UNIVERSIDAD COMPLUTENSE DE MADRID

FACULTAD DE CIENCIAS BIOLÓGICAS

Departamento de Genética

TESIS DOCTORAL

Caracterización de AcNMCP1 una proteína implicada en organización nuclear de plantas

Characterization of AcNMCP1 a protein implicated in the nuclear organization in plants

MEMORIA PARA OPTAR AL GRADO DE DOCTOR

PRESENTADA POR

Malgorzata Ciska

Directoras

Susana Moreno Díaz de la Espina
Concepción Romero Martínez

Madrid, 2014

UNIVERSIDAD COMPLUTENSE DE MADRID

CONSEJO SUPERIOR DE INVESTIGACIONES CIENTÍFICAS

CENTRO DE INVESTIGACIONES BIOLÓGICAS

LABORATORIO DE MATRIZ NUCLEAR Y REGULACIÓN DE LA ORGANIZACIÓN Y FUNCIONALIDAD NUCLEAR

Caracterización de AcNMCP1 una proteína implicada en organización nuclear de plantas

Characterization of AcNMCP1 a protein implicated in the nuclear organization in plants

TESIS DOCTORAL

Malgorzata Ciska

Madrid, 2013

UNIVERSIDAD COMPLUTENSE DE MADRID

FACULTAD DE CIENCIAS BIOLÓGICAS

DEPARTAMENTO DE GENÉTICA

Caracterización de AcNMCP1 una proteína implicada en organización nuclear de plantas

Characterization of AcNMCP1 a protein implicated in the nuclear organization in plants

MEMORIA PARA OPTAR AL GRADO DE DOCTOR
PRESENTADA POR

MALGORZATA CISKA

Vº Bº DIRECTORES DE TESIS

Fdo. Dra.Susana Moreno Díaz de la Espina

Vº Bº TUTOR DE TESIS

Fdo.: Dra. Concepción Romero Martínez

Fdo.: Malgorzata Ciska

MADRID, 2013

CONSEJO SUPERIOR DE INVESTIGACIONES CIENTÍFICAS

CENTRO DE INVESTIGACIONES BIOLÓGICAS

LABORATORIO DE MATRIZ NUCLEAR Y REGULACIÓN DE LA ORGANIZACIÓN Y FUNCIONALIDAD NUCLEAR

In the first place I would like to thank the people who made it possible to finish this work. Dr. Susana Moreno who has put a trust in me and has allowed me to develop as a scientist while working on such an inspiring project. Dr. Kyoshi Masuda whose collaboration and professional expertise allowed us to perform experiments and obtain results of importance in the plant cell biology. My parents who has always believed in me and supported me through thick and thin even though I know many times it was not easy for them. My biggest failure would be to let them down. I could not forget about Merce, our technician who helped me with the experiments more than once and who always spared a smile and a chat when I needed.

I would like to thank CSIC for granting me the JAE fellowship (JAEPre_08_00012/JAEPre027) and providing financial: support [PIE 201020E019] as well as the Spanish Ministry of Science and Innovation [BFU2010-15900].

Dr. Francisco García Tabares and Ms María Fernández López-Lucendo from proteomics fascility, Dr. Mª Teresa Seisdedos Domínguez from confocal microscopy, Dr. Fernando Escolar Antunez from electron microscopy and Dr. Perdo Lastres Varo from the flow cytometry facility for expert technical assistance. Also my tutor at the UCM, Dr. Concepción Romero.

The people who helped me in the professional manner, as well as on the personal level. Dr Livia Donaire who helped me performing the northern blot analysis and whose friendship made my first years in a foreign country much easier. Dr Cesar Llave who allowed me to perform the northern blot in his lab. Mrs Elzbieta Smolczynska from the State Plant Health and Seed Inspection Service who kindly supported me with cereal seeds. Dr Alberto Garcia, “un sol” who always had a good advice, professional and concerning private life.

Also I would like to thank dr Javier Gallego from the UCM for making the administrative steps of the thesis so much easier and more pleasant. And also people who might not remember me but who inspired me and awoke the passion for science during The Wilhelm Bernard workshop in Riga: prof Yossif Gruenbaum and prof David Jans.

I do have to mention my "CIB team" as if not for them I would probably run back to Poland after the first weeks. People that welcomed me and quickly became my friends: Fati, Meme, Fran and Ana Castro. Jose Ramon, who introduced me to the lab and to his friends and help me to intergrate in spite of the language barrier. Also Hector, Maite and Vanessa who are great companions in scientific and social affairs.

My partner, Quike, without whom I wouldn´t have had decided on coming to Spain and whose help made it possible to start the fellowship and also a completely new life. Michiel Janssens, my good friend who always have motivated me even from a 2,000 km distance.

Finally I would like to thank all the staff from CIB for creating such a friendly working environment as it was a great pleasure working there for the last five years.

RESUMEN

La lámina es una estructura filamentosa adosada a la membrana nuclear interna presente en el núcleo de numerosos eucariotas, incluyendo protozoos, metazoos y plantas. Está constituida por una red proteínica compleja asociada a la membrana nuclear interna y a los poros nucleares complejos. En metazoos la lámina consiste en un polímero de filamentos de laminas con numerosas proteínas asociadas que regulan su asociación con la membrana nuclear interna, poros nucleares y cromatina. Los principales componentes de la lámina de metazoos son las laminas que constituyen la clase V de la superfamilia de filamentos intermedios. Las laminas tienen importantes funciones en el núcleo como son la regulación de la organización y posición de la cromatina, replicación, transcripción y reparación del DNA, mantenimiento de la morfología nuclear, transducción de señales, conexión física del núcleoesqueleto y citoesqueleto, etc. Estas funciones se realizan de forma similar en el núcleo de plantas aunque carecen de genes codificantes de laminas y de la mayoría de las proteínas que se asocian con ellas. Además la lámina ha sido descrita repetidamente en varias especies de plantas mono y dicotiledóneas aunque su composición proteínica no es conocida. Por estos motivos se ha postulado que las plantas tendrían una lámina compuesta por un tipo diferente de proteínas. Hasta el presente se han propuesto varias proteínas específicas como candidatas para realizar las funciones de las laminas en plantas. Entre ellas se encuentran proteínas reconocidas por anticuerpos contra laminas y filamentos intermedios y también proteínas *coiled coil* específicas de plantas. Entre estas últimas están las proteínas constitutivas de la matriz nuclear (NMCP) que son las candidatas mas sólidas para reemplazar a las laminas en plantas ya que al igual que estas presentan una

estructura *coiled coil* tripartita, localizan en la periferia nuclear y están implicadas en la regulación de la morfología nuclear.

El objetivo de este trabajo era por una parte la caracterización de la familia de proteínas NMCP estableciendo las relaciones filogenéticas entre los distintos ortólogos en varias especies de mono y dicotiledóneas, así como la determinación de sus principales características: estructura secundaria, distribución de dominios conservados y sitios de modificación postranscripcional. Asimismo nos planteamos el análisis de la proteína NMCP1 en *Allium cepa* (AcNMCP1) incluyendo su secuencia y la caracterización de la proteína endógena. Finalmente efectuamos la comparación de las principales características de NMCPs y laminas que permitieran establecer si las proteínas NMCPs realizan funciones de laminas en plantas.

La búsqueda en la base de datos Phytozome v8 demostró que la familia está muy conservada ya que todas las plantas excepto las unicelulares expresan al menos dos proteínas NMCP. El análisis filogenético reveló que la familia está dividida en dos grupos uno conteniendo las proteínas NMCP1 y el otro las NMCP2. El primero está a su vez dividido en dos subgrupos NMCP1 y NMCP3. Las monocotiledóneas expresan una proteína NMCP1 y una NMCP2 mientras que las dicotiledóneas tiene una proteína NMCP2 y dos o más del tipo NMCP1. La forma ancestral de las NMCPs parece pertenecer al grupo NMCP2 ya que los dos ortólogos del musgo *Physcomitrella patens* están incluidos en ese grupo.

El análisis exhaustivo de las secuencias NMCP demostró que comparten muchas características con las laminas. La predición de segmentos *coiled coil* con el programa MARCOIL reveló que todas las NMCPs tienen una estructura tripartita conservada con un segmento central *coiled coil* análogo al

de las laminas aunque el doble de largo. Este está dividido en dos segmentos separados por un *linker* corto que no tiene estructura *coiled coil* y en algunos casos interrumpidos por *linkers* internos. La predicción de sitios de modificación postranslacional demostró que las NMCPs tienen sitios de fosforilación para cdk1 flanqueando el dominio *coiled coil* central al igual que las laminas. La búsqueda de motivos conservados con MEME demostró la presencia de regiones muy conservadas en ambos extremos del dominio *coiled coil*, en las posiciones de los *linkers* y en la cola de la proteína, entre estas una región de localización nuclear, un dominio de aminoácidos ácidos (en las NMCP1) y el extremo carboxy terminal de la proteína (excepto en las NMCP2 de dicotiledóneas). Todas estas características son compartidas con las laminas.

El análisis mediante "Western blot" usando un anticuerpo dirigido contra una región muy conservada de la proteína incluyendo la cabeza y el principio aminoterminal del segmento *coiled coil* reveló que el peso molecular de las proteínas endógenas es muy variable entre especies, aunque los deducidos de los cDNAs son similares, sugiriendo que las proteínas experimentan modificaciones post-tranlacionales.

También analizamos la secuencia y propiedades bioquímicas de un ortólogo de *Allium cepa*: AcNMCP1. El cDNA codifica una proteína de 1.217 aminoácidos que presenta la estructura compartida con el resto de las NMCPs. Su peso molecular es mucho mas alto (200 kDa) que el deducido de la secuencia (139 kDa). La posibilidad de dimerización de la proteína fue descartada en base a las extracciones con altas concentraciones de urea, tiocianato de guanidina y alta temperatura y pH, sugiriendo que la proteína experimenta modificaciones post-translacionales. AcNMCP1 es altamente insoluble y un componente del núcleoesqueleto como demuestra la extracción secuencial con detergentes no iónicos, nucleasa y tampones de baja y alta fuerza iónica. Mediante inmunofluorescencia e inmunomicroscopía

electrónica de fracciones de núcleoesqueletos demostramos la localización predominante de AcNMCP1 en la lámina y en menor grado en el núcleoesqueleto interno.

El análisis de fracciones nucleares mediante inmunofluorescencia demuestra que AcNMCP1 localiza mayoritariamente en la periferia nuclear y en menor grado en el nucleoplasma. El análisis de alta resolución mediante microscopía electrónica permitió localizar la proteína mayoritariamente en la lámina y con menor concentración en los dominios intercromatínicos en las zonas de contacto entre la cromatina condensada y descondensada.

La expresión y distribución nuclear de AcNMCP1 están reguladas en el desarrollo en células de raíz, como demuestran los experimentos de western blot e inmunofluorescencia. La proteína es muy abundante en los núcleos meristemáticos tanto proliferantes como quiescentes y decrece gradualmente en los de las zonas de elongación y diferenciación. La distribución de AcNMCP1 cambia cuando las células pasan del estado quiescente al proliferante y los focos intranucleares de la proteína típicos de células quiescentes desaparecen en el núcleo en proliferación. Durante la diferenciación cambia la distribución periférica de la proteína obsevándose en los núcleos diferenciados regiones carentes de AcNMCP1 en contraste con la distribución periférica uniforme de los núcleos meristemáticos.

Las funciones de las NMCPs son poco conocidas aunque varios estudios independientes han confirmado su implicación en la regulación del tamaño y forma nuclear. Nosotros investigamos los efectos de las mutaciones *linc1, linc2* y *linc1linc2* en la organización nuclear de células meristemáticas de raíz de *Arabidopsis thaliana,* no observando cambios evidentes en la organización de los diferentes componentes nucleares de ninguno de los mutantes en relación con los de las plantas silvestres. Estos resultados podrían deberse a complementación con las proteínas LINC3 y LINC4 presentes en los mutantes.

Nuestros resultados nos permiten concluir que las NMCPs son proteínas específicas presentes en todas las plantas multicelulares pero no en las unicelulares, que constituyen una familia muy conservada con dos grupos las de tipo NMCP1 y las de tipo NMCP2. Las monocotiledóneas tienen un gen de NMCP1 y otro de NMCP2 mientras que las dicotiledóneas expresan dos o tres del tipo NMCP1 y uno solo del tipo NMCP2. Los dos ortólogos del musgo *Physcomistrella patens* están incluídos en el grupo de las de tipo NMCP2 lo cual sugiere que la forma ancestral de las proteínas sería de este tipo.

Todas las NMCPs tienen una estructura tripartita con un dominio central en α-hélice con una alta probabilidad de formar *coiled coils* y dimerizar. Todos los miembros de la familia contienen dominios altamente conservados: cinco en el dominio central y tres en la cola de la proteína. La distribución de los dominios conservados es similar a la de las laminas ya que los extremos del dominio *coiled coil*, los *linkers*, el extremo carboxiterminal y los sitios de reconocimiento de cdk1 que flanquean el dominio central están muy conservados en ambos. La presencia de múltiples sitios de modificación post translacional y las diferencias de peso molecular entre las proteínas endógenas y los valores deducidos de las secuencias sugieren que las proteínas NMCP experimentarían modificaciones post translacionales.

La proteína NMCP1 de *Allium cepa* tiene la misma estructura y características del resto de las NMCP1s. La proteína endógena tiene un peso molecular de 200 kDa, mucho mayor que el esperado de la secuencia, y un punto isoeléctrico de 5.2 y 5.8. Está distribuída preferentemente en la periferia nuclear y en menor cantidad en el nucleoplasma. La inmunomicroscopía de alta resolución demuestra su localización preferencial en la lámina. AcNMCP1 es muy insoluble y forma parte de la lámina y el núcleoesqueleto interno lo mismo que las laminas. La expresión y distribución nuclear de AcNMCP1 estan reguladas con el desarrollo en raíces. La proteína es abundante en los

meristemos, ya sean proliferantes o quiescentes, mientras que en las zonas de elongación y diferenciación sus niveles disminuyen gradualmente. En los meristemos quiescentes la proteína tiene una distribución regular en la periferia nuclear análoga a la de los meristemos proliferantes, pero forma agregados grandes en el nucleoplasma que desaparecen en los núcleos en proliferación. En las células diferenciadas los núcleos presentan una distribución discontinua en la periferia nuclear con zonas grandes carentes de la proteína.

Nuestros resultados demuestran que las proteínas NMCP comparten importantes características estructurales y funcionales con las laminas, como son:

a) Una estructura tripartita con un dominio central *coiled coil* con alta probabilidad de dimerización.
b) La presencia de dominios altamente conservados en los dos extremos del dominio *coiled coil* central
c) La presencia de sitios de fosforilación para cdk1 flanqueando el dominio *coiled coil* central
d) Alta conservación del dominio C-terminal de la proteína
e) Localización en la lámina y en menor proporción en el núcleoesqueleto interno.
f) Expresión regulada en el desarrollo.

Todo ello y los datos de su funcionalidad en el control del tamaño y forma nuclear sugiere que las proteínas NMCP podrían ser análogos de las laminas en plantas y realizar algunas de sus funciones.

ABSTRACT

The lamina is a filamentous structure underlying the inner nuclear membrane. It has been described in many eukaryotes including protozoa, metazoans and plants. In metazoans, lamins which constitute the class V of the intermediate filament superfamily are the main components of the lamina. They play important functions in the nucleus such as the regulation of chromatin organization, maintenance of nuclear morphology, mechanotransduction, physical connection between the cytoskeleton and the nucleoskeleton etc. These functions are also fulfilled in the plant cells although they lack genes encoding lamins and most lamin-binding proteins. The plant lamina was described repeatedly in various species but the composition of this structure is still not known. However, few plant-specific proteins have been proposed as candidates to play functions of lamins in the plant cell. The candidates include nuclear proteins cross-reacting with anti-lamin and anti-IF antibodies and plant specific coiled-coil proteins. In amongst them are the Nuclear Matrix Constituent Proteins (NMCPs) that are so far the best candidate to be a lamin analogue in plants as they display a similar secondary structure to lamins, are localized at the nuclear periphery and play a critical role in the regulation of nuclear morphology. Mutations of NMCP proteins in *Arabidopsis thaliana* cause a reduction in nuclear size and changes in nuclear shape which are the funtions regulated by lamins in the metazoan cell.

The objective of this work was to characterize NMCP protein family. We describe the phylogenetic relationships between the NMCP orthologues in various species, as well as the features characterizing the protein family: secondary structure, distribution of conserved motifs and the presence of post-translational modification sites. We also investigated the sequence, biochemical properties, the nuclear distribution and the high-resolution

localization of an onion orthologue, AcNMCP1. Finally, we compare the features of NMCPs with that of lamins and discuss the possibility that they play some of the functions of lamins in the plant cell.

A search on Phytozome v8 database revealed that all land plants express at least two NMCP proteins. Extensive analysis of NMCP sequences demonstrated they share many features with lamins. The phylogenetic analysis revealed the family is divided into to clusters, one containing NMCP1-type and the second NMCP2 proteins. The former is divided into two subclusters, one containing NMCP1 and the second NMCP3 protens. The coiled-coil prediction with MARCOIL programme demonstrated that all NMCPs represent a conserved tripartite structure with a central coiled-coil domain analogous to lamin´s although it is twice as long as that of the later. The rod domain is divided into two coiled-coil segments separated by a short non-coiled-coil linker and sometimes interrupted by internal linkers. A search for predicted post-translational modification sites demonstrated NMCPs contain cdk1 phosphorylation sites flanking the rod domain, as lamins. Analysis with MEME, a programme searching for conserved motifs demonstrated the presence of highly conserved regions at both ends of the rod domain, at the positions of linkers and in the tail domain. It also demonstrated the presence of a conserved nuclear localization signal in the tail domain and of a stretch of acidic amino acids at the C-extreme in the NMCP1-type proteins. The C-terminus of the protein is also conserved (except for NMCP2 in dicots) These features are also characteristic for lamins.

Western blot analysis using an anti-AcNMCP1 antibody raised against a highly conserved region which includes the head and the conserved begining of the rod domain demonstrated that the molecular weights of the endogenous NMCP orthologues is highly variable between species, although the predicted MWs calculated based on the cDNA sequenes were comparable between the

NMCPs suggesting that NMCP proteins undergo post-translational modifications.

We also report the sequence and biochemical properties of an onion orthologue, AcNMCP1. The cDNA encodes a protein containing 1,217 amino acids which shares the predicted structure with other NMCPs. Its molecular weight is higher (200 kDa) than the predicted value (139 kDa) which is probably caused by post-translational modification. The possibility of dimer formation was excluded after treatments with high concentrations of urea, guanidine thiocyanate and high pH and temperature values. The AcNMCP1 is highly insoluble and a component of the nucleoskeleton as shown in the sequential extraction with non-ionic detergent, and low and high- salt buffers after nuclease digestion. Immunofluorescence microscopy and a high resolution immunolabelling in NSK fractions confirmed the predominant localization of the AcNMCP1 in the lamina and less abundant fraction in the internal NSK. Analogous distribution is characteristic for lamins.

Immunofluorescence microscopy analysis demonstrated that the protein is localized predominantly at the nuclear periphery and in a minor fraction in the nucleoplasm. High resolution localization of AcNMCP1 using electron microscopy demonstrated the protein is abundant in the lamina but also is present in the fibrillar network of the interchromatin domains and at the boundaries between condensed and decondensed chromatin in the nucleoplasm.

We report that the expression of AcNMCP1 is developmentally regulated in root cells as was shown by the immunoblot and immunofluorescence analyses. The protein is most abundant in meristems, either quiescent or proliferating, while in the elongation and differentiated root zones the levels gradually decrease. The distribution of the AcNMCP1 changes when root cells switch from quiescent to proliferating state as the accumulations of the

protein observed in quiescent nuclei in form of nucleoplasmic foci are not present in the proliferating nuclei. The distribution at the nuclear periphery changes during differentiation as in differentiated nuclei we observed regions depleted of AcNMCP1 in contrast with the uniform peripheral distribution in the proliferating nuclei.

The functions of NMCPs are still scarcely described although several independent studies confirmed its implication in the regulation of nuclear size and shape. We investigated the effects of *linc* mutations in root meristems of single and double *A. thaliana* mutants: *linc1*, *linc2* and *linc1linc2* by electron microscopy. No obvious changes in nuclear morphology were observed in comparison to the wild type probably caused by the presence of two remaining functional NMCP homologues (LINC3 and LINC4) which may have complemented the functions of LINC1 and LINC2 in the regulation of nuclear morphology.

In conclusion, NMCPs are plant-specific and are expressed in multicellular plants but are absent in the single-cell plants. They form a highly conserved protein family which consists of two clusters, one containing NMCP1-type and the second containing NMCP2-type proteins. Monocots express one NMCP1 and one NMCP2 protein whereas dicots express two or three NMCP1-type proteins and a single NMCP2-type. The progenitor form of NMCPs seem to belong to NMCP2 cluster as the two orthologs expressed in a moss *Physcomitrella patens* are included in this cluster.

All NMCPs represent a conserved tripartite structure with a central α-helical rod domain predicted to form coiled coils and dimerize. The NMCP family members contain highly conserved motifs: five within the coiled-coil and three within the tail domain. The distribution of the conserved domains is similar to the one in lamins, as the ends of the rod domain, the linkers and the C-terminus are highly conserved in both. The presence of multiple predicted

post-translational modification sites and the difference between the molecular weights of endogenous proteins and the predicted values strongly suggest NMCPs undergo post-translational modifications.

The AcNMCP1 shares predicted structure and characteristic features with other NMCP1 proteins. The endogenous protein has a molecular weight of 200 kDa and an isoelectric point of 5.2 and 5.8. It is predominantly distributed at the nuclear periphery and to a lower extent in the nucleoplasm. It is preferentially localized in the lamina as revealed by high resolution immunogold localization. AcNMCP1 is highly insoluble and a constituent component of the lamina and the internal NSK. The expression of AcNMCP1 is developmentally regulated. It is abundant in root meristems (proliferating and quiescent) whereas in the elongation and differentiated root zones the levels decrease gradually. The subnuclear distribution of AcNMCP1 changes depending on the differentiation states in onion root. In quiescent meristems the protein is abundant at the nuclear periphery but also forms large aggregates in the nucleoplasm. In the differentiated nuclei as the levels of the protein decrease, the nuclei display a discontinuous distribution at the nuclear periphery with large areas depleted of AcNMCP1.

Our results demonstrate that NMCP proteins share important structural and physiological characteristics with lamins such as:

a) a tripartite structure containing a central coiled-coil domain predicted to dimerize

b) presence of highly conserved motifs at both ends of the rod domain

c) the presence of cdk1 phosphorylation sites in close proximity to the rod domain

d) highly conserved C-terminus of the protein

e) localization in the lamina and to a lesser extent in the internal NSK

f) developmentally regulated expression

All above suggest that these proteins could be the analogues of lamins in plants and play some of their functions.

INDEX

LIST OF ABBREVIATIONS

2,4-D: 2,4-Dichlorophenoxyacetic acid

2-DE: Two dimensional electrophoresis

ACN: acetonitrile

ARP: Actin Related Protein

BAF: Barrier to Autointegration Factor

BSA: Bovine serum albumin

C: Celcius

CaMV: Califlower Mosaic Virus

CB: Cajal Body

CBH: Cellobiohyrdolase

cdk1: cyclin dependent kinase 1

CHAPS: 3-[(3-cholamidopropyl) dimethylammonio]-1-propanesulfonate

CSK: Cytoskeleton

CskB: Cytoskeleton Buffer

DAPI: 4',6' diamidino-2-phenylindole

DB: Digestion Buffer

DFC: Dense Fibrillar Component

DIC: Differential Interference Contrast

DNA: Deoxyribonucleic acid

DTT: Dithiothreitol

EDTA: Ethylenediaminetetraacetic acid

EGFP: Enhanced Green Fluorescent Protein

EGTA: Ethylene Glycol Tetraacetic Acid

EtOH: Ethanol

FA: Formaldehyde

FC: Fibrillar centers

FISH: Fluorescence In Situ Hybridization

FPP: Filament-like Plant Proein

FRET: Forster Resonance Energy Transfer

GC: Granular Component

GFP: Green Fluorescent Protein

GITC: Guanidine thiocyanate

HGPS: Hutchinson-Gilford progeria syndrome

HIFD: Human Inermediate Filament Database

HMM: Hidden Markov Model

HRP: Horseradish peroxidase

IF: Intermediate Filament

IM: Isolation Medium

INM: Inner Nuclear Membrane

IPTG: Isopropyl-beta-D-thiogalactopyranoside

KASH: Klarsicht, ANC-1, SYNE/Nesprin 1 and 2 homology domain

LB: Lysogeny Broth

LBR: Lamin B Receptor

LEM: LAP2, Emerin, MAN (domain)

LINC: Linker of the Nucleoskeleton to the Cytoskeleton (complex)

LINC: *Little Nuclei* (gene)

LysB: Lysis Bufer

MAR: Matrix Attachment Region

MARBP: Matrix Attachment Region-Binding Protein

MEGA5: Molecular Evolutionary Genetics Analysis 5

MEME: Multiple EM for Motif Elicitation

ML: Maximum Likelihood (method)

MOPS: 3-morpholinopropane-1-sulfonic acid

MS: Murashige and Skoog

MW: Molecular Weight

NAA: Naphthalene Acetic Acid

NAC: Nuclear Acidic Coiled-coil (protein)

NCBI: National Center of Biotechnology Information

NE: Nuclear Envelope

NJ: Neighbour-Joining (method)

nLC-MS/MS: Nano-scale liquid chromatographic tandem mass spectrometry

NLS: Nuclear Localization Signal

NMCP: Nuclear Matrix Constituent Protein

NOR: Nucleolus Organizing Region

NPC: Nuclear Pore Complex

NSK: Nucleoskeleton

NUA: Nuclear pore anchor

NuMA: Nuclear Mitotic Apparatus

ONM: Outer Nuclear Membrane

PBS: Phosphate Buffered Saline

PCR: Polymerase Chain Reaction

PIPES: Piperazine-N,N'-bis(2-ethanesulfonic acid)

PKA: cyclic AMP-dependent Protein Kinase

PKC: Protein Kinase C

PKG: cyclic GMP-dependent Protein Kinase

PLF: nuclear Pore-Linked Filament

PSSM: Position Specific Scoring Matrix

RNA: Ribonucleic acid

RNP: Ribonucleoproteins

rpm: Revolutions per minute

SDS: Sodium dodecyl sulfate

SDS-PAGE: Sodium dodecyl sulfate polyacrylamide gel electrophoresis

SSC: Saline-Sodium Citrate buffer

SUN: Sad1, UNC domain

TCA: Trichloroacetic acid

TEM: Transmission Electron Microscopy

TFA: Trifluoroacetic acid

TPR: Translocated Promoter Region

TRIS: Tris(hydroxymethyl) aminomethane

TX-100: Triton X-100

X-gal: 5-bromo-4-chloro-indolyl-β-D-galactopyranoside

INTRODUCTION

1. Nuclear morphology and nuclear matrix

The nucleus is the defining feature of eukaryotic cells which separates the nuclear genome from cytoplasm with a double membrane (Wilson and Berk 2010). This subnuclear compartment was observed for the first time by the Scottish botanist Robert Brown who described a "circular areola" or "nucleus of the cell" in orchid epidermis (Fig 1 a, b, c) (Brown 1833). The shape and the size of the nucleus differ between species and tissues but few common structural features can be distinguished: the Nuclear Envelope (NE), chromatin, several types of nuclear bodies and the nucleolus. The NE defines the nucleus and consists of two bordering membranes interrupted by Nuclear Pore Complexes (NPCs) that enable transport of molecules from and to the cytoplasm (Strambio-De-Castillia et al. 2010). The nucleolus is the site of rDNA gene expression as well as ribosome formation (Nemeth and Langst 2011).

Another nuclear component that is less evident and more controversial is the nucleoskeleton (NSK) also called the nuclear matrix, which is a protein assembly thought to provide a structural support to other nuclear components. First hints about a possible existence of the nuclear matrix date as far as 1948 when a nuclear protein fraction resistant to extraction with high salt buffer was reported (Zbarsky and Debov 1948; Pederson 2000). In the following years it was described by few independent research groups (Georgiev and Chentsov 1962; Narayan et al. 1967; Pederson 2000; Berezney and Coffey 1974). Also, light and electron microscopic observations of salt-extracted nuclei revealed retention of nuclear shape which suggested the presence of a structural protein matrix in nuclei similar to the cytoskeleton

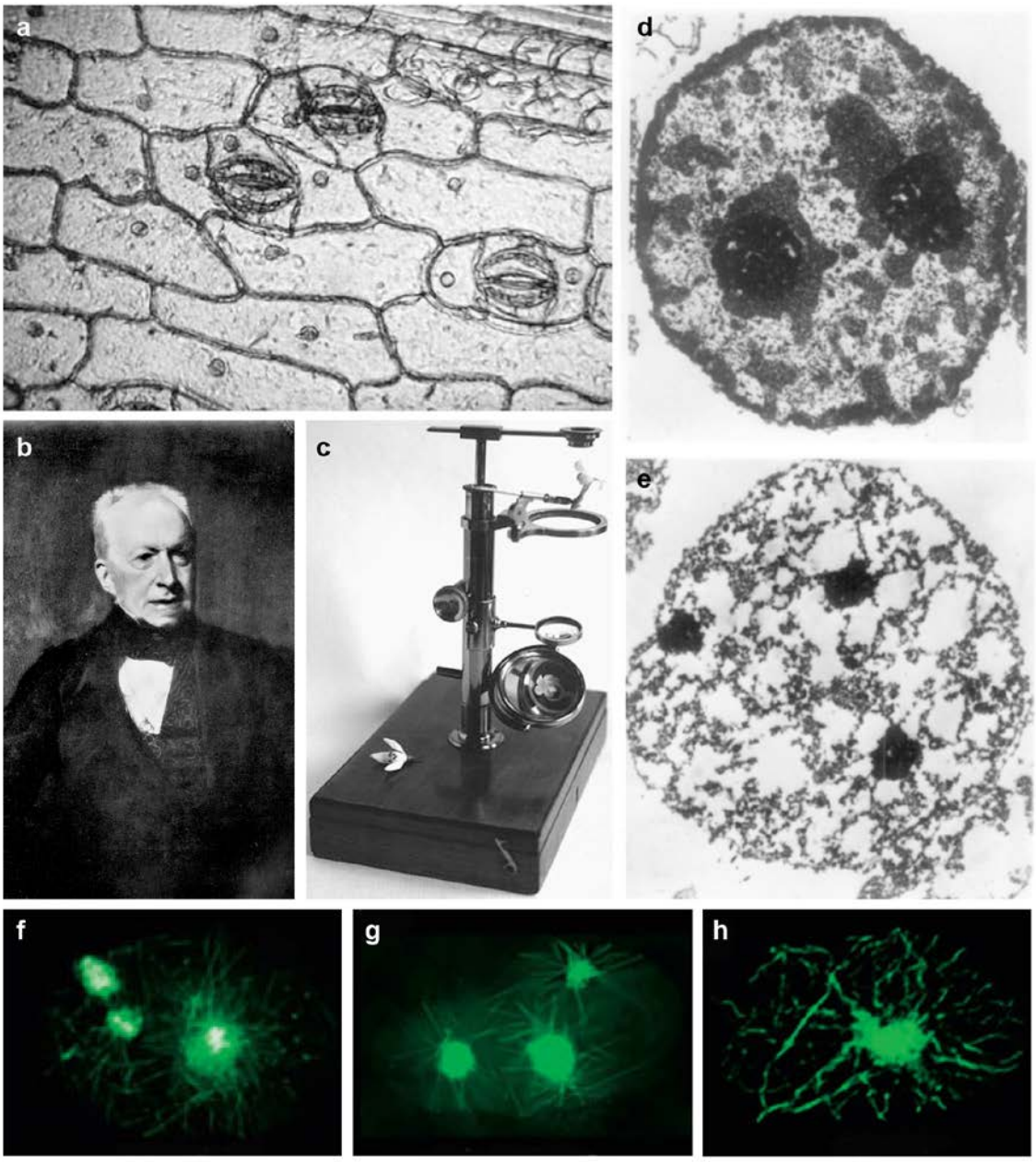

Figure 1. First discoveries of nucleus and NSK. a, **b** Cells within orchid *Cymbidium* epidermis (a) as seen by Robert Brown (b) (Ford 2009). **c**. Model of a single-lens microscope used by Robert Brown (Ford 2009). **d**, **e** Nucleus (d) and isolated NSK fraction observed by TEM (e) (Berezney and Coffey 1974) **f**, **g**, **h** EGFP-Cdc14B pattern in fixed (f) and living mammalian cells (g) demonstrate that Cdc14B phosphatase associates with intranuclear filaments. The filaments are also seen in detergent and nuclease extracted NSK (h) (Nalepa and Harper 2004).

(Georgiev and Chentsov 1962; Narayan et al. 1967). The term NSK was for the first time used in the seventies and referred to a filamentous meshwork that remains after extraction of nuclei with high-salt buffer and DNA

digestion (Fig 1 d, e) (Berezney and Coffey 1975, 1974, 1977). Since then the opinions of scientists were contradictory: some reckoned that the structure is just an extraction artefact and others that it is a functional nuclear component (Pederson 2000). Currently, the existence of the nuclear matrix is commonly accepted since few proteins typical for CSK as actin, myosin, IFs (lamins) were also detected inside the nucleus and they are thought to be functional components of the NSK (Simon and Wilson 2011). A breakthrough in the discussion was reached when the intranuclear filamentous framework was demonstrated in the living mammalian cells by immunofluorescent staining of Cdc14B, a phosphatase that binds to the NSK filaments (Fig. 1 f, g, h). The phosphatase which is critical for nuclear structure maintenance is tightly associated with long nucleoskeletal filaments that stretch from nucleolar periphery to NE, frequently making close connections with NPCs (Nalepa and Harper 2004).

At first the NSK was thought to be only a structural component of the nucleus with strictly mechanical functions as preventing rupture of the nucleus under force and maintaining nuclear structure (Dahl and Kalinowski 2011). The extended studies on the NSK showed its components are involved in cellular signaling and gene regulation by providing binding sites for regulatory proteins (Stenoien et al. 2000; Wilson and Berk 2010). The NSK is also implicated in DNA replication (Berezney and Coffey 1975), RNA splicing (Wagner et al. 2003), control of cell cycle checkpoints (Mancini et al. 1994) and regulation of apoptosis (Gerner et al. 2002). The NSK is thought to be an important player in mechanostransduction, a process of channelling extracellular physical forces which mediates simultaneous activity changes of multiple molecules in cytoplasm and nucleus. This provides a more rapid and efficient way to convey information over long distances than diffusion-based chemical signalling (Wang et al. 2009; Lombardi et al. 2011).

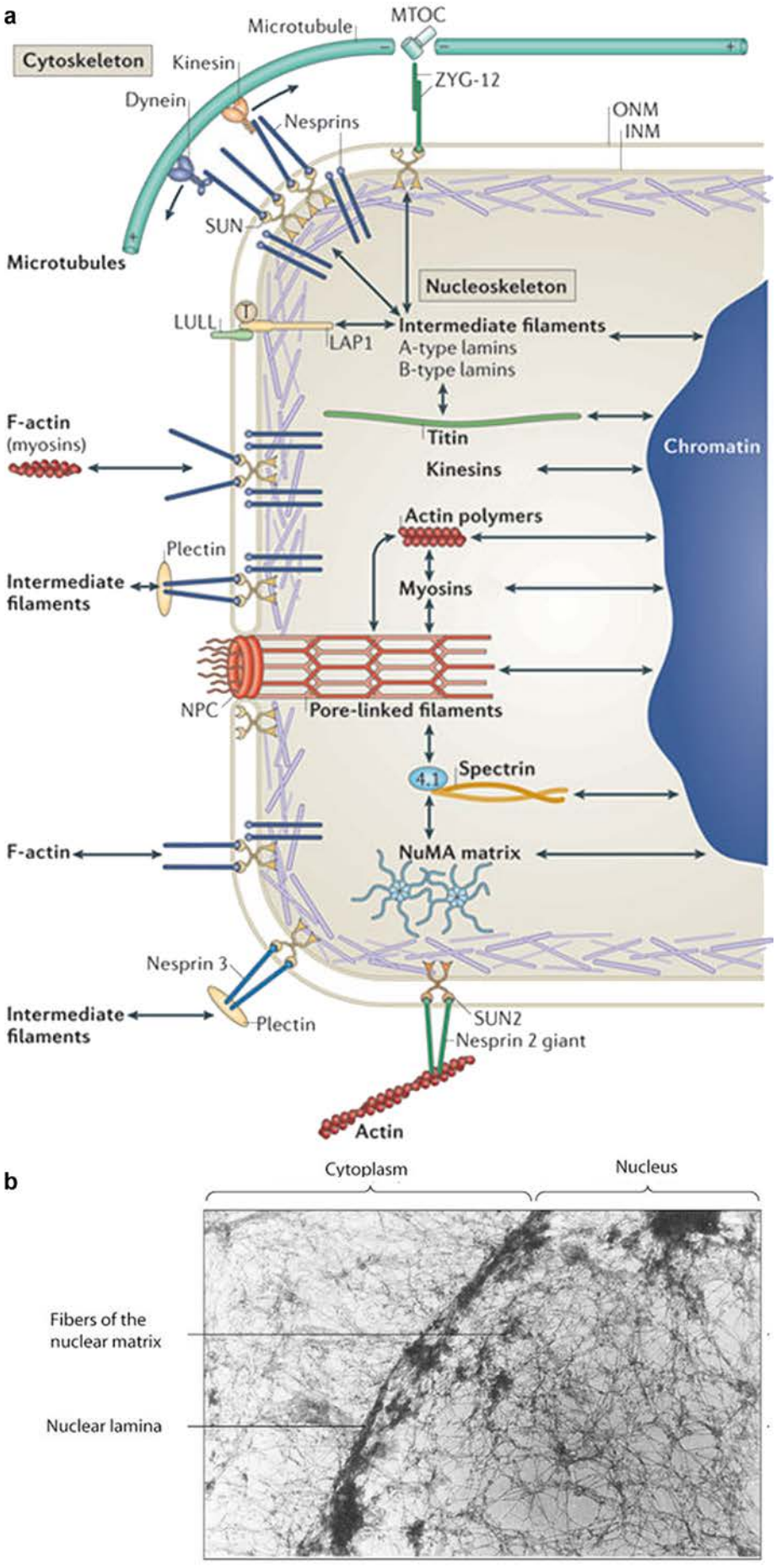
a
Microtubule
MTOC
Cytoskeleton
Kinesin
ZYG-12
Dynein
Nesprins
ONM
INM
SUN
Microtubules
Nucleoskeleton
LULL
LAP1
Intermediate filaments
A-type lamins
B-type lamins
F-actin
(myosins)
Titin
Chromatin
Kinesins
Actin polymers
Plectin
Intermediate
filaments
Myosins
NPC
Pore-linked filaments
4.1
Spectrin
F-actin
NuMA matrix
Nesprin 3
Intermediate
filaments
Plectin
SUN2
Nesprin 2 giant
Actin
b
Cytoplasm
Nucleus
Fibers of the
nuclear matrix
Nuclear lamina

The NSK is linked to the elements of the cytoskeleton by the LINC (LInker of the Nucleoskeleton to the Cytoskeleton) complex (Fig 2 a, b) (Padmakumar et al. 2005; Crisp et al. 2006). Disruption of its components or the components of the NSK (for example lamin A) results in altered cytoskeletal mechanics (Lombardi et al. 2011; Lammerding et al. 2005). In the metazoan cell the nucleoskeleton includes nuclear-Pore Linked Filaments (PLFs), A-type and B-type lamin filaments, Nuclear Mitotic Apparatus (NuMA) networks, spectrins, tintin, nuclear actin polymers and myosin and kinesin motors (Fig 2) (Simon and Wilson 2011).

Lamin filaments are present in the lamina where they form a meshwork attached to the INM but they are also present in the nucleoplasm (Dechat et al. 2010b). The structure and composition of lamin filaments and their possible plant analogues are discussed in the next chapters.

The PLFs are filaments attached to the basket of NPCs on the nucleoplasmic side of NE and can extend at least 350 nm into the nucleoplasm. They are open filaments with eightfold symmetry and 8-10 nm in diameter and are connected to the nucleolus and Cajal bodies (Simon and Wilson 2011; Strambio-De-Castillia et al. 2010). The main component of PLFs is probably Translocated Promoter Region (TPR) (Megator in *Drosophila melanogaster*), a

Figure 2 (on the left). The nucleoskeleton is connected to the cytoskeleton through the LINC complex. a. Scheme of main proteins of the CSK and the NSK and their interactions. The components of the CSK: cytoskeletal IF, microtubules and F-actin filaments attach to LINC complexes which consist of nesprins located on the ONM (outer nuclear membrane) binding in the NE lumen SUN proteins residing on the INM (inner nuclear membrane). The NE also contain complexes formed by LULL1 (luminal domain like LAP1), LAP1 (lamina-associated polypeptide 1) and torsin (T). LINC complexes transmit mechanical forces to the nucleoskeleton and chromatin. The nucleoskeletal components include; lamin intermediate filaments, nuclear mitotic apparatus (NuMA), spectrins, protein 4.1, titin, actin, myosins, kinesins and NPC-linked filaments. MTOC (microtubule-organizing center) binds to ZYG12 (zygote defective 12) which binds to SUN proteins (Simon and Wilson 2011) b. Attachment of nucleoskeletal fibers to the nuclear lamina (He et al. 1990).

long coiled-coil protein forming dimers (Cordes et al. 1997; Fontoura et al. 2001). The function of this structure is still not resolved but it was proposed that the filaments maintain chromatin-free channels facilitating diffusion into and out of the nucleus. Also, actin, protein 4.1 and myosin MYO1C were detected on PLFs and it was suggested that PLF-associated motors might facilitate the export of large cargos like for example ribosomal units (Simon and Wilson 2011). TPR is also a main component of the nuclear pore basket in vertebrates (Frosst et al. 2002) and is involved in multiple functions such as transcriptional regulation, RNA biogenesis, regulation of SUMO homeostasis, chromatin maintenance and the control of cell division (Strambio-De-Castillia et al. 2010). NUA, a plant protein described in *A. thaliana* displays some sequence homology to TPR, has a similar size to the animal homologue and shares some of its functions (Xu et al. 2007; Jacob et al. 2007). It is involved in the control of SUMO protease activity at the nuclear pore and mRNA export as TPR (Jacob et al. 2007; Xu et al. 2007). Also, NUA interacts with AtMAD1 as TPR in mammalian system (Lee et al. 2008) and is needed for proper localization of AtMAD1 and AtMAD2 at the NE (Ding et al. 2012). Filaments extended from the distal ring of the basket towards the nuclear interior, similar to PLF were also observed in plant nucleus but it is still to be resolved if these filaments are formed by NUA (Fiserova et al. 2009).

NuMA is a large protein (238 kDa) with a long central coiled-coil domain (1,500 amino acids) and globular head and tail domains. The coiled-coil domain mediates formation of homodimers which self-assemble *in vitro* in groups of 24 to form three-dimensional space-filling structures (Harborth et al. 1999). It is spread throughout the nucleus, except for the nucleolus and almost as abundant as lamins (at 10^6 copies per nucleus) which suggests it is next to lamins the major component of the NSK (Radulescu and Cleveland 2010). During mitosis NuMA is an essential player in mitotic spindle assembly and maintenance; it organizes spindle microtubules and tethers them to

spindle poles using its cross-linking properties. Its role in the interphase nuclei is not well understood, but its properties and abundance suggest it plays structural functions (Radulescu and Cleveland 2010; Simon and Wilson 2011). Although, no NuMA-like protein sequence was identified in plants, the antibodies against animal NuMA recognize in immunoblots three bands of 210-230 kDa and also react with epitopes on the nuclear core filaments of onion NSK and the spindle matrix *in situ* (Yu and Moreno Diaz de la Espina 1999).

Two proteins, spectrin and titin which crosslink and provide elasticity to the cytoskeleton were also found in the nucleus and are thought to play analogous functions in the nucleoskeleton. In the cytoskeleton spectrins crosslink F-actin and protein 4.1 to the cell membrane proteins, forming elastic networks required for cell shape maintenance. The functional unit is a tetramer which consists of two α-β heterodimers (Baines 2009). Mammals contain seven spectrin genes and their products undergo alternative transcripts to produce multiple forms ranging between 30-430 kDa. Three forms are found in the nucleus; βII spectrin, βIVΣ5 spectrin and αII spectrin (Simon and Wilson 2011; Young and Kothary 2005). The latter is implicated in chromosome maintenance and DNA repair (McMahon et al. 2009) and co-immunoprecipitates with lamin A, emerin, actin, protein 4.1 and βIVΣ5 spectrin (Sridharan et al. 2006). In plants, antibodies raised against α- and β-spectrin chains cross-react with nuclear proteins which are components of the NSK fraction (Perez-Munive and Moreno Diaz de la Espina 2011).

Titin is a large actin-binding protein (3MDa) which in muscle sarcomeres functions as a mechanical spring. It also undergoes alternative splicing and at least one of the multiple isoforms associates to chromatin and is required for mitotic condensation (Simon and Wilson 2011). The C terminus of titin binds directly to A-type and B-type lamins in human (Zastrow et al. 2006).

The actin superfamily which consists of actins and ARPs (Actin Related Proteins) is characterized by the actin fold, a tertiary structure centered on the nucleotide-binding pocket binding ATP and/or ADP which results in major conformational changes in the proteins (Kandasamy et al. 2004). In the cytoplasm actin is present as monomeric and polymeric F-actin forms. In the nucleus around 20% of actin is polymeric though conventional phalloidin-stainable F-actin is not detected, which caused a controversy concerning the functionality of actin in the nucleus for many years. Currently, it is proposed that polymeric nuclear actins include short F-actin forms that fall below the treshold of detection by phalloidin, and also alternative polymeric forms which are recognized by monoclonal antibodies recognizing unconventional actin polymer forms: 2G2 produced against the actin-profilin complex and 1C7 against a chemically cross-linked actin dimer (Simon and Wilson 2011; Schoenenberger et al. 2011). Nuclear actin is a component of several chromatin remodeling complexes and has roles in mRNA processing, nuclear export and nuclear envelope assembly (Visa and Percipalle 2010; Spencer et al. 2011; Simon and Wilson 2011). It is involved in different phases of gene transcription and binds to RNA polymerase I, II and III (Percipalle 2013). ARP4-ARP9 share 17-45% sequence homology with actin and are found in the nucleus in yeast, human, mouse, flies and plants. Most of the nuclear ARPs are essential components of chromatin-modifying complexes (Kandasamy et al. 2004).

Actins are found in all eukaryotic kingdoms and even in bacteria proteins with some sequence similarity and similar structure were found. MreB, bacterial actin-like protein can also polymerize into actin-like filaments (Egelman 2003). It is required for DNA segregation and co-immunoprecipitates with RNA polymerase which suggests nuclear functions of actins are ancient and highly conserved (Kruse and Gerdes 2005).

Studies using the 1C7 and 2G2 antibodies demonstrated the presence of nuclear actins in plant cells as the antibodies cross-reacted with proteins in various nuclear and NSK fractions and displayed nuclear staining in the nucleolus, transcription foci and the endonucleoskeleton in immunofluorescence experiments (Cruz and Moreno Diaz de la Espina 2009). Later three nuclear actins were identified in *A. thaliana*; ACT2, ACT8 and ACT7 (Kandasamy et al. 2010). The latter is concentrated in the nucleoplasm in form of speckles and is also abundant in the nucleolus and ACT2 and ACT8 are localized diffusively throughout the nucleoplasm (Kandasamy et al. 2010). Also two actin related proteins; ARP4 and ARP7 were detected in the interphase nuclei in *A. thaliana* (Kandasamy et al. 2003).

Another important group of proteins found in CSK and NSK are motor proteins: myosin and kinesin. Myosins constitute a large protein superfamily whose members share a conserved motor domain that mediates binding to actin. They contain three functional domains: the motor head domain which also binds ATP, the neck domain binding light chains or calmodulin and the tail domain which anchors and positions the motor domain so it can interact with actin (Sellers 2000). MYO1C (myosin 1β) is the most extensively characterized nuclear myosin. Alternatively spliced *MYO1C* gene encodes cytoplasmic myosin 1C and the nuclear isoform myosin 1β which contains 16 additional residues in comparison to otherwise identical cytoplasmic MYO1C (Pestic-Dragovich et al. 2000; Hofmann et al. 2006). Nuclear myosin associates to the three classes of RNA polymerases and chromatin remodeling complexes, it interacts with the transcription initiation factor TIF1A and also binds directly to DNA (Simon and Wilson 2011). In proliferating human fibroblasts myosin 1β is distributed throughout the nucleoplasm as well as at INM and in the nucleolus. In quiescent cells it is detected in large aggregates within the nucleoplasm but is absent at the NE and in the nucleolus (Mehta et al. 2010). Other examples of nuclear myosins are MYO6 and two paralogues

of MYO5; MYO5A and MYO5B (Simon and Wilson 2011). MYO6 is the only known example of minus-end-directed myosin (Sweeney and Houdusse 2010) and it contains six predicted NLS in the tail domain. It is distributed diffusely in the nucleoplasm but is absent from nucleoli (Vreugde et al. 2006) and associates with RNA polymerase II at promoters and at coding regions of active genes modulating their transcription (Vreugde et al. 2006). MYO5A co-localizes with splicing component SC35 (SRSF2) at nuclear speckles (Pranchevicius et al. 2008) and MYO5B is distributed in nucleoplasm and nucleolus where it binds to RNA polymerase I and actin (Lindsay and McCaffrey 2009). In plants, the antibody against myosin Iβ recognizes a protein of similar size in immunoblots and in immunofluorescence in nuclei isolated from meristematic root cells of *A. cepa* (Cruz and Moreno Diaz de la Espina 2009). Plant myosins belong to XI and VII class and they contain the typical myosin features; highly conserved N-terminal motor head domain which binds actin and ATP, neck domain with IQ motifs and C-terminal domain responsible for binding cargo (Sellers 2000; Peremyslov et al. 2011; Sparkes 2011). Myosin XI-I was localized using GFP expression at the nuclear envelope and in punctuate structures in cytoplasm in *A. thaliana* (Avisar et al. 2009).

Two kinesins are found in the interphase nuclei; KIF4A and KID. They are called chromokinesins due to their ability to bind DNA (Mazumdar and Misteli 2005). KID is distributed throughout the nucleus and is enriched in the nucleolus and at the nuclear envelope (Levesque and Compton 2001). Other kinesins found in the nucleus are; mitotic centromere-associated kinesin (MCAK or KIF2C) and KIF17B. MCAK regulates microtubule dynamics in the mitotic spindle but is also detected in the interphase nuclei and can bind to nucleoporin Nup89 (Simon and Wilson 2011). KIF17B probably shuttles between nucleus and cytoplasm (Macho et al. 2002).

Another group of nucleoskeletal proteins are Matrix Attachment Region Binding Proteins (MARBPs) which anchor MARs (Matrix Attachment Regions) and mediate formation of DNA loop domains. MARs are DNA sequences that bind preferentially to nuclear matrices. They are about 200 bp long AT-rich sequence motifs that often reside near cis-acting regulatory sequences. MARBPs are involved in chromosome maintenance, regulation of gene expression, cell development and induction of cell apoptosis (Wang et al. 2010a). They include highly conserved proteins as histone H1 and actin, as well as animal and plant specific proteins. MARBPs expressed only in plants include MFP1 (Meier et al. 1996; Gindullis and Meier 1999; Samaniego et al. 2006; Samaniego et al. 2008), MAF1 (Gindullis et al. 1999), AT hook-containing MAR binding protein 1 (AHM1) (Morisawa et al. 2000), AT-hook motif nuclear localized protein 1 (AHL1) (Fujimoto et al. 2004), MARBP-1, MARBP-2 (Hatton and Gray 1999) and NtMARBP61 (Fujiwara et al. 2002). In animals this group includes lamins and other proteins as NMP-1, NMP-2, ARBP, HnRNP-U/SAF-A, SAF-B, SATB1, SATB2 etc (Wang et al. 2010a).

2. The Lamina

The lamina is a prominent compartment of the NSK attached to the INM. The first descriptions of this structure date as far as the fifties (Pappas 1956; Beams et al. 1957) but it was not till it was described for the first time in mammalian cells that the interest in the fibrous lamina rose (Fig 3 a, d) (Fawcett 1966). The lamina defines a structure observed in many eukaryotes under the electron microscope as a typical fibrous layer between the nuclear envelope and the condensed masses of chromatin on the nuclear periphery (Pappas 1956; Beams et al. 1957; Fawcett 1966; Masuda et al. 1993; Masuda et

al. 1997; Moreno Diaz de la Espina et al. 1991; Minguez and Moreno Diaz de la Espina 1993; Moreno Diaz de la Espina 1995; Li and Roux 1992).

2.1. Metazoan Lamina

The fibrous structure of the lamina was discovered by two groups during a research on the nuclear pore complex in amphibian oocytes (Scheer et al. 1976) and rat liver (Aaronson and Blobel 1975; Dwyer and Blobel 1976). After subfractionation of nuclei they observed under the electron microscope in the nuclear envelope fraction nuclear pores interconnected by fibrils (Scheer et al. 1976). Although this was a significant discovery the best known picture of a fibrous lamina was published ten years later by Aebi et al. (1986) who observed a filament meshwork with a crossover spacing of 52 nm in well preserved areas of the nuclear envelope isolated from *Xenopus* oocytes after metal shadowing (Fig. 3b). The three main protein components of metazoan lamina were identified in 1978 (Gerace et al. 1978) and later called lamins A, B, and C due to their localization at the peripheral lamina (Gerace and Blobel 1980).

2.2. Lamins, discovery and classification

Lamins belong to the highly conserved IF protein family. All IFs represent a typical tripartite structure with a central coiled-coil domain. Lamins are the only IFs found in the nucleus and are thought to be the founding members of the protein family. All metazoans express at least one lamin. Invertebrates contain one or two and vertebrates three or four lamin-coding genes.

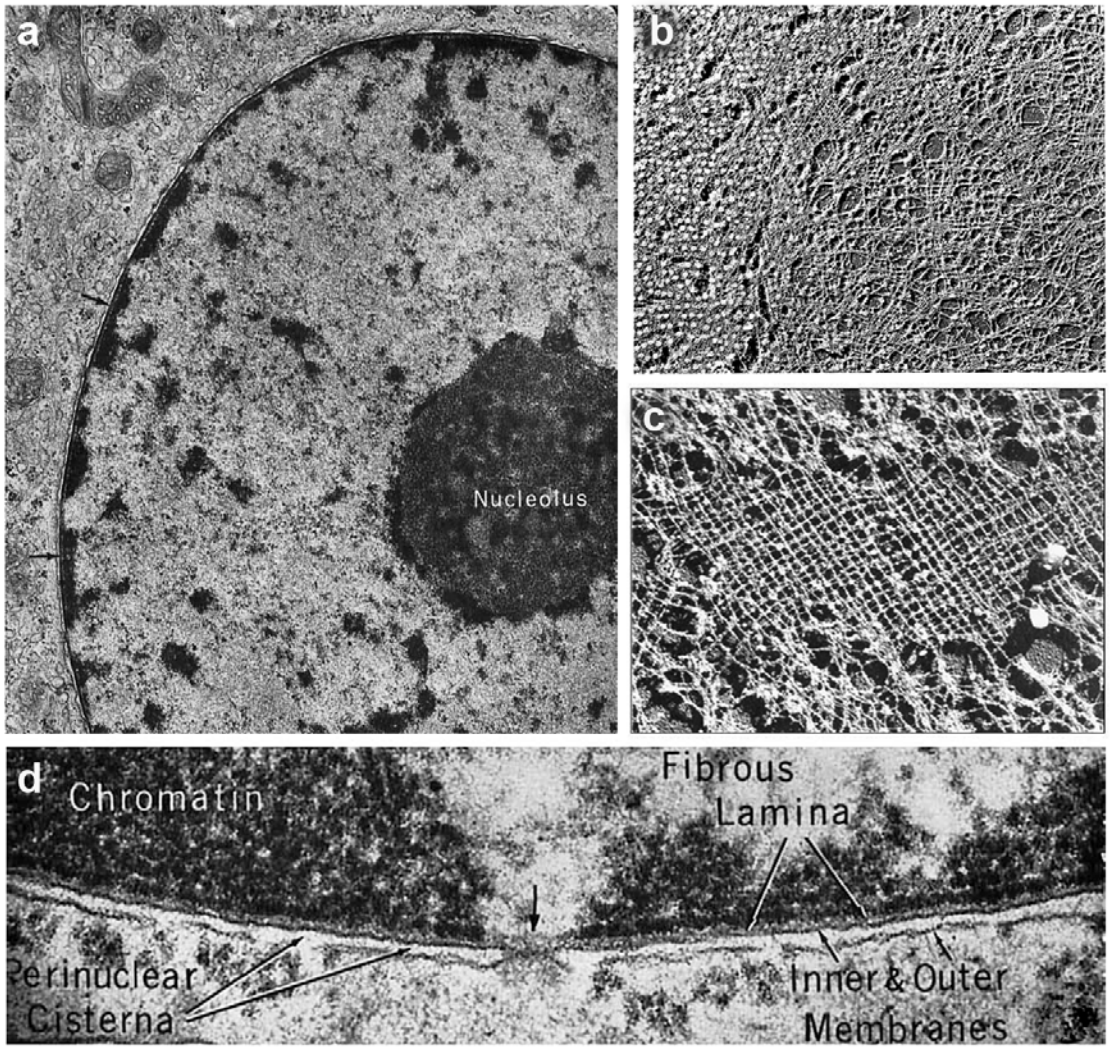

Figure 3. Nuclear lamina. **a**, **d** Micrographs of nuclei in vertebrate cells; cat interstitial cell (a) and smooth muscle (d). Fibrous lamina (indicated with arrows in a) is seen as a thin layer of lower density between the dense chromatin and the inner nuclear envelope (visible as a dark line). Peripheral accumulation of the heterochromatin (dark masses) is interrupted at the sites of nuclear pores (arrow in d). (Fawcett 1966); **b**, **c** Freeze-dried/metal-shadowed nuclear envelope of *Xenopus* oocytes extracted with Triton X-100 reveals the nuclear lamina meshwork with arrays of nuclear pore complexes (b) which displays two set of near-orthogonal filaments (c) (Aebi et al. 1986).

The first study describing the components of the rat liver lamina fraction is dated from 1978 and reports three proteins nominated P70, P67 and P60 according to their size established by separation on SDS-PAGE gel (Gerace et al. 1978). Two years later the same research group designatd them as lamins

A, B and C, respectively, due to their localization in the nuclear lamina (Gerace and Blobel 1980). Analogous studies using *Xenopus* eggs report lamins L_I, L_{II}, L_{III} (Benavente et al. 1985), L_{IV} (Benavente and Krohne 1985) and lamin A (Wolin et al. 1987). At this point the characterization of lamins was limited to biochemical and microscopic studies but this changed in 1986 when the first lamin cDNA sequence was published (McKeon et al. 1986). This discovery enabled classification of lamins as IF proteins based on the sequence similarity (McKeon et al. 1986; Franke 1987), along with the confirmation that lamins form a filament meshwork (Aebi et al. 1986). Sequence of lamin B1 was published in 1988 (Hoger et al. 1988) and shortly afterwards lamin B2 was identified (Vorburger et al. 1989; Hoger et al. 1990). Although it was assumed that lamins A and C are products of one gene (McKeon et al. 1986; Fisher et al. 1986) it was confirmed definitively when the structure of human *LMNA* gene was published (Lin and Worman 1993). Availability of the lamin sequences enabled identification of *Xenopus* lamin L_I as lamin B1 orthologue and lamin L_{II} as an orthologue of lamin B2. Lamin L_{III} is a germ cell-specific lamin sometimes confusingly called lamin B3 which corresponds to a mammalian germ cell-specific product of *LMNB2* gene (von Moeller et al. 2010). Lamin L_{IV} is also germ cell-specific and its classification was resolved in a recent study demonstrating that it is a splice variant of L_{III} gene (von Moeller et al. 2010).

In conclusion, vertebrates contain four lamin genes which is in agreement with the hypothesis that two rounds of genome duplications have occurred in the ancestral vertebrate (Lundin et al. 2003). Mammals have lost L_{III} gene (Zimek and Weber 2005) and evolved germ cell-specific splice products of *LMNA* and *LMNB2* genes. In addition, transcripts of lamin genes are alternatively spliced to create multiple isoforms. The information on lamin splices in *Xenopus* and mammals is summed up in table 1. Lamins also undergo various post-translational modifications such as farnesylation, phosphorylation

gene	Proteins		Characteristics	Expression
	Mammals	***Xenopus***		
LMNB1	lamin B1	Lamin B1 (L_I)	Vertebrate ortholog of invertebrate lamins (Zimek and Weber 2008)	somatic cells
LMNB2	lamin B2	Lamin B2 (L_{II})	Typical lamin structure	somatic cells
	lamin B3	-	Unique N-terminus (Schutz et al. 2005)	postmeiotic stages of spermatogenesis
LMNA	lamin A	lamin A (L_A)	Tail domain 50-100 aa longer than B-type (Stick 1992)	differentiated cells
	Progerin (lamin AΔ50)	-	Lacks 50 aa region in the tail domain, permanently farnesylated (De Sandre-Giovannoli et al. 2003; Eriksson et al. 2003)	Expressed in HGPS patients together with lamin A and at low level in normal aged cells (McClintock et al. 2007)
	lamin C	-	Unique C-terminus (lacks Caax box) (Lin and Worman 1993)	differentiated cells
	lamin AΔ10	-	Lacks 30 aa in the tail domain (Machiels et al. 1996)	Differentiated cells (minor fraction)
	lamin C2	-	Unique N-terminus with myristoylation site (Alsheimer et al. 2000)	meiotic stages of spermatogenesis
L_{III}	-	lamin L_{IIIa} (*X*LB3a)	Becomes soluble in meiotic metaphase (Hofemeister et al. 2000)	oocytes (major fraction), few specialized cell types of adult tissue (Benavente et al. 1985)
	-	lamin L_{IIIb} (*X*LB3b)	Palmitoylation site, stable membrane association (Hofemeister et al. 2000)	oocytes (minor fraction)
	-	lamin L_{IV}	40 additional residues in coil 2A of the rod domain (von Moeller et al. 2010)	Male germ cells

Table 1. List of lamins expressed in *Xenopus* and mammmals.

and sumoylation that play a role in the retention of lamins in the INM or in the control of the polymerization state (Simon and Wilson 2013; Dittmer and Misteli 2011).

Lamins constitute the class V of IFs and are thought to be the founding members of this vast protein family (Franke 1987; Weber et al. 1989b; Weber et al. 1988; Peter and Stick 2012). IFs are highly conserved and display a typical tripartite structure with a central coiled-coil domain. The rod domain of lamins consists of two clusters of coiled coils: the first including coils 1A and 1B, and the second 2A and 2B separated by non-coiled-coil linkers (Fig. 4) (Parry et al. 1986; Kapinos et al. 2010). The central domain of lamins is flanked by a short head domain containing a cdk1 phosphorylation site and a long tail domain containing a cdk1 phosphorylation site, an NLS, an Ig fold, and a CaaX box at the C-terminus (Fig. 4) (Dechat et al. 2010a).

First classification of lamins into general classes was proposed by Wolin et al. (1987) to establish the homology between mammalian lamins A, B, C and amphibian lamins L_I, L_{II}, L_{III} and L_A. At this point only the sequence of lamin A/C was known and the classification was based on the cross-reactivity with the anti-lamin A and anti-lamin B antibodies. This division of lamin family was accepted by other researchers and developed into type-A and type-B lamins based on structural and biochemical features, as well as expression patterns (Stick 1988). Nevertheless, even at this point Reimer Stick was conscious about the limitations of such classification since lamin L_{III} was not easily classified into any subgroup. Although today the complete sequences of lamins in many species are known, and it is clear that the proposed classification not always reflects homology between the proteins (Peter and Stick 2012), the classification into A and B types is still commonly used. Invertebrates have generally one gene encoding a B-type lamin. Additional lamin genes were found in the mosquitos and the fruit fly but strong genomic

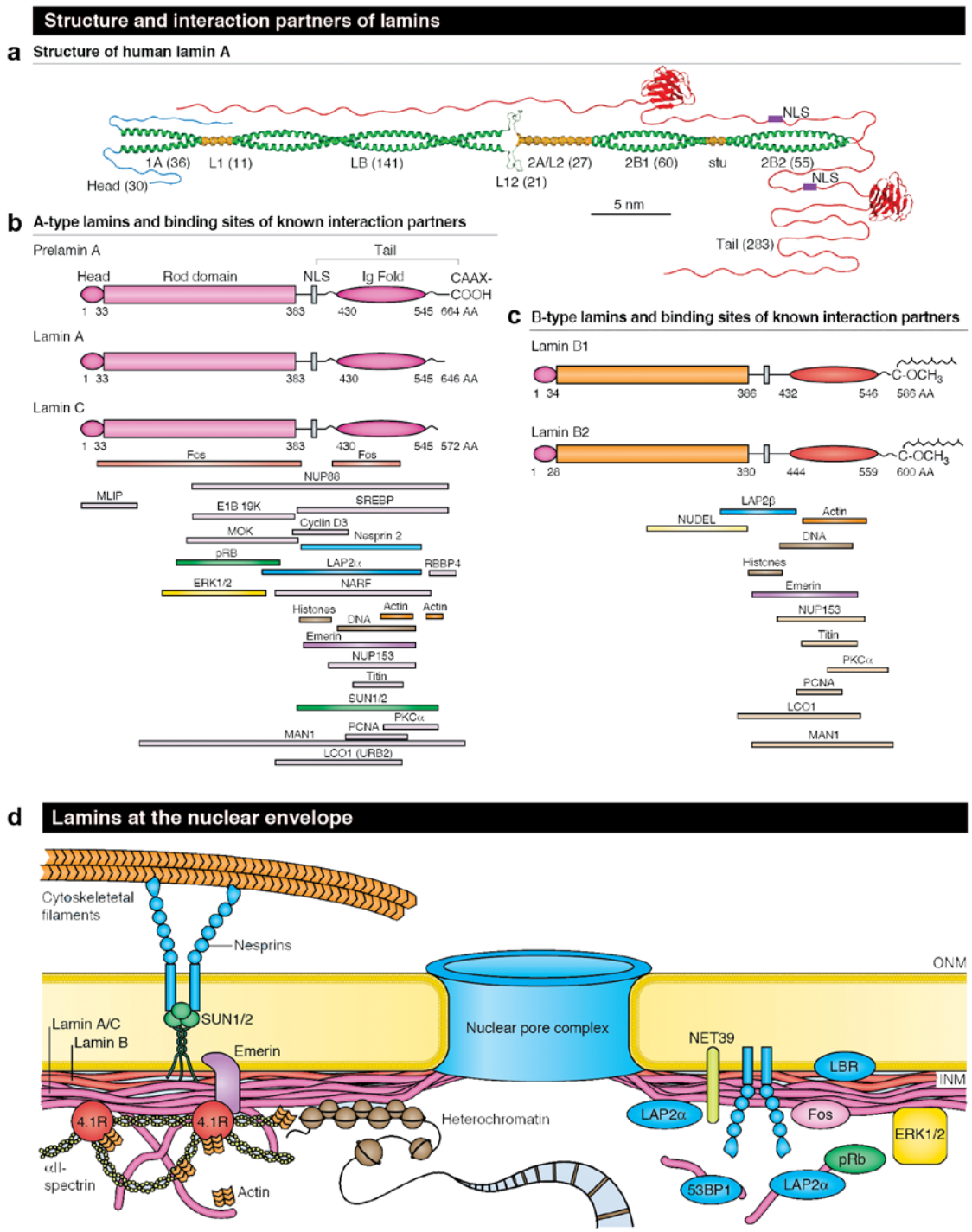

Figure 4. The structure and partners of lamins and interactions of lamins at the nuclear envelope. a. Detailed structure of lamin A dimer. Coiled coils of two lamins mediate formation of dimers. Coil 1a contains 36 residues, coil 1B; 141; coil 2A 27 (including the linker L2) and coil 2B; 115 residues interrupted by stutter (stu). Linkers L1 and L2 also display α-helical structure. The tail domain contains a nuclear localization signal (purple box) and a globular Ig-fold (red yarn) **b**, **c** Scheme displaying the proteins interacting with A-type (b) and B-type lamins (c) **d**. At the nuclear envelope lamins bind the integral INMproteins, components of the LINC complex, heterochromatin, regulatory factors and components of the NSK. (Ho and Lammerding 2012).

drift observed in insects suggest they are an exception (Peter and Stick 2012). Selected invertebrate lamins are listed in table 2. The fruit fly has one gene encoding a B-type lamin Dm_0 and another coding for LamC (Melcer et al. 2007), name given based on the analogy to mammalian lamin C since the two proteins lack the CaaX box (Bossie and Sanders 1993). It is classified as A-type lamin since it is expressed only in differentiated cells similar to A-type lamins in vertebrates (Riemer et al. 1995). Nevertheless, from an evolutionary point of view this classification is not justified since the vertebrate lamin A/C gene evolved in vertebrate lineage and both LamC and Dm_0 evolved from archetypal lamin gene (Peter and Stick 2012).

All invertebrate lamins show the same overall gene organization and resemble the vertebrate B-type lamins which seem to confirm these appeared first in the evolution (Peter and Stick 2012). Lamin B1 is thought to be the vertebrate ortholog of the invertebrate lamin since the same gene flanks the single lamin gene in Nematostella (sea anemone- a member of the cnidaria, a very old metazoan phylum) and *LMNB1* in *Xenopus* and man (Zimek and Weber 2008). Also, positions of introns are conserved between Nematostella lamin gene and the human lamin B genes, which have only one (lamin B1) or two (lamin B2) additional introns (Zimek and Weber 2008).

2.2.1. The expression of lamins is developmentally regulated

All vertebrate lamins are differentially expressed to a different extent but in all vertebrate as well as invertebrate cells at least one B-type lamin is expressed (Peter and Stick 2012). Lamin B2 is nearly ubiquitously expressed in all somatic cells whereas lamin B1 expression is more restricted

species	lamin	gene	characterisctics
Cnidaria (*Hydra* sp. and *Taelia* sp.)	AJ005934 (Hydra) AJ005937 (Taelia)	no name	Archetypal lamin features: coils, phosphorylation sites, NLS, Ig fold, CaaX box (Erber et al. 1999)
Ciona intenstinalis (tunicate)	AJ251957	no name	Lacks the Ig fold (Riemer et al. 2000; Peter and Stick 2012)
Caenorhabditis elegans	*Ce*-lamin	*lmn-1*	Lacks two heptads in 2b coil and the cdk1 phosphorylation site preceeding coil 1a, short tail domain (Riemer et al. 1993)
Drosophila melanogaster	Dm_0	*Dm_0*	Typical B-type lamin features (Gruenbaum et al. 1988)
	LamC	*LamC*	Lacks Caax box, expressed in differentiated tissues (Riemer et al. 1995)
Mosquitos (*Aedes aegypti* and *Anopheles gambiae*)	L1	no name	Lack first seven heptads of coil 2b (Peter and Stick 2012)
	L2	no name	

Table 2. Characteristics of selected invertebrate lamins (specific features of some invertebrate lamins)

(Broers et al. 1997; Benavente et al. 1985; Stick and Hausen 1985; Lehner et al. 1987; Stewart and Burke 1987). Lamin A and A-type lamins in a few invertebrates are expressed in late development and usually their appearance correlate with differentiation (Broers et al. 1997; Lehner et al. 1987; Rober et al. 1989; Bossie and Sanders 1993). There are also known germ cell-specific lamins as L_{III} expressed in fish, amphibians and birds in oocytes and at early embryotic stages (Benavente et al. 1985; Stick and Hausen 1985; Hofemeister

et al. 2002; Peter and Stick 2012); L_{IV} (an alternative splice product of L_{III} in amphibians) expressed in male germ cells; lamin C2 (an alternative splice product of *LMNA* in mammals) expressed in meiotic stages of spermatogenesis and lamin B3 (an alternative splice product of *LMNB2* in mammals) expressed in postmeiotic male germ cells (von Moeller et al. 2010). Until recently it was believed that the presence of at least one lamin is indispensable and required for maintaining nuclear integrity, cell proliferation and development (Harborth et al. 2001; Vergnes et al. 2004) but recent studies on conditional knockout mice showed that depletion of B-type lamins does not result in obvious phenotype in mouse embryonic stem cells (Kim et al. 2011) or in some differentiated tissues as hepatocytes and keratinocytes (Yang et al. 2011). Although stem and some differentiated cells can function without B-type lamins, they are needed for proper organogenesis and organism survival (Kim et al. 2011).

2.2.2. Lamins form filaments

In vitro the coil-coiled rod domains of two lamin polypeptides assemble in dimers visible under the electron microscope as 52 nm rods flanked at one end by two tightly packed globules which correspond to their tail domains (Fig. 5a) (Karabinos et al. 2003). Lamin polymer exhibiting a 48 nm axial repeat is formed by head-to-tail parallel association between two or more dimers with a short overlap (Fig 5 b, c) (Geisler et al. 1998). This step involves conserved regions at the beginning of coil 1A and at the end of 2B (Strelkov et al. 2004; Kapinos et al. 2010). The polymers associate laterally and eventually form lamin filaments *in vivo* or paracrystalline fibres *in vitro* and also *in vivo* when overexpressed (Karabinos et al. 2003; Stuurman et al. 1998). Up to date *Ce*-lamin is the only lamin assembled into 10 nm filaments *in vitro*

(Karabinos et al. 2003; Ben-Harush et al. 2009). Although A- and B-type lamins can bind directly *in vitro* (Ye and Worman 1995; Schirmer and Gerace 2004), in living cells lamins A, C and B1 form homodimers and homopolymers (Shimi et al. 2008; Delbarre et al. 2006; Kolb et al. 2011).

The ultrastructure of the filamentous lamina is best characterized in amphibian oocytes and consists of lamin L_{III} filaments arranged in a regular meshwork pattern formed by two sets of parallel filaments arranged at right angles to each other (Aebi et al. 1986). This model was later re-examined and the results suggest that L_{III} lamina consists of a single set of parallel filaments with distinct regular cross-connection (Goldberg et al. 2008b). The lattices formed by B2 and A-type lamins expressed in *Xenopus* eggs differ significantly from this model (Goldberg et al. 2008b). Lamin B2 filaments are thinner than L_{III} filaments and are arranged in a similar but less regular lattice. On the other hand, lamin A filaments are thicker and form a compact irregular layer which covers the entire nuclear lamina but leaves the regions of the NPCs free (Goldberg et al. 2008b). The filaments form three-dimensional bundles of filaments and the cross-connections between the filaments are not observed (Goldberg et al. 2008a). A-type and B-type lamins probably also form homopolymers in the nucleoplasm (Kolb et al. 2011). Nucleoplasmic A-type lamins display much higher mobility in comparison to the lamina-associated pool and B-type lamins in the nuclear interior compared to those associated to the lamina (Broers et al. 1999; Moir et al. 2000b; Shimi et al. 2008).

2.2.3. Functions of lamins

It is difficult to define the functions of lamins. At the beginning it was believed that they were strictly structural proteins based on their biochemical

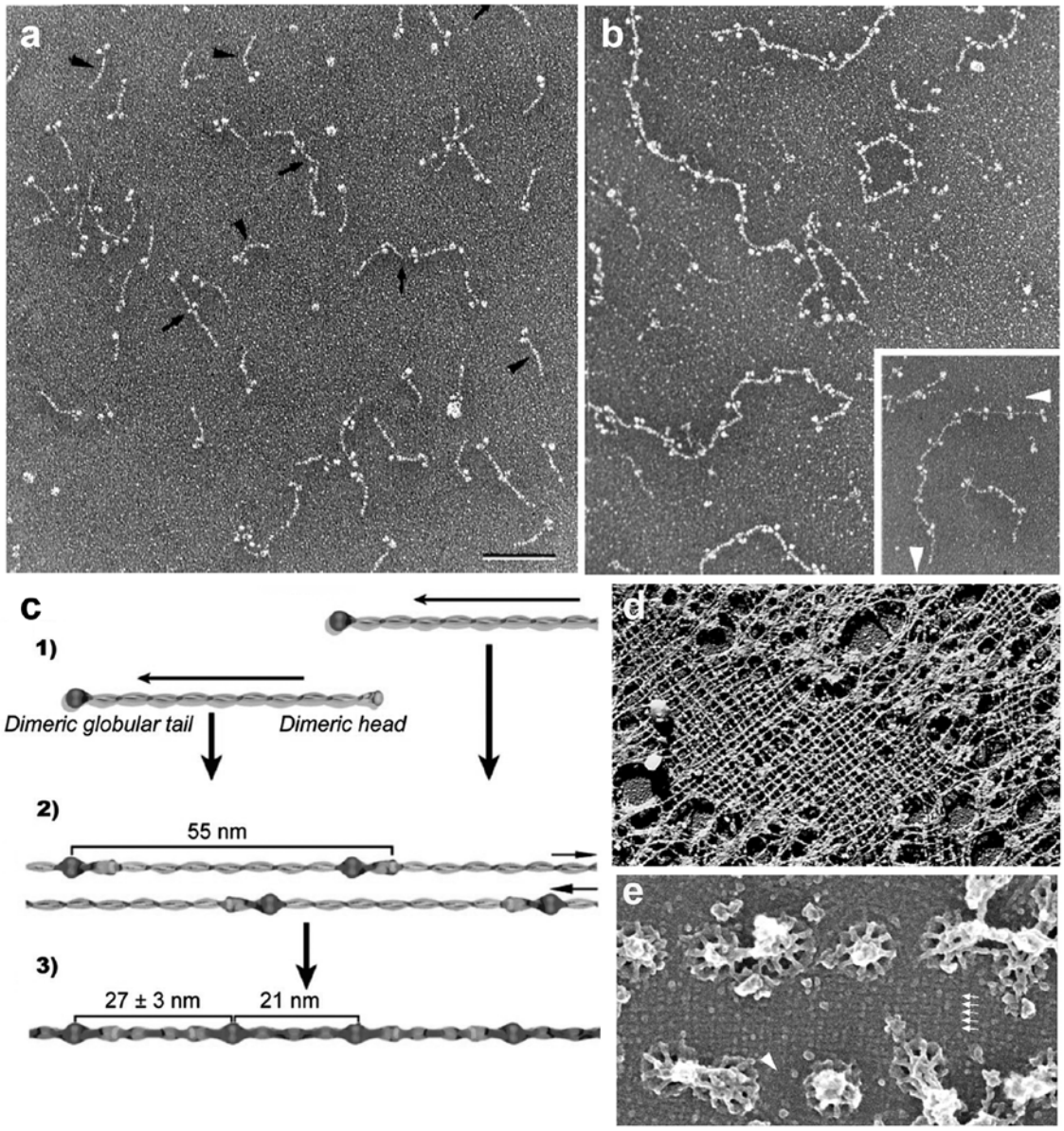

Figure 5. Assembly of lamins in vitro into dimers (a) and linear head-to-tail polymers (b,c) and in vivo in the lamina (d, e). **a**, **b**, Transmission electron microscopy of glycerol sprayed samples (Stuurman et al. 1998) **c**. Steps of lamin polymerization; 1). Lamins form dimers that assemble into a polar head-to-tail polymer of dimers. 2). Two antiparallel head-to tail polymers form a protofilament. 3). lateral assembly of the polymers into tetrameric protofilaments which assemble into filaments (Bank and Gruenbaum 2011a); **d**, **e** Filaments of lamins observed on the cytoplasmic (d) (Aebi et al. 1986) and nucleoplasmic (e) (Goldberg et al. 2008b) face of the nuclear envelope.

properties such as insolubility, filament-forming properties and lack of obvious enzymatic activity (Burke and Stewart 2013). Indeed, many studies confirm that lamins are important contributors in nuclear mechanics (Zwerger et al. 2011). Nevertheless, the diverse phenotypes found in numerous laminopathies caused by different mutations in *LMNA* gene (the mutations in B-type coding genes are usually viable) could not be explained by nuclear damage alone. This observation mobilized numerous studies on lamins and other proteins of the nuclear envelope and proved the straightforward approach was not enough to predict the effects of lamin mutations. Mutations at many positions resulted in severe changes in some tissues, whereas other mutations affected other tissues (Dittmer and Misteli 2011; Szeverenyi et al. 2008).

Lamins are involved in many nuclear functions such as maintaining nuclear shape and architecture; connecting nucleoskeleton to cytoskeleton through interaction with SUN domain proteins; chromatin organization and positioning; DNA replication, repair and transcription; cell cycle progression; mitosis and differentiation, etc which are revieved in table 3 (Dechat et al. 2010a; Mejat and Misteli 2010).

Today the common understanding is that the multiple and diverse effects of lamin mutations are caused by impaired nuclear stability, disruptions in the interactions between lamins and regulatory factors and in chromatin organization, which could modulate tissue-specific gene expression (Ho and Lammerding 2012).

Function	Lamin	Reference
NUCLEAR STRUCTURE AND MECHANICS		
Regulation of nuclear shape and mechanical properties	Lamin A/C	(Lammerding et al. 2004; Lammerding et al. 2006)
Physical connection of the nucleus to the cytoskeleton	Lamin A/C	(Houben et al. 2007)
Regulation of nuclear size	B-type lamins	(Levy and Heald 2010) (Meyerzon et al. 2009)
Incorporation and spacing of nuclear pores	B-type lamins	(Liu et al. 2000) (Lenz-Bohme et al. 1997)
CHROMATIN ORGANIZATION AND GENE SILENCING	B-type lamins, Lamin A/C	(Guelen et al. 2008) (Dorner et al. 2007)
DNA REPLICATION AND DNA REPAIR	B-type lamins Lamin A	(Moir et al. 1994; Moir et al. 2000a) (Spann et al. 1997) (Kennedy et al. 2000) (Mahen et al. 2013)
DEVELOPMENT AND ORGANOGENESIS	B-type lamins Lamins A/C	(Kim et al. 2011) (Vergnes et al. 2004) (Zuela et al. 2012) (Burke and Stewart 2013)
SPINDLE MATRIX	Lamin B1	(Tsai et al. 2006)
SENESCENCE	Lamin B1 Lamin A/C	(Shimi et al. 2011) (Pekovic et al. 2011)

Table 3. The functions of lamins.

2.3. Lamin-binding proteins (LBPs)

Up to date, 54 binding partners are known for lamin A, 23 for lamin B1 and seven for lamin B2 in human (Simon and Wilson 2013). The much higher number of lamin A-binding proteins characterized could be caused by the fact that in contrast to B-type lamins a fraction of the interphase nuclear pool of lamin A can be extracted in mild conditions, for example with a buffer containing 1% of Triton X-100, a non-ionic detergent (Muralikrishna et al. 2004; Moir et al. 2000b). This biochemical feature enables application of a number of approaches such as co-immunoprecipitation (co-IP) in which whole protein complexes are extracted in mild conditions that do not disrupt the bonds between the units. Selected LBPs are listed in table 4.

Among LBPs a group of proteins involved in nuclear architecture and chromatin organization that contain a conserved LEM (LAP2, Emerin, MAN) domain can be distinguished. The LEM domain is a 45-residue motif that folds as two α-helices and binds to Barrier to Autointegration Factor (BAF), a chromatin binding protein (Laguri et al. 2001; Wilson and Foisner 2010). BAF also binds to lamin A. Most LEM proteins are integral INM proteins and contain one or two transmembrane domains. The interaction between lamins, LEM proteins, BAF and probably other INM proteins is involved in anchoring chromatin to the NE and the lamina (Wilson and Foisner 2010).

Lamin B Receptor (LBR) is an INM-localized sterol reductase that binds to lamins B and is required for nuclear shape maintenance and reorganization of chromatin in differentiating cells (Hoffmann et al. 2002).

Sad1, UNC84 (SUN)-domain proteins are an example of the few lamin binding proteins which are highly conserved across the kingdoms. The SUN proteins spanning the INM bind KASH (Klarsicht, ANC-1 and SYNE/Nesprin-1 and -2 Homology) proteins residing in the ONM. This

PROTEIN	LAMIN	Functional character of the bidning	references
LEM-domain proteins: -emerin -LAP2 -MAN1 -LEM2/NET25	B-type lamins Lamin A/C	Nuclear architecture and chromatin organization	(Sakaki et al. 2001; Lee et al. 2001; Vaughan et al. 2001; Dechat et al. 2000; Furukawa and Kondo 1998; Mansharamani and Wilson 2005; Brachner et al. 2005)
BAF	Lamin A/C		(Holaska et al. 2003)
LBR	Lamin B1		(Ye and Worman 1994)
histones	B-type lamins, Lamin A/C		(Taniura et al. 1995)
SUN- and KASH-domain proteins: -SUN1 and SUN2 (components of LINC complex) -nesprin 1α -nesprin 1β	Lamin A/C	Mechanotransduction, positioning of the nucleus and chromosomes	(Haque et al. 2006; Crisp et al. 2006; Mislow et al. 2002; Libotte et al. 2005)
REGULATORY FACTOTORS -transcription factors (Rb, cFos, Oct-1, SREBP1, MOK1)	Lamin A/C Lamin B1 (Oct-1)	Transcription	(Simon and Wilson 2013)
-PCNA	Lamin A/C	DNA replication	
-kinases (PKC, cdk1)	All lamins		
Nucleoporins -Nup153	all lamins	Positioning of NPCs	(Al-Haboubi et al. 2011)
-Nup88	Lamin A/C		(Lussi et al. 2011)
IINTERNAL NSK PROTEINS -F-actin	Lamin A/C Lamin B1	Structural and motor functions	(Simon et al. 2010)
-αII spectrin -βIV spectrin -p4.1	Lamin A/C		(Sridharan et al. 2006)
-titin	Lamin B1		(Zastrow et al. 2006)

Table 4. The list of selected proteins binding to lamins.

complex constitutes the core of the LINC complex connecting the NSK to the CSK. The C-terminal SUN domain resides in the lumen of the NE and interacts to the luminal KASH peptide containing terminal PPPX motif, where X is the very terminal residue (Sosa et al. 2013). SUN proteins form a trimer in a way that the three SUN domains form a globular head from which expand the N-terminal extensions forming a right-handed, trimeric coiled-coil (Sosa et al. 2012; Zhou et al. 2012). SUN and KASH proteins associate with 3:3 stoichiometry and the structure of this complex was recently reported (Sosa et al. 2012; Wang et al. 2012). SUN proteins with localization at the nuclear envelope were recently identified in rice, *Arabidopsis thaliana* and maize (Moriguchi et al. 2005; Graumann et al. 2010; Murphy et al. 2010). They contain the highly conserved C-terminal SUN-domain, preceded by a transmembrane domain and a coiled-coil region possibly involved in protein oligomerization, as in case of animal SUN1 and SUN2 proteins (Graumann et al. 2010). While single cell organisms seem to carry only one SUN domain protein, multicellular organisms express multiple orthologs, for example in human are found five (Sun1-5), from which Sun1 and Sun2 are widely expressed (Crisp et al. 2006; Padmakumar et al. 2005) and Sun3, Sun4 and Sun5 display testis-specific expression pattern (Gob et al. 2010). Maize contain up to five SUN proteins, ZmSUN1 and ZmSUN2 containing a typical C-terminal SUN domain and three (SUN3, SUN4, SUN5) containing an internal SUN domain (Murphy et al. 2010). Proteins with an internal SUN domain were also described in other organisms including Protozoa (Shimada et al. 2010; Field et al. 2012), fungi (Field et al. 2012) and mammals (Sohaskey et al. 2010; Field et al. 2012) but their localization does not seem to be exclusive for the NE as they were also detected in the ER (Murphy et al. 2010; Sohaskey et al. 2010).

Lamins bind to the components of the internal NSK like actin, spectrins and titin. Funtions that require polymerizable actin and lamins are mRNA export,

intranuclear chromatin movement and transcription (Chuang et al. 2006; Dundr et al. 2007; Louvet and Percipalle 2009). The interaction with spectrins is thought to have a role in maintaining chromosome stability and DNA damage repair (Sridharan et al. 2006; McMahon et al. 2009). The interaction of lamins with titin plays a role in nuclear shape maintenance and is required for proper localization of B-type lamins (Zastrow et al. 2006).

Lamins bind directly to a number of transcription and regulatory factors (Wilson and Foisner 2010; Simon and Wilson 2013). Transient or stable binding of these factors to lamins in vivo suggests that they and the pathways they represent require or are regulated by lamins. The factors that bind to lamins include transcription factors cFos, Oct-1, SREBP1, MOK2m, kinases; protein kinase C α (PKCα), cdk1, JIL-1 and, proliferating cell nuclear antigen (PCNA) involved in DNA replication (Wilson and Foisner 2010; Simon and Wilson 2013; Shumaker et al. 2008).

Only two nucleoporins have been reported to bind lamins. Nup153 binds to lamins directly and helps anchor NPCs to the lamina. It also binds mRNA and facilitates mRNA transport, and is directly involved in gene expression (Al-Haboubi et al. 2011). Nup88 binds the tail domain of lamin A but not of B-type lamins (Lussi et al. 2011).

3. Lamina in Protozoa

The lamina was for the first time observed in an amoeba in the fifties (Pappas 1956; Frajola et al. 1956). Later, it was described also in other protozoa (Chen et al. 1994; Beams et al. 1957; Lang and Loidl 1993; Minguez et al. 1994; Rudzinska 1956). The proteins building up the structure cross-reacted with anti-lamin antibodies in some species and displayed similar molecular weight

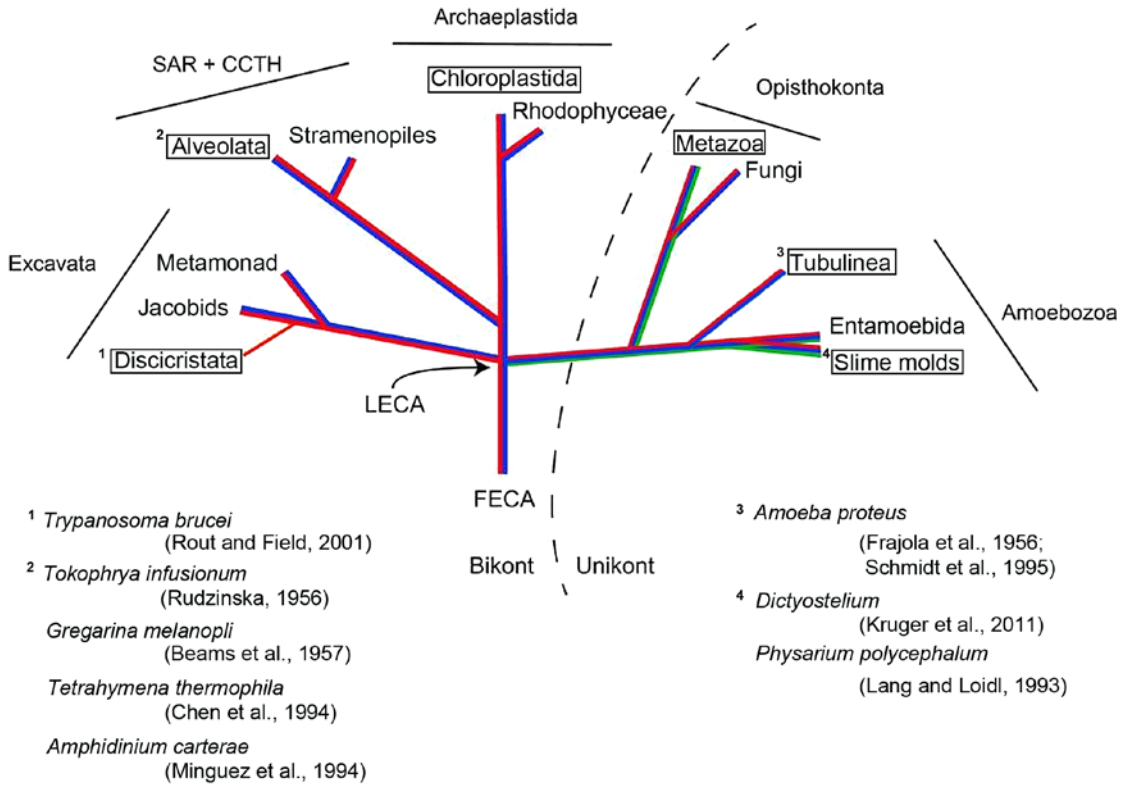

Figure 6. A lamina is present in diverse Protoza, metazoans and plants. The evolutionary distributions of the nuclear pore complex/importins (red), LINC complex (blue) and lamins (green). The presence of lamina was described in Protozoa species that belong to Discicristata (1), Alveolata (2), Tubulinea (3) and slime molds (4). The lamina in Dictyostelium is thought to be formed by a protein prototype of lamins (Kruger et al. 2012; Batsios et al. 2012).

(Lang and Loidl 1993; Chen et al. 1994). Protozoa is a diverse group which includes unicellular eukaryotic organisms which might be phylogenetically unrelated therefore the proteins making up the lamina in various protozoa species might have evolved separately. The species in which a lamina was described and their phylogenetic relationships are displayed in the Fig 6. The lamina described in *Amoeba proteus* and *Gregorina melonopli* displays different properties than the metazoan lamina (Frajola et al. 1956; Beams et al. 1957; Schmidt et al. 1995). It resembles a honeycomb structure and is not tightly anchored to the nucleoplasmic side of NPC or to the INM (Schmidt et al. 1995).

Recently, two lamin-like proteins building up the nuclear lamina in Dictyostelium and Trypanosoma have been described and confirmed to play some functions of lamins (Kruger et al. 2012; Dubois et al. 2012).

Dictyostelids belong to a group of Amoebozoa which are relatively close to the metazoans in comparison to other Protozoa (Fig. 6). They undergo closed mitosis and under certain environmental conditions (lack of food) they are capable of forming a multicellular body (Kessin 2000). The *Dictyostelium* NE81 protein has been considered an evolutionary precursor of metazoan lamins (Kruger et al. 2012) since they share some structural features. For example, the distribution of predicted coiled coils in the rod domain resembles that of lamins, also the rod domain is preceded by a cdk1 phosphorylation consensus sequence. The tail domain also share features with lamins as it contains a basic nuclear localization sequence and a CaaX box at its C-terminal end with a methionine at the X-position which indicates it undergoes farnesylation . The CaaX box is required for proper localization at the nuclear envelope (Kruger et al. 2012). The protein is associated with the NE during the entire cell cycle. Knockout and overexpression mutants demonstrated that it has an important role in nuclear integrity, chromatin organization and mechanical stability of the cells.

Trypanosomatids are highly divergent unicellular eukaryotes that undergo closed mitosis. The African trypanosome *T. brucei* is an obligate parasite living in blood, lymphatics, and cerebrospinal fluid in mammalian host (bloodstream form; BSF) and in midgut and salivary glands in the Tsetse fly (procyclic form; PCF). The different environments encountered by the parasite in the two hosts demand rapid and complex transcriptional changes since different sets of genes are activated or silenced in different hosts (Navarro et al. 2007). The NUP-1 in *Trypanosoma brucei* is a coiled-coil protein, containing 20 near-perfect repeats of a 144-amino acid sequence and is localized at the inner face of the NE (Rout and Field 2001). Similar to lamins, it is a major component of the

nucleoskeleton and is implicated in functions such as, organization of the nuclear periphery NPCs and heterochromatin, as well as control of developmentally regulated groups of genes (Dubois et al. 2012). A single ORFs encoding NUP-1 orthologues with similar structure was found in other trypanosomatid genomes although the size, the repeated sequences and the number of the repeats varies between the species (Dubois et al. 2012).

4. The lamina in plants

A well-defined lamina was observed using electron microscope also in isolated NSKs of monocot and dicot plants (Masuda et al. 1993; Masuda et al. 1997; Moreno Diaz de la Espina et al. 1991; Minguez and Moreno Diaz de la Espina 1993; Moreno Diaz de la Espina 1995; Li and Roux 1992). Recent results using fe-SEM electron microscopy revealed that the structure of the plant lamina resembles the one in *Xenopus* oocytes (Fig 7) (Fiserova et al. 2009). Since well-defined, tightly packed filaments were observed at the INM of tobacco cells it is believed that the lamina is formed by proteins that assemble into filaments (Fiserova et al. 2009). The filaments in the plant lamina were 10-13 or 5-8 nm thick. Before, similar filaments of 6-12 nm in diameter had been observed in an isolated lamina fraction of pea nuclei highly resistant to urea treatment (Fig 7 e) (Li and Roux 1992; Blumenthal et al. 2004).

Lamins play basic functions in the metazoan cell such as regulation of nuclear morphology, chromatin organization, development etc. which are also fulfilled in the plant cell which suggests plants express functional homologues of lamins with similar characteristics. Plant analogues of lamins seem to lack clear sequence similarity with the latter as the genome searches demonstrated no lamin orthologues in any plant species (Mans et al. 2004; Rose et al. 2004). Nevertheless, it is possible that lamin analogues bind to the plant homologs of

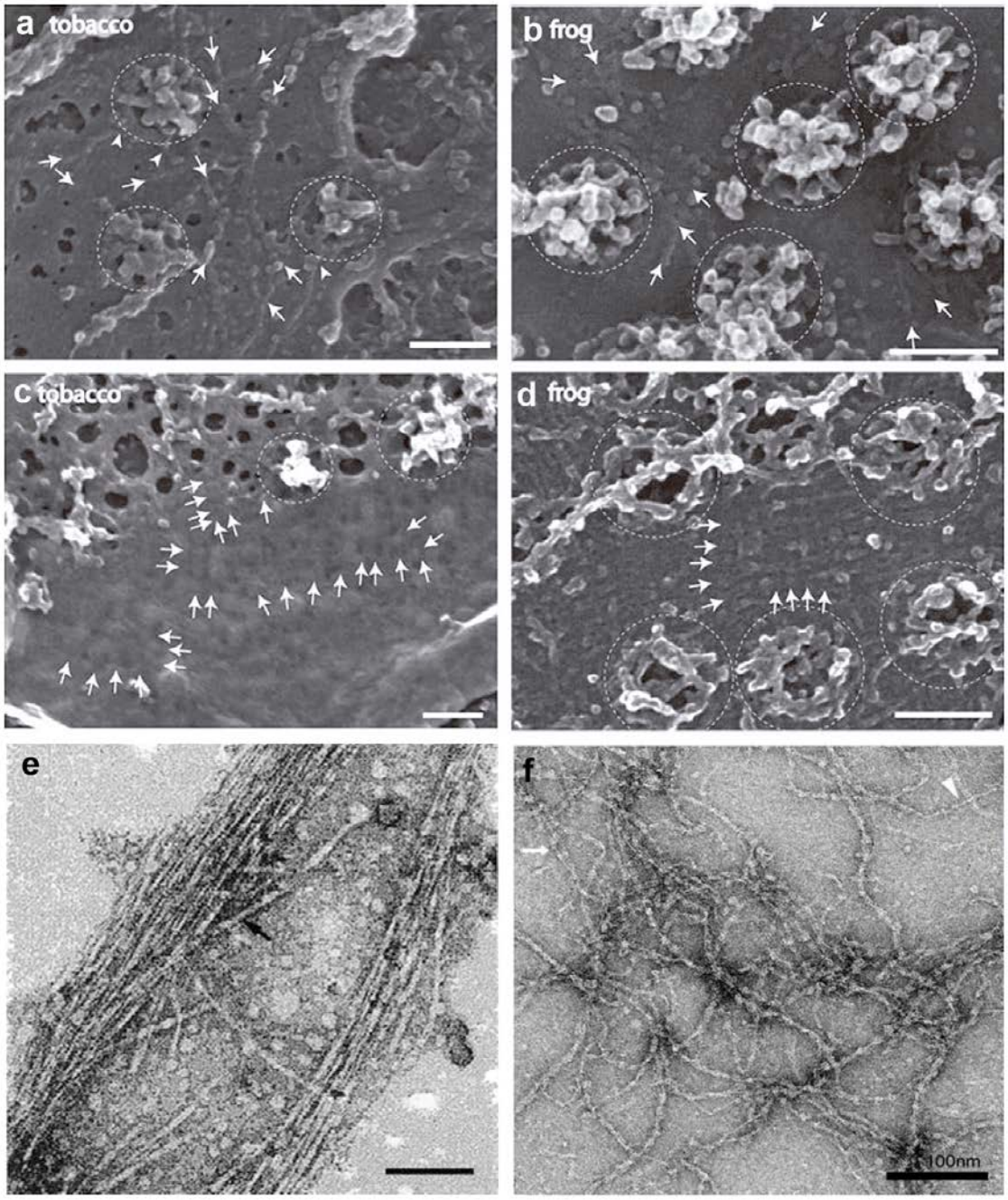

Figure 7. Comparison of lamina in plants and metazoans and filaments observed in isolated lamina fractions with *Ce*-lamin filaments assembled in vitro. a, c, Nucleoplasmic views of the filamentous structure underlying the inner nuclear membrane in tobacco BY-2 cells (Fiserova et al. 2009). **b, d** Nucleoplasmic views of the lamina structure in *Xenopus* (Fiserova et al. 2009). **e, f** Electron micrographs of negatively stained pea lamina fraction (e) (Blumenthal et al. 2004) and *Ce*-lamin filaments (f) (Foeger et al. 2006).

lamin-binding proteins like SUN- domain proteins which are conserved widely across all kingdoms (Graumann et al. 2010; Murphy et al. 2010; Field et al. 2012). Also, a functional homolog of Nup153 a lamin-binding nucleoporin was found in plants (Nup 136). As Nup153, it is involved in regulation of nuclear morphology even though they do not share sequence similarity (Tamura and Hara-Nishimura 2011).

The presence of proteins with similar characteristics to lamins was also suggested in an indirect study. It was reported that a mammalian lamin-binding protein, the human LBR, when expressed in transformed tobacco BY2 cells is directed to the NE and interacts weakly with proteins present in this structure (Irons et al. 2003; Graumann et al. 2007; Evans et al. 2009).

In conclusion, the presence of a filamentous lamina, expression of two lamin-binding proteins and the fulfilment of the main lamin functions in the plant nucleus strongly suggest that even though plant genomes lack obvious homologs of lamins they may express proteins that functionally replace them. There are few lamin-like candidates that can be classified into two groups, one including proteins with some biochemical similarities to lamins (pI, MW) that cross-react with anti-IF antibodies and another containing proteins with structural analogies and biochemical properties analogous to lamins.

4.1. Proteins that cross-react with anti-IF antibodies

Early biochemical studies suggested that lamins were present in plants since the general anti-IF antibody cross-reacted with proteins of 60-70 kDa in monocots and dicots (Li and Roux 1992; McNulty and Saunders 1992; Minguez and Moreno Diaz de la Espina 1993; Moreno Diaz de la Espina 1995). Nevertheless, lack of sequence information on any protein from this group makes it impossible to identify homology and verify their conservation

across species. Blumenthal et al. (2004) tried to obtain the sequences of three lamin-like proteins in pea lamina by peptide mapping. The peptides showed high sequence similarity to keratins (including human keratins) and gave no significant match in a BLAST search against *A. thaliana* nr database which undermines the reliability of the sequence results. Also, most of these proteins localize abundantly to the nucleoplasm and internal NSK and not predominantly to the nuclear periphery as it is in case of lamins (Frederick et al. 1992; McNulty and Saunders 1992; Minguez and Moreno Diaz de la Espina 1993; Blumenthal et al. 2004; Perez-Munive et al. 2012). An onion protein belonging to this group seems to be localized at the nuclear periphery in isolated onion nuclei but the distribution changes in the isolated NSK fraction which displays abundant internal staining (Minguez and Moreno Diaz de la Espina 1993; Perez-Munive et al. 2012).

4.2. Coiled-coil proteins

The second group is focused on proteins containing long coiled-coil domains. The selection of these candidates is based on the hypothesis that proteins with long coiled-coil domain are able to form filaments and fulfill some of the lamin functions.

4.2.1. Coiled-coil structure

The coiled coil is one of the first described protein folds (Crick 1952; Crick 1953a) and enables protein assemblies into large, mechanically stable structures like fibres, tubes, sheets, spirals and funnels (Lupas and Gruber 2005). Coiled coils are bundles of α-helices that are wound around each other into super-helical structures (Fig 8 b, d). Commonly they consist of two, three

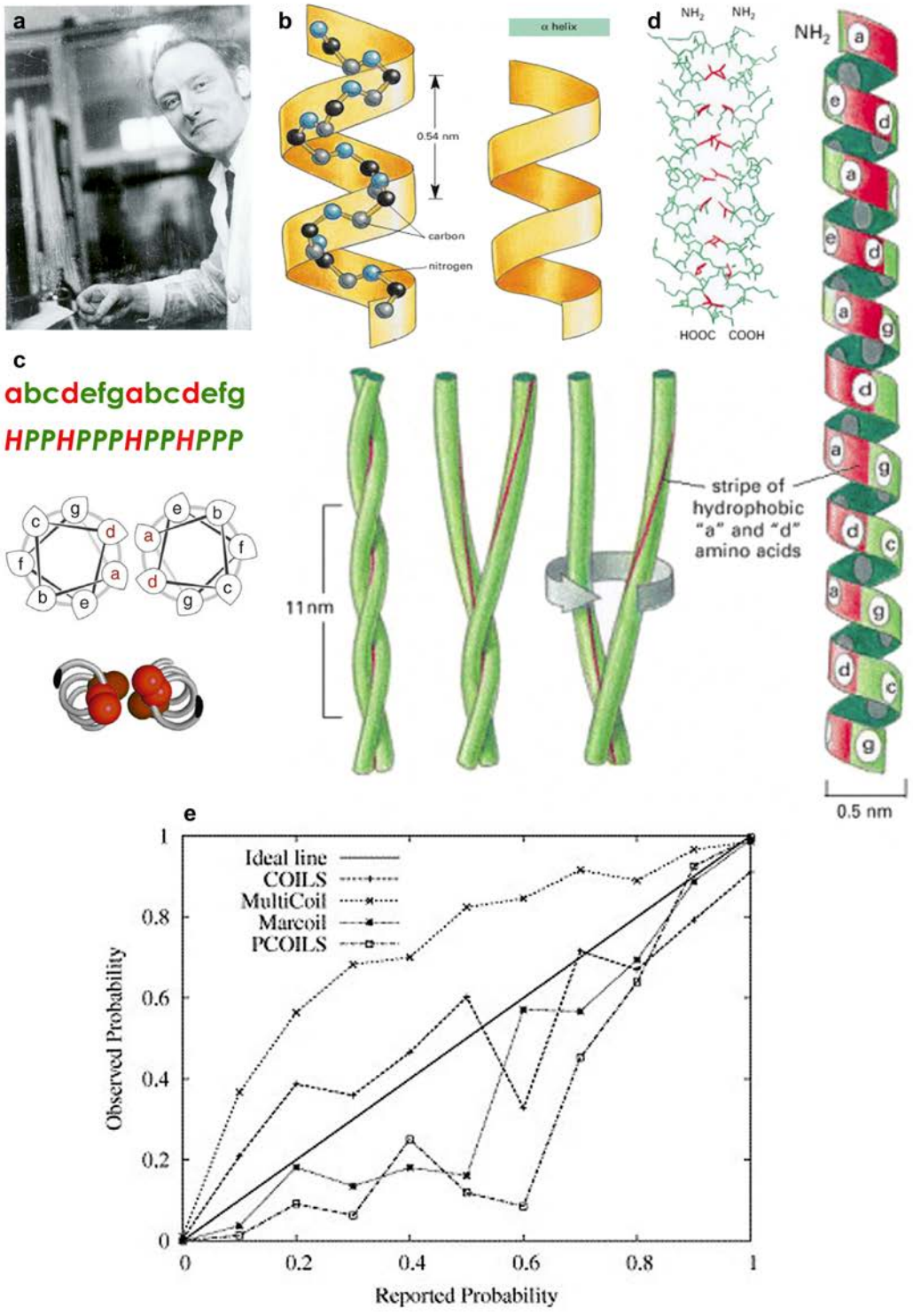

Figure 8. Coiled-coil structure. a Francis Crick **b**, **c**, **d** Coiled coils consist of α-helical folds (b) formed by sequences diplaying heptad repeat pattern where the first and the fourth residue are hydrophobic (c). The hydrophobic residues form a stripe stretched along the polypeptide and the interaction between two or more coiled coils is mediated by these regions in a way that hydrophobic residues are buried inside the dimer/polymer (d). **e** Information quality of the given probabilities obtained using various coiled-coil prediction tools. Probabilities provided by Multicoil are generally too low, while probabilities from Marcoil too high although its performance is better in comparison to other tools in the range 0.6-1 (Gruber et al. 2006).

or four helices running in the same or opposite direction. The name for this structure was for the first time used by Crick (Crick 1952; Crick 1953a; Crick 1953b) and is formed by polypeptide chains with typical heptad repeat. Schematically the seven structural positions are labeled a-g, where at the a and g positions are present hydrophobic residues or HPPHPPP where H stands for hydrophobic and P for polar (hydrophilic) amino acids (Fig. 8 c). Proteins containing coiled-coil domains are implicated in multiple functions in the cell: organization of structures such as nuclear pore complexes (Devos et al. 2006) and spindle pole body (Newman et al. 2000), formation of IF filaments in cytoplasm and nucleus (Strelkov et al. 2003), directing protein trafficking and quality control (Kim et al. 2006), chromatin organization and maintenance, transcription and translation, signal transduction and motility, etc (Rose et al. 2005).

The strong heptad periodicity of coiled coils made it possible to develop a large number of computational coiled-coil prediction tools. There are three common approaches applied by prediction programs: Fourier transform (Parry 1975), Position Specific Scoring Matrix (PSSM) (Parry 1982; Lupas et al. 1991; Lupas 1996) and the Hidden Markov model (HMM) (Delorenzi and Speed 2002). The two last are commonly used to predict coiled coils based on sequences of proteins of unknown structure. The PSSM uses a frame of 28 (four heptads), 21 (three heptads) or 14 (two heptads) in the search for coiled-coil domains and assign probabilities for each residue depending on the occurrence of correlated residues. A disadvantage of this approach is that when the window is longer than the domain it contains neighboring non-coiled-coil residues and when it is shorter, some of the information is not included in the prediction (Delorenzi and Speed 2002). Also, the factors included in the algorithm seem to be specific only for few classes of coiled-coil domains whereas for the general identification of new classes of coiled coils it is too specific (Delorenzi and Speed 2002; Gruber et al. 2006). On the

other hand, HMM is computationally more complex and more flexible and since it is a windowless method it does not have the limitations of the former (Delorenzi and Speed 2002; Gruber et al. 2006). The comparative study on a group of prediction tools established definitely the superiority of HMM approach (Fig 8 e) (Gruber et al. 2006).

4.2.2. Filament-like Plant Proteins (FPPs)

Filament-like Plant Proteins (FPPs) make up a vast and diverse protein family and are expressed in land plants. Gindullis et al. (2002) described for the first time members of this family in *Arabidopsis thaliana* which represented different sizes and structures and shared four conserved motifs. Analysis using Phytozome suggests that in other species also diverse orthologs are expressed. FPPs contain one or two long coiled-coil domains separated by non-coiled-coil regions of diverse lenghts (Tab. 5). Most of these proteins seem to lack an NLS site and their nuclear localization was never confirmed in situ. The assumption that they localize in the nucleus was made based on results from yeast two hybrid screen which showed that LeFPP (tomato FPP) binds to MAF1, a protein originally assigned as NE protein (Gindullis et al. 2002) but later also found in the Golgi (Patel et al. 2005). FPPs were proposed to be the candidates for plant lamin analogues due to the presence of long coiled-coil domains, nevertheless, relatively low degree of conservation and diverse size and structure between the members of this protein family undermines the classification as such. Also, the lack of NLS site creates further doubts about their functionality as nuclear IF-like proteins in the plant nucleus.

4.2.3. NAC (Nuclear Acidic Coiled-coil) proteins

NAC proteins are orthologues of AtNAC1 (NP_175138), a nuclear coiled-coil protein expressed in *A. thaliana* (Blumenthal et al. 2004). Preliminary phylogenetic analysis using Phytozome database demonstrated that one or multiple NACs are expressed in land plants. The predicted molecular weight ranges between 80-130 kDa and isoelectric point between 4.8-5.8. They represent a tripartite structure including a central coiled-coil domain and non-coiled coil long head and short tail domains. Most of them are predicted to contain a basic NLS but their localization in situ was never confirmed. The functions of these proteins are also not known (Tab. 5).

4.2.4. Nuclear Matrix Constituent Proteins (NMCPs)

The most promising and well described candidate for lamin substitute in plants is NMCP (Nuclear Matrix Constituent Protein). NMCP1 was for the first time described in carrot (DcNMCP1) as a constituent component of NSK which localized predominantly at the nuclear periphery. Immunoblot analysis demonstrated it is an acidic protein with a pI similar to the one of B-type lamins (5.4-5.6) although representing a molecular mass roughly twice that of lamins (130 kDa) (Masuda et al. 1993). Determination of the cDNA sequence enabled analysis of the predicted structure and sequence analysis. The DcNMCP1 was predicted to represent a structure similar to that of lamins featuring a central coiled-coil domain flanked by non-coiled coil head and tail domains, the latter containing an NLS motif. The rod domain was predicted to mediate dimerization (Masuda et al. 1997). Searches against plant genomes revealed genes encoding NMCP homologs (Rose et al. 2004; Dittmer et al. 2007; Kimura et al. 2010). All NMCP proteins contain coiled coils with high sequence similarity while head and tail domains show lower

degree of sequence conservation. Most plants contain genes coding for two or more NMCP proteins implying the existence of several NMCP variants with different roles (Tab. 5) (Kimura et al. 2010).

High resolution immunogold labelling in membrane-depleted carrot nuclei using a specific antibody demonstrated the localization of NMCP1 at the nuclear periphery, in the lamina (Masuda et al. 1997). Predominant peripheral localization was also confirmed for other NMCP orthologs by IF ot GFP expression (Dittmer et al. 2007; Dittmer and Richards 2008; Kimura et al. 2010; Sakamoto and Takagi 2013) although few localized also or exclusively in the nucleoplasm (Dittmer et al. 2007; Sakamoto and Takagi 2013).

Biochemical and sequence analysis demonstrated that carrot and celery contain at least two variants of NMCP proteins designated NMCP1 and NMCP2 (Kimura et al. 2010). The two display different distribution during mitosis suggesting they might play some non-overlapping functions. In metaphase NMCP1 is predominantly distributed within the mitotic spindle (Masuda et al. 1999; Kimura et al. 2010) while NMCP2 is dispersed throughout the cytoplasm where it remains until the end of anaphase (Kimura et al. 2010). NMCP1 accumulates on the surface of segregating chromosomes at anaphase while its accumulation in mitotic spindle decreases (Masuda et al. 1999; Kimura et al. 2010). NMCP2 also accumulates on the chromosomes at telophase and both proteins localize at the nuclear envelope in entirely enclosed reforming nuclei (Kimura et al. 2010). Similar changes in distribution during mitosis were observed in *A. thaliana* as LINC1/AtNMCP1 was co-localized with chromosomes from prometaphase to anaphase while other orthologs were dispersed in the cytoplasm (Sakamoto and Takagi 2013).

Biochemical studies demonstrated that NMCPs are constituent components of the nucleoskeleton (Masuda et al. 1993; Sakamoto and Takagi 2013) suggesting that similar to lamins they are components not only of the lamina but probably also of the internal NSK.

Little is known about the functions of NMCPs. Functional studies were performed only in *A.thaliana* mutants (Dittmer et al. 2007; Dittmer and Richards 2008; Sakamoto and Takagi 2013). *A. thaliana* contains four ORFs encoding NMCP proteins identified by Rose et al. (2004) based on sequence similarity to DcNMCP1. In a reverse genetic study Dittmer et al. (2007) characterized these genes and found that mutation in two of them affected nuclear size and morphology. The proteins were called LINC1-4 (Little Nuclei) proteins 1-4 due to the phenotype observed in *linc1linc2* double mutants (Dittmer et al. 2007). Unfortunately, the name coincides with that of the LINC (Linker of the Nucleoskeleton to the Cytoskleleton) protein complex therefore it is recommended to use NMCP nomenclature. Distruption of one or two genes encoding LINC1/AtNMCP1 and LINC4/ATNMCP2 highly affected nuclear size and shape (Dittmer et al. 2007; Sakamoto and Takagi 2013) which demonstrated that these proteins are important determinants of nuclear morphology like lamins in metazoan nuclei. Interestingly, a similar phenotype was observed after disruption of Nup136, the plant functional homolog of Nup156 which suggests these two proteins may interact and play a key role in maintenance of nuclear size and shape (Tamura and Hara-Nishimura 2011). Dittmer et al. (2007) reported that LINC1 and LINC2 proteins affect heterochromatin organization as a decrease in the number of chromocenters was observed in *linc1linc2* mutants. Nevertheless, independent analysis of these mutants did not confirm the role of NMCP proteins in chromatin organization (van Zanten et al. 2011; van Zanten et al. 2012) and the decrease in chromocenter number could be affected by the decrease in nuclear volume, which could cause fusion of these structures. On the other hand, NMCP proteins may have overlapping functions in chromatin organization and other processes which is difficult to verify as disruption of four genes and some combinations of triple mutants are inviable (Richards, personal communication).

	NMCP	**FPP**	**NACs**	**NIFs**
species	Land plants	Land plants	Land plants	Described in pea, onion
isoforms	2-4	1-7	1-3	3 in pea
Sequence conservation	Highly conserved	conserved	conserved	unknown
structure	Central coiled-coil domain, long tail	Two coiled-coil domains interrupted by central non-coiled coil domain	Central coiled-coil domain, long head	unknown
MW, pI	130-160 kDa 5.6-5.8 pI	70-130 kDa 4.8-5.8 pI (predicted)	65-120 kDa 4.8-6.4 pI (predicted)	60, 67 and 71 kDa 4.8-6.0 pI
Subnuclear localization	Nuclear periphery (predominant), Nucleoplasm; cointain NLS	Unknown, does not contain NLS	Unknown, contains predicted NLS	Uniform nuclear distribution, nuclar periphery and nucleoplasm
Known functions	Nuclear size and shape	unknown	unknown	unknown

Table 5. The comparison of plant protein candidates to be lamin analogues.

OBJECTIVES

The final objective of this work was to characterize plant-specific proteins that could be lamin analogues in plants. For this, we investigated the NMCP protein family and the NMCP1 protein in onion. The analogies between plant specific NMCPs and metazoan lamins were also analysed.

For this, the following specific objectives were proposed:

1. Characterization of the NMCP family based on sequence conservation.

2. Establishment of phylogenetic relationships between NMCPs.

3. Analysis of predicted coiled-coil structures of NMCPs and comparison with those of lamins.

4. Identification of conserved motifs characterizing the NMCP family.

5. Determination of the AcNMCP1 sequence and characterization of the endogenous protein (molecular weight and isoelectric point) using technics of biochemistry.

6. Investigation of the association of AcNMCP1 with the NSK.

7. Analysis of the subnuclear distribution and high-resolution localization of AcNMCP1 in meristematic nuclei.

8. Comparative analysis of the AcNMCP1 levels and distribution patterns in nuclei of cells in various differentiation states: proliferating and quiescent meristems, and cells in the elongation and differentiation root zones.

9. Comparative analysis of the nuclear ultrastructure in *Arabidopsis thaliana* single *linc1* and *linc2* and double *linc1linc2* mutants and in wild type nuclei.

10. Comparative analysis of the features of NMCP proteins with those of lamins including the predicted structures, distribution and pattern of conserved domains, biochemical characteristics, subnuclear localization and expression levels.

MATERIALS AND METHODS

1. MATERIALS

1.1. Plant material- species

The following species were used for the analysis:

- *Allium cepa* L. francesa
- *Arabidopsis thaliana* L.
- *Triticum aestivum* L.
- *Secale cereale* L.
- *Zea mays* L.
- *Pisum sativum* L.
- *Nicotiana benthamiana* L.
- *Allium sativum* L.

1.2. Plant material- mutants

Seeds of *Arabidopsis thaliana* single *linc1* and *linc2* mutants and *linc 1-1 linc2-1* double mutants were obtained through the courtesy of Dr Eric Richards (Department of Biology, Washington University).

1.3. Antibodies

The following antibodies were used:

- an anti-AcNMCP1 polyclonal antibody produced in rabbit against a region corresponding to the 313 N-terminal residues
- a DMA1 (anti-tubulin) monoclonal antibody (Sigma-Aldrich T9026)

- an anti-HRP polyclonal antibody produced in rabbit (GenScript A00619)

2. METHODS

2.1. Callus culture

Callus of *Allium cepa* was induced from root tips of aseptically grown seedlings and maintained on agar-solidified Murashige and Skoog (MS) medium (Sigma-Aldrich M9274) supplemented with 200 μM naphthalene acetic acid (NAA) (Sigma-Aldrich N0640), 5 μM 2,4-D (Sigma-Aldrich D7299), and 5 μM zeatin (Sigma-Aldrich Z0164).

2.2. Plant culture

External layers of *Allium cepa* L. francesa var. bulbs and *Allium sativum* L. cloves were eliminated and plant organs were extensively washed in tap water for 30 min and then grown in filtered tap water at room temperature for at least two days. Root meristems and root segments of *A. cepa* were excised at different lengths from the tips and used for nuclear isolation. Quiescent meristems of *A. cepa* were excised directly from unsoaked bulbs.
Triticum aestivum (wheat), *Secale cereale* (rye), *Zea mays* (maize), *Pisum sativum* (pea), *Arabidopsis thaliana* and *Nicotiana benthamina* seeds were surface sterilized for 10-12 minutes in 5% bleach and washed in MQ water tree times. Wheat, rye, maize and pea seeds were grown on Whatmann 3MM paper in Petri dishes for 3-4 days.

Arabidopsis thaliana and *Nicotiana benthamiana* seeds were grown in soil in a growth chamber under 16:8 light:dark cycle at 19-22 °C (*A. thaliana*) or 22-24 °C (*N. benthamiana*) with 60-75% humidity. Plants were grown for three weeks. The seeds of *Arabidopsis thaliana* single and double *linc* mutants were surface sterilized and grown on agar-solidified MS medium with sucrose (Sigma-Aldrich M9274) for two weeks in the same conditions as above.

2.3. Cloning and sequencing of cDNAs for AcNMCP1

RNA was extracted from *Allium cepa* callus using Trizol reagent (Invitrogen 15596-018) according to manufacturer's instructions. First-strand cDNA was synthesised from RNA with Transcriptor Reverse Transcriptase (Roche 03531317001) by priming with the 3'-CDS primer (Clontech 634901). In 3'-RACE, forward degenerate primers AcF2 (GGGGCTKCTTTTGATTGAGA) and AcF3 (ATTGAGAAAAARGARTGGAC) and reverse primers UPM and NUP (Clontech 634922) were used for primary and nested PCR. In 5'-RACE, first-strand cDNA was tailed with oligo-dG using terminal deoxyribonucleotidyl transferase in the presence of dGTP. The first-strand cDNA with the dG tail was primed with a forward tag-primer 5T that has oligo-dC at the 3'-terminus, and double-stranded using *Taq* DNA polymerase (Invitrogen 10342). Then the 5'-terminal region of cDNA was amplified using the forward primer N5T, which has a partial sequence of 5T and the sequence-specific reverse primers Ac5RACE-R2 (TAATATGCCTCTGCCCATCAA) and Ac5RACE-R3 (GCAAATGCTCTTTTTGTTCAG).

For sequencing, the cDNA was ligated into the pGEM T-Easy vector (Promega A1360) with the TA-cloning method, and the vectors were cloned into *Escherichia coli* DH5 alpha cells. The plasmid DNA was extracted from the

clones, and the cDNA sequence was determined. The accession number for AcNMCP1 in GenBank/EMBL/DDBJ is AB673103.

2.4. Bioinformatic analysis

2.4.1. Genome searches for NMCP homologs

Sequence similarity searches against sequenced genomes were performed using BLASTP and BLASTX on Phytozome v8.0 (Goodstein et al. 2012) (www.phytozome.net). The Phytozome is a database that provides access to complete plant genomes of land plants and selected algae, as well as sequences and functional information about single genes and putative gene families (groups of extant genes descended from a common ancestral gene). The presented search included 31 genomes of species included in table 6.
Additional BLASTP searches against non-redundant protein sequences (nr) were performed on NCBI webpage (http://www.ncbi.nlm.nih.gov/).
The estimation of predicted molecular weight (MW) and isoelectric point (pI) was performed on ExPASY webpage (www.expasy.org).

2.4.2. Phylogenetic analysis

The phylogenetic analysis and tree construction was made using MEGA5 (Molecular Evolutionary Genetics Analysis) software (Tamura et al. 2011). The phylogenetic tree was constructed based on two recommended methods: Neighbour Joining method (Saitou and Nei 1987) which is the most widely used distance matrix method and Maximum Likelihood Method

No	name	species	Common name	Genome Source
1	**Vca**	*Volvox carteri*	Volvox	JGI annotation 2.0 on assembly v2
2	**Cre**	*Chlamydomonas reinhardtii*	Green algae	Augustus update 10.2 (u10.2) annotation of JGI assembly v4
3	**Ppa**	*Physcomitrella patens*	Moss	JGI assembly release v1.1 and COSMOSS annotation v1.6
4	**Smo**	*Selaginella moellendorffii*	Spikemoss	JGI v1.0 assembly and annotation
5	**Bdi**	*Brachypodium distachyon*	Purple false brome	JGI 8x assembly release v1.0 of strain Bd21 with JGI/MIPS PASA annotation v1.2
6	**Osa**	*Oryza sativa*	Rice	MSU Release 7.0 of the Rice Genome Annotation
7	**Sit**	*Setaria italica*	Foxtail millet	JGI 8.3X chromosome-scale assembly release 2.0, annotation version 2.1
8	**Zma**	*Zea mays*	Maize	5b.60 annotation (filtered set) of the maize "B73" genome v2 produced by the Maize Genome Project
9	**Sbi**	*Sorghum bicolour*	Sweet Sorghum	Sbi1.4 models from MIPS/PASA on v1.0 assembly
10	**Aco**	*Aquilegia coerulea*	Colorado blue columbine	JGI 8X assembly v1.0, annotation v1.1
11	**Mgu**	*Mimulus guttatus*	Monkey flower	JGI 7x assembly release v1.0 of strain IM62, annotation v1.0
12	**Vvi**	*Vitis vinifera*	Grape	12X assembly and annotation from Genoscope (March 2010)
13	**Egr**	*Eucalyptus grandis*	Eucalyptus	JGI assembly v1.0, annotation v1.1
14	**Ccl**	*Citrus clementina*	Clementine	JGI v0.9 assembly and annotation
15	**Csi**	*Citrus sinensis*	Sweet orange	JGI v1.1 annotation on v1 assembly
16	**Cpa**	*Carica papaya*	Papaya	ASGPB release of 2007
17	**Tha**	*Thellungiella halophila*	Salt cress	JGI annotation v1.0 on assembly v1

18	**Bra**	*Brassica rapa*	Napa cabbage	Annotation v1.2 on assembly v1.1 from brassicadb.org
19	**Cru**	*Capsella rubella*	Red shepherd's purse	JGI annotation v1.0 on assembly v1
20	**Ath**	*Arabidopsis thaliana*	Thale cress	TAIR release 10 acquired from TAIR
21	**Aly**	*Arabidopsis lyrata*	Lyre-leaved rock cress	JGI release v1.0
22	**Mdo**	*Malus domestica*	Apple	GDR prediction v1.0 on Malus x domestica assembly v1.0
23	**Ppe**	*Prunus persica*	Peach	JGI release v1.0
24	**Csa**	*Cucumis sativus*	Cucumber	Roche 454-XLR assembly and JGI v1.0 annotation
25	**Gma**	*Glycine max*	Soybean	JGI Glyma1.0 annotation of the chromosome-based Glyma1 assembly
26	**Pvu**	*Phaseolus vulgaris*	Common bean	JGI annotation v0.91 on assembly v0.9 using published ESTs, and JGI RNAseq
27	**Mtr**	*Medicago truncatula*	Barrel medic	Release Mt3.0 from the Medicago Genome Sequence Consortium
28	**Ptr**	*Populus trichocarpa*	Poplar	JGI assembly release v2.0, annotation v2.2
29	**Lus**	*Linum usitatissimum*	Flax	BGI v1.0 on assembly v1.0
30	**Rco**	*Ricinus communis*	Castor bean	TIGR release 0.1
31	**Mes**	*Manihot esculenta*	Cassava	Assembly version 4, JGI annotation v4.1

Table 6. Genomes included in genomic searches.

(Jones et al. 1992). The distances were computed using the p-distance method and the reliability of the results was tested by bootstrap method (Felsenstein 1988).

2.4.3. Search for conserved domains

The multiple alignment of collected NMCP sequences was derived with ClustalW2 (Larkin et al. 2007) and visualized in Jalview (Waterhouse et al. 2009).

The search for conserved regions was conducted using MEME (Multiple EM for Motif Elicitation) program which discovers shared motifs in a set of unaligned sequences (Bailey et al. 2009). The MEME form allowed analysis of 54 NMCP sequences at a time. Sequences from various species and of various types were selected and the presence and position of detected conserved regions was confirmed in the rest of the sequences.

2.4.4. Coiled-coil domain prediction

The prediction of coiled-coil domains (CCD) was performed by MARCOIL which uses HMM (Delorenzi and Speed 2002). To avoid negative matches and improve the results reliability the cutoff was set at 0.6 at which MARCOIL showed the best performance (Gruber et al. 2006). A control analysis was performed on a collection of lamin amino-acid sequences from various species which confirmed that in this analysis MARCOIL outperforms Multicoil2 or Multicoil programs commonly used for coiled-coil domain prediction. The coiled-coil prediction was performed on 76 NMCP sequences which included the sequences collected in genome searches and previously described NMCP members in carrot, celery and *A. thaliana*.

Additionally, we performed prediction of oligomerization state of NMCPs by Multicoil2 (Trigg et al. 2011). The Multicoil2 is a recent version of the Multicoil program based on paircoil algorithm. The paircoil algorithm uses a

probabilistic framework to detect CCDs based on residue-pair frequencies in known coiled-coils. The program derives dimer and trimer propensities using sequence databases constructed from authentic coiled-coil dimers and trimers.

2.4.5. Prediction of nuclear localization signals (NLS) and post-translational modification (PTM) sites

The search of post-translational modification sites was performed using PROSITE and the localization of nuclear localization signals using NucPred (Brameier et al. 2007).

2.5. Northern Blot analysis

2.5.1. Probe production

2.5.1.1. Probe design

For probe production a highly conserved region was selected. Primers were designed using DNAMAN program, focusing on the primer pairs of similar

1.	**325F** 5'- CGTGAGTCTCTTGCTTCG -3'	**631R** 5'- CGGTATACTTAACCTCGGC -3'
2.	**325F** 5'- CGTGAGTCTCTTGCTTCG -3'	**676R** 5'- CAATACTTGCTTCCAATGC -3'
3.	**310F** 5'- TGCTACAAGAAAGATCGTG -3'	**628R** 5'- TATACTTAACCTCGGCGA -3'
4.	**313F** 5'- TACAAGAAAGATCGTGAGTC -3'	**634R** 5'- CAGCGGTATACTTAACCTC -3'
5.	**338F** 5'- CTTCGAGAATCATTGAGC -3'	**634R** 5'- CAGCGGTATACTTAACCTC -3'
6.	**363F** 5'- GGATCTTCACGAGTACCA -3'	**647R** 5'- GTCATCTTCTTCTCAGCG -3'

Table 7. List of the primer pairs used in PCR reactions.

melting temperatures that do not self-align or align between themselves. Six primer pairs listed in table 7 were selected and used in PCR reactions. Only one primer pair aligned and gave specific product. The size of the product was bigger than predicted therefore cDNA was produced in reverse transcription reaction using AMV Reverse Transcriptase (Promega M5101) according to manufacturer's instructions. The fragment chosen for probe production was amplified in PCR reaction using the cDNA as matrice

2.5.1.2. Transformation

The amplified fragment was purified twice with phenol:chloroform (Amresco 0883) in proportion 1:1, centrifuged at 12 000 rpm for 5 min, precipitated with 2.5 volumes of ethanol and 0.2 volume of 3 M sodium acetate and dissolved in sterile MQ water. Next the fragment was ligated to pGEM-T (Promega A1360) vector using T4 DNA Ligase (Promega A1360) according to manufacturer's instructions. The ligation was followed by transformation using JM109 High Efficiency Competent Cells (Promega L2004). A 50 μl aliquot of competent cells was shortly thawed on ice. The ligation reaction was dialysed for 10 minutes using Milipore 0.025 μm filter (VSWP01300). Next 5 μl of ligation reaction was mixed with competent cells, the mixture was transferred into an E. coli Pulser Cuvette (BIO-RAD 165-2086) and electroporated with a single 2.5 kV pulse. Immediately after the shock 1 ml of SOC medium (Sigma-Aldrich S1797) was added. Next the cells were incubated for 1 h at 37 ºC with constant shaking (150 rpm) and plated onto LB/ampicillin/IPTG/X-Gal plates. After overnight incubation at 37 ºC positive colonies were selected and the sequence of the insert was confirmed in colony PCR and subsequent sequencing. Transformed *E. coli* was inoculated in lysogeny broth (LB) and incubated overnight at 37 ºC with constant shaking. Next the vector was isolated using the

High Pure Plasmid Isolation Kit (Roche 11754777001) and the insert was amplified in a PCR reaction. PCR reaction product was separated in agarose gel, the band corresponding to the insert was cut out and DNA was extracted with phenol:chloroform as above. The DNA content was quantified using NanoDrop 1000 sepctrophotometer and the sample stored at -20 °C until Random Priming was performed.
PCR conditions are listed in table 8.

PCR	Reaction mix	Conditions
PCR with genomic DNA or cDNA	4 µl DNA matrice 10 µl HF buffer 5x 2x 0.5 µl primers 20 mM 1 µl dNTPs 0.5 µl Phusion DNA polymerase (NEW ENGLAND BioLabs M0530S) MQ water up to 50 µl	Denaturation- 4 min, 98 ºC Cycle: denaturation- 30 s, 98 ºC Alignment- 30 s, 50 ºC Elongation- 30 s, 72 ºC Cycle x35 Final elongation- 4 min, 72 ºC
Colony PCR	2 µl PCR buffer 10x 1.2 µl $MgCl_2$ 25 µM 0.4 µl M13F oligo 10 µM 0.4 µl M13R oligo 10 µM 0.4 µl dNTPs 10 µM 0.2 µl Taq DNA polymerase (Invitrogen) MQ water up to 20 µl	Denaturation- 4 min, 94 ºC Cycle: denaturation- 45 s, 94 ºC Alignment- 30 s, 55 ºC Elongation- 1 min, 72 ºC Cycle x35 Final elongation- 10 min, 72 ºC

Table 8. Conditions of PCR reactions.

2.5.1.3. Random Priming

Random priming (extension of random oligonucleotides) was performed using Klenov fragment and ^{32}P-dCTP. First 2 µg of template DNA in 30 µl of sterile

MQ water was combined with 2 μl of random deoxynucleotide primers (Roche 11277081001) and denatured for 2 min in a boiling water bath. Then the tube was placed on ice and the sample was mixed with 2 μl dNTP solution 10x, 1 μl of Tris-CBH buffer and 5 μl of ^{32}P-dCTP (sp. act. 3000 Ci/mmole) and sterile MQ water was added up to 50 μl. Next 1.5 μl of the *E. coli* polymerase I Klenov fragment (New England BioLabs M0210) was added, sample was mixed gently and the reaction was incubated for 45 min at 37 °C. Finally, the radiolabeled probe was separated from unincorporated dNTPs by P30 chromatography column (BIO-RAD 732-6223).

2.5.2. RNA extraction and electrophoretic separation in denaturating conditions

RNA from root meristem of *Allium cepa* and *Allium sativum*, 2-week-old *Arabidopsis thaliana* plants and 3-day-old *Triticum aestivum* sprouts was extracted with Trizol reagent (Invitrogen, 15596-018) according to manufacturer's instructions. The RNA content was quantified with NanoDrop. RNA isolated from mouse lymphocytes was used as negative control. Samples containing 25 μg of RNA were mixed with 5x loading buffer (0.03% bromophenol blue, 5 mM EDTA, 7.4% formaldehyde, 20% glycerol, 30% formamide, 80 mM MOPS, 20 mM sodium acetate, 0.2 μg/μl ethidium bromide). The samples and the RNA molecular weight marker (Millenium range 0.5-9 kbp; Ambion AM7150) were denatured at 65 °C for 5 min then loaded on 1.5 % agarose gel containing 0.5 M MOPS pH 7 and 6% formaldehyde and separated according to size in buffer containing 0.5 M MOPS pH 7 and 6% formaldehyde at 60 V.

2.5.3. Northern Blot

RNA was transferred overnight in upward capillary transfer to positively charged nylon membrane and cross-linked. The membrane was blocked for 4 h at 38 °C in PerfectHyb hybridization buffer (Sigma-Aldrich H7033). Next the random priming reaction was added to the hybridization buffer and the membrane was incubated for 16 h at 38 °C, washed three times at 50 °C for 30 min in 2x SSC/2x SDS buffer, then in 1x SSC/0.5x SDS buffer and finally in 0.1xSSC/0.1xSDS buffer. The Kodak Biomax XAR film (853-2665) was exposed overnight.

2.6. Anti-AcNMCP1 antibody production

2.6.1. Polypeptide synthesis with partial sequences of AcNMCP1

The cDNA fragment encoding the N-terminal 313 amino acids of AcNMCP1 (indicated in figure 16) was sub-cloned into expression vector pET28-b (Novagen 69865), and the vectors were transformed into *E. coli* strain Rosetta II (Novagen 71403). Protein expression was induced by incubation with 1 mM IPTG at 37 °C for 4 h, and the cells were then harvested. The cells were extracted several times with PBS containing 0.2% TX-100, and the proteins in the insoluble fraction were extracted with 8 M urea, 10 mM Na-phosphate buffer (pH 8.0), and 1.0 mM 2-mercaptoethanol. The N-terminal region of AcNMCP1 with a 6X histidine tag was affinity-purified through iMAC resin (BIO-RAD 156-0121). The fraction retained in the gel at 10 mM imidazole was eluted with 300 mM imidazole and dialysed against 6 M urea in 10 mM Tris-acetate, pH 7.6. Protein in the dialysed solution was then precipitated by adding 1.5 volumes of acetone and collected by centrifugation.

2.6.2. Antibody production

The protein precipitate was dissolved in PBS containing 0.04% SDS, which was used for immunisation. The anti-AcNMCP1 antibody was made commercially at Sigma Genosys Co (Ishikari), using rabbits for immunisation.

2.7. Isolation of nuclei

Selected root segments were isolated and submerged in freshly prepared Isolation Medium pH 7.8 (IM; 2% arabic gum, 1.25% ficoll, 2.5% dextran, 0.01% BSA, 0.5 mM EDTA, 50 mM magnesium acetate, 8 mM β-mercaptoethanol, 4 mM n-octanol, 25 mM TRIS, 7 mM diethylpyrocarbonate, 30% glycerol) containing 1% protease inhibitor cocktail (Sigma-Aldrich P9599). The tissue was incubated in vacuum on ice for 15 min and then homogenized 3x 20 s at 20,000 rpm with an ULTRA-TURRAX homogenizer IKA T25 digital with dispersor IKA S25-10G. Next, the homogenate was filtrated through a set of 100, 50 and 30 μm nylon sheets. The homogenization and filtration was repeated three times and each batch was collected separately. The homogenates were centrifuged at 2,500 rpm, for 15 min at 4 ºC. The supernatant containing the cytoplasmic fraction was transferred to a fresh centrifuge tube, precipitated with 10% v/v trichloroacetic acid (TCA) for 1 h on ice, centrifuged 5 min at 12,000 rpm and mixed with Laemmli Buffer 2x or Lysis Buffer (LysB). The pellets containing the nuclei were washed with Isolation Medium containing 0.1% protease inhibitor cocktail (Sigma-Aldrich P9599) and stored at -20 ºC until used. The purity and integrity of isolated nuclei were controlled using a light microscope after methyl green staining (Sigma-Aldrich M8884).

2.8. Isolation of the nucleoskeleton

The isolation of the NSK fraction was obtained in a sequential nuclear extraction with non-ionic detergent, DNase and high salt buffer according to laboratory´s protocol (Perez-Munive and Moreno Diaz de la Espina 2011) with minor changes as follows.

Freshly isolated nuclei were incubated for 5 minutes with cytoskeleton buffer (CSKB; 10 mM PIPES pH 6.8, 100 mM KCl, 300 mM sucrose, 3 mM $MgCl_2$, 20 mM DTT, 1 mM EGTA) containing 1% protease inhibitor cocktail (Sigma-Aldrich P9599) and 0.5% TX-100. Next, soluble and membrane associated nuclear proteins were removed by centrifugation at 3,000 rpm for 10 min at 4 ºC and collected in supernatant (**S1**). The pellet containing the nuclear insoluble fraction (**F1**) was digested with 75 U of Benzonase (Sigma-Aldrich E1014) in Digestion Buffer (DB; 10 mM PIPES pH 6.8, 50 mM KCl, 50 mM NaCl, 300 mM sucrose, 3 mM $MgCl_2$, 20 mM DTT, 1 mM EGTA, 1% protease inhibitor cocktail, 0.5% TX-100) for 1h. Then 1 M $(NH_4)_2SO_4$ was added slowly to a final concentration of 0.25 M to remove the DNA and DNA-associated proteins, then the sample was incubated for 15 minutes and centrifuged. The soluble proteins were collected in the supernatant (**S2**). 4 M NaCl was added to the pellet (**F2**) containing loosely bound proteins to a final concentration of 2 M and was incubated for 5 minutes and then centrifuged. This step released proteins bound to the NSK (**S3**) and revealed the insoluble **NSK** fraction. All steps were performed at 4 ºC. Compilation of all the steps is presented in table 9.

Extraction step	Fractions obtained
Suspension of nuclei in CSKB containing 0.5% of non-ionic detergent TX-100 Incubation for 15 min on ice Centrifugation at 3,000 rpm for 10 min at 4 °C	**S1**- supernatant containing soluble and membrane associated nuclear proteins **F1**- pellet containing insoluble nuclear proteins
Suspension of F1 pellet in DB containing 75 U Benzonase. Incubation for 1 h on ice Addition of $(NH_4)_2SO_4$ (final concentration 0.25 M) to remove DNA and associated proteins Incubation for 15 min on ice Centrifugation at 3,000 rpm for 10 min at 4 °C	**S2**- supernantant containing proteins associated with DNA **F2**- pellet containing insoluble nuclear proteins associated with the NSK and not associated with genomic DNA
Suspension of F2 pellet in DB buffer and extraction of ionically bounded proteins by addition of NaCl (final concentration 2M).	**S3**- supernatant containing proteins ionically bound to the NSK **NSK**- pellet containing resident proteins of the NSK

Table 9. Steps included in the isolation of NSK.

2.9. Protein analysis

2.9.1. Protein sample preparation for electrophoresis

2.9.1.1. Nuclear fractions

Fractions containing soluble proteins (S1, S2 and S3) were precipitated with 10% v/v trichloroacetic acid (TCA) (Sigma-Aldrich T9159) for 1 h on ice. Next, samples were centrifuged for 5 min at 12,000 rpm at 4 ºC and washed with ethanol/ether (1:1 v/v) to eliminate TCA. The insoluble fractions (F1, F2, NSK) were washed with DB buffer and mixed with lysis buffer (LysB; 100mM TrisHCl pH 7.5; 4.5 M urea; 1 M thiourea; 2% CHAPS; 0,5% TX-

100; 10 mM DTT, 75 U Benzonase) and then with 6x Laemmli Buffer (125 mM TRIS-HCl pH 6.8, 10% SDS, 30% 2-mercaptoethanol, 30% glycerol 0.012% bromophenol blue). Nuclear extracts were stored at -20 ºC until used.

2.9.1.2. Protein extraction from whole tissues

The 4-day-old sprouts of pea, wheat, maize and rye, *A. sativum* roots and whole 3-week-old whole plants of *A. thaliana* and *N. benthamiana* were grounded in liquid nitrogen. For each 100 μg of grounded tissue 100 μl of LysB containing protease inhibitor cocktail (Sigma-Aldrich P9599) and 75 U of Benzonase (Sigma-Aldrich E1014) were added. The samples were incubated 45 min on ice and then centrifuged at 14,000 rpm, for 10 min at 4 ºC. Protein extracts were stored at -20 ºC until used.

2.9.1.3. Measurement of protein concentration

Protein content was measured with modified Bradford Protein Assay (Berkelman 2008) as follows.

1. Sample dilutions and BSA standards were prepared as indicated in table 10.
2. 20 μl of each standard and diluted sample were transferred to 1.5 ml microcentrifuge tubes. For best results replicates of each standard and unknown sample were run.
3. 1 ml of Bradford dye reagent (BIO-RAD 500-0205) was transferred to each microcentrifuge tube. The content was mixed by inverting the tubes few times.

4. Mixtures were incubated for 5 min at room temperature and transferred into UVette cuvettes (eppendorf 952010051).
5. The absorbance at 595 nm and protein concentration were measured using an eppendorf BioPhotometer.

Preparation of BSA protein standard dilutions				
Tube	Standard volume (µl)	Source of standard	Diluent volume (LysB) (µl)	Final prot conc.(µg/ml)
1	70	2 mg/ml stock	0	2,000
2	75	2 mg/ml stock	25	1,500
3	70	2 mg/ml stock	70	1,000
4	35	Tube 2	35	750
5	70	Tube 3	70	500
6	70	Tube 5	70	250
7	70	Tube 6	70	125
8 (BLANK)	-	-	70	0
Dilution of unknown sample				
Dilution factor	Volume of sample (µl)		Volume of diluent (LysB) (µl)	
4	12.5		37.5	
10	5		45	

Table 10. Preparation of sample dilutions and BSA standards for modified Bradford protein assay.

2.9.1.4. Treatments with urea and guanidine thiocyanate

To compare the mobility of the detected bands in various conditions three batches of nuclear pellets were solubilised in different buffers: a) 6 M guanidine thiocyanate (GITC) (Sigma-Aldrich G9277) in 100 mM TRIS-HCl pH 7.5; b) 7 M urea (MERCK 08488), 2 M thiourea (MERCK 07979), 4% CHAPS (Sigma-Aldrich 53195), 18.2 mM DTT, 100 mM TRIS-HCl pH 7.5; c) 2x Laemmli Buffer (125 mM TRIS-HCl pH 6.8, 4% SDS, 10% 2-mercaptoethanol, 20% glycerol, 0.012% bromophenol blue). Samples in GITC or urea buffer were mixed in proportion 1:1 with 2x Laemmli Buffer. The samples, except for the one in urea were heated at 85 ºC for 5 minutes before loading on SDS-PAGE gels. The sample containing urea was loaded at room temperature.

2.9.2. Sodium dodecyl sulfate-polyacrylamide gel electrophoresis (SDS-PAGE)

Samples containing 50-100 μg of protein extract in 10 μl and Precision Plus Protein Dual Color (BIO-RAD 161-0374) molecular weight standards were loaded into the wells of a polyacrylamide gel. Electrophoretic separation was carried out using discontinuous buffer system in 8% (w/v) polyacrylamide gels containing 4% (w/v) stacking gel. Electrophoresis was performed at room temperature using a Mini-PROTEAN Tetra system tank (BIO-RAD 165-8001) and a PowerPac Basic power supply (BIO-RAD 164-5050) at constant current 10 mA per gel for 40 min and subsequently at 20 mA per gel for 1-2 h until the bromophenol blue front reached the end of the gel. Next, the gel was washed shortly with MQ water.

2.9.3. Alternative SDS-PAGE protocols

SDS-PAGE was also performed using different gels as follows:

- 4-15% linear gradient precast gels (BIO-RAD 161-1104)
- 8% (w/v) polyacrylamide gels containing 4M Urea
- 8% (w/v) polyacrylamide gels prepared using 0.5 M Tris-HCl (9.5 pH).

In all cases the electrophoresis was run in the same conditions as described in 2.9.2).

2.9.4. Two dimensional electrophoresis (2-DE)

Two dimensional electrophoresis (2-DE) was performed in a Protean IEF Cell System (BIO-RAD 165-4001) using nonlinear pH 3-10 (for *A. cepa* nuclear extract) or linear pH 4-7 (for *A. thaliana* extract) gel strips and SDS-PAGE gels. Protein extracts were precipitated with chlorophorm:methanol and resuspended in 2x Sample Buffer (7 M urea, 2 M thiourea, 4% CHAPS, 18.2 mM DTT and 3 μg/ml bromophenol blue). The gel strips were actively rehydrated at 50 V with 200 μg of the protein extract in the sample buffer for 12 h at 20ºC, and run at 20ºC. After running the first dimension, the gel strips were equilibrated in 2 ml of equilibration buffer (50 mM Tris-HCl pH 8.8, 2% SDS, 6 M urea, 30% glycerol) containing 52 mM DTT for 15 min and then in 2 ml of equilibration buffer containing 130 mM iodoacetamide for 15 min. The second dimension was resolved by standard 8% SDS-PAGE.

2.9.5. Coomassie Brilliant Blue staining

The gel was fixed overnight in 40% methanol: 10% acetic acid and then stained with Coomassie Brilliant Blue G-250 (BIO-RAD 161-0406) as described in Neuhoff et al. (1988). Coloidal Coomassie Brilliant Blue G-250 solution was prepared as described below. Gels were stained for 12 or 24 hours. Next the gels were washed few times in MQ water for 6h.

Coomasie Brilliant Blue solution

1. *5% Coomasie Brilliant Blue G-250 was prepared in 30 ml MQ water.*
2. *1.5 L of 10% ammonium sulphate was prepared and mixed with 30 ml of 85% sulphuric acid.*
3. *Coomasie Brilliant Blue G-250 was added slowly to ammonium sulphate and sulphuric acid on magnetic mixer and mixed for 30 min. The stock was stored in dark.*
4. *Before use the stock was mixed well on a magnetic mixer and methanol was added in proportion 1:4 methanol:stock.*

2.9.6. Protein transfer and western blot analysis

The gel was equilibrated for 10 min in transfer buffer (50 mM TRIS pH 8.2, 200 mM glycine, 20% methanol, 0.1% SDS). The electrotransfer was performed using a Mini-PROTEAN Tetra Cell with a Mini Trans-Blot module (BIO-RAD 170-3935). The immunoblot sandwich was assembled and proteins were transferred to PROTRAN nitrocellulose transfer membrane with 0.45 μm pores (Whatman 10401196) at 80 V for 1.5 h on ice.

After the transfer membranes were washed shortly in MQ water and stained with 2% Ponceau red (Sigma-Aldrich 7767) for a control of transfer efficiency, they were washed in 0.05% Tween-20 in PBS to remove the dye and blocked overnight in 10% (w/v) non-fat milk at 4 °C. Next, membranes

were washed shortly and incubated for 1 h in an antibody dilution; anti-AcNMCP1 at 1:1000, anti-tubulin (Sigma-Aldrich T9026) at 1:500 or anti-HRP (GenScript A00619) at 1:1000 and washed three times in blocking solution. Then the membranes were incubated for another hour with a peroxidase-coupled anti-rabbit or anti-mouse secondary antibody (Amersham NA931) at 1:3000 and washed three times in blocking solution and finally briefly washed in PBS. Negative controls were performed omitting incubation with a primary antibody. The reaction was revealed by the ECL system (Amersham RPN2209) according to manufacturer´s instructions. Determination of MW values for the reactive bands was done with the Quantity One 1-D analysis software (BIO-RAD).

2.9.7. Mass spectrometry

The scan of the 2-DE gel stained with Coomassie Brilliant Blue was compared with the results from 2-D immunoblots with anti-AcNMCP1 of an electrophoretic separation run in the same conditions, and the spots that corresponded to the detected proteins were selected. The selected spots were cut with an EXQuest Spot Cutter (BIO-RAD 165-7200). The excised spots were further cut in small pieces and destained in 50 mM ammonium bicarbonate/50% acetonitrile (ACN), dehydrated with ACN and dried. The gel pieces were rehydrated with 12.5 ng/mL trypsin solution in 50 mM ammonium bicarbonate and incubated overnight at 30 ºC. Peptides were extracted at 37 ºC using ACN 100% and, then 0.5% trifluoroacetic acid (TFA), dried by vacuum centrifugation, purified using ZipTip (Millipore) and, finally, reconstituted in 0.1% formic acid/2% ACN for HPLC sample injection.

The peptide mixtures from in-gel tryptic digestions were analyzed using nLC-MS/MS. The peptides were loaded onto a C18-A1 EASY-Column 2 cm, ID 100 μm, 5 μm precolumn (Proxeon SC001) and then eluted with a linear gradient of 2–99.9% ACN in 0.1% aqueous solution of formic acid.

The gradient was performed by a ThermoEasy-nLC (Proxeon LC120) at a flow-rate of 300 nL/min onto a NS-AC-11-dp3 Biosphere C18 capillary column, 75 um, 16 cm, 3 um (Nano Separations) to a stainless steel nano-bore emitter (Proxeon).

The peptides were scanned and fragmented with an LTQ-Orbitrap Velos (ThermoScientific). Mass spectra *.raw files were compared to AcNMCP1 sequence using SEQUEST search engine through Thermo Proteome Discoverer.

2.10. Immunofluorescence confocal microscopy

2.10.1. Nuclear fractions

Nuclear or nucleoskeleton fractions were fixed in 2% formaldehyde (FA) freshly prepared from paraformaldehyde (PFA) powder in PBS buffer (pH 7.4) containing 0.5% TX-100 for 30 minutes. Then samples were centrifuged at 2 500 rpm for 15 min and washed in PBS buffer containing 0.5% TX-100 for 30 min. Pellets were resuspended in 20 mM glycine and incubated for 30 min, then blocked in 2% BSA in PBS with 0.05% Tween-20 for 30 min. Next, the anti-AcNMCP1 antibody was added to the blocking solution to a final dilution 1:100, incubated overnight at 4 ºC in constant shaking and washed 3x 15 min in PBS with 0.05% Tween-20. Pellets were incubated with A488-coupled secondary antibody (Molecular Probes) at 1:100 for 45 min in the

dark at room temperature, washed 2x 15 min in PBS with 0.05% Tween-20 and stained with 1 μg/ml 4',6' diamidino-2-phenylindole (DAPI) to counterstain DNA in the nuclei. Pellets were washed again 3x 15min in PBS with 0.05% Tween-20. All steps were performed at room temperature and in constant shaking if not stated differently. The labelled fractions were layered onto 0.1% poly-L-lysine coated multi-wells slides, air dried and mounted with Vectashield (Vector H-1000).

Negative controls were prepared by omitting the primary antibody.

Samples were examined in a Confocal Microscope Leica TCS-SP2-AOBS, using the Leica-confocal software.

2.10.2. Whole cells

For immunofluorescence preparation of the whole cells, root meristems or root segments were fixed in 2% FA freshly prepared from PFA powder in PBS containing 1% TX-100 for 1 h and washed 3x 10 min with PBS. Next, tissues were digested for 45 min at 37 ºC with an enzyme cocktail containing 1% Pectinase (Serva 31660), 2% cellulase R10 (Serva 16419), 0.5% macerozyme R10 (Serva 28302) and 0.4 M mannitol (Merk 05983) in PBS pH 7.4. Samples were washed 2x 15 min in PBS then squashed onto 0.1% poly-L-lysine coated multi-wells slides and air dried. Blocking, incubation with antibodies and mounting were performed on wells as described in 3.12.1, changing anti-AcNMCP1 antibody dilution to 1:50.

Negative controls were prepared by omitting the primary antibody.

Samples were examined in a Confocal Microscope Leica TCS-SP2-AOBS, using the Leica-confocal software.

2.11. Electron microscopy

2.11.1. Pre-embedding immunogoldlabelling

Nuclei isolated from root meristems were fixed in 0.25% FA freshly prepared from PFA powder in PBS buffer pH 7.2 with 0.5% TX-100 for 30 min at 4 ºC, washed in PBS 2x 10 min and then blocked in 2% BSA in PBS buffer pH 7.2 for 30 min. The anti-AcNMCP1 antibody was added to the blocking solution to a final dilution of 1:50, and the nuclei were incubated overnight at 4 ºC then washed 3x 15 min in PBS with 0.05% Tween-20. Pellets were incubated with 5 nm gold conjugated anti-rabbit secondary antibody (Sigma-Aldrich G7277) (1:50) for 45 min at room temperature and washed 2x 15 min in PBS with 0.05% Tween-20. Then, the pellets were fixed in 2% FA in PBS buffer pH 7.2 for 1 h at 4 ºC, washed in PBS, embedded in 2% agarose and dehydrated in an ethanol series as indicated in table 11. Next, samples were embedded in LR White resin (London Resin) in three steps: **1**. 100% EtOH:LR White 2:1 for 2 h; **2**. 100% EtOH:LR White 1:2 for 2 h; **3**. LR White for 3 days changing resin each12h. Embedding was performed at 4 °C. Finally, samples were closed in gelatin capsules with resin and cured at 60 ºC for 20-22 h. Ultrathin sections

30% EtOH	30 min	4 °C
50% EtOH	30 min	4 °C
70% EtOH	overnight	4 °C
90% EtOH	1 h	4 °C
100% EtOH	45 min	4 °C
100% EtOH	45 min	4 °C
100% EtOH	45 min	4 °C

Table 11. Ethanol series used for dehydration of the sample.

were cut on an ultramicrotome with a diamond knife and mounted on nickel grids coated with a Formvar film. Samples were contrasted using 5% uranyl acetate and examined in a Jeol 1230 electron microscope at 80 kV. Negative controls were performed by omitting the primary antibody.

2.11.2. Post-embedding immunogoldlabelling

Nucleoskeleton fractions were fixed in 4% FA freshly prepared from PFA powder in PBS buffer pH 7.2 for 2 h at 4 ºC, then washed in PBS buffer pH 7.2 and embedded in 2% agarose. Samples were dehydrated in an ethanol series and then embedded in LR White resin (London Resin) and cured at 60 ºC as described in 2.11.1. Post-embedding immunogold labelling was performed on ultrathin sections mounted on nickel grids coated with a Formvar film. Blocking, incubations with the antibodies and washes were performed as in 2.10.1 changing the primary antibody dilution to 1:20. The samples were contrasted with 5% uranyl acetate and examined in a Jeol 1230 electron microscope at 80 kV. Negative controls were performed by omitting the primary antibody.

2.11.3. Conventional electron microscopy of *Arabidopsis thaliana*

Root tips from *Arabidopsis thaliana* (wild type, *linc1*, *linc2* single mutants and *linc1linc2* double mutant) were excised from two-week-old plants and fixed in 4% FA freshly prepared from PFA powder in PBS buffer pH 7.2 for 2h at 4 ºC. The samples were incubated in vacuum for 15 minutes at 4 ºC and then incubated on ice. The roots were washed in PBS buffer pH 7.2, dehydrated in an ethanol series as described in 2.11.1, then embedded in LR White resin

(London Resin) and cured at 60 ºC for 20-22 h. The zones of interest within the tissues were selected using semi-thin sections controlled under an optical microscope. Blocks containing the zones were prepared and cut on an ultramicrotome with a diamond knife to produce ultra-thin sections about 80–100 nm thick.

Ultrathin sections were mounted on nikel grids coated with a Formvar film, stained with 5% uranyl acetate and examined in a Jeol 1230 electron microscope at 80 kV.

2.12. Flow cytometry analysis

For estimation of DNA content by flow cytometry, various root segments were isolated and fixed for 30 min at 4 ºC in 2% (w/v) FA in TRIS buffer (10 mM TRIS pH 7.5, 10 mM EDTA, 100 mM NaCl) containing 0.1% TX-100. Then samples were washed 3x with TRIS buffer and homogenizated in lysis buffer (15 mM TRIS pH 7.5, 2 mM EDTA, 80 mM KCl, 20 mM NaCl, 0.1% TX-100) 3x 20 s with an Ultra-Turrax homogenizer IKA T25 with dispersor IKA S25-10G at 20 000 rpm. Next, homogenates were filtered through a 30 μm nylon-mesh. The nuclear suspensions were centrifuged at 2,500 rpm for 20 minutes at 4 ºC and resuspended in 300 μl of lysis buffer. Before the analysis the nuclei were incubated with RNaseA (Sigma-Aldrich R6513) at 30 μg/ml concentration for 30 minutes and stained with 20 μg/ml propidium iodide (Sigma-Aldrich P4170). After 10 min, flow-cytometry analysis was performed with an EPICS XL analyzer (Coulter) equipped with an argon laser tuned at 488 nm, and fluorescent signals from propidium iodide-labelled nuclei collected by a 620 nm band-pass filter.

RESULTS

1. Analysis of AcNMCP1 sequence and characterization of the NMCP protein family

1.1. AcNMCP1 sequence

The cDNA sequence of AcNMCP1 was obtained in RACE-PCR using RNA isolated from callus of *A. cepa* and B-degenerate primers. AcNMCP1 was predicted to contain 1,217 amino acids (3,998 bp) with a molecular weight (MW) of 139 kDa and an isoelectric point of 5.39 pH. The GenBank accession numbers are: for cDNA AB673103 and for amino-acid sequence BAM10996. The protein sequence is presented in figure 9. AcNMCP1 contains two stretches of basic amino acids (residues 1,010-1,014 and 1,041-1,046) that may function as nuclear localization signal (NLS). It also contains a stretch of negatively charged amino acids at the C-terminus (1,191-1,201) interrupted by a single methionine.

1.2. NMCP orthologs found in genomic searches

Genomic searches were performed to investigate if NMCP orthologs are commonly present in plants. The AcNMCP1 amino-acid and DNA sequences were used for BLASTP and BLASTX searches using Phytozome v8.0 database (Goodstein et al. 2012). The gene family with the highest score and e-value (2.2e-177 for DNA and 2.1e-123 for amino-acid sequence) was selected. The family was made up of 74 genes of which some were repeated and it also produced high scores using DcNMCP1 and AgNMCP1 sequences.

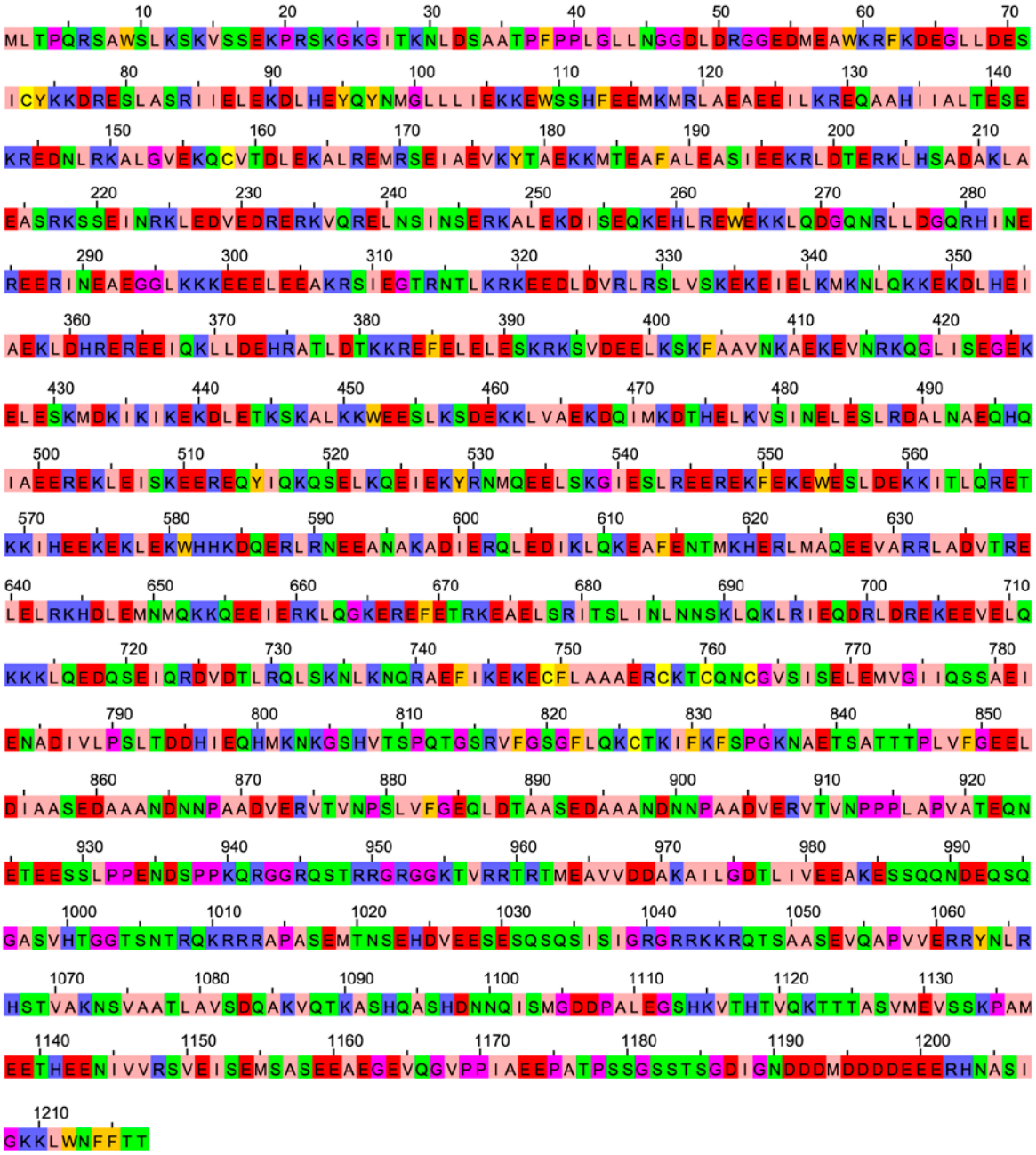

Figure 9. AcNMCP1 amino-acid sequence. The residues are coloured according to their physico-chemical properties as follows: aliphatic/hydrophobic residues (I, L, V, A, M)- pink; aromatic (F, W, Y)- orange; positive (K, R, H)- blue; negative (D, E)- red; hydrophilic (S, T, N, Q)- green; proline/ glycine (P, G)- magneta; cysteine (C)- yellow. The figure was made in Jalview.

The matches represented 27 out of 31 plant genomes. The following species lacked NMCP homologs: *Volvox carteri* and *Chlamydomonas reinhardtii* (unicellular algue), *Selaginella moellendorffii* (clubmoss) and *Medicago truncatula* (a dicot). In the selected gene family were included ORFs from a moss (*Physcomitrella patens*) and from various monocot and dicot species listed in table 12. Most species, including moss had at least two genes encoding NMCPs. The proteins were initially classified as NMCP1 or NMCP2 based on the sequence similarity to the previously described carrot and celery NMCP1 and NMCP2. Most dicot species had one additional gene encoding NMCP1-related protein, that was designated NMCP3. Few dicots contain two genes ORFs encoding NMCP3 proteins.

Additional BLASTP searches against non-redundant protein sequence databases (nr) of the species that lacked NMCP homologs were performed on NCBI webpage. The NMCP sequences of *Glycine max* were used in the search against *Medicago* nr database since soya was phylogenetically the most related species with known NMCP orthologs and the sequence similarity was expected to be high. The *Physcomitrella* NMCP sequences were used in the search against *Volvox*, *Chlamydomonas* and S*elaginella* nr databases. One short sequence with high similarity to NMCP was identified in *Medicago* (MtrA; ACJ86244.1) and two in *Selaginella* (SmoA; XP_002993584.1 and SmoB; XP_002992724.1). The matched sequences were shorter than the typical length of NMCP but included highly conserved regions in the rod domain which suggested that *Selaginella* and *Medicago* expressed NMCP proteins but the sequence entries were not complete (Fig. 10). Two additional sequences showed significant similarity to NMCP in *Medicago* but they did not contain the highly conserved motifs characteristic for the family therefore were not

Species	NMCP homologs		
Allium cepa	AcNMCP1		?
Apium graveolens	AgNMCP1	?	AgNMCP2
Aquilegia coerulea	Aco1		Aco2
Arabidopsis lyrata		Aly3	
Arabidopsis thaliana	LINC1	LINC2/3	LINC4
Brachypodium distachyon	Bdi1		Bdi2
Brassica rapa	Bra1	Bra3	Bra2
Capsella rubella	Cru1	Cru3	Cru2
Carica papaya	Cpa1	Cpa3	
Citrus clementina	Ccl1		Ccl2
Citrus sinensis	Csi1	Csi3	Csi2
Cucumis sativus	Csa1	Csa3	Csa2
Daucus carrota	DcNMCP1	DcNMCP3/4	DcNMCP2
Eucalyptus grandis	Egr1	Egr3	Egr2
Glycine max	Gma1	Gma3	Gma2
Linum usitatissimum	Lus1	Lus3	Lus2
Malus domestica	Mdo1	Mdo3	Mdo2
Manihot esculenta	Mes1	Mes3	Mes2
Mimulus guttatus	Mgu1	Mgu3	Mgu2
Oryza sativa	Osa1		Osa2
Phaseolus vulgaris	Pvu1	Pvu3	Pvu2
Physcomitrella patens			Ppa1, Ppa2
Populus trichocarpa	Ptr1	Ptr3	Ptr2
Prunus persica	Ppe1	Ppe3	Ppe2
Ricinus communis	Rco1	Rco3	Rco2
Setaria italica	Sit1		Sit2
Sorghum bicolour	Sbi1		Sbi2
Thellungiella halophila	Tha1	Tha3	Tha2
Vitis vinifera	Vvi1	Vvi3	Vvi2
Zea mays	Zma1		Zma2

Table 12. NMCP proteins found in genomic searches and the previously described proteins in carrot and celery. The species are listed alphabetically. Most contain at least two NMCP proteins. The NMCP3 proteins in *Apium graveolens* have not yet been described and the genomes of these species are not available (?).

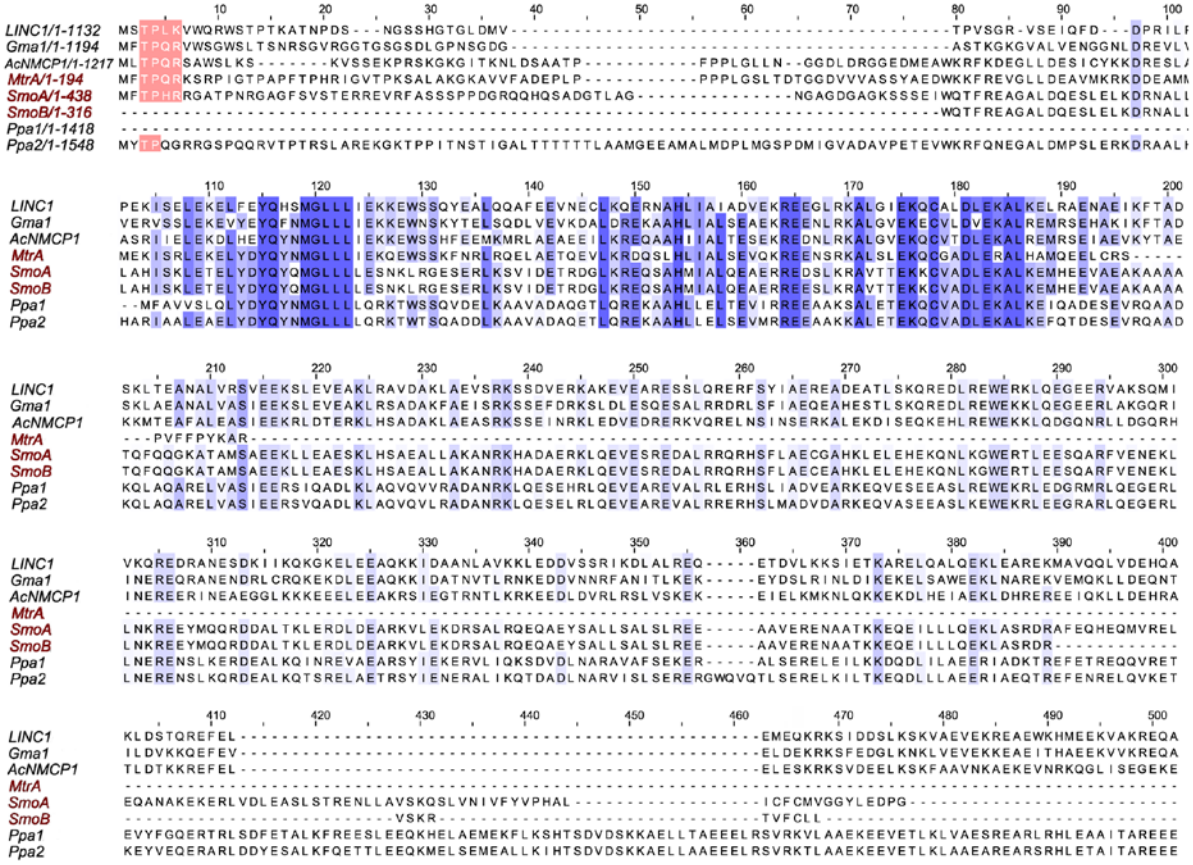

Figure 10. The alignment of Ppa1, Ppa2, Gma1, AcNMCP1, AtNMCP1/LINC1 sequences and partial sequences of NMCP orthologs in *Medicago* and *Selaginella*. The conserved phospohorylation site at the N-terminus of NMCP proteins marked with pink boxes. The most conserved residues are marked in dark blue, the less conserved in light blue. Short sequences MtrA (ACJ86244.1), SmoA (XP_002993584.1) and SmoB (XP_002992724.1) (marked in red) were found in BLAST search against nr databases and contain the conserved phosphorylation site and the conserved region between 105-200 residues, but do not represent full NMCP sequences. The alignment was generated using ClustalW2 and the figure was made using Jalview.

listed. The searches against *Volvox* and *Chlamydomonas* did not give significant results. Also, in searches against animal, yeast or bacteria genome databases no significant matches were found.

The genomic searches revealed that NMCP proteins are present in land plants. No sequences showing high sequence similarity were found in animals or single cell organisms suggesting NMCP family is plant-specific.

1.3. Phylogeny and NMCP family classification

Phylogenetic analyses were performed to determine the relationships between NMCP proteins. A phylogenetic tree of NMCP family was constructed using Neighbour-Joining Method (NJ) in MEGA5 (Fig. 11). NJ is a widely used distance matrix method which searches for minimum pairwise distances according to the distance metric, and also for sets of neighbors that minimize the total length of the tree. As shown on the phylogenetic tree the whole family can be divided into two clusters. The two *Physcomitrella patens* NMCPs evolved from the common *NMCP* progenitor gene and are included in the NMCP2 cluster suggesting the archetypal NMCP progenitor was an NMCP2 protein. In vascular plants NMCPs evolved from two genes: *NMCP1* progenitor and *NMCP2* progenitor. Monocots contain one NMCP1 protein but most dicots (18 out of 20) contain two: NMCP1 and NMCP3 which evolved separately. *A. thaliana* has three *NMCP1* genes (previously reported as *LINC1*, *LINC2*, *LINC3*) from which AtNMCP1/LINC1 protein is closely related to NMCP1 and LINC2 and LINC3 are related to NMCP3. Our recent analysis conducted using the latest data suggests that species closely related to *Arabidopsis thaliana*; *Capsella rubella* and *Brassica rapa*, as well as *Dacus carota* also contain two NMCP3-type proteins. On the other hand, two species: *Solanum tuberosum* (potato) and *Solanum lycopersicum* (tomato) lack NMCP3-type protein and express two NMCP1 proteins (not included in Fig. 11). In *Arabidopsis lyrata*, which is closely related to *A. thaliana* only one NMCP was detected

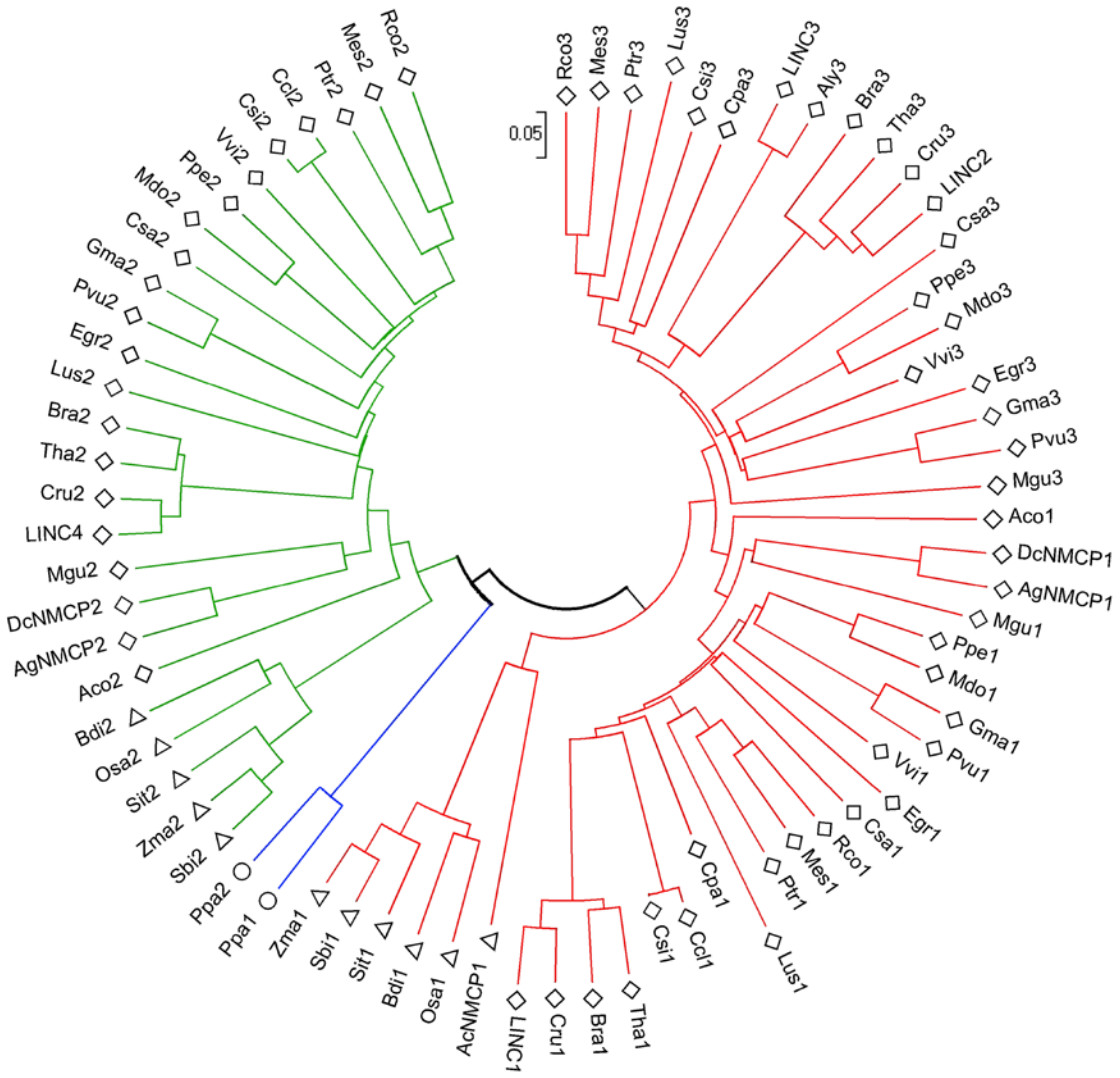

Figure 11. Evolutionary relationships of NMCP protein family. Phylogenetic relationship of NMCPs inferred using the Neighbour-Joining method. Evolutionary distances were calculated using the p-distance method and are presented as the number of amino-acid differences per site. The phylogenetic tree is drawn to scale. Sequences belonging to the NMCP1 cluster are marked in red, the ones belonging to NMCP2 cluster in green, the two members in *Physcomitrella patens* in blue. Dicotyledon species are represented by rhombi; monocotyledons by triangles, and moss by circles.

which was an NMCP3-related protein (closely related to LINC3; see on the phylogenetic tree Fig. 11) suggesting that the available *A. lyrata* genome version is not complete.

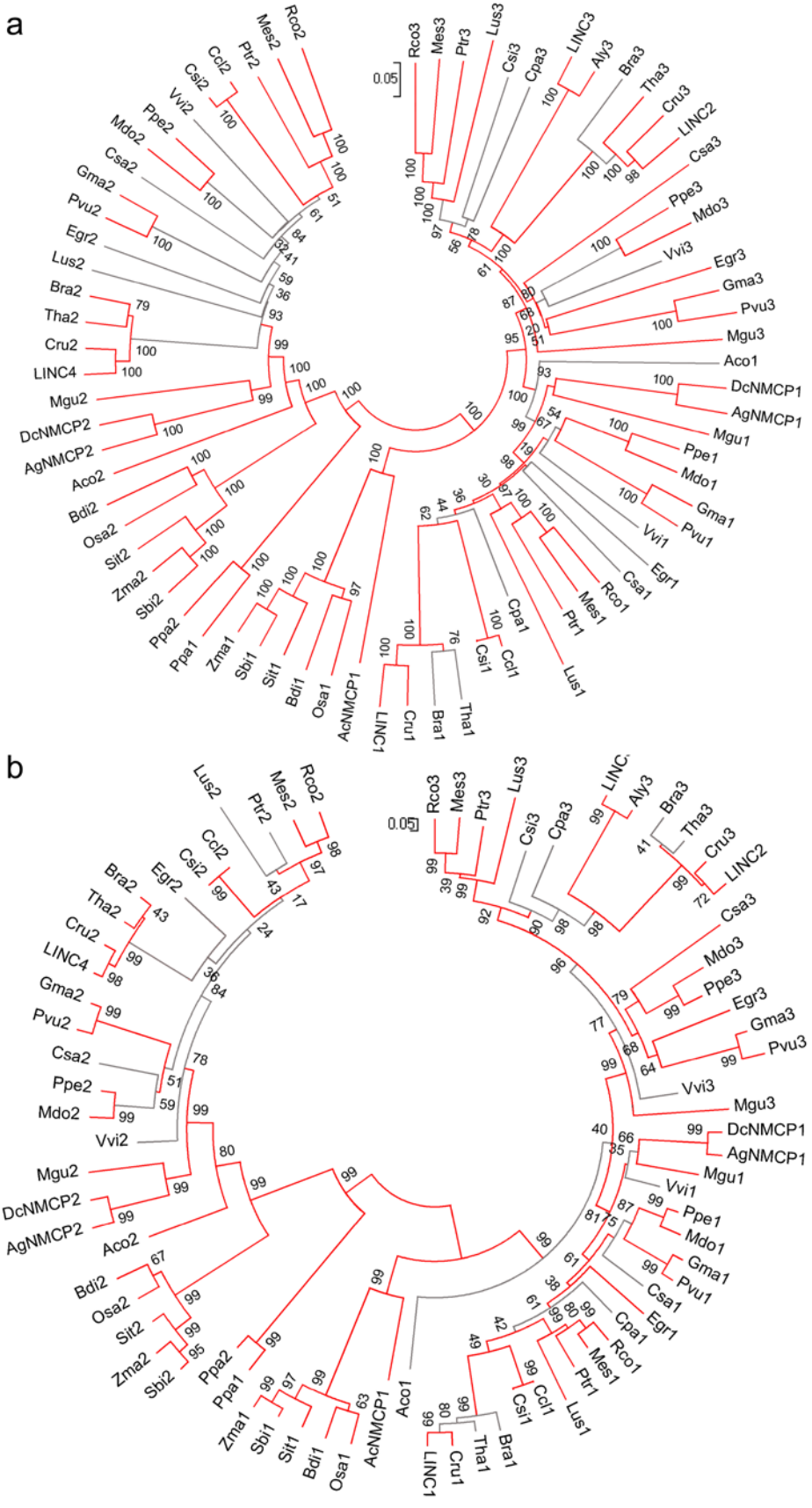
a
0.05
Rco2
Mes2
Ptr2
Ccl2
Csi2
Vvi2
Ppe2
Mdo2
Csa2
Gma2
Pvu2
Egr2
Lus2
Bra2
Tha2
Cru2
LINC4
Mgu2
DcNMCP2
AgNMCP2
Aco2
Bdi2
Osa2
Sit2
Zma2
Sbi2
Ppa2
Ppa1
Zma1
Sbi1
Sit1
Bdi1
Osa1
AcNMCP1
LINC1
Cru1
Bra1
Tha1
Csi1
Ccl1
Lus1
Cpa1
Mes1
Ptr1
Rco1
Csa1
Egr1
Vvi1
Pvu1
Gma1
Mdo1
Ppe1
Mgu1
AgNMCP1
DcNMCP1
Aco1
Mgu3
Pvu3
Gma3
Egr3
Vvi3
Mdo3
Ppe3
Csa3
LINC2
Cru3
Tha3
Bra3
Aly3
LINC3
Cpa3
Csi3
Lus3
Ptr3
Mes3
Rco3
b
0.05
Lus2
Rco2
Mes2
Ptr2
Ccl2
Csi2
Egr2
Bra2
Tha2
Cru2
LINC4
Gma2
Pvu2
Csa2
Ppe2
Mdo2
Vvi2
Mgu2
DcNMCP2
AgNMCP2
Aco2
Bdi2
Osa2
Sit2
Zma2
Sbi2
Ppa2
Ppa1
Zma1
Sbi1
Sit1
Bdi1
Osa1
AcNMCP1
Aco1
LINC1
Cru1
Bra1
Tha1
Csi1
Ccl1
Lus1
Cpa1
Mes1
Ptr1
Rco1
Csa1
Egr1
Vvi1
Pvu1
Gma1
Mdo1
Ppe1
Mgu1
AgNMCP1
DcNMCP1
Vvi3
Mgu3
Pvu3
Gma3
Egr3
Ppe3
Mdo3
Csa3
LINC2
Cru3
Tha3
Bra3
Aly3
LINC3
Cpa3
Csi3
Lus3
Ptr3
Mes3
Rco3

All analysed plants have one gene encoding NMCP2. In *A. thaliana* a protein previously described as chloroplast protein LINC4 was classified as NMCP type 2.

Based on sequence and structure analogies as well as phylogenetic relationships between NMCPs we propose a classification of the protein family into two clusters; one that includes NMCP1 proteins and the second that includes NMCP2.

The phylogenetic relationships between NMCP members were verified constructing a phylogenetic tree with another widely used method: Maximum Likelihood (ML). This method is probabilistic and it evaluates every possible tree topology. It also searches for the optimal choice by assigning probabilities to every possible evolutionary change and by maximizing the total probability of the tree. The ML analysis is thorough but very time consuming and for this reason the NJ method is more often used. The comparison of the phylogenetic trees generated using both methods and bootstrap test values are presented in figure 12.

As seen in the figure 12 phylogenetic interferences using both methods were mostly in agreement, and the main relationships between NMCPs were confirmed. NMCP1 and NMCP2 proteins evolved separately in vascular plants and both *Physcomitrella patens* orthologs seemed to be NMCP2-related suggesting the archetypal origin of the latter.

Figure 12 (on the left). Comparison of the phylogenetic trees obtained using the NJ and ML methods. Presentation of phylogenetic trees constructed using Neighbour-Joining (NJ; **a**) and Maximum Likelihood (ML; **b**) methods. Both phylogenetic trees were generated in MEGA5 suite. The relationships confirmed by both methods are marked in red and the relationships that differed in grey. The values of bootstrap test are indicated in both phylogenetic trees.

1.4. Distribution of predicted coiled coils in NMCPs

Previously described NMCP proteins were predicted to contain a central domain forming coiled coils and mediating dimerization. This structure is similar to the highly conserved structure of IF proteins. To investigate if the predicted structure was conserved across the NMCP family coiled-coil prediction was performed using all available NMCP sequences.

To select the most suitable method for coiled-coil prediction and to optimize program parameters a control analysis on a set of lamin sequences was performed. Methods used for the analysis included MARCOIL, COILS, Multicoil and Multicoil2. The method that produced most accurate prediction was MARCOIL (with cut-off set at 0.6) and was used for prediction of NMCP structures. The comparison of the coiled-coil prediction methods on human lamin A amino-acid sequence (GenBank: NP_733821.1) is presented in figure 13.

Predictions were generated for 76 NMCP sequences, including the sequences collected in the genome searches and the proteins previously described in carrot, celery and *A. thaliana*. The coiled-coil domain prediction confirmed that all NMCPs contain a central coiled-coil domain.

NMCP sequences can be classified into two classes based on sequence similarity and predicted structure. The rod domains of most NMCPs type 1 (31 out of 49; 64%) contain two segments of coiled coils of similar lengths (first coil between 250 and 300 residues and the second between 350 and 400). The segments are separated by a short linker (approximately 20 residues), that is not detected by MARCOIL in seven out of 49 NMCP1 members (14%). In nine sequences (18%) the MARCOIL analysis revealed a short linker inside the second segment dividing it into two coils of around 200 and 150 residues, respectively. The predicted structure of NMCP2 members resembled the

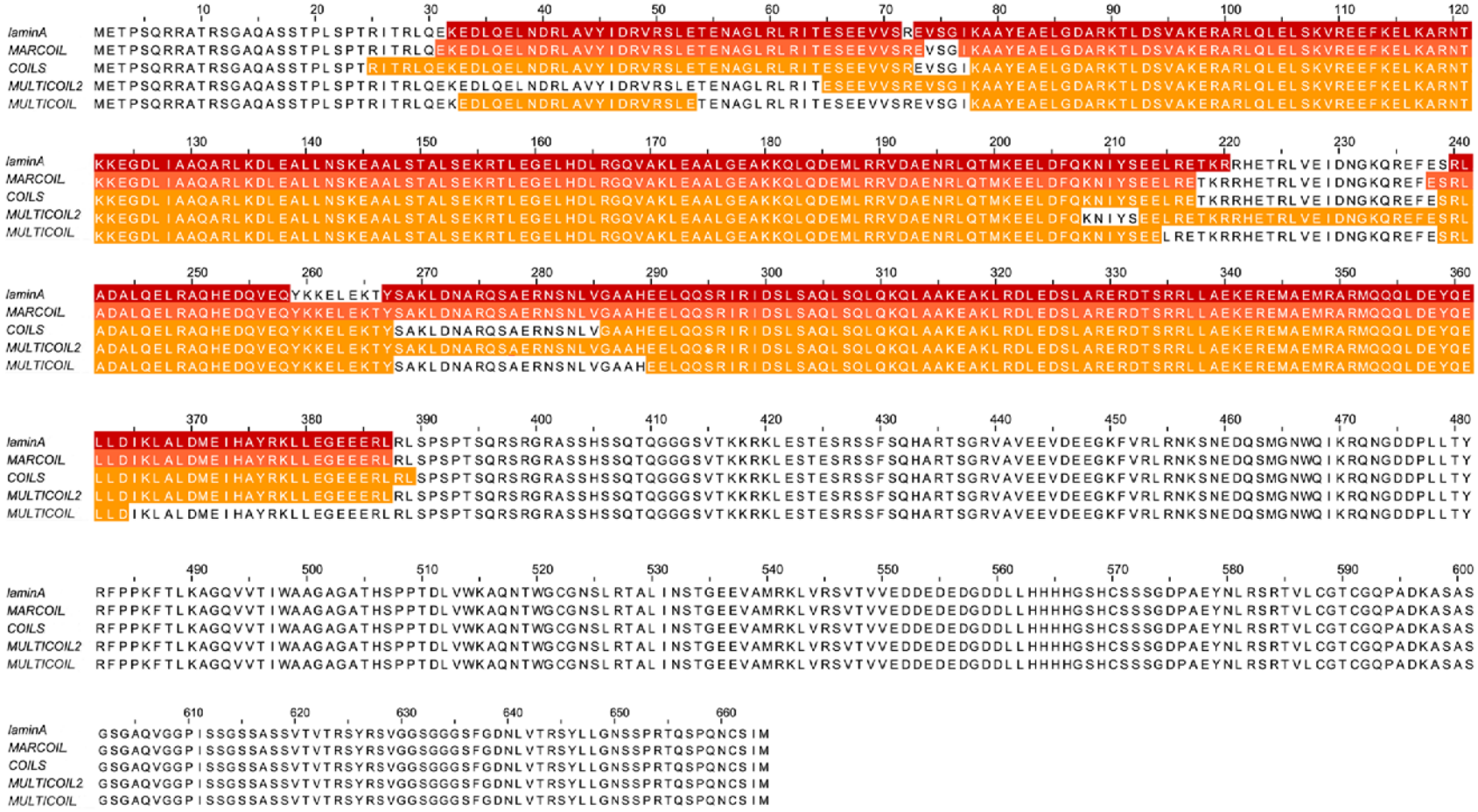

Figure 13. Comparison of coiled-coil prediction tools. Coiled-coil prediction performed on lamin A sequence using different tools (coiled coils marked as orange boxes). Confirmed positions of coiled-coil regions were taken from Human Intermediate Filament Database (http://www.interfil.org/). The confirmed structure is marked in red and predicted coiled-coil segments are marked as orange boxes. The prediction by MARCOIL is the most precise although it did not reveal the L2 linker. Figure was made using Jalview.

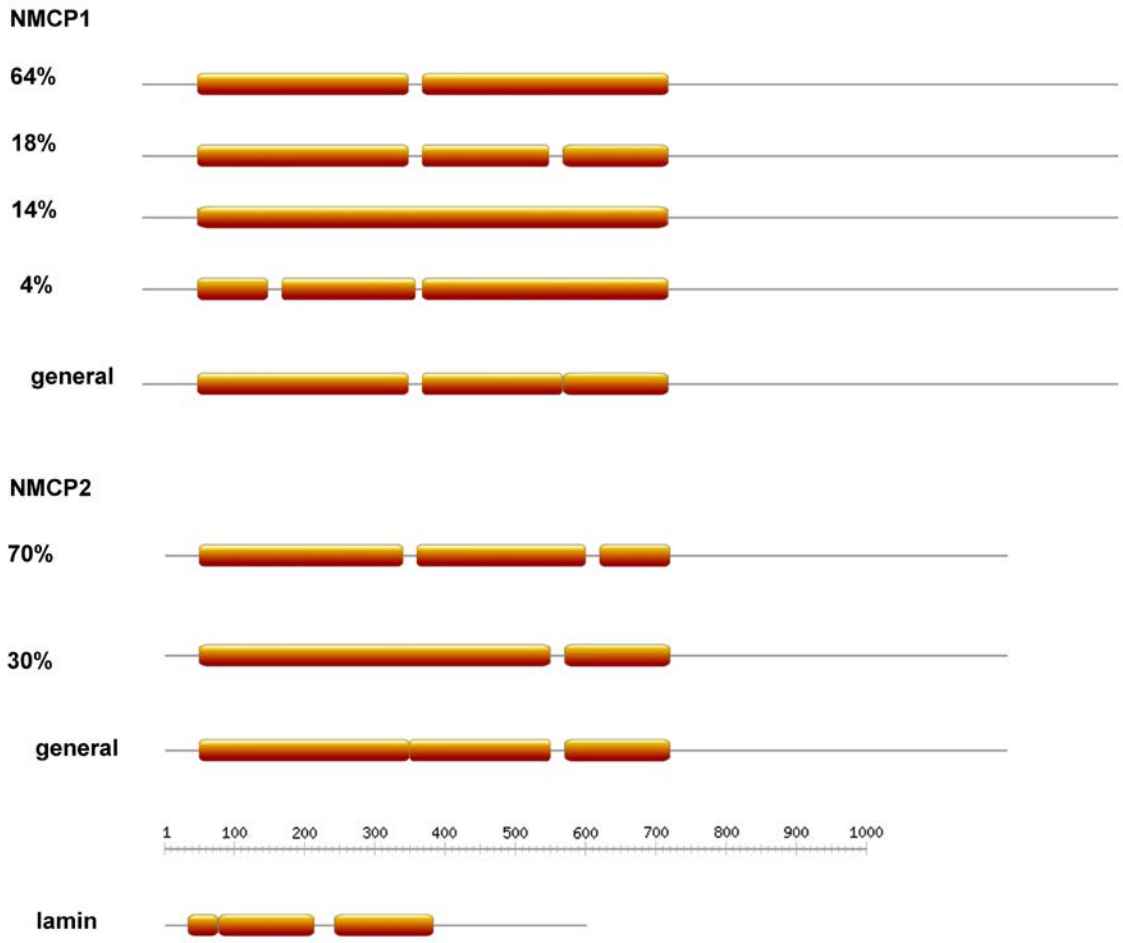

Figure 14. Schematic representation of the predicted coiled-coil structure of NMCP proteins and lamins. Prediction of the coiled coils was performed using MARCOIL with a cutoff set at 0.6. Medium lengths of the sequences are presented to scale with grey lines, coiled-coil segments are represented as orange boxes. Most NMCP1 proteins contain a rod domain consisting of two coiled coils of similar lengths which resemble the coiled coil arrangement in lamins. In several sequences the program did not predict any linker or an additional linker in the second coiled coil. Most NMCP2 proteins contain three coiled coils, the position of the first linker corresponds to the linker in NMCP1. In several NMCP2 sequences MARCOIL did not predict this linker.

latter arrangement although in eight out of 27 sequences (30%) the linker between the second and the third coils was not detected (Fig. 14).

The sequences of NMCPs in *Physcomitrella patens* are longer than other NMCP proteins (Ppa1- 1,418 aa; Ppa2- 1,548 aa). They contain inserts in rod (insert

of around 200 aa) and tail domains showing no sequence similarity with other NMCPs. This insertion resulted in a unique distribution of coiled-coils and different positions of linkers in Ppa proteins. Since no other NMCP sequences in non-vascular land plants are known we cannot determine if it is a feature of archetypal NMCPs or a result of adaptation in *Physcomitrella*.

The positions of the linkers in the rest of NMCP1 and NMCP2 proteins corresponded, suggesting that the structure of the rod domain is conserved across the NMCP family. The prediction of coiled-coils is an approximation based on an algorithm and the lack of the predicted linkers in some sequences does not mean these sequences lack it but that the distortion in the coiled-coil heptad pattern is not as significant as in other sequences. In lamins MARCOIL predicted the linker L12 between coil 1 and coil 2 but linker L1 was predicted only in few sequences and linker L2 in none (Fig. 14). Linkers L1 and L2 are shorter (7 aa) in comparison with L12 (20 aa) and although they interrupt the heptad periodicity they are likely to adopt an α-helical conformation which makes the computational analysis more difficult. In fact linker L1 is thought to form a continuous coiled coil with segments 1A and 1B. On the other hand, MARCOIL always predicted correctly the start and the end of lamin coiled-coil rod domains and the predictions were more precise than for Multicoil or Multicoil2. This, together with the fact that the start and the end of the NMCP coiled-coil domain were conserved in all NMCPs strengthens the assumption that the rod domain is conserved across the NMCP family and that it could play an important role in oligomerization.

The oligomerization state predicted by Multicoil2 indicated that all coiled-coil regions have a high probability of forming dimers.

The coiled-coil prediction confirmed that all NMCPs contain a central coiled-coil domain with conserved structure which is predicted to dimerize. Until

today, no structure of NMCP is available in PDB database. Hopefully, in the future the predicted structures will be verified by structural biology methods.

1.5. Conserved motifs in NMCPs

Multiple sequence alignment confirmed all NMCPs share high degree of sequence similarity along the central rod domain. IF proteins also share high sequence similarity along the coiled-coil domain, and at both extremes of this domain they contain highly conserved regions which probably play an important function in oligomerization and filament formation. To find the conserved regions characteristic for the NMCP family a search using MEME (Bailey et al. 2009) was performed. The MEME form allowed analysis of 54 NMCP sequences at a time. NMCP1 and NMCP2 sequences from various species were selected and the presence and positions of the conserved regions was confirmed in the rest of the sequences. The MEME search detected multiple conserved motifs within the rod domain (see Fig. 15) and several in the tail domain although the general sequence similarity in the tail domain was relatively low. Selected regions with high e-value and conserved localization are shown in figure 5 and listed in table 13. Regions conserved across all NMCPs are located at the extremes of the rod domain (region 1 at the N-extreme followed by region 2 and at the C-extreme region 5) and inside the second coil, just before the second linker (region 4).

Region 3 which includes the linker separating two coils is conserved in all NMCPs except for those in *Physcomitrella patens*. This can be caused by the different distribution of coiled coils in these proteins. Region 7 was present only in NMCP1 proteins suggesting it is involved in functions specific for this group. Region 8 was present in NMCP1 cluster and monocot NMCP2 but

was absent from dicot NMCP2 which coincides with the appearance of NMCP3 proteins, and may suggest this new protein class took up some of the functions played by NMCP2. This region was preceded by a stretch of acidic amino acids.

The search also revealed a stretch of basic amino acids in the tail domain of NMCP1 proteins which can function as nuclear localization signal (Kalderon et al. 1984). The predicted NLS is followed by the conserved region 7. The region 6, on the other hand is followed by consensus sequence recognized by cdk1 kinase SPXK/R (Blom et al. 2004).

A NucPred prediction indicated that almost all (62 out of 76) NMCPs contain NLS consensus sequence although its localization and pattern was only conserved in NMCP1-type proteins. In the search for possible conserved post-translational modification sites a few phosphorylation sites for cdk1, PKA and PKC were found in the head and tail domains (Fig. 15).

The analysis revealed that the distribution of conserved regions at the extremes of the rod domain is similar to that in IF proteins. This may suggest NMCP proteins could oligomerize and form filaments in a mechanism similar to that of IF. MEME search also revealed highly conserved regions in the tail domain that probably play important functions and an NLS conserved across NMCP1-type proteins.

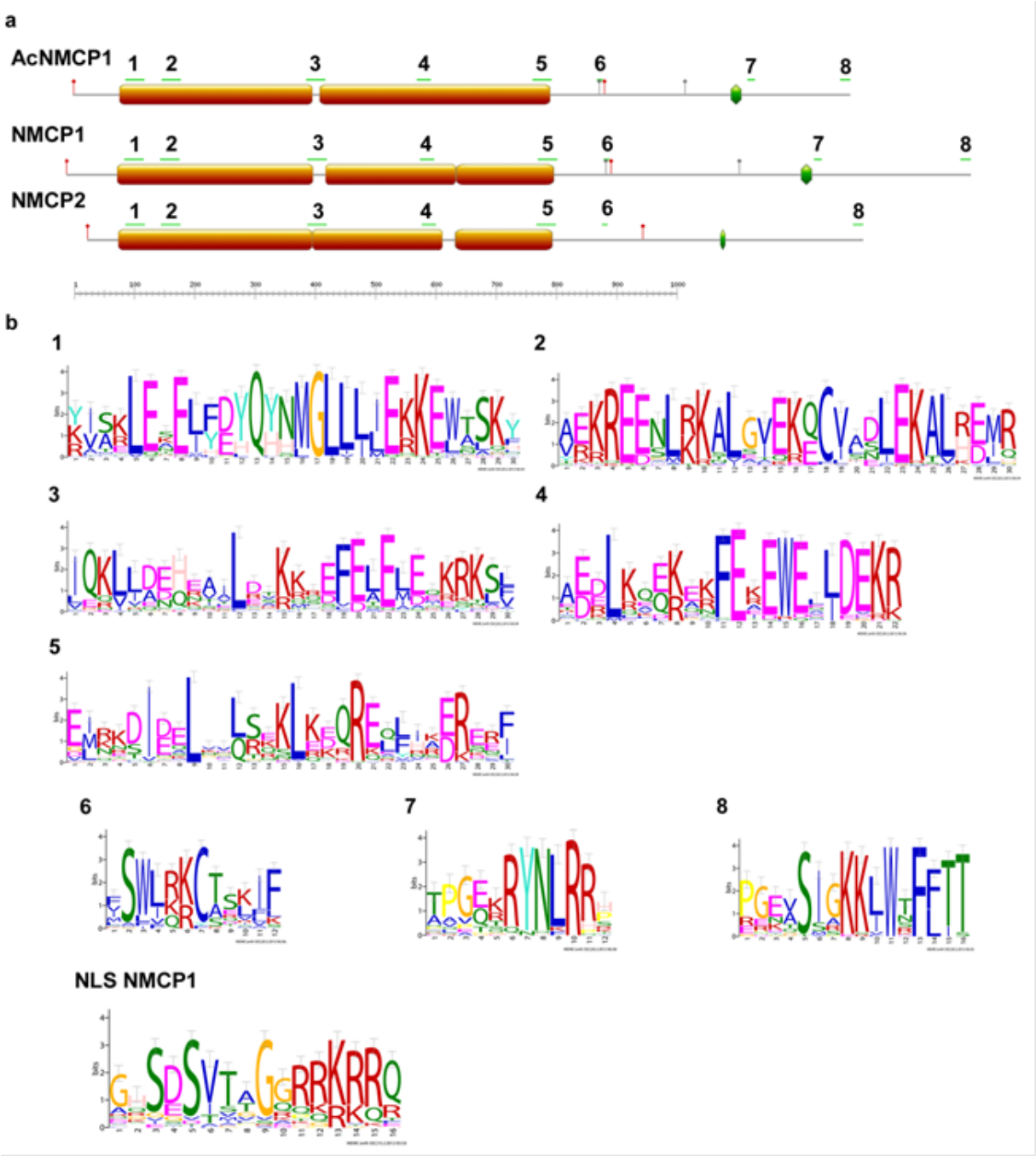

Figure 15. Conserved regions and phosphorylation sites in NMCP proteins. a. Schematic representation of conserved regions, predicted NLSs (green boxes) and phosphorylation sites (red bar, cdk1; grey bar, PKA/PKG) in AcNMCP1, and in NMCP1 and NMCP2 types. Localization of the conserved regions is indicated by green bars with corresponding numbers. Coiled coils are represented as orange boxes. **b** MEME motifs displayed as "sequence LOGOS". The height of each letter reflects the probablility of its localization at this position. Letters are coloured using the same colour scheme as the MEME motifs based on the biochemical properties of the amino acids.

Region	NMCP1	NMCP2	Ppa
1	yes	yes	yes
2	yes	yes	yes
3	yes	yes	no
4	yes	yes	yes
5	yes	yes	yes
6	yes	yes	no
7	yes	no	no
8	yes	monocot	yes

Table 13. List of conserved motifs characteristic for the NMCP family. Regions were found using MEME program. The motifs conserved in all NMCPs are regions 1, 2, 4 and 5; regions 3 and 6 were absent in *Physcomitrella patens*; region 7 in NMCP2 and *P. patens* proteins and region 8 was not present in dicot NMCP2 proteins but was present in monocots.

1.6. Characteristic features of NMCP family

NMCP proteins make up a highly conserved plant-specific protein family. They share high degree of sequence similarity (Fig. 16) and have a conserved tripartite structure resembling the one in IF proteins. The structure contains a central rod domain that is predicted to form coiled coils and to dimerize and non-coiled-coil head and tail domains. The rod domain is highly conserved and contains multiple conserved motifs localized at the N- and C- extremes and at the positions of predicted linkers. Also, conserved cdk1 phosphorylation sites are localized in proximity to the extremes of the rod

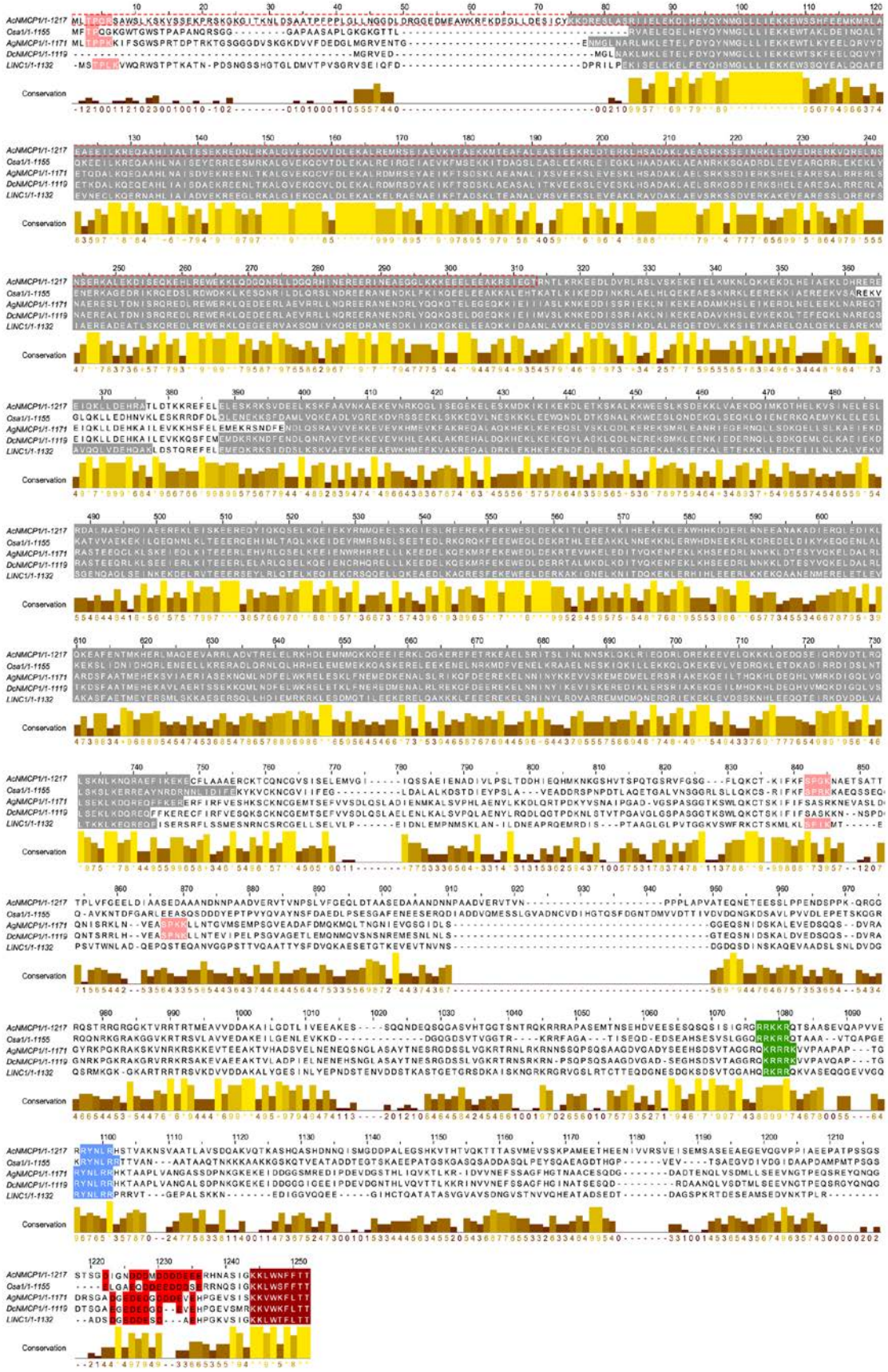
AcNMCP1/1-1217
Csa1/1-1155
AgNMCP1/1-1171
DcNMCP1/1-1119
LINC1/1-1132
Conservation

domain. Several conserved motifs were also found in the tail domain, although in general it does not show high degree of sequence similarity. In the tail domain a stretch acidic amino acids is also present except for dicot NMCP2. Most NMCP proteins contain an NLS consensus sequence in the tail domain. The members of the NMCP protein family can be divided into two clusters based on phylogenetic relationships, sequence similarity and predicted structure.

Figure 16 represents NMCP features revealed by bioinformatics analysis on several well described NMCP1 sequences and AcNMCP1.

The bioinformatic analysis of NMCP family revealed many analogies to metazoan lamins. Their similar structure and distribution of highly conserved regions may suggest NMCPs could play some functions similar to those played by lamins.

Figure 16 (on the left). NMCP1 sequence similarity. The NMCP1 sequences from *Oryza sativa* (Osa1; LOC_Os02g48010), *Apium graveolens* (AgNMCP1; BAI67715.1), *Daucus carota* (DcNMCP1; BAA20407) and *Arabidopsis thaliana* (LINC1; NP_176892.1) were aligned with that of AcNMCP1 (BAM10996.1) using ClustalW2 (Larkin et al. 2007) and edited in Jalview (Waterhouse et al. 2009). The coiled-coil segments predicted using MARCOIL (Delorenzi and Speed 2002) are shaded in grey, the cdk1 consensus sequences in pink, the predicted NLSs in green, the NMCP1-specific conserved regions in blue and brown and the stretch of acidic amino acids in red. The degree of conservation is represented by yellow and brown bars beneath the alignment (generated by Jalview). The region of AcNMCP1 used for antibody production is contained in a red dotted box.

2. Protein characterization

2.1. Detection of endogenous NMCPs by Western blotting

2.1.1. Detection of endogenous NMCP in various species

For the identification of endogenous AcNMCP1 an antibody was raised against the N-terminal part of the protein that includes the highly conserved regions 1 and 2 (figure 16). The cross-reactivity of the antibody was evaluated in monocot species: *Allium cepa, Allium sativum, Triticum aestivum, Secale cereale, Zea mays* and in the dicots: *Arabidopsis thaliana, Nicotiana benthamiana* and *Pisum sativum*. In western blots the antibody specifically recognised bands in all species except for *Nicotiana benthamiana*. The antibody raised against a highly conserved region specifically recognised in immunoblots proteins with different molecular weights in various species. In onion the molecular weight of the detected band was higher than expected. No bands were detected in negative controls when the incubation with the primary antibody was omitted which indicates that there was no non-specific binding of the secondary antibody.

Although the NMCP transcripts were similar in size; generally between 3,300-3,600 bp (1,100-1,200 aa) for NMCP1 and 2,700-3,000 bp (900-1000 aa) for NMCP2 (Addendum) the molecular weights of the detected bands were variable across the species (figure 17). In *Arabidopsis thaliana* the antibody recognised a major band of 150 kDa sometimes visible as a doublet roughly corresponding to the predicted MW of AtNMCP/LINC proteins (120-130 kDa; www.arabidopsis.org). In monocots such as garlic, wheat and rye the antibody cross-reacted with proteins of 100 kDa, while in maize the antibody

recognised a triplet of about 80 kDa. In pea a major band of similar size (70 kDa) to one of the proteins highly resistant to urea and localized in pea peripheral nuclear matrix was detected (Blumenthal et al. 2004). The diversity of MWs across species may indicate that NMCP proteins undergo alternative splicing and/or post-translational modifications.

In onion the antibody recognised a major band of 200 kDa though some minor bands between 150 and 100 kDa were also observed. The presence and intensity of the minor bands varied between experiments suggesting that they were proteolytic products.

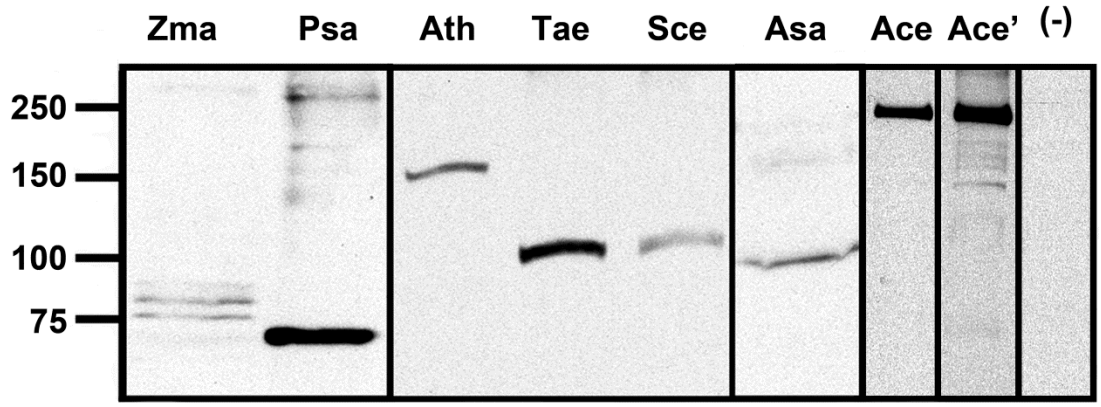

Figure 17. Immunoblot detection of NMCP proteins in various species. Immunoblot was performed using the anti-AcNMCP1 antibody and detected bands in monocots: *Zea mays* (Zma; 80 kDa), *Triticum aestivum* (Tae; 100 kDa), *Secale cereal* (Sce; 100 kDa), *Allium sativum* (Asa; 100 kDa) and *Allium cepa* (Ace, Ace´) and in dicots: *Pisum sativum* (Psa; 70 kDa) and *Arabidopsis thaliana* (Ath, 150 kDa). In onion the antibody recognised a major band of 200 kDa (Ace) but in longer exposures also lower bands (between 100 and 150 kDa) were visible (Ace´). No bands were detected in negative controls when the incubation with the primary antibody was omitted (-).

2.1.2. Influence of various conditions favouring protein denaturation on AcNMCP1 band migration

The molecular weight of the band detected with anti-AcNMCP1 in onion was 60 kDa higher than the predicted value (139 kDa). Also, as shown in immunoblot analysis, when a high amount of protein was loaded on gel, AcNMCP1 aggregated in the upper part of the gel (Fig. 18 a). Similar results were obtained when a high amount of the isolated peptide used for antibody production was separated in conventional electrophoresis (Fig. 18 b). Together, these results suggested that the high molecular weight of the band could be caused by a high tendency to dimerize and to form higher order oligomers even in the presence of SDS. This feature is characteristic for many

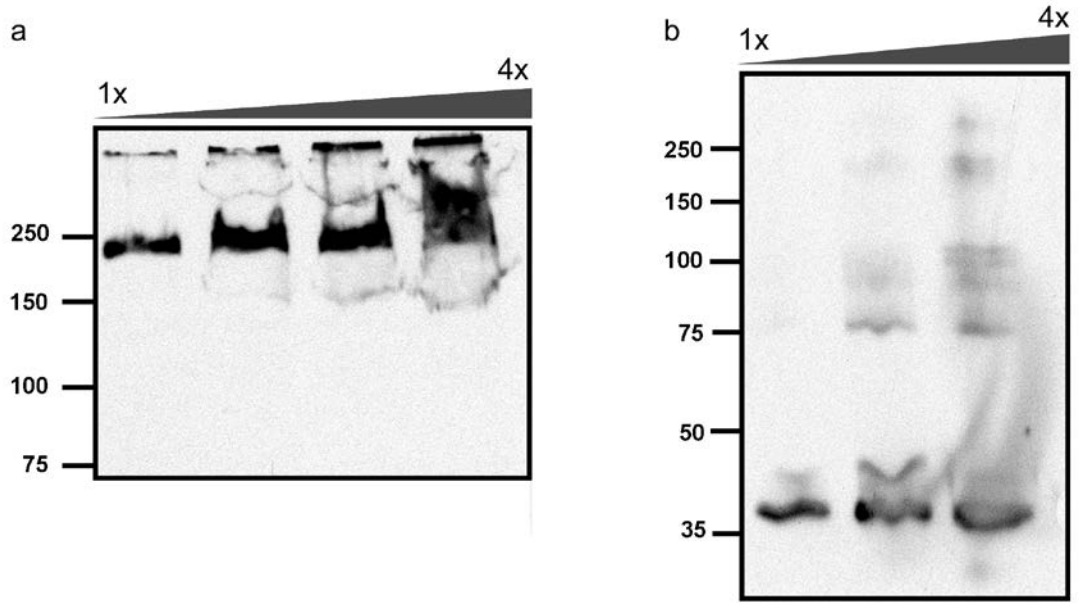

Figure 18. AcNMCP1 forms aggregates in the upper part of the gel at high concentrations. **a** Immunoblot displaying increasing amounts of the onion nuclear protein loaded on an 8% SDS-PAGE gel (from 1x to 4x). In the upper part of the gel aggregates of AcNMCP1 protein were visible. **b** Immunoblot displaying different amounts of the isolated peptide used for antibody production (from 1x to 4x).

IF proteins therefore in following experiments the treatment of the sample in various denaturating conditions was investigated.

To exclude the possibility that the 200 kDa band corresponded to a dimer the protein samples were treated in various conditions favouring denaturation. High concentrations of chaotropic agents: urea (7 M) or guanidine thiocyanate (6 M) were used as well as exposure to high temperatures for different periods of time, electrophoretic separation in presence of urea and in high pH (9.5 pH) which is known to favour depolimerization of IF proteins (Fig. 19 a, b).

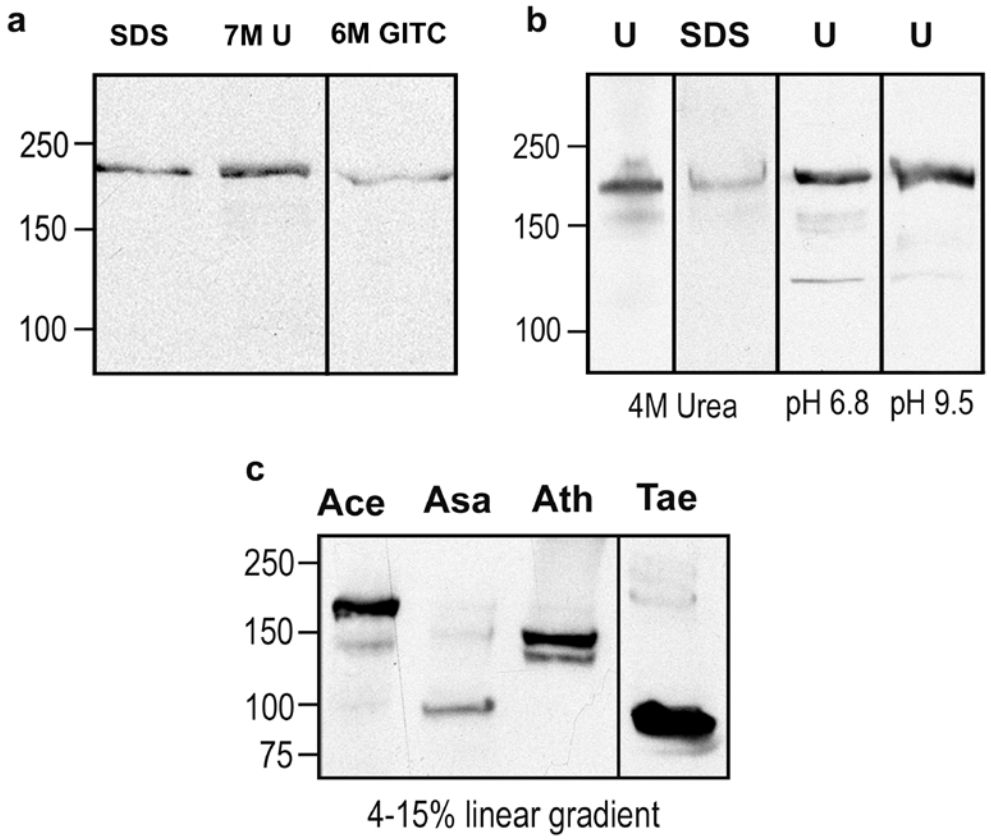

Figure 19. Migration of the NMCP proteins in various conditions favouring protein denaturation. **a** Migration of AcNMCP1 in onion nuclear fractions extracted in SDS (Laemmli Buffer 2x), 7 M U (7 M urea/2 M thiourea) and 6 M GITC (6 M guanidine thiocyanate). AcNMCP1 migrated at 200 kDa in all these conditions. **b** Migration of AcNMCP1 in onion nuclear fractions extracted in SDS (Laemmli Buffer 2x) or U (4M urea, 2M thiourea) and separated in presence of 4 M urea or optimal (6.8) and high (9.5) pH **c** Separation of onion (Ace), garlic (Asa), *A. thaliana* (Ath) and wheat (Tae) protein fractions in a 4-15% linear gradient gel. The migration of bands detected in onion and other species was not altered by any of the denaturating conditions used.

The treatments had no effect on band mobility suggesting that the 200 kDa band represented the real MW of AcNMCP1 and that the difference between the predicted and detected MW might be caused by post-translational modification (PTM). A PTM that can alter the molecular weight so significantly is glycosylation due to attachment of long glycan chains.

To rule out any possible protein aggregation in the stacking gel the sample was resolved in 4-15% linear gradient gels. As shown in figure 19 there was no apparent effect on band migration in different species in these conditions.

Together, these results excluded the possibility that the high molecular weight of the 200 kDa band detected in onion could have been caused by uncomplete denaturation, aggregation or dimerization.

2.1.3. Two dimensional electrophoretic separation (2-DE) and detection of AcNMCP1 and an NMCP in *A. thaliana*

Two dimensional electrophoresis (2-DE) was performed for the estimation of the isoelectric point and better electrophoretic separation of AcNMCP1. After the 2-DE separation of onion nuclear and *A. thaliana* whole protein fractions the proteins were transferred onto nitrocellulose membranes and then immunoblots with the anti-AcNMCP1 antibody were performed (Fig. 20). In onion, two major spots were detected at pI 5.2 and 5.8 which roughly corresponded to the predicted pI value of the AcNMCP1 protein (5.39). Long exposures revealed additional spots of 200 kDa with isoelectric points in the range between 3 and 5.8.

In *Arabidopsis thaliana* a major spot of 150 kDa and pI 4.9 was detected. In overexposed membranes additional minor isoforms of pI 4 and 5 were

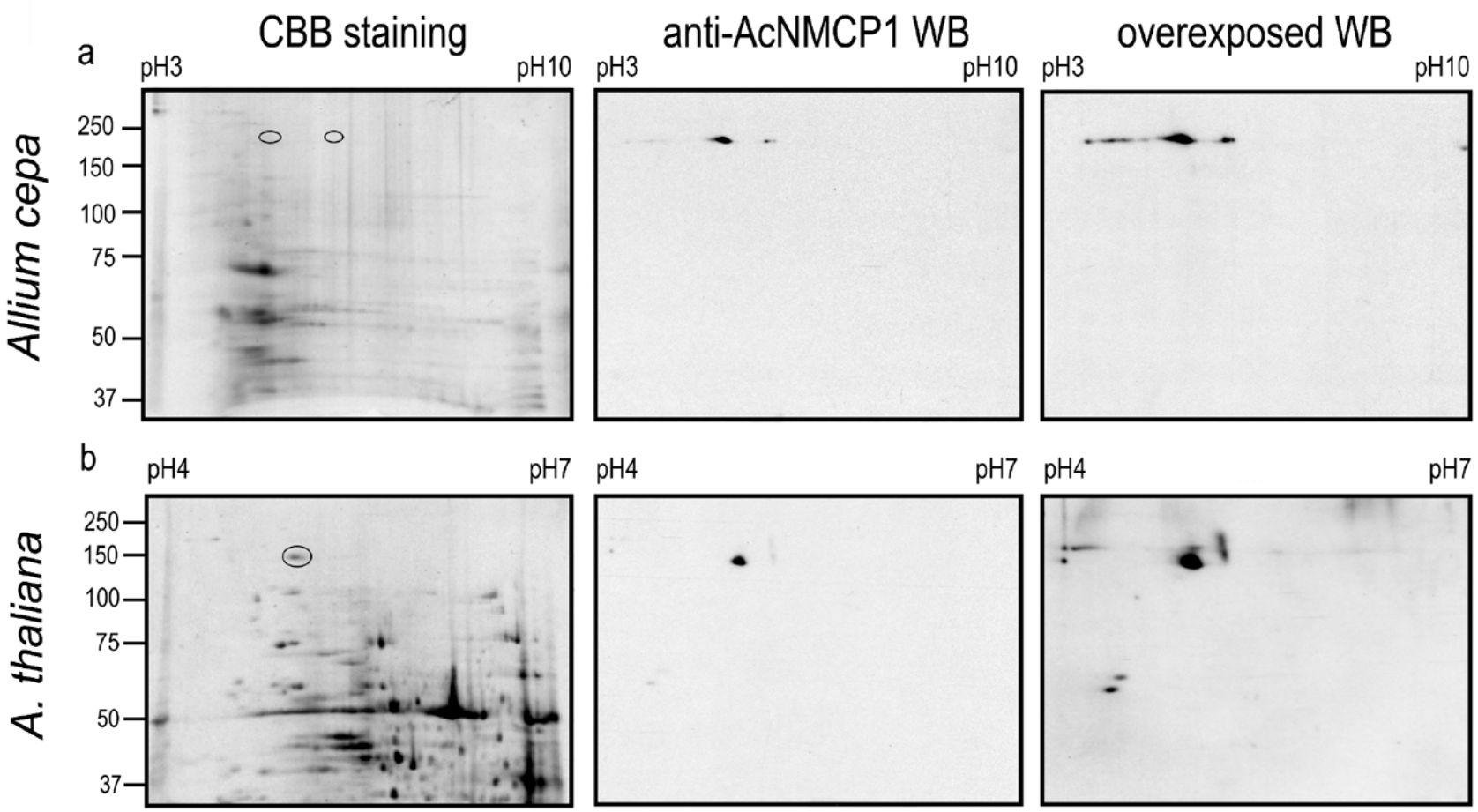

Figure 20. Two dimensional electrophoretic separation of proteins from *Allium cepa* root meristem nuclear fractions and 2-week-old *Arabidopsis thaliana* whole plants and the corresponding 2D-immunoblots probed with anti-AcNMCP1 antibody. Spots corresponding to the immunoblot signal are marked in black oval frames. **a** In onion two major spots of 200 kDa and isoelectric points 5.2 and 5.8 were detected. In overexposed membrane additional spots in the range between 3 and 5.8 pH were observed. **b** In *A. thaliana* a major spot of 150 kDa and pI 4.9 was detected. In long exposure additional spots of 150 kDa were detected that could correspond to the doublet sometimes observed in 1-DE immunoblots. Also, spots of around 55 kDa were observed that could be proteolytic products.

observed (Fig. 20 b). The isoelectric points are in agreement with the predicted values for AtNMCP/LINC proteins: 4.96 for LINC1, 4.8 for LINC2, 4.99 for LINC3 and 4.84 for LINC4 (www.arabidopsis.org). These could correspond to the doublet sometimes observed in 1-DE immunoblots (Fig. 19 c). The antibody may have recognised more than one NMCP form with different isoelectric points since it was raised against a region conserved among all NMCP proteins, but also the different isoelectric points might have corresponded to differently phoshporylated isoforms. Spots of lower molecular weight could be proteolytic products.

The positions of the spots detected in onion and *Arabidopsis thaliana* are in agreement with predicted pI values confirming the specificity of the anti-AcNMCP1 antibody in various species.

2.1.4. Protein identification with nLC-MS/MS

To confirm that the protein detected in onion corresponded to AcNMCP1, 2-DE and subsequent identification of the main spots by nLC-MS/MS were performed (Fig. 21). The major spots of pI 5.2 and 5.8 were cut out and identified by nLC-MS/MS. In the first spot 61 peptides (41.6% AcNMCP1 amino acid sequence coverage) were confirmed by SEQUEST with score of 193.4 whereas in the second 49 peptides (34.9% sequence coverage) with score of 174.6. The values were sufficient to confirm that the two spots corresponded to AcNMCP1 confirming the specificity of the antibody.

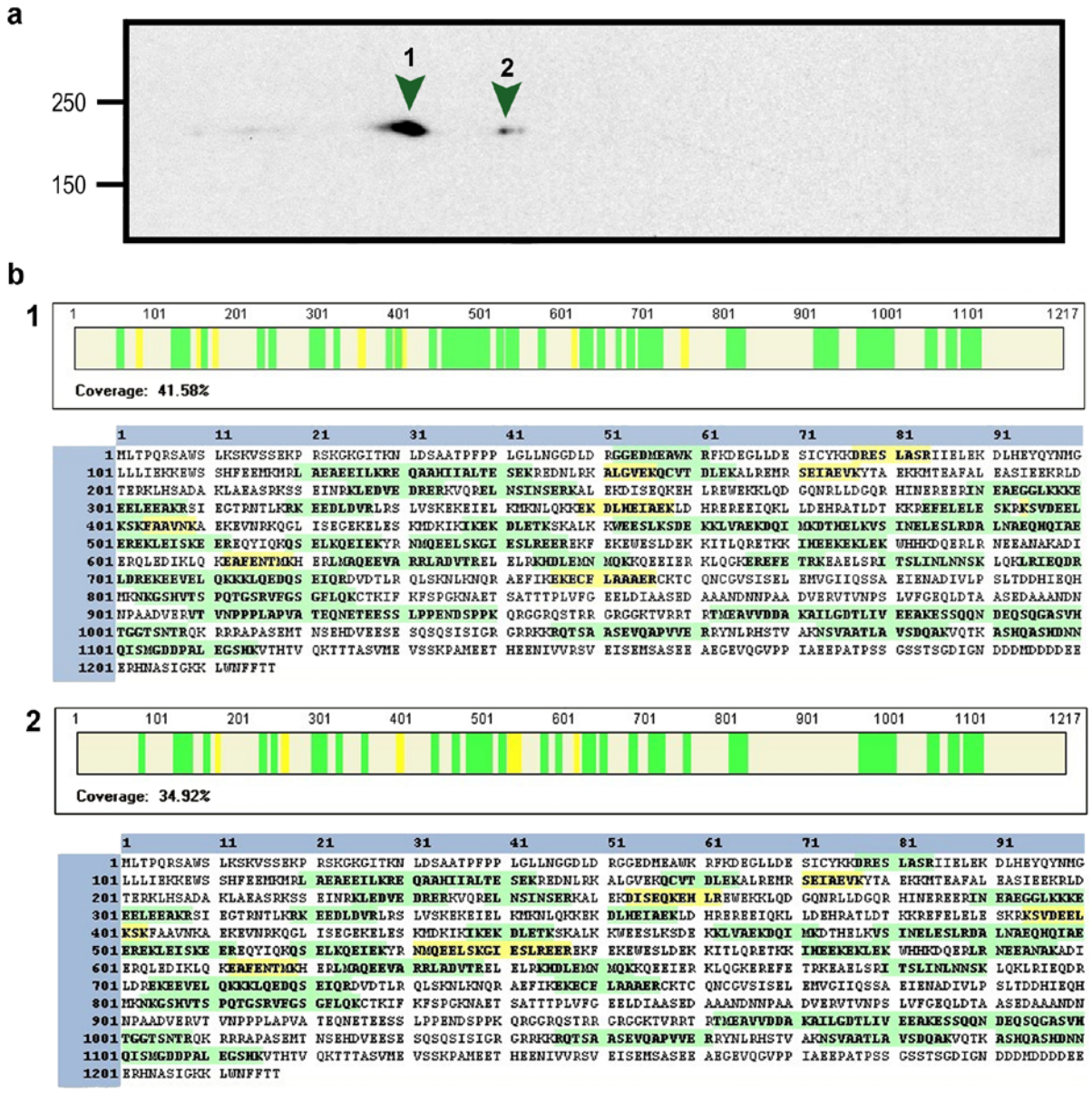

Figure 21. Identification of the two major spots detected using anti-AcNMCP1 antibody in 2-D immunoblots of onion nuclear extracts by nLC-MS/MS. a Identification of the two main spots in 2-D western-blots. **b** The sequence and positions of peptides identified by nLC-MS/MS. In the first spot (1) peptides representing 41.58% amino acid sequence coverage were identified with high scores and in the second (2) representing 34.92%. Peptides identified with very high scores are marked in green and those identified with high scores in yellow.

3. Estimation of the sizes of NMCP transcripts by northern blot analysis

The high molecular weight of the endogenous NMCP proteins in relation with the predicted values could be a result of alternative splicing or post-translational modifications. To investigate if the modification causing the rise in MW occurs at the transcript level, northern blot analysis was performed. The aim was to determine the definitive size of NMCP transcripts in onion, garlic, wheat and *A. thaliana* and to compare their sizes. The analysis would also reveal the presence of alternative transcripts in these species as the Phytozome data on NMCP genes generated based on genomic information, revealed alternative transcripts for several of them. In *A. thaliana*, for example LINC2 is expressed as primary transcript At1g13220.2 (1,128 aa) and alternative At1g13220.1 (391 aa). Also, LINC4 is expressed in multiple forms but the differences in size are not as significant (At5g65770.2- 1,042 aa primary; At5g65770.1- 1,010 aa; At5g65770.3- 1,010 aa). The list of all transcripts is presented in the Addendum.

The region selected for production of probe was highly conserved across species (Fig. 22).

Six primer pairs were designed for amplification of the region but only one aligned to the genomic DNA and gave a positive result; (363F GGATCTTCACGAGTACCA and 647R GTCATCTTCTTCTCAGCG). The electrophoretic separation of the PCR product revealed that its size was 800 bp which was higher than expected. The sequencing confirmed the selected region was interrupted with an intron of 352 bp therefore the cDNA had to be produced from the selected region. (Fig. 23).

The PCR reaction using as matrice the cDNA produced in reverse transcription gave a specific product of 300 bp which corresponded to the size of the selected fragment (Fig. 24).

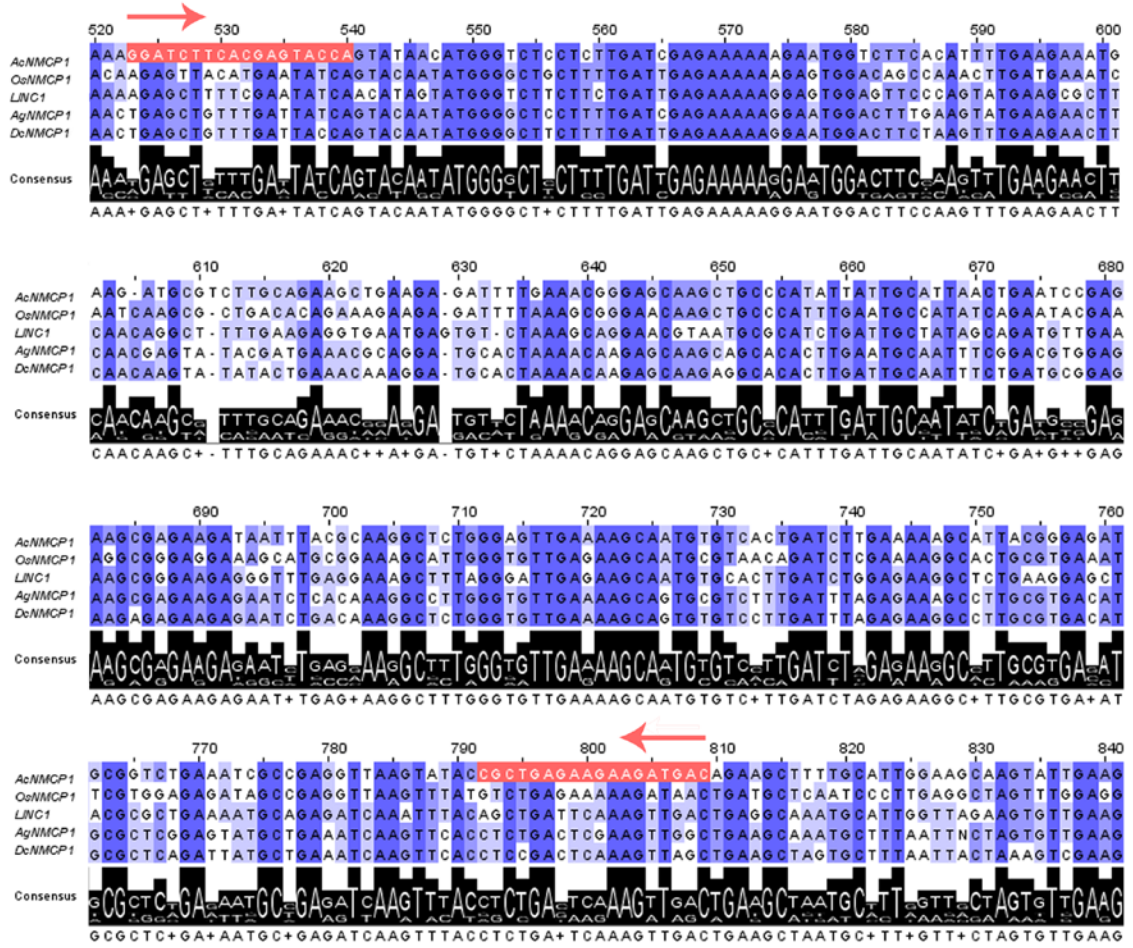

Figure 22. Region selected for probe production. The region selected for the production of the probe used later in the northern blot is a highly conserved region. Forward and reverse primers are marked in pink boxes, highly conserved residues are marked in dark blue and less conserved in light blue. The alignment consensus sequence is shown below and represents the level of conservation at given residue. Alignment was generated in ClustalW2 and the graphic was made in Jalview.

Although the probe used in northern blot analysis was designed in agreement with all the recommendations and the protocol was performed with care, the probe did not align to the RNA samples (Fig. 24) therefore the sizes of the transcripts could not be definitively confirmed. Weak signal observed in several samples was also present in negative control (RNA extracted from

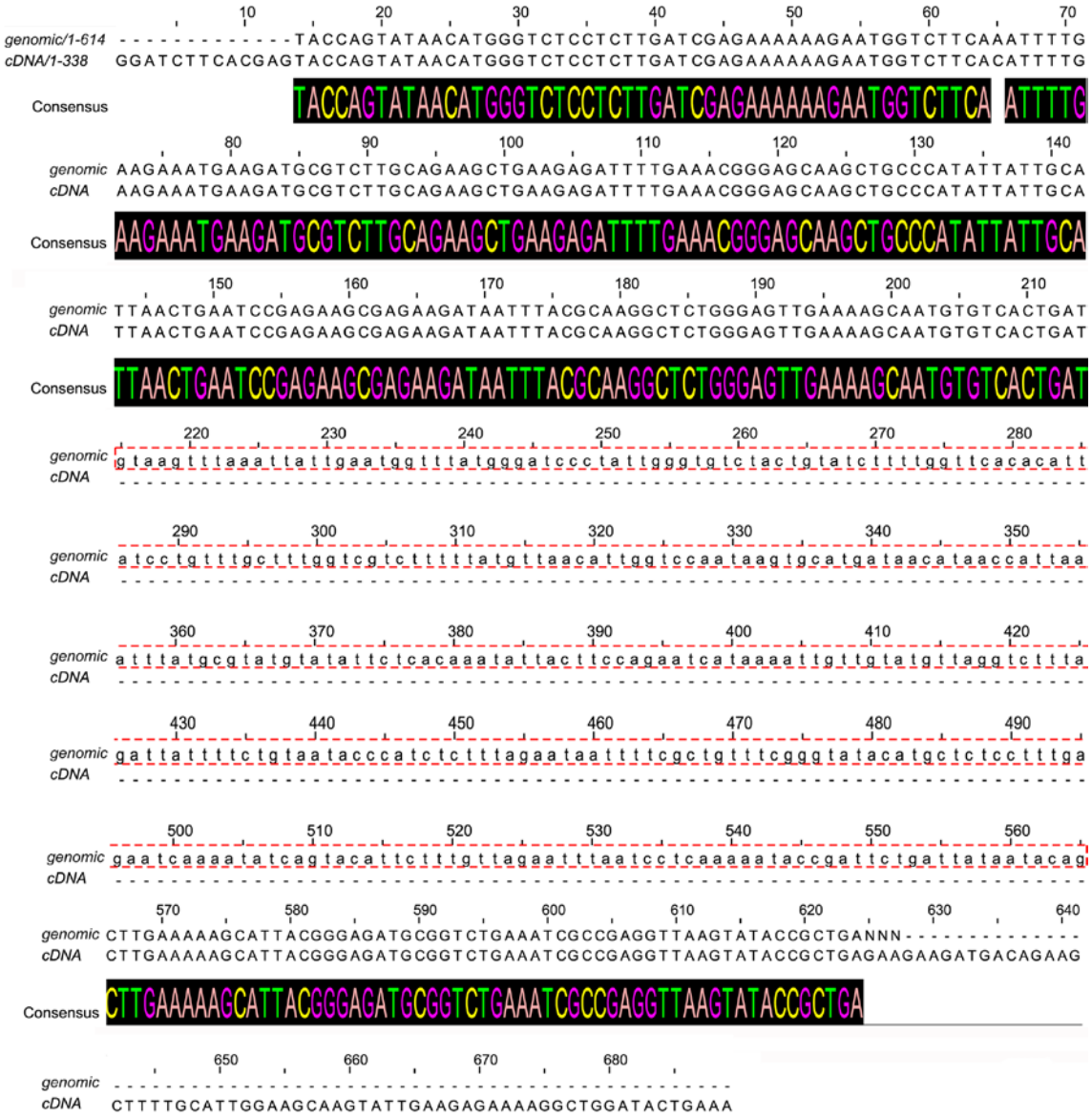

Figure 23. The region amplified in PCR reaction using genomic DNA as matrice contained an intron. Alignment of the region amplified in PCR reaction (genomic DNA) and cDNA corresponding to the region selected for probe production. The intron is contained in the red dotted box.

mouse lymphocytes) meaning that the signal was unspecific since NMCPs are plant-specific. To establish the sizes of the transcripts in *Arabidopsis thaliana*,

onion, garlic and wheat the production of four probes specific for each species could improve the reactivity but time restriction of the project did not allow us to perform such an elaborated experiment in the frame of this research. Nevertheless, the information about the localization of the intron in the AcNMCP1 gene could be useful for future studies.

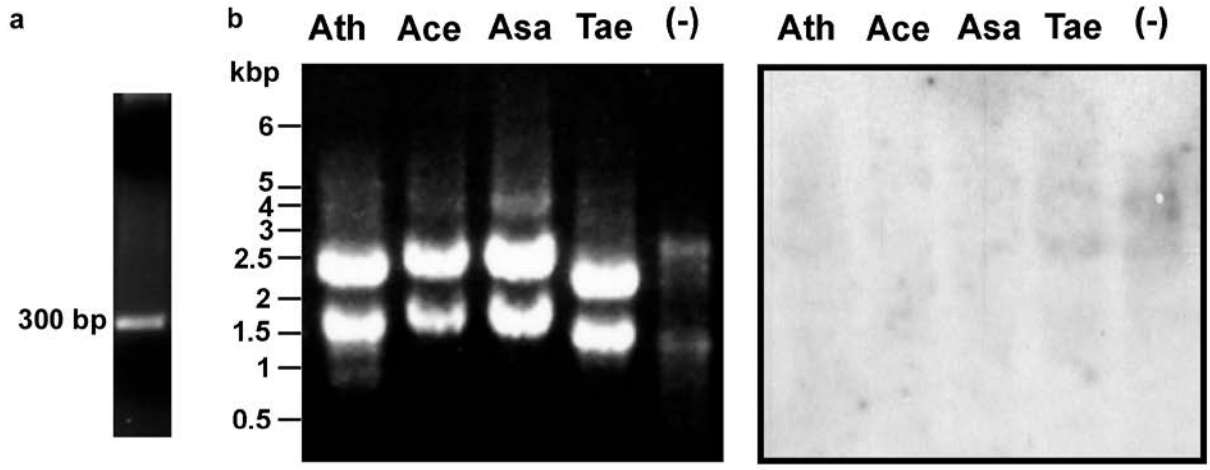

Figure 24. Northen blot analysis. a Electrophoretic separation of the region selected for probe production amplified in a PCR reaction using cDNA as matrice. The PCR reaction generated a specific product of 300 bp **b** Electrophoretic separation in denaturating conditions of RNA isolated from *Arabidopsis thaliana* (Ath), *Allium cepa* (Ace), *Allium sativum* (Asa), *Triticum aestivum* (Tae) and mouse lymphocytes (negative control). The ribosomic RNA is visible as a doublet. The probe did not align as seen on the membrane (right). Weak signal observed in the plant samples is unspecific as it was also seen in negative control (-).

4. Detection of glycosylated proteins in onion nuclear fraction

One of the possible post-translational modifications that may alter protein molecular weight in such a degree as described for AcNMCP1 is glycosylation. To investigate if NMCP proteins contain possible sites for glycosylation a

PROSITE search was performed which confirmed that AcNMCP1 as well as most NMCP sequences contain at least three predicted glycosylation sites (Fig. 25 a).

The possibility that AcNMCP1 could be glycosylated was investigated by performing immunoblots with a rabbit anti-HRP antibody which recognises complex-type *N*-glycans with α1->3 fucose and β1->2 xylose residues characteristic for plant glycoproteins (Faye et al. 1993). The anti-HRP antibody recognised in nuclear fractions three major bands of calculated MW 148, 167 and 271 kDa and a group of minor bands (Fig. 25 b). The results did not confirm definitely if AcNMCP1 is glycosylated since no clear band was detected with the anti-HRP antibody with a similar mobility to AcNMCP1 protein.

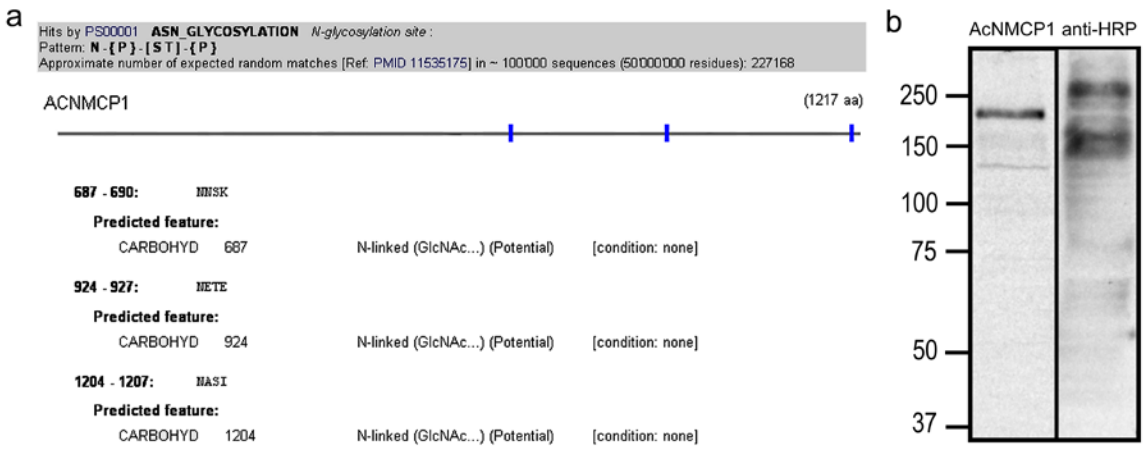

Figure 25. AcNMCP1 predicted glycosylation sites and detection of nuclear glycoproteins in onion nuclei. a AcNMCP1 contains three predicted glycosylation sites as predicted using PROSITE. **b** Detection of AcNMCP1 with anti-AcNMCP1 antibody (left lane) and glycoproteins with anti-HRP antibody (right lane) in onion nuclear fractions. No clear band is seen at the level of AcNMCP1 therefore it is not confirmed that the protein is glycosylated.

In the future N-glycan specific removal assay could be performed using endoglycosidase H (endo H) which cleaves *N*-linked glycan from the protein carrier. After the incubation of protein sample with enzyme the changes of band migration are monitored. If the band migrates faster it means that the glycan was removed and native protein is glycosylated (Kobata 1979; Cladaras and Kaplan 1984).

5. Subnuclear distribution of AcNMCP1 in meristematic nuclei

5.1. Nuclear distribution of AcNMCP1 analysed by immunofluorescence confocal microscopy

To investigate the distribution of AcNMCP1 in onion nuclei, immunofluorescence confocal microscopy was performed. Isolated onion meristematic nuclear fractions (free of contaminating cytoplasm) were probed with the anti-AcNMCP1 and an A488-coupled secondary antibody. The analysis revealed a consistent distribution of AcNMCP1 labelling forming a peripheral layer in the nucleus (Fig. 26 a, c). At high magnification some discontinuity of the labelling was observed, with a more intense staining in some areas than in others (Fig. 26 e).

Variable intranuclear staining in form of spotted foci was also observed in several preparations (Fig. 26 b, d). In these preparations a very intense labelling at the nuclear periphery was always observed. The intranuclear staining corresponded to interchromatin domains as revealed by DAPI counterstaining of nuclei (Fig. 26 d´, f´). The labelled foci seemed to form a network in the nucleoplasm. The intensity of the labelling was higher close to the nuclear periphery and decreased towards the nuclear interior. This may suggest that in these preparations the penetration of the antibody was more

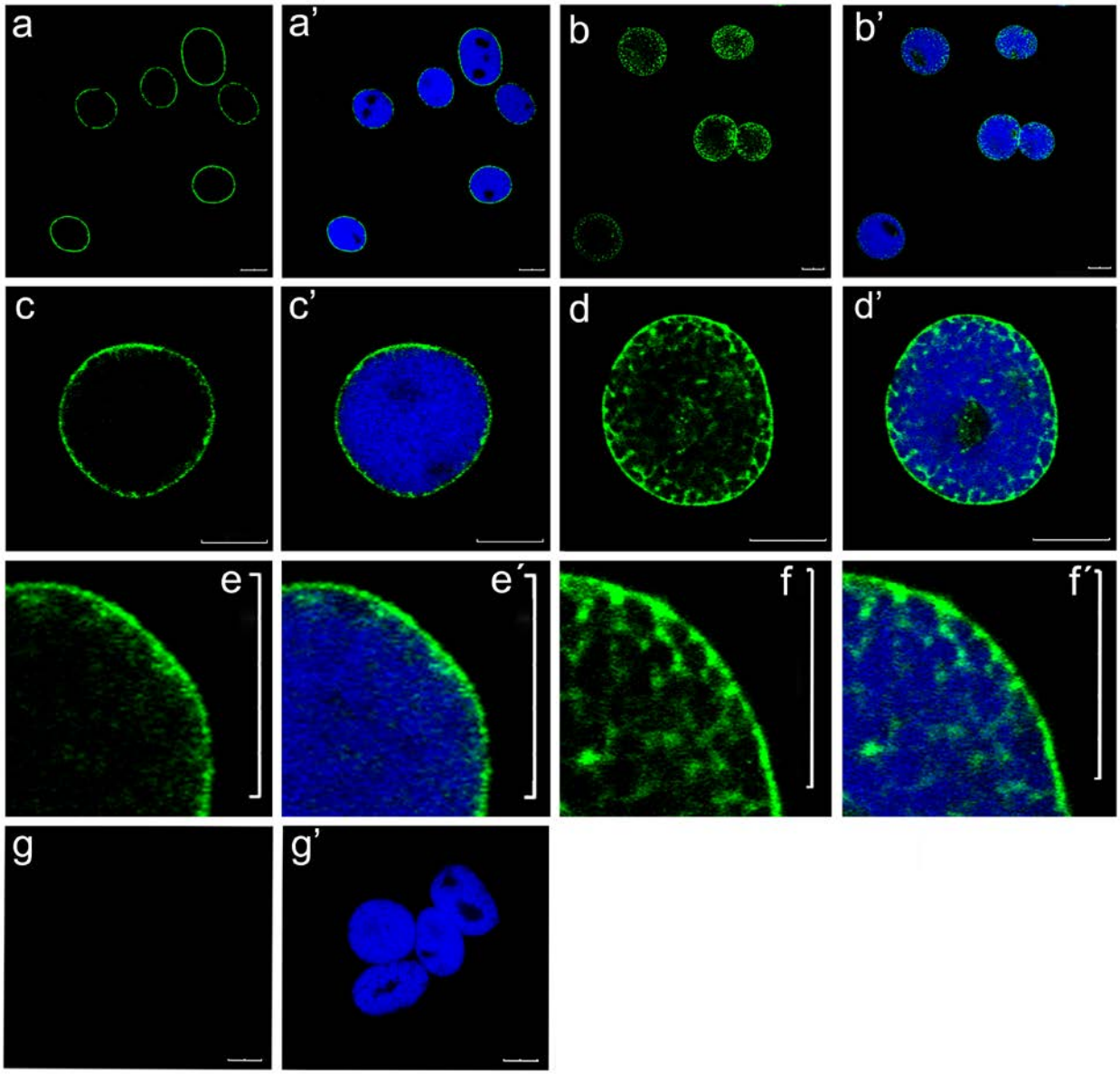

Figure 26. Distribution of AcNMCP1 in the meristematic nucleus. Confocal sections of meristematic nuclear fractions after incubation with the anti-AcNMCP1 antibody, demonstrating the distribution of the protein along the nuclear periphery (**a** to **f**) and in the nucleoplasm on occasion (**b**, **d**, **f**) with stained foci forming a network in the interchromatin domains as demonstrated by DAPI staining (**d'** and **f'**) **g** Negative control incubated with the secondary antibody alone. **a´**, **b´**, **c´**, **d´**, **e´**, **f'** and **g´** overlay of the corresponding anti-AcNMCP1 and DAPI stained images. Scale bars = 10 μm

effective and it could react with proteins in the intranuclear domains. Only very rarely positive foci were observed in the nucleolus (Fig. 26 d').

The negative controls incubated without the primary antibody showed no staining (Fig. 26 g).

These results confirm that the distribution of AcNMCP1 in onion nuclei is similar to that of lamins in metazoan nuclei. The latter are predominantly localized at the nuclear periphery in the lamina where they play structural and other functions, but they are also localized in the nucleoplasm where they are involved in DNA replication, transcription and other processes.

5.2. High resolution localization of AcNMCP1 using electron microscopy

Electron microscopy was used to determine the localization of AcNMCP1 in onion nuclei at high resolution. The conventional protocol for post-embedding immunogold labelling did not give any significant results due to very low signal therefore, a new protocol of pre-embedding labelling was developed to increase the labelling. For that isolated nuclei were fixed in 2% FA, depleted of membranes by adding 0.5% TX-100 and then incubated with the anti-AcNMCP1 antibody and a 5 nm gold conjugated secondary antibody before fixing again in 4% FA and embedding.

Pre-embedding immunogold labelling of isolated nuclei provided a better reactivity of the protein with the antibodies in situ, and also a good preservation of nuclear ultrastructure (Fig. 27).

Allium cepa is a diploid plant with a high DNA content (33,5 pg/nucleus) and have a reticulated nucleus. In the analysed sections the nucleus was organized in abundant dense heterochromatin masses and loose interchromatin domains, which is typical for reticulated nuclei.

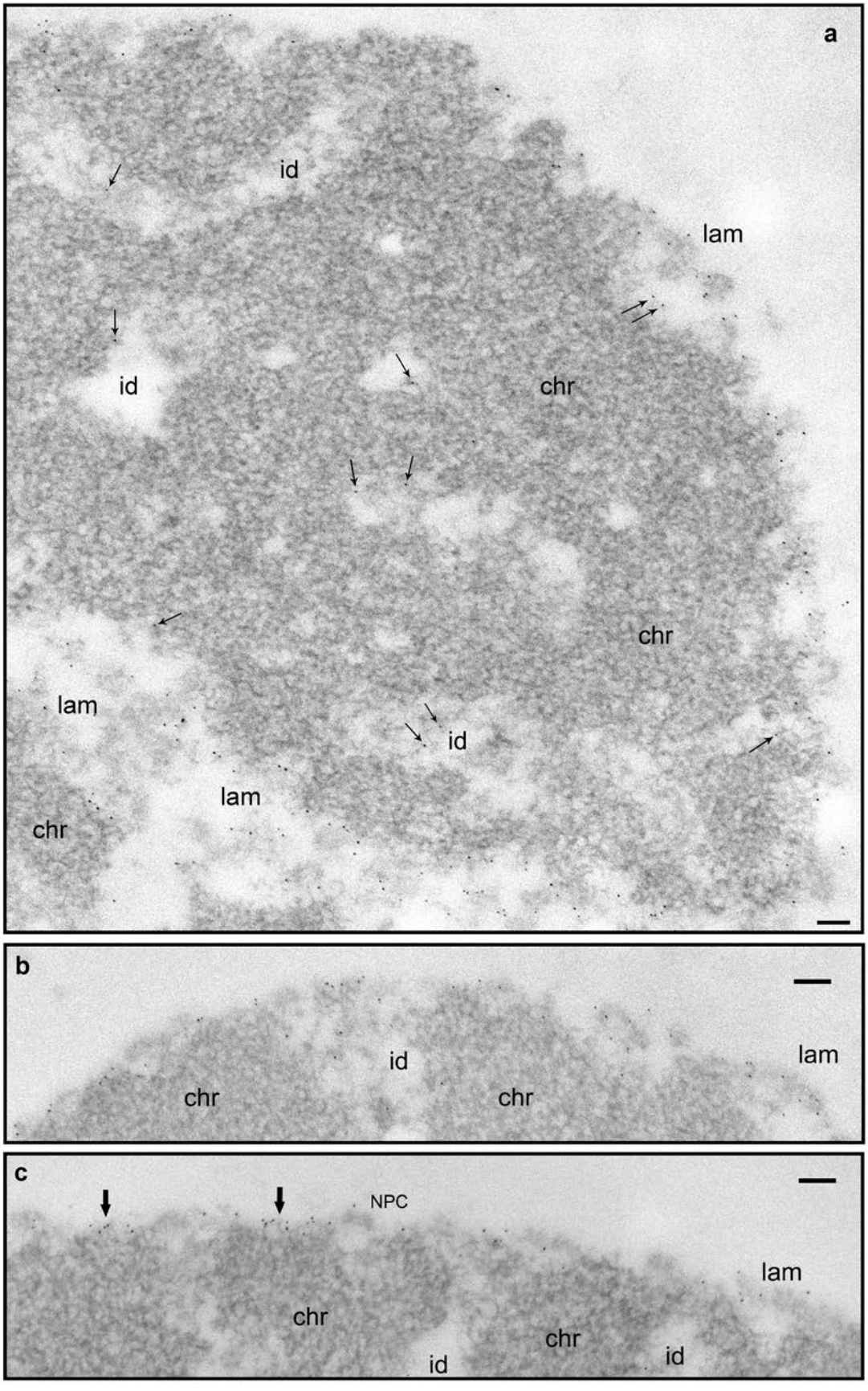
a
id
lam
id
chr
chr
lam
id
lam
chr
b
id
lam
chr
chr
c
NPC
lam
chr
chr
id
id

Electron microscopy images of membrane-depleted nuclei showed clearly the lamina at the nuclear periphery in close proximity with the dense heterochromatin masses and the interchromatin network. In the lamina we observed associated pore complexes and closely attached condensed chromatin masses as well as the interchromatin domains. The labelling confirmed the distribution of AcNMCP1 observed in the immunofluorescence analysis and permitted to establish its association with various nuclear structures visualized at high resolution.

Clusters of gold particles were visible mostly at the nuclear lamina confirming that AcNMCP1 resides mainly in this structure. Also, single gold particles were visible in the fibrillar network of the interchromatin domains and at the boundaries between condensed and decondensed chromatin in the nucleoplasm (Fig. 27).

The abundant immunogoldlabelling of AcNMCP1 in the lamina strongly suggests it is a main component of this structure.

6. AcNMCP1 is bound to the nucleoskeleton

To investigate the association of AcNMCP1 with the NSK, nuclear fractions were submitted to sequential extraction with non-ionic detergent, and low- and high- salt buffers after nuclease digestion for isolation of the NSK. When

Figure 27 (on the left). Subnuclear localization of AcNMCP1 in isolated onion nuclei. High resolution pre-embedding immunogold labelling using anti-AcNMCP1 and 5 nm gold-conjugated secondary antibody. Nuclei (a) and portions of nuclei (b, c) that exhibit accumulation of gold particles in the peripheral lamina (lam) attached to the heterochromatin masses (arrows in c) and also some labelling in the fibrillar network of interchromatin domains (id) marked with arrows in a. **a** Displays a nucleus and a fragment of another nucleus (bottom left corner). The labelling is abundant in the zones where heterochromatin associates to the lamina (arrows in c). NPC- nuclear pore complex in c. Scale bars = 100 nm.

western blots of the different fractions were probed with the anti-AcNMCP1 antibody the protein was always present in the insoluble fractions and absent from the soluble ones, being resistant to extraction with non-ionic detergent, DNase and high salt concentration. These results demonstrate that AcNMCP1 is a highly insoluble nuclear protein and a component of the NSK (Fig. 28).

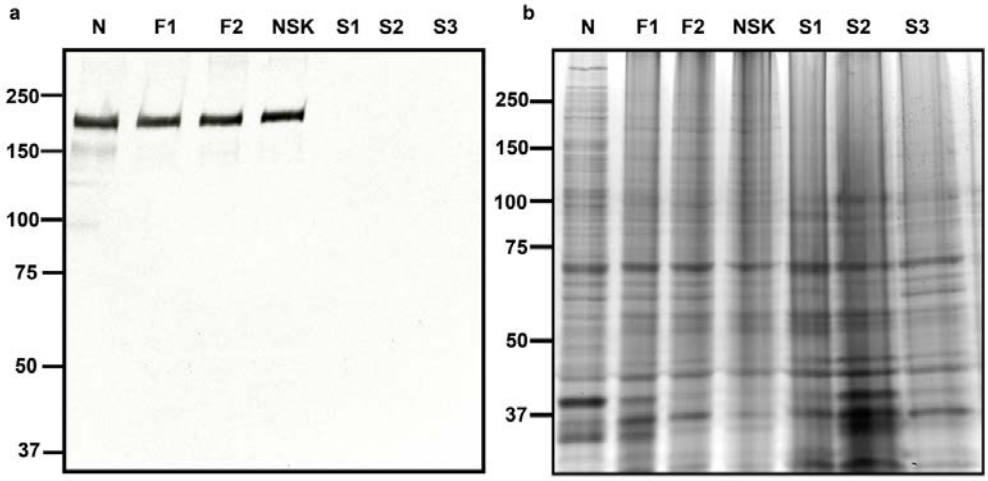

Figure 28. AcNMCP1 is extracted with unsoluble proteins and nucleoskeleton. a Detection of AcNMCP1 in the nuclear (N), insoluble (F1, F2, NSK) and soluble (S1, S2, S3) fractions obtained during NSK extraction in immunoblots probed with anti-AcNMCP1. The 200 kDa band of AcNMCP1 was present in all the insoluble fractions but not in the soluble ones. **b** Coomasie blue staining of a gel run in parallel showing the complex protein composition of the insoluble and soluble fractions.

Immunofluorescence confocal microscopy of nucleoskeletal fractions confirmed that AcNMCP1 is located in the NSK structures. The images revealed that the protein is mainly associated with the lamina and to a lesser extent with the internal NSK, revealing a similar distribution pattern to that found in isolated nuclei although the internal labelling was weaker than in the nuclei (Fig. 29 a, b).

High resolution immunogoldlabelling confirmed the immunofluorescence results and revealed abundant labelling at the lamina and weaker in the internal NSK (Fig. 29 c).

Together, these results confirm AcNMCP1 as a constituent protein of the NSK.

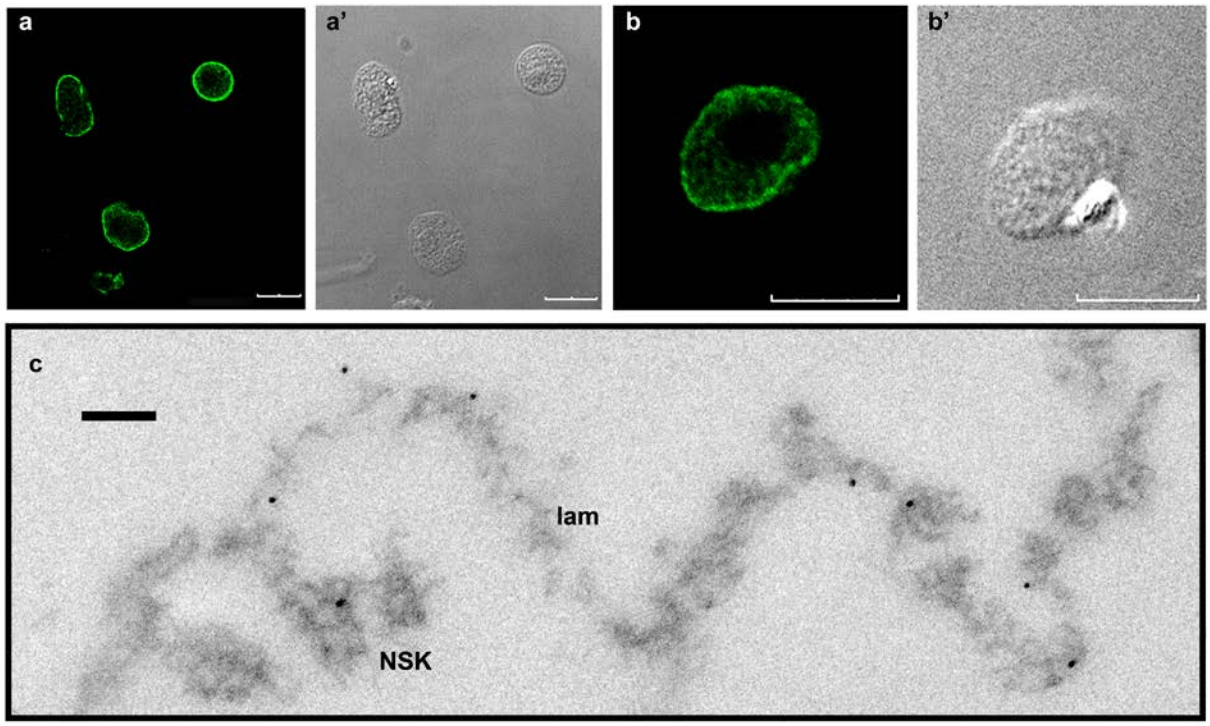

Figure 29. AcNMCP1 is a component of the nucleoskeleton. a, b Confocal images of nucleoskeletons showing the predominant accumulation of AcNMCP1 in the lamina and the weaker staining associated with the internal NSK. **a′, b′** DIC (differential interference contrast) images of the corresponding fields. **c** Immunogold labelling of a section of a NSK showing the accumulation of gold particles in the lamina (lam) and a weaker labelling of the internal NSK. Scale bar in a, a', b, b' = 10 μm; in c = 100 nm.

7. Levels and nuclear distribution of AcNMCP1 in root cells with different proliferating stages

Western blot analysis was performed to investigate if the AcNMCP1 levels changed in root zones with different activities: proliferating root meristem, elongation and differentiation zones and also in the quiescent meristems isolated from unsoaked onion bulbs, as it is the case of metazoan lamins whose expression is developmentally regulated.

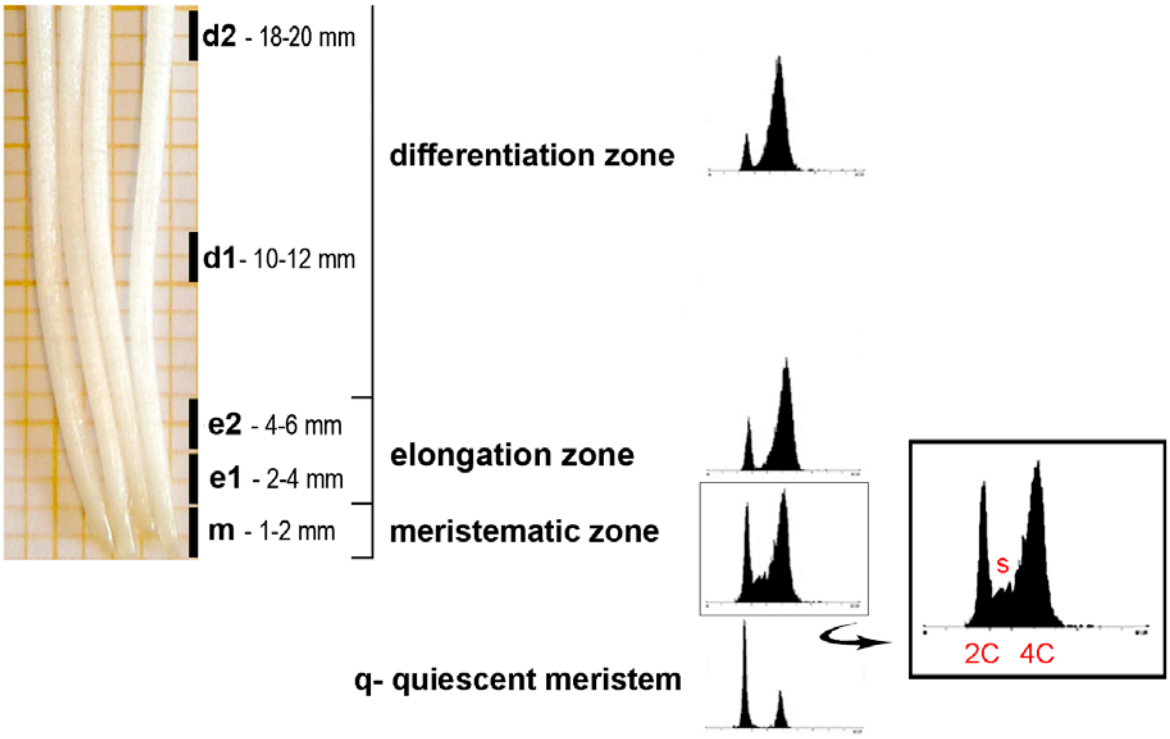

Figure 30. Localization of the onion root zones used in the analysis and their corresponding DNA content determined by flow cytometry. Indicated root fragments were excised and nuclei were isolated. Their DNA contents were determined by flow cytometry. Cells in the meristematic zone (m) proliferate as indicated by abundant nuclei with a DNA content between 2C and 4C corresponding to S period. Cells in quiescent meristem, the elongation (e1, e2) and differentiation (d1, d2) zones were mostly non-proliferating.

The flow cytometry analysis of nuclei isolated from the different segments of onion root revealed a diploid DNA content in all of them. The cells in the root meristem (1-2 mm from the tip) proliferate as it is indicated by the presence of abundant nuclei with a DNA content ranging from 2C to 4C corresponding to the S period of the cell cycle. On the other hand, the cells in the elongation (2-4 mm) and differentiation (10-24 mm) zones were mostly non-proliferating and contained abundant nuclei in G2 phase (4C). The cells

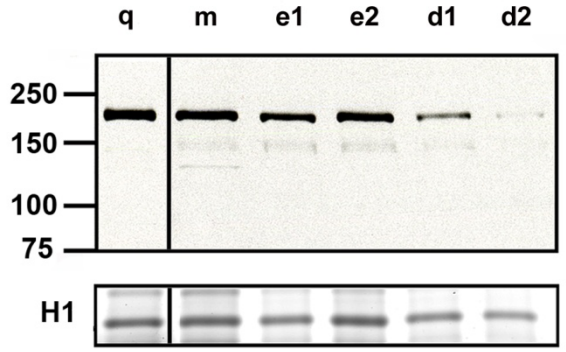

Figure 31. AcNMCP1 levels in the different root zones detected by immunobloting with the anti-AcNMCP1 antibody. AcNMCP1 expression was abundant in the cells of quiescent (q) and proliferating (m) meristems, although it decreased significantly in non-meristematic cells of the elongation (e1, e2) and differentiated (d1, d2) zones. H1 histones were stained with Coomasie Blue for loading controls.

of quiescent meristems were mostly in G_{01} phase (2C) and in a minor proportion in G_{02} phase, with no cells in the S-phase (Fig. 30).

Immunoblots revealed that AcNMCP1 was most abundant in meristematic cells, either proliferating or quiescent. Its levels decreased slightly in the elongation zone while in the mature zone they decreased dramatically, with very weak levels in the cells located 18-20 mm from the root tip (Fig. 31).

Confocal immunofluorescence microscopy was performed to analyse the distribution of AcNMCP1 in the nuclei from meristematic and differentiated cells. To compare the distribution at the nuclear periphery and in the

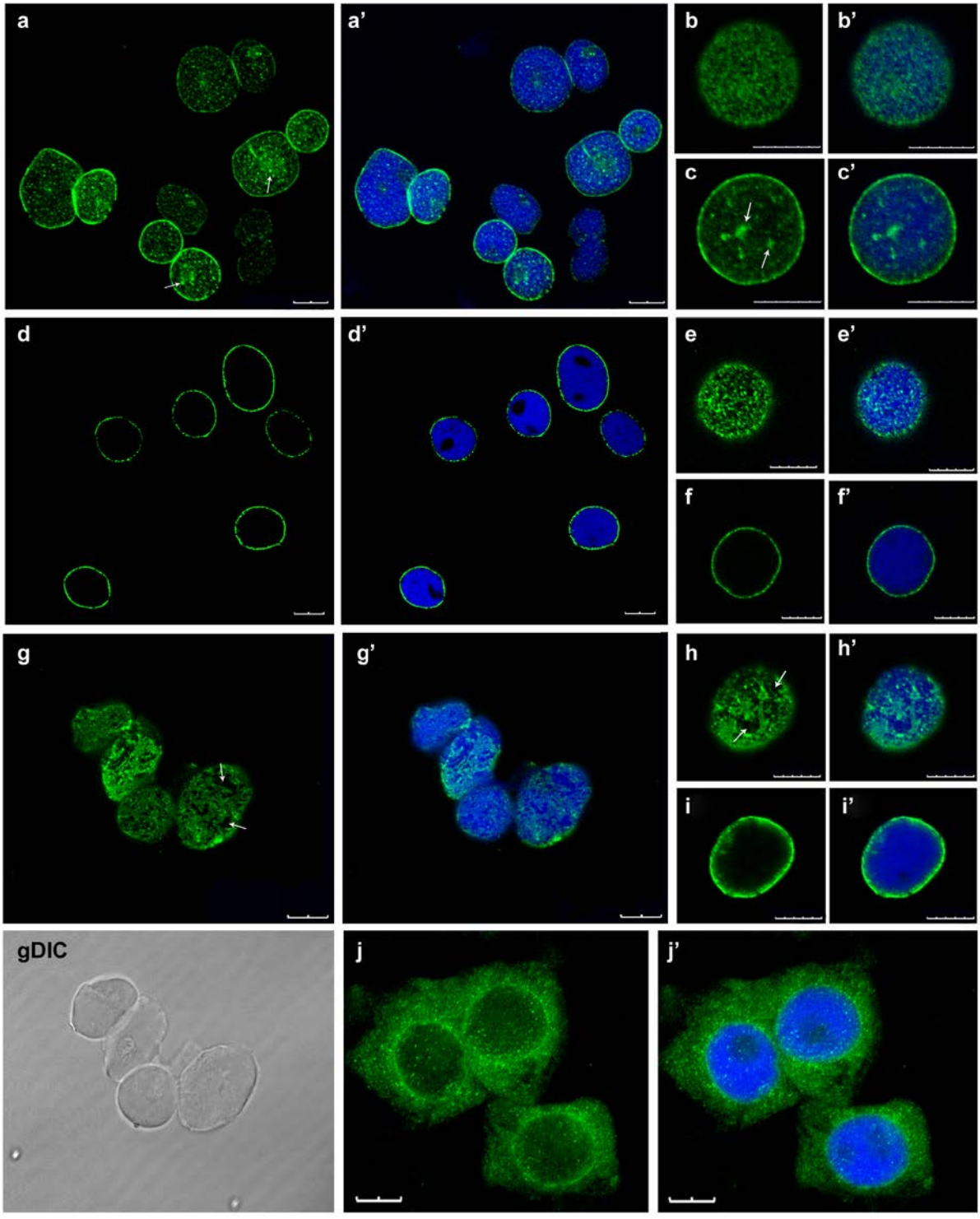
a
a'
b
b'
c
c'
d
d'
e
e'
f
f'
g
g'
h
h'
i
i'
gDIC
j
j'

nucleoplasm, peripheral and central confocal sections from selected nuclei were recorded and analysed. The confocal sections confirmed a general pattern of AcNMCP1 distribution at the nuclear rim and sometimes in the nucleoplasm in all the cell types. In addition, large intranuclear accumulations of AcNMCP1 were frequently observed in the quiescent meristematic nuclei (Fig. 32 a, c). In nuclei isolated from elongation and mature zones there was a discontinous distribution of AcNMCP1 along the nuclear periphery with non-reactive islands (Fig. 32 g, h, i). The gaps in AcNMCP1 staining at the nuclear periphery could be a result of damage in the integrity of nuclear envelope. The isolation of nuclei from upper parts of the root is more problematic than in case of root meristems due to their high fibre content and it may cause mechanical damage in the nuclear envelope. Nevertheless, the corresponding DIC images appear to rule out any damage in the nuclear envelope since

Figure 32 (on the right). Distribution of AcNMCP1 in nuclei isolated from different root cell types and whole cells. Central (a, c, d, f, i) and peripheral (b, e, g, h) sections showing the distribution of AcNMCP1 in the lamina and nuclear interior of quiescent (a, b, c) and proliferating (d, e, f) meristems, and in differentiated cells (g, h, i). **a**. Central confocal section of a group of quiescent nuclei displaying AcNMCP1 staining at the nuclear rim and intranuclear staining including large aggregates that were not observed in nuclei from proliferating meristem (arrows in a and c). At higher magnification the peripheral section (**b**) revealed a regular distribution of the protein in the lamina while in the central section (**c**) besides the intense staining in the lamina big aggregates and nucleoplasmic staining were observed. **d** Central confocal section of a group of proliferating nuclei displaying AcNMCP1 staining at the nuclear rim. At higher magnification the peripheral (**e**) and central (**f**) sections display a regular staining in the lamina. **g**. Peripheral confocal section of a group of nuclei isolated from differentiated cells displaying irregular distribution of the AcNMCP1 at the nuclear rim. **h** Peripheral confocal section of a nucleus isolated from differentiated cell displaying irregular distribution as gaps in AcNMCP1 staining in the lamina (arrows in g and h). The irregular distribution is also visible in central confocal section of the nucleus (**i**). **gDIC** represents differential interference contrast image of the group of differentiated nuclei presented in g and proves uninterrupted integrity of nuclear envelope of these nuclei. **j** In squashed meristematic cells an intense staining of the lamina was observed but also weaker unspecific staining in the cytoplasm. **a'**, **b'**, **c'**, **d'**, **e'**, **f'**, **g'**, **h'**, **i'** and **j'** represent overlays of AcNMCP1 and DAPI staining. Scale bar = 10 μm

nuclei preserved their shape and no leakage of nuclear content was visible (Fig. 32 gDIC). Immunofluorescent staining in whole cells that would permit the observation of nuclei without the risk of damage was not successful because of non-specific cross-reaction of the anti-AcNMCP1 antibody in the cytoplasm (Fig. 32 j). The signal was not caused by non-specific binding of the secondary antibody, as revealed by the negative controls (not shown), nor was it observed in immunoblots of cytoplasmic fractions with the anti-AcNMCP1 antibody (not shown).

Together, these results revealed that the level of AcNMCP1 decreased during cell differentiation and also that the distribution of AcNMCP1 changed depending on the activity and developmental stage of the cell.

8. Nuclear ultrastructure in *Arabidopsis thaliana linc* single and double mutants analysed by electron microscopy

AtNMCP/LINC proteins have been suggested to play a role in maintaining nuclear shape and structure. To investigate this, we compared the ultrastructure of nuclei in meristematic root cells of wild type *A. thaliana* and *linc* single and double mutants by electron microscopy. The main subnuclear compartments in plants are the nuclear envelope, heterochromatin, nucleoplasm, nucleolus and Cajal bodies and we focussed the analysis on these structures.

In wild type cells we observed spherical nuclei located centrally in the cell with a chromocentric chromatin organization typical for species with low DNA content (0.5 pg/ 2C nucleus in *A. thaliana*). This nuclear organization is characterized by a loose nucleoplasm made up of fibrils and granules and they contain 10 chromocenters and four NORs that can fuse. In the analysis scarce heterochromatin that is confined to compact dense fibrillar patches

corresponding to chromocenters (small pericentromeric regions of the five *A. thaliana* chromosomes) and to the two nucleolus organizing regions (NORs) per haploid complement. Root meristem cells are mostly diploid therefore usually from 0 to three chromocenters were observed per section as dense fibrillar masses firmly attached to the inner part of the nuclear envelope (Fig. 33 a). Although, the nuclear envelope with attached nuclear pore complexes was clearly seen, the underlying lamina was not visible in the sections.

The NORs appeared as heterochromatin masses associated to the nucleolus and sometimes attached to the nuclear envelope (Fig. 33 b). Diploid *A. thaliana* cells contain four NORs on chromosomes 2 and 4 respectively. NORs are composed of several hundred of tandemly-arranged repeats of ribosomal RNA genes encoding the 45S precursor transcript for the three largest ribosomal RNAs (18S, 5.8S, and 28S).

Transcription of rRNA genes by RNA polymerase I results in formation of a nucleolus in the interphase nuclei. The nucleolus is the site for transcription and processing of pre-RNA and for ribosome subunit assembly. In analysed sections nuclei contained a single nucleolus visible as a spherical membrane-less structure. The nucleoli displayed an organization typical for active nuclei where the three canonical components can be distinguished: small and numerous light fibrillar centers (FC) surrounded by dense fibrillar component (DFC) where transcription occurs, and intermingled with this a loose granular component (GC) containing the pre-ribosomal particles. Most nucleoli contained a central cavity with a similar density to that of the nucleoplasm and a fibrillo-granular composition (Fig. 33 d).

Cajal bodies (CBs), formerly known as coiled bodies are round membrane-less nuclear bodies of about 0.5-1.0 μm, in which splicing components concentrate. They are dynamic structures that move, split, rejoin and exchange contents with the surrounding nucleoplasm. The size and the number of Cajal.

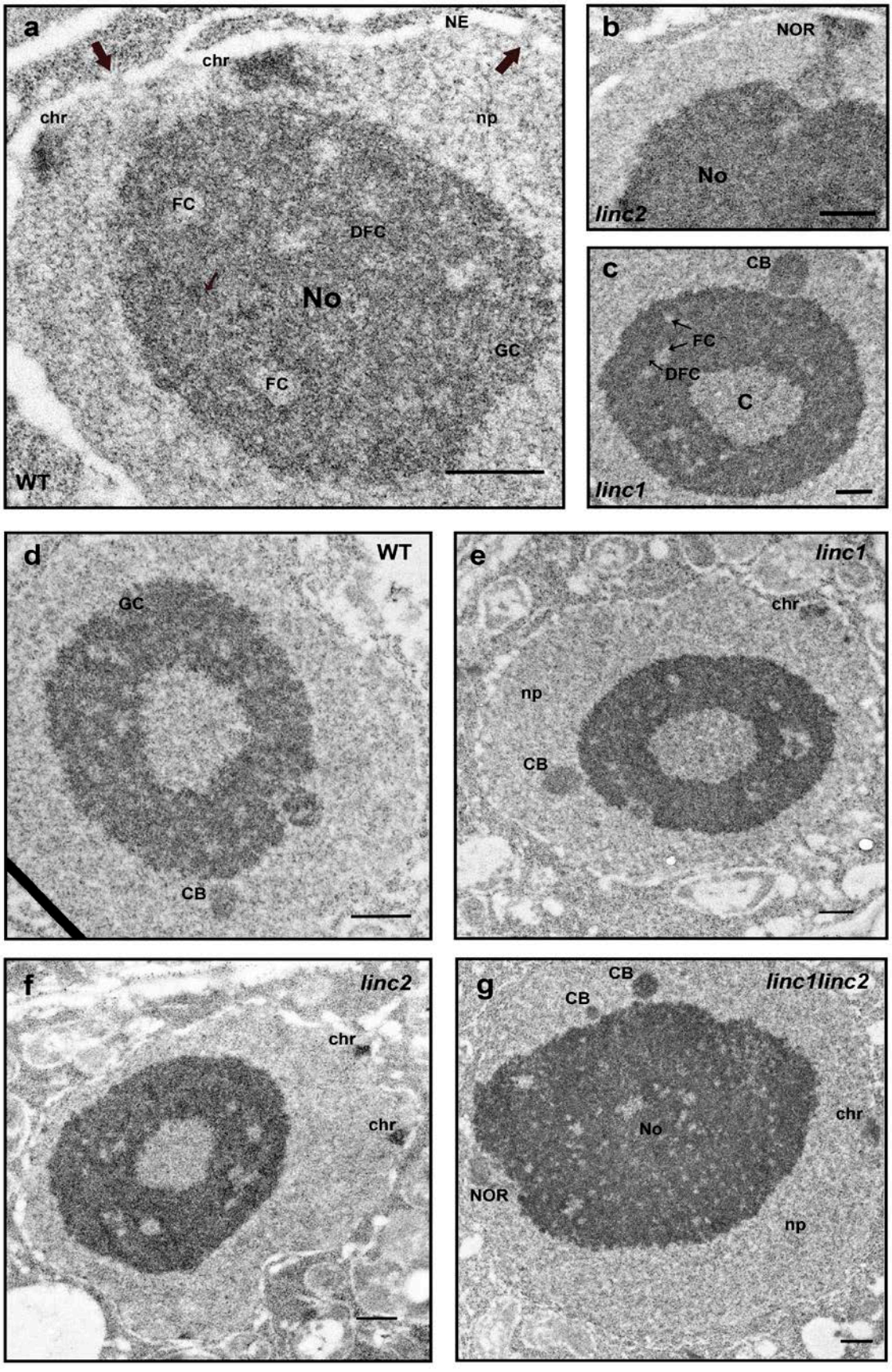
a
NE
chr
chr
np
FC
DFC
No
GC
FC
WT
b
NOR
No
linc2
c
CB
FC
DFC
C
linc1
d
WT
GC
CB
e
linc1
chr
np
CB
f
linc2
chr
chr
g
CB
CB
linc1linc2
No
chr
NOR
np

bodies depend on cell type, cell cycle and metabolic activity and are more numerous in rapidly dividing or highly active cells. CBs are made up of RNA and proteins and are involved in assembly and maturation of small nuclear RNA (snRNA) as well as small nucleolar RNA (snoRNA). In sections from WT root cells CBs were observed as compact discrete structures bound to the nucleolus made up of coiled fibrils (Fig. 33 d).

No apparent changes in the nuclear shape or in the ultrastructure and numbers of the studied subnuclear components were observed in *linc* single and double mutants in comparison to the wild type nuclei (Fig. 33 b, c, e, f, g). The chromocentres in numbers of 0-3 per nuclear section appeared always associated to the inner nuclear envelope (Fig. 33 e, f, g). The nucleolus presented the same central location and ultrastructure as in WT nuclei with small and numerous fibrillar centers, an abundant dense fibrillar component intermingled with the granular component and a central cavity (Fig. 33 c, e, f, g). The NORs were also similar in nuclei of WT and mutants (Fig. 33 b, g). CBs presented the same ultrastructure and association to the nucleolus as in WT nuclei (Fig. 33 c, d, e, g). Together, these results suggest that mutations of *LINC1* and *LINC2* genes do not affect nuclear ultrastructure in meristematic root cells.

Figure 33 (on the left). Transmission Electron Microscopy of nuclei from meristematic root cells of *A. thaliana* wild type, single *linc1* and *linc2* mutants and double *linc1linc2* mutant. **a, d:** wild type. **c, e:** *linc1* mutant. **b, f:** *linc2* mutant. **g:** *linc1linc2* mutant. The nuclei of single and double mutants did not show significant differences in nuclear size or ultrastructure in comparison to nuclei in wild type cells. The different images display roundish nuclei with a loose fibrillo granular nucleoplasm (np) and centrally located single spherical nucleoli (No) displaying the typical nucleolar components: small and numerous light fibrillar centers (FC) surrounded by the dense fibrillar component (DFC), the granular component (GC) intermingled with the later and a central cavity (C). Cajal bodies (CB) were observed at the nucleolar periphery. The heterochromatin containing structures: chromocenters (chr) and nucleolar organizing regions (NOR) are attached to the inner nuclear envelope (NE). Nuclear pores are indicated with arrows at the NE. Scale bar = 500 μm

.

DISCUSSION

1. Proteins forming the lamina in non-metazoans

The filamentous lamina is a structure observed in the electron microscope as a low-density layer underlying the inner nuclear membrane and attached to heterochromatin masses. It was described repeatedly in many eukaryotes, including plants (Fawcett 1966; Kruger et al. 2012; Moreno Diaz de la Espina et al. 1991; Li and Roux 1992; Masuda et al. 1993; Rout and Field 2001). In metazoans it is formed by tightly packed 8-10 nm filaments of lamins. Recent studies suggest that different types of lamins form separate layers; B-type lamins form a meshwork lining the INM and A-type lamins form bundles of filaments upon this layer (Goldberg et al. 2008a). In non-metazoans the lamina is not made up of lamins since they are expressed only in metazoans but it is formed by different proteins.

In the amoebae Dictyostelium a structure resembling metazoan lamina was observed in electron micrographs as a typical low electron-density layer more than four decades ago. The images were not published until recently when the identity of the protein forming this structure was revealed. Searches for lamin orthologs against sequenced genomes of Dictyostelia gave no convincing results but Kruger et al. (2012) described a protein, NE81 that shares structural features and functions with lamins, although sequence similarity between the two is low. NE81 contains a central coiled-coil domain flanked by short head and long tail domains. The rod domain is of similar length to that of lamins and is directly preceded by a cdk1 phosphorylation consensus sequence. The tail domain also shares features with the metazoan counterpart, for example a basic NLS and a CAAX box at the C-extreme with a

methionine at the X-position which indicates farnesylation (Kruger et al. 2012). The protein is associated with the NE during the entire cell cycle and its mobility in this membrane is probably regulated during mitosis by phosphorylation of S122 within the putative cdk1 site (Batsios et al. 2012). The NE81 knockout and overexpression mutants revealed an important role of this protein in nuclear integrity, chromatin organization and mechanical stability of the cells, which are functions fulfilled by lamins in metazoan cells (Kruger et al. 2012; Batsios et al. 2012). Today, many arguments suggest that NE81 could be a prototype of lamins (Batsios et al. 2012).

The NUP-1 found in the parasitic protozoa *Trypanosoma brucei* is another lamin-like protein. It does not seem to be evolutionary related to lamins and its size is much bigger (400 kDa) than the size of the latter (60-65 kDa) nevertheless, it plays some functions of metazoan lamins. Analogous to them, NUP-1 is a component of nucleoskeleton and plays key roles in the maintenance of nuclear shape and structure, organization of the heterochromatin and distribution of NPCs (Dubois et al. 2012). NUP-1 contains a large central coiled-coil domain and is restricted to trypanosomatids, although the orthologs do not share high degree of sequence similarity and display differences in size and structure between the species (Dubois et al. 2012; Rout and Field 2001).

The lamina was also observed under the electron microscope in plant cells (Moreno Diaz de la Espina et al. 1991; Li and Roux 1992; Masuda et al. 1993). Recently, in–lens field-emission scanning electron microscopy enabled observation of the fibrous structure of a well-preserved lamina underlying the nuclear envelope in plants and metazoans (Fiserova et al. 2009; Goldberg et al. 1992; Goldberg et al. 2008a). An observation of tobacco NE using this method revealed a complex filamentous lattice which is made up of two classes of filaments (10-13 nm and 5-8 nm thick) closely attached to the INM

and interconnecting the NPCs. The lattice resembled in the filament organization and dimensions the arrangement of the nuclear lamina in *Xenopus* oocytes (Goldberg et al. 2008a).

The similar ultrastructure of the lamina in plants and the fact that lamins play important roles that are fulfilled in any complex multicellular eukaryotic organism such as regulation of nuclear architecture, mechanotransduction, chromatin organization, etc. (Dechat et al. 2010a) suggest that the plant lamina plays similar roles to the metazoan lamina. Similarities in functionality were suggested by few lines of study although the mayor components of plant lamina are still not resolved. A study revealed that a part of a metazoan lamin-binding protein, LBR fused to the GFP and expressed in tobacco cells under the control of enhanced 35S promoter was directed to the nuclear envelope (Irons et al. 2003). This part of the protein contains a lamin binding domain (1-60), a chromatin binding region and a transmembrane domain (Ye and Worman 1994). The mobility of the LBR region in plant NE was much higher than in animal INE, suggesting lack of strong interactions between LBR and plant NE proteins. Nevertheless, the deletion of the lamin-binding domain from LBR increased the diffusion rate of the protein within the plant NE, which suggests that LBR might be interacting with components of the plant nucleoskeleton similar in structure to lamins (Graumann et al. 2007).

Also, the presence of plant homologs for some lamin-binding proteins further supports this hypothesis. Proteins with highly conserved SUN domain were reported in *A. thaliana* and maize (Graumann et al. 2010; Murphy et al. 2010; Oda and Fukuda 2011) as well as nucleoporin Nup136 in *A. thaliana*, a functional homologue of the animal Nup153 (Tamura and Hara-Nishimura 2011). Recent studies using FRET suggest a possible interaction between AtSUN1/AtSUN2 proteins and a candidate for lamin analogue AtNMCP1/LINC1, which could mean that in plant cell there is an interaction

between the two proteins, similar to that of SUN-proteins and lamins in metazoan cells (Graumann et al. 2013).

Several plant-specific proteins have been proposed as lamin analogues, including proteins that cross-react with anti-IF and anti-lamin antibodies (Li and Roux 1992; McNulty and Saunders 1992; Minguez and Moreno Diaz de la Espina 1993), FPPs (Gindullis et al. 2002), NACs (Blumenthal et al. 2004) and NMCPs (Masuda et al. 1993). Up to date, the best candidate for lamin-like proteins is the NMCP protein family made up of conserved nuclear coiled-coil proteins with a tripartite organization similar to that of lamins (Masuda et al. 1993; 1997; Dittmer et al. 2007; Kimura et al. 2010).

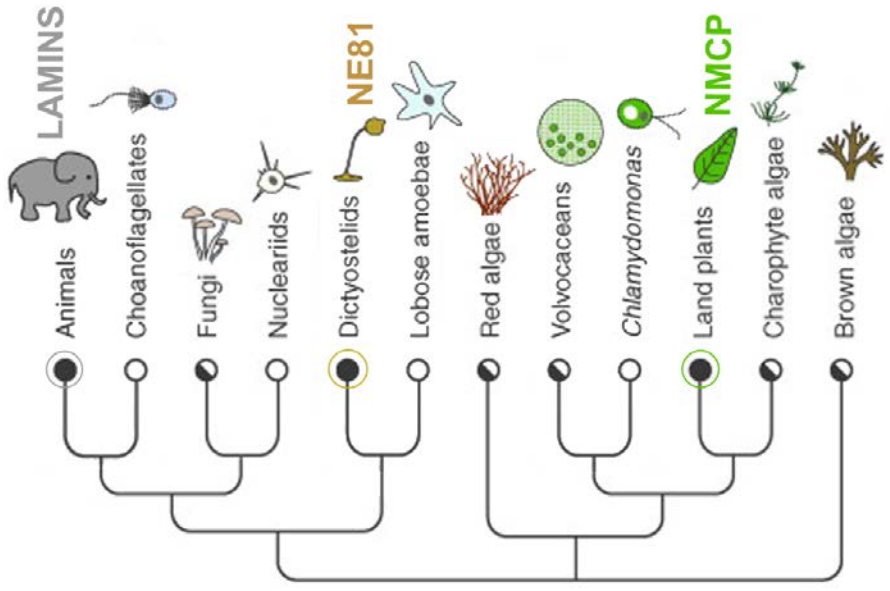

Figure 34. Phylogenetic relationships of multicellular eukaryotes and their closest unicellular and colonial relatives. As indicated by the phylogenetic relationships among selected unicellular, colonial and multicellular eukaryotic lineages the multicellularity evolved multiple times. Lineages strictly multicellular are represented by filled circles, unicellular or those that form undifferentiated colonies by open circles, lineages that contain unicellular, colonial and multicellular forms are represented by half-filled circles. Multicellular organisms express lamins (grey circle) or lamin-like coiled-coil proteins: NE81 (orange circle) and NMCP (green circle). Edited from Abedin and King (2010).

New insights into lamin-like proteins brought back the long-time debate about the origin of lamins and other nuclear coiled-coil proteins. Since nuclear lamina was revealed by electron microscopy in distant eukaryotes, also those lacking lamins, it was proposed that divergent proteins with extended coiled-coil domains might form filaments and perform some functions of lamins in these organisms.

It was suggested that the evolution of proteins forming the lamina coincided with the switch to multicellularity and facilitated the interaction of various cell types into elaborated tissues. The presence of a lamina in a unicellular Dictyostelia which forms multicellular aggregates with cells performing diverse functions under starvation conditions seem to confirm this hypothesis (Kessin 2000). Also, the presence of B-type lamins in multicellular metazoans and their role in the development of many organs support it (Zuela et al. 2012). Since, multicellularity evolved multiple times and separately in plants, animals and Dictyostelids (Fig. 34) (Abedin and King 2010) it is highly probable that plant proteins fulfilling lamin functions evolved independently. On the other hand, unicellular organisms express a limited number of proteins with a long coiled-coil domain while multicellular plants and animals express many more (Rose et al. 2005). Most of the long coiled-coil proteins in multicellular eukaryotes are kingdom-specific and include proteins crosslinking cytoskeletal components with membranes, IFs and proteins involved in mitosis and in structural integrity (Rose et al. 2005). The dynamic evolution of long coiled-coil proteins in multicellular organisms suggests that the proteins forming the lamina evolved independently which explains the lack of significant sequence similarity between lamins and the plant analogues.

On the other hand, a lamina was also found in a strictly unicellular organisms, for example in a parasitic Protozoa; *Trypanosoma brucei* (Rout and Field 2001). The protein forming the lamina in this organism is implicated in lamin

functions such as repression of developmentally regulated genes, the positioning of telomers, regulation of NPC distribution at the nuclear envelope, nuclear size and organization of chromatin (Dubois et al. 2012). It is possible that the presence of developmentally regulated genes was the impulse for the evolution of lamina in *Trypanosoma* and other organisms.

2. The NMCP family

NMCP1 was described for the first time in carrot as a constituent protein of the nucleoskeleton which is localized predominantly at the nuclear periphery (Masuda et al. 1993). DcNMCP1 was predicted to represent a tripartite structure similar to intermediate filament proteins with a central coiled-coil domain. Partial amino acid sequences revealed relatively high similarities with myosin, tropomyosin and IFs (Masuda et al. 1997). Further studies revealed the presence of another homolog, NMCP2 in carrot and celery and the distribution of NMCPs during mitosis, similar to that of lamins (Masuda et al. 1999; Kimura et al. 2010). In spite of the fact that NMCP does not display high sequence similarity to lamins, the predicted structure and subnuclear distribution suggested these proteins might form the lamina in the plant nucleus. It was not until 2007 that the function of NMCP proteins in the regulation of nuclear morphology was confirmed in *A. thaliana* (Dittmer et al. 2007) which has supported their classification as lamin-like proteins. Single or multiple mutations of three out of four *A. thaliana* NMCP genes (*LINC1*, *LINC2* and *LINC4*) affect nuclear size and morphology (Dittmer et al. 2007; Sakamoto and Takagi 2013) which is also the phenotype characteristic for lamin mutants (Dechat et al. 2010a; Levy and Heald 2010; Meyerzon et al. 2009). In addition, changes in heterochromatin distribution and increased

nuclear DNA packaging densities were described for *linc1linc2* mutants in comparison to the WT (Dittmer et al. 2007) although the role in chromatin organization was not confirmed by an independent study on the same mutant (van Zanten et al. 2011; van Zanten et al. 2012). Nonetheless, features observed in *linc* mutants are influenced by lamins in metazoan nuclei (Dechat et al. 2010a) therefore NMCPs seem to be, up to date, the most promising candidates for lamin analogues in plants.

Here, we apply bioinformatics and biochemistry tools to analyze the proteins of the NMCP family. We determine their predicted structures, conservation and phylogenetic relationships, and based on our results we classify them into two clusters: NMCP1 and NMCP2. In addition, we characterize NMCP1 in the monocot *A. cepa* by determining its sequence, biochemical properties, nuclear distribution and levels in cells at different differentiation states. Our results, together with previous studies, suggest that NMCPs could be the proteins that make up the lamina and fulfill some functions of lamins in plants.

2.1. Sequence and phylogenetic analysis of the NMCP family

Previous knowledge about the NMCP family was restricted to few species (carrot, celery, *A. thaliana* and sequences from the genomic projects in *Oryza sativa*, *Vitis vinifera* and *Populus trichocarpa*) (Dittmer et al. 2007; Kimura et al. 2010).

The first sequence analysis of NMCP1 suggested homology between these proteins and myosins (Masuda et al. 1997), however, it is difficult to judge on the significance of the low sequence similarity scores in establishing the homology between two proteins in distant organisms. For instance, the best match for AcNMCP1 sequence (BAM10996.1) in a BLAST search against

animal nr database is a heavy chain of non-muscle-like myosin in *Amphimedon queenslandica* (XP_003382828.1) with the total score 46.6 and e-value 0.012. The shared sequence similarity between the two is limited to the coiled-coil regions. This myosin sequence aligned with a mouse lamin B1 sequence (NP_034851.2) gives a total score of 141 and an e-value 8e-05, producing even better match than for AcNMCP1 and as before, sequence similarity is limited to the coiled-coil domain. Up to now, there is no evidence of homology between lamins and myosins. Therefore, it is clear that not only searches for plant homologs using sequence similarity are not efficient, but also in case of proteins containing extended coiled-coil domains they are very misleading since the periodic character of these domains produce false matches. A new approach that would include the structural analogies, functionality and biochemical properties is needed and joining the tools of bioinformatics, biochemistry and molecular biology could be more efficient and complete in the search for potential homologues or analogues of lamins.

Previous studies by Kimura et al. (2010) revealed a rudimentary NMCP phylogenetic tree based on ten NMCP sequences, which disabled definite classification of *A. thaliana* LINC proteins (Fig D35 a, b). Fast growing databases providing new sequenced genomes each year enabled us a more complete analysis of the well-conserved NMCP family. To search for NMCP homologs we used the Phytozome, an annually updated comparative platform providing up-to-date plant genome and gene family data (Goodstein et al. 2012). Using AcNMCP1 sequence we have found a gene family with high score and e-value which also produced high scores using previously described DcNMCP1 and AgNMCP1 sequences. Members of the NMCP family share high degree sequence similarity and have been identified in all land plants (Embryophytes) analyzed, including a moss (*P. patens*) and vascular plants (Tracheophyte), although they seem to be absent in single cell plants. Based

not only on sequence similarities but also on structural analogies and phylogenetic relationships we classified these proteins into two clusters. Our classification agrees with that proposed by Kimura et al. (2010) which was based only on the sequence similarity to carrot and celery orthologs: DcNMCP1, AgNMCP1, DcNMCP2 and AgNMCP2. In our study we characterize each cluster including not only phylogenetic relationships, but also specific structures and conserved domains.

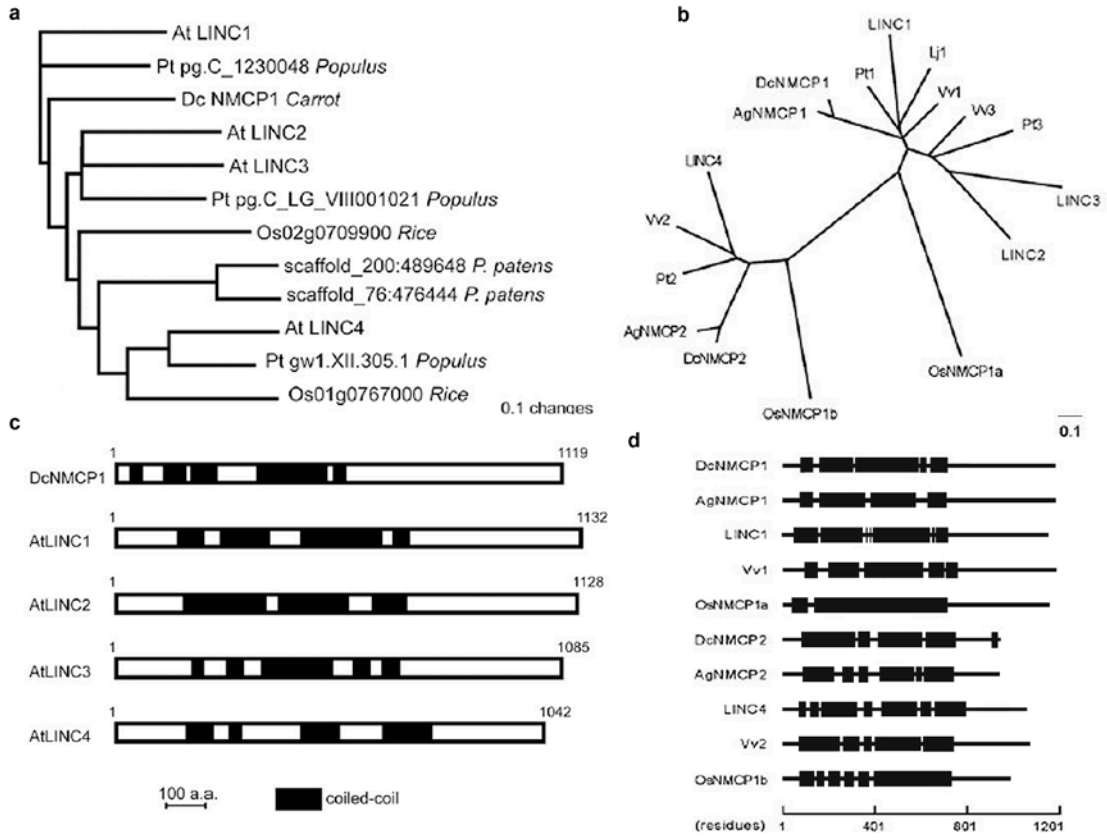

Figure 35. Previous phylogenetic analyses and coiled-coil predictions of NMCP proteins. a, b Phylogenetic relationships of NMCP proteins as proposed by Dittmer et al. (2007) (a) and Kimura et al. (2010) (b). **c, d** Coiled-coil predictions of selected NMCP proteins performed using Multicoil (Dittmer et al. 2007) (c) and COILS (Kimura et al. 2010) (d). Coiled coils are represented by black boxes.

According to our results performed on 71 protein sequences, NMCPs in vascular plants evolved from two genes, the *NMCP1* and *NMCP2* progenitor, while the two *P. patens* homologues evolved from the common NMCP ancestor which seems to be related to NMCP2 (Fig. 11). Monocots carry one *NMCP1* and one *NMCP2* gene, while dicots carry an additional gene encoding an NMCP1-related protein, designated *NMCP3* (Fig. 11). *A. thaliana* carries four genes, *LINC1-4* (Dittmer et al. 2007). We found that LINC1 is an ortholog of the NMCP1, whereas LINC2 and LINC3 are classified as NMCP3 proteins (Fig 11). Dittmer et al. (2007) focused their research on LINC1 and LINC2 proteins suggesting their important functions in the nucleus. Nevertheless, our phylogenetic results suggest that LINC4 could be also implicated in basic NMCP functions as it is the only NMCP2-type protein expressed in *A. thaliana* as already suggested (Fig. 35) and despite its previous annotation as a chloroplast protein in a proteomic study (Kleffmann et al. 2006). The presence of a predicted NLS also suggests that LINC4 is present in the nucleus, as it has been confirmed recently by the expression of LINC4-GFP under the control of the cauliflower mosaic virus (CaMV) 35S promoter (Sakamoto and Takagi 2013). Our recent results obtained using an actualized version of Phytozome suggest that more dicots contain two NMCP3 proteins (*Capsella rubella*, *Brassica rapa* and *Dacus carota*) and also, that tomato and potato lack NMCP3 and instead, express two NMCP1 proteins.
The subnuclear distribution of NMCP1 and NMCP2 during mitosis differs, indicating that they probably have different partners and mediate different functions (Kimura et al. 2010).

2.2. The predicted structures of NMCPs

NMCPs have a tripartite structure featuring a central coiled-coil rod domain and non-coiled-coil head and tail domains. The previous predictions of coiled-coil domains in NMCP proteins were performed using Multicoil (Wolf et al. 1997) and COILS based on Lupas algorithm (Lupas et al. 1991) (Fig. 35 c, d). However, a comparative analysis on a group of tools by Gruber et al. (2006) revealed the former methods are too restrictive and tend to unpredict coiled-coil domains. On the other hand, the analysis discloses that MARCOIL, a tool based on Hidden Markov Model (Delorenzi and Speed 2002) performs the best in the coiled-coil prediction and for that reason we have chosen it in our analysis. Our prediction with the MARCOIL programme suggests that the distribution of coiled-coil domains in NMCPs is much more conserved than suggested by the previous predictions obtained with Multicoil or COILS (Dittmer et al. 2007; Kimura et al. 2010). Most NMCPs contain two coiled coils separated by a linker of around 20 residues and forming a central rod domain. Our prediction also revealed short linkers inside the coiled-coil segments in some cases. The predicted coiled-coil structures were compared to the structure of lamins. Similarities in predictions for lamins and NMCPs confirmed that their general structure and organization of coiled coils are alike, although the rod domain of the latter is twice as long (Fig. 36).

NMCPs exhibit a high degree of sequence similarity in the rod domain, which contains five highly conserved regions at each end and at the positions of the predicted linkers. Lamins exhibit a similar distribution of conserved motifs although the sequence does not show significant degree of similarity between the two proteins. Based on a search against MyHits-PROSITE database, all NMCP conserved motifs appeared to be specific to this family.

The regions located at either end of the coiled-coil domain in lamins are prime candidates to mediate head-to-tail associations (Kapinos et al. 2010). The analogous structure and location of conserved motifs in NMCPs and lamins

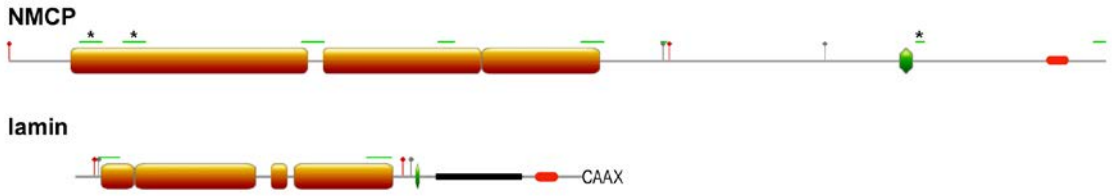

Figure 36. Schematic representation of structural analogies between typical NMCP protein and lamin. NMCPs and lamins display similar distribution of coiled coils (orange boxes) and conserved regions (green bars) at the ends of rod domain. NMCP also contain predicted phosphorylation sites preceding and following the coiled-coil domain. Both proteins contain an NLS (green boxes) and a stretch of acidic amino acids in the tail domain (red boxes), although NMCP does not contain an Ig fold (black box). Three regions which mediate the localization of NMCP1 at the nuclear periphery are marked with asterisks (*). NMCP lacks CAAX box but contains a highly conserved region at the C-extreme.

may suggest a similar mechanism of oligomerization and protofilament formation. This hypothesis is further supported by the presence of consensus sequences recognized by cdk1 (Blom et al. 2004) at each side of the rod domain as in lamins (Fig. 36). A recent study has shown that the region corresponding to the 141 amino acids of the N-terminus of DcNMCP1, which includes the two highly conserved regions at the beginning of the rod domain, together with the conserved RYNLRR region in the tail domain mediate localization of the NMCP1 proteins to the nuclear periphery (Masuda, unpublished results). The tail domain, also contain five amino acids identical to a specific region of lamin A (E**YNLR**S**R**T) (Peter and Stick 2012) that probably serves as an actin-binding site (Simon et al. 2010). Thus, the conservation of the sequence suggests that this region of NMCP1 may also be a binding site for actin. Punctual mutations in this conserved sequence in lamins cause severe laminopathies like Hutchinson-Gilford progeria syndrome (HGPS; mutation E578V) and Dunningan type Familial Lipodystrophy (FPLD2; mutations R582H, R584H) (Human Intermediate Filament Database: www.interfil.org) (Szeverenyi et al. 2008; Csoka et al. 2004; Speckman et al. 2000; Boschmann et al. 2010; Vigouroux et al. 2000; Hegele et

al. 2000) which suggests that the actin-binding site plays an important role in lamin A functions.

Like lamins, most NMCPs (62 out of 76) contain a predicted NLS in the tail domain although the position and the sequence are conserved only in NMCP1-type proteins. The functionality of the conserved NLS was confirmed for DcNMCP1 using EGFP-fused constructs transiently expressed in *Apium graveolens* epidermal cells (Masuda, unpublished results). Although few sequences lack a predicted NLS two of such proteins (AgNMCP2 and DcNMCP2) still localize in the nucleus, to which they are probably directed via an alternative pathway (Kimura et al. 2010).

The retention of lamins in the INM is mediated by the farnesylated C-terminal CAAX box (Krohne et al. 1989; Kaufmann et al. 2011; Peter and Stick 2012), although as seen for lamin C, this motif is not an absolute requirement for INM association (Dittmer and Misteli 2011). While NMCPs lack a CAAX box, the C-terminus of most members (except for the dicot NMCP2) contains a highly conserved region. It could mediate the localization of NMCP1 to the nuclear periphery together with the conserved regions at the beginning of the rod and in the tail domains (Fig. 36). The conserved C-terminal region is preceded by a stretch of acidic amino acids that is also present at the end of the tail domain of vertebrate lamins (Erber et al. 1999).

2.3. The endogenous NMCP proteins

We analyzed the endogenous NMCP proteins using the anti-AcNMCP1 antibody, which is directed against the most conserved part of the protein. While the predicted molecular weights of NMCPs from dicot and monocot species were similar (~130-140 kDa for NMCP1 and 110-120 kDa for NMCP2), immunoblots revealed that the sizes of the endogenous proteins are

highly variable across species. In some cases, the molecular weights of the bands detected were higher than the predicted values: 60 kDa higher in onion and 20-30 kDa in *A. thaliana*. The experimental MWs of NMCP1 proteins in carrot and celery are also 20-40 kDa higher than the predicted values (Kimura et al. 2010). These differences could reflect incomplete denaturation or post-translational modifications of the native protein, although the first possibility appears unlikely given the protein's behaviour in conditions favouring denaturation. The experiments using high concentration of urea (7M) or guanidine thiocyanate (6M), high temperature and high pH values (9 pH) which are known to favour denaturation of the most resistant IFs, keratins (Herrmann and Aebi 2004) did not change the mobility of the detected bands. Therefore, we suggest that NMCP1 proteins probably undergo post-translational modifications. Moreover, the lower MW detected in monocots, including garlic that belongs to the same genus as onion suggests the involvement of alternative splicing or post-translational modification like a proteolytic cleavage. Lamins undergo these two modifications. For example, lamin C, an alternative transcript of *LMNA* is 92 amino acids shorter than lamin A (Human Intermediate Filament Database: www.interfil.org) while the latter undergoes a proteolytic cleavage of the 15 C-terminal amino acids by the protease Zmpste24 (Weber et al. 1989a).

NMCP genes may also encode multiple transcripts as it is suggested by the data on Phytozome database. For example, an NMCP1 protein in *Sorghum bicolor* (Sb04g030240.1) is predicted to contain 1,156 amino acids but a protein product of the alternative transcript is predicted to lack 134 amino acids at the C-terminus (Sbi04g030240.3) (Addendum 1). We intended to investigate by Northern blot the presence of alternative transcripts and the possibility that the differences in NMCP size between the species were present at the transcript level. We designed and produced a probe based on a highly

conserved region which included the end of the head and the beginning of the rod domain and intended to detect and compare the sizes of NMCP transcripts in various species. Unfortunately, the probe failed to align.

In pea the anti-NMCP1 antibody recognized a band with the size (70 kDa) of one of the three main constituent proteins of the isolated lamin fraction (L) obtained by nuclease digestion, high salt and detergent extraction and incubation in high concentration of urea followed by dialysis (Li and Roux 1992). The last two steps take advantage of a characteristic IF feature of being soluble at high urea concentrations but then becoming insoluble when dialyzed out of the urea solution into one not containing urea (Ward and Kirschner 1990). Interestingly, TEM analysis of the negatively stained pea L fraction revealed bundles of filaments ranging in diameter between 6-12 nm (Li and Roux 1992; Blumenthal et al. 2004) which could suggest that the pea ortholog of NMCP1 protein would be a component of the filaments observed in L fraction. Nevertheless the identity of the proteins forming pea filaments cannot be confirmed since no sequence data is available.

3. AcNMCP1- a monocot NMCP1 ortholog

3.1. Biochemical features of AcNMCP1

The experimental MW of the endogenous AcNMCP1 in immunoblots (200 kDa) is much higher than the predicted value (139 kDa). The results of experiments using different denaturation conditions such as 7 M urea, 6 M guanidine thiocyanate, high temperature and high pH values discarded the presence of dimers and higher oligomerization states. The MW could be altered by post-translational modification such as glycosylation (Wilson et al.

2009) which is further supported by the presence of predicted glycosylation sites in NMCP sequences, including AcNMCP1. Our immunoblot results using an anti-HRP antibody, which recognizes complex-type *N*-glycans with α1->3 fucose and β1->2 xylose residues characteristic for plant glycoproteins (Faye et al. 1993) do not confirm this hypothesis but further studies using more specific methods is needed to verify if AcNMCP1 undergoes glycosylation as occurs with lamins (Ferraro et al. 1989; Wang et al. 2010b; Alfaro et al. 2012).

Although endogenous NMCP proteins show a wide range of MW the experimental isoelectric point of AcNMCP is in agreement with the predicted and detected pI values for other NMCPs and similar to pI of B-type lamins (Addendum 1) (Masuda et al. 1993).

3.2. Nuclear distribution and localization of AcNMCP1

The NMCP proteins show different intranuclear distribution which was investigated by immunofluorescence and GFP expression. AcNMCP1 demonstrated a consistent association with the nuclear periphery by immunofluorescence confocal microscopy. Nevertheless, a minor fraction was also localized in the nucleoplasm. Exclusive localization at the nuclear periphery in the interphase nuclei was previously reported for the corresponding carrot and celery proteins using the same method (Masuda et al. 1997; Kimura et al. 2010) and for *A. thaliana* proteins by expression of LINC1-GFP (Dittmer et al. 2007; Dittmer and Richards 2008) and LINC4-GFP (Sakamoto and Takagi 2013). Exclusive nucleoplasmic localization was described for rice NMCP1a (Moriguchi et al. 2005), *Arabidopsis* LINC2 (Dittmer et al. 2007) and LINC3 (Sakamoto and Takagi 2013) using

YFP/GFP:35SV, although the intranuclear staining of AcNMCP1 was not as abundant as in latter cases and in all our preparations the predominant labeling of AcNMCP1 at the nuclear periphery was evident. Some variability of the intranuclear staining may have been produced by the reduced accessibility of the internal AcNMCP1 pool to the antibody, as suggested by the gradient of internal staining and would explain differences in abundance and intensity of nucleoplasmic labelling. Lamins are also localized in the nucleoplasm where they are involved in gene transcription, cell cycle progression, differentiation and chromatin organization (Dechat et al. 2010b). Immunogold-EM of detergent extracted nuclei clearly demonstrated that onion NMCP1 preferentially localizes in the nuclear lamina, close to the condensed heterochromatin masses. This suggests a role of NMCP1 in anchoring peripheral heterochromatin to the lamina, one of the functions fulfilled by lamins in metazoan nuclei (Fawcett 1966; Bank and Gruenbaum 2011b). Many lines of studies suggest that the lamina not only supplies an anchor for heterochromatin but also regulates chromatin organization and activity (Guelen et al. 2008; Peric-Hupkes et al. 2010; Bank and Gruenbaum 2011b; Zuleger et al. 2011; Mekhail and Moazed 2010). Transcriptionally silent regions of the genome, such as centromers, telomers and the inactive X chromosome are preferentially positioned at the nuclear lamina (Fawcett 1966; Belmont et al. 1993; Peric-Hupkes and van Steensel 2010; Guelen et al. 2008; Pickersgill et al. 2006). Also, in plants heterochromatic centrometers localize at the nuclear periphery in close association to the lamina (Fang and Spector 2005). On the contrary, active chromatin is preferentially associated with the nuclear interior (Osborne et al. 2004; Shopland et al. 2006) and this global distribution is dynamic during the cell cycle, differentiation and development (Peric-Hupkes et al. 2010; Pickersgill et al. 2006). Recent models of nuclear architecture include lamins and lamin-associated proteins as determinants of

chromosome positioning through direct or indirect anchoring chromatin to the nuclear lamina and organizing chromatin inside the nucleus on nucleoplasmic scaffold (Goldman et al. 2002; Dorner et al. 2007; Vlcek and Foisner 2007; Bank and Gruenbaum 2011b; Zuleger et al. 2011). The interaction between lamins and chromatin appears to involve at least two chromatin-binding regions: one located in the tail domain between the end of the rod domain and the Ig fold and the other within the rod domain (Taniura et al. 1995; Bruston et al. 2010). Lamins also bind nonspecifically to DNA *in vitro* through contacts in the minor groove of the double helix (Taniura et al. 1995; Shoeman and Traub 1990) and associate with MAR (matrix attachment region) sequences which are involved in transcriptional regulation, DNA replication, chromosome condensation and chromatin organization (Luderus et al. 1994). It is possible that NMCPs also bind to peripheral chromatin via a similar mechanism.

AcNMCP1 is localized in the lamina in close proximity to associated NPCs suggesting that the protein may associate to these macromolecular assemblies. In metazoan nuclei lamins control spatial distribution of the NPCs on the nuclear envelope by physical binding to the NPCs through the C-terminal domain of Nup153 (Liu et al. 2000; Lenz-Bohme et al. 1997). Although plants do not contain a Nup with high sequence similarity to Nup153, a plant-specific functional homolog of this nucleoporin, Nup136 was described in *A. thaliana* (Tamura et al. 2010). Interestingly, a mutant overexpressing this protein displays elongated nuclei, while the knockdown mutant displays more spherical nuclei (Tamura and Hara-Nishimura 2011), a phenotype characteristic for *linc1linc2* mutants (Dittmer et al. 2007). This suggests that Nup136 influences the nuclear shape through the interaction between NPCs and NMCP proteins present in the plant nuclear lamina (Tamura and Hara-Nishimura 2011).

AcNMCP1 was also detected in the fibrillar network of interchromatin domains, suggesting that it is involved in nuclear functions associated with these domains. Lamins are also localized in the nuclear interior and this intranuclear pool is thought to be implicated in functions such as regulation of cell cycle, chromatin organization and DNA replication (Dechat et al. 2010b). Both lamin types are found in the nucleoplasm where A-type lamins form a mobile fraction and B-type lamins are more static (Shimi et al. 2008). Lamin B co-localizes in the nucleoplasm with DNA replication sites (Moir et al. 1994) whereas A-type lamins are involved in the regulation of the cell cycle through the interaction with retinoblastoma protein (pRb), a major cell cycle regulator and transcriptional repressor (Ozaki et al. 1994; Dechat et al. 2010b). Lamins bind to DNA and histones as well as to proteins regulating chromatin transcription which suggests their role in the organization of chromatin throughout the nucleus (Dechat et al. 2010b). Further studies have to be performed to establish the possible roles of both, nucleoplasmic and lamina-associated pools of NMCPs, in chromatin organization.

3.3. AcNMCP1 is a component of the NSK

AcNMCP1 is highly insoluble and is an abundant component of the nucleoskeleton, as determined by the sequential extraction of lipids, soluble proteins and DNA from nuclei (Ciska et al. 2013) and has been reported for DcNMCP1 (Masuda et al. 1993). A recent study by (Sakamoto and Takagi 2013) revealed that not only NMCP1 but also the other NMCP/LINC proteins are components of the NSK fraction extracted by sequential extraction with non-ionic detergent, DNase and RNase (but omitting the high salt extraction) in *A. thaliana* which confirms the structural function of these

proteins. Our immunofluorescence and immunogold EM results in nucleoskeletons are the first report of the distribution of NMCP1 in the NSK in situ. We confirm that the protein is a key component of the lamina and it is also present in a minor fraction in the internal NSK. These results demonstrate that NMCP1 is a structural protein that may be involved in the organization of the lamina and also of the multimeric complexes in the internal plant NSK, function fulfilled by lamins in the metazoan NSK (Simon and Wilson 2011).

3.4. The levels and the distribution of AcNMCP1 are developmentally regulated along the root

Immunoblots with proteins extracted from nuclei of the different root cell populations show that the expression of AcNMCP1 is developmentally regulated. AcNMCP1 is abundant in meristems, either proliferating or quiescent while in the cells of the mature zone it is expressed at much lower levels.

Onion quiescent meristematic cells have smaller nuclei than proliferating ones (Risueno and Moreno Diaz de la Espina 1979). Since NMCP1 is necessary for the increase of nuclear size during germination (van Zanten et al. 2012) it may be also the case during the switch from quiescent to proliferating meristem which could explain its accumulation in quiescent meristems. Cells in the onion root quiescent meristem are stopped in pre-replicative (G_{01}) and post-replicative (G_{02}) states as showed by the flow cytometry analysis (Fig. 30). After water activation cells undergo dramatic metabolic changes to undertake the first post-quiescent cell cycle followed by cell division (den Boer and Murray 2000). Some of the factors necessary for this activation are stored in the quiescent meristem (Jakob and Bovey 1969). NMCP proteins may be

implicated in the regulation of the cell cycle, DNA processing and also transcription as microarray data suggest (Dittmer et al. 2007). It is possible that NMCP1 proteins are needed for cell cycle progression and the quick activation of quiescent cells which could also explain the high AcNMCP1 levels detected in the quiescent meristem.

In line with our results in proliferating meristems, Dittmer and Richards (2008) reported that GFP-LINC1 was expressed predominantly in proliferating tissues but no GFP signal was detected in the differentiated cells. On the contrary, our results using immunoblotting and immunofluorescence demonstrated that AcNMCP1 is expressed in the differentiated cells of the onion root although at a low level. Our results are in agreement with those of Sakamoto and Takagi (2013) who reported that all *LINC* genes are expressed in the whole *A. thaliana* plants. Microarray data show that in *A. thaliana* root tissues *LINC1*/*AtNMCP1*, *LINC4*/*AtNMCP2* and *LINC3* genes are expressed at the highest levels whereas *LINC2* is generally expressed at the lowest levels (Birnbaum et al. 2003; Brady et al. 2007). Also, in agreement with our results is the observation that the expression of *LINC1* decreases between the elongation and the differentiated root zones (Birnbaum et al. 2003; Brady et al. 2007; Dinneny et al. 2008). Regarding other NMCP proteins, the expression of *LINC2* and *LINC3* also decreases from the meristem to the differentiated root zone and displays an especially steep decrease in *LINC2* expression between the meristematic and the elongation root zone (Brady et al. 2007; Birnbaum et al. 2003; Dinneny et al. 2008). The expression of *LINC4* decreases in the elongation zone but slightly increases again in the differentiated root zone (Birnbaum et al. 2003; Brady et al. 2007; Dinneny et al. 2008).

One of the confirmed functions of NMCP proteins is the regulation of the nuclear size and shape (Dittmer et al. 2007; van Zanten et al. 2011; Sakamoto

and Takagi 2013) which may change significantly during cell differentiation. In the plant root several zones can be distinguished containing cells at different developmental stages. The changes in nuclear size and shape in the root have been described by Tamura and Hara-Nishimura (2011) in the model plant *Arabidopsis thaliana*. In the meristem, undifferentiated cells undergo mitosis and the nuclei are small and spherical. When they cease to proliferate they undergo a period of elongation defining the elongation zone (Bennett and Scheres 2010). The nuclei of these cells increase the volume maintaining the spherical shape (Tamura and Hara-Nishimura 2011). The accumulation of NMCP in the elongation zone could be related to the increase of nuclear size in the cells of this zone.

On the other hand, the decrease in NMCP1 levels in the fully differentiated cells could be caused by a reduction of a function performed by this protein. Many coiled-coil proteins, including lamins fulfill important structural functions in the cell (Lammerding et al. 2006; Schape et al. 2009; Lupas and Gruber 2005). It is probable that NMCP proteins also play these functions since they are highly insoluble and contain an extensive coiled-coil domain, as lamins. The structural functions of the latter are well described but plant cells react to mechanical forces differently than animal cells as they are encased in an "exoskeleton" in form of a rigid cell wall (Zhong and Ye 2007; Hamant et al. 2008). Therefore, the animal nucleus is more vulnerable to mechanical forces and at least one lamin is expressed in the metazoan cell at all developmental stages (Peter and Stick 2012). In plant cell the rigidness of the cell wall is modified during cell differentiation, in the meristematic cells being more elastic than in the differentiated cells. The cell wall becomes more rigid as the cell elongates, when cellulose microfibrils undergo a dynamic reorientation and the rigidification of other cell wall components takes place which provides a structure capable of resisting force along any axis (Anderson

et al. 2010). In result, a rigid cell wall in differentiated cell provides a protection against external mechanical forces which could reduce the mechanical functions of NMCP proteins and explain their low levels in these cells.

Lamin expression is also developmentally regulated (Takamori et al. 2007). The AcNMCP1 and LINC1/AtNMCP1 expression profile resembles that of lamin B1, which is abundant in proliferating and quiescent meristematic cells but is weakly expressed in differentiated cells (Lehner et al. 1987; Broers et al. 1997; Shimi et al. 2011). Lamin B1 plays a role in regulation of the proliferation rate since silencing the expression of lamin B1 results in decreased cell proliferation whereas its over-expression increases the proliferation rate (Shimi et al. 2011). Likewise, NMCP1 could be implicated in the regulation of proliferation as its levels are high in the meristematic cells, but further studies are needed to resolve its involvement in this function.

The AcNMCP1 distribution in the nucleus varies in different root cell populations. In quiescent nuclei NMCP1 forms accumulations in form of speckles in the nucleoplasm that are not present in proliferating meristems. Similar structures were previously reported to contain packed nuclear ribonucleoproteins (RNPs) and actin in quiescent root meristems and were suggested to serve as storage sites for frozen transcription and splicing factors, ready to be used early after release from the root dormancy (Cui and Moreno Diaz de la Espina 2003; Cruz and Moreno Diaz de la Espina 2009). The sites of accumulation of AcNMCP1 could correspond to the quiescent micro-speckles since microarray expression data suggested that the *LINC* genes in *A. thaliana* are involved in transcription, cell cycle and DNA processing (Dittmer et al. 2007). The AcNMCP1 speckles observed in the nucleoplasm of root quiescent meristematic cells could be the reservoir of this protein prepared for early activation during root germination.

Our results also reveal alterations in the distribution of AcNMCP1 in differentiated cells: while AcNMCP1 is regularly distributed along the nuclear envelope in meristematic cells, its distribution in differentiated cells is discontinuous, with gaps depleted of AcNMCP1. A similar distribution pattern has been reported also for lamin B2 in lamin B1-silenced cells (Shimi et al. 2008) and for *Ce*-lamin in aging cells of *C. elegans* (Haithcock et al. 2005). Changes in the distribution of the latter were accompanied by changes in nuclear shape, loss of peripheral heterochromatin and appearance of condensed chromatin in the nucleoplasm. Alterations of the AcNMCP1 distribution in the differentiated cells could be correlated with changes in the distribution of heterochromatin that take place during cell differentiation.

4. *linc1* and *linc2* mutations do not alter nuclear ultrastructure in *Arabidopsis thaliana* root meristem

Mutations of *LINC1* and *LINC2* genes resulted in reduction in nuclear size, changes in nuclear shape and in the number of chromocenters in *A. thaliana* (Dittmer et al. 2007) but the effects of these mutations on nuclear ultrastructure have not been described. The functional analysis conducted on these mutants by Dittmer et al. (2007) was focused on the changes in differentiated cells (root and leaf epidermis and anthers) which displayed decrease in nuclear size and increase in nuclear DNA packing density.

The analysis of ultrathin sections of root meristems isolated from WT and *linc1* and *linc2* double and single mutants did not reveal any evident changes in the ultrastructure and distribution of the different nuclear domains such as nucleolus or chromocenters between the mutant and WT cells.

Although the involvement of LINC1 and LINC2 proteins in maintenance of nuclear shape and size was confirmed by several research groups (Dittmer et

al. 2007; van Zanten et al. 2011; Sakamoto and Takagi 2013) their role in chromatin organization is still discussed. Our analysis using EM revealed that nuclei of root meristematic cells of *linc1linc2* mutants display no changes in chromatin ultrastructure in comparison to WT which is in agreement with the results obtained for *linc1linc2* mutants by van Zanten et al. (2011) during seed maturation and germination. Nuclei decrease their size and increase the chromatin condensation during seed maturation and reverse effects take place during germination. The research revealed that LINC1 and LINC2 proteins are required for the increase in nuclear size during germination (van Zanten et al. 2011). Nevertheless, the changes in relative heterochromatin fraction and distribution of heterochromatic regions (labeled using FISH: centromeric 180-bp repeat, pericentromeric subtelomeric 45s rDNA repeats and pericentromeric sequences) during germination were the same for the *linc1linc2* mutants as for the WT (van Zanten et al. 2011; 2012). Ours and the latter results would indicate that at least LINC1 and LINC2 proteins are not major factors involved in the control of chromatin compaction. Nevertheless, the *linc1linc2* mutant contains functional LINC3 and LINC4 proteins which may complement some functions of LINC1 and LINC2, therefore the involvement of other LINC proteins in these functions cannot be discarded. Further analysis of nuclear ultrastructure in mutants including mutations of the remaining *LINC* genes is needed to verify their role in chromatin organization.

5. NMCPs as analogues of lamins

The origin of lamins is still to be resolved. Despite the lack of lamin homologs in non-metazoans, the universal presence of a lamina and the fulfillment of lamin functions in most eukaryotes, suggest that lamins are just one of many

possible solutions. Here, we summarize the main similarities between NMCPs and lamins, which are also presented in table 14, and that could be the key factors in resolving the nature of the protein components of the lamina in plants. These similarities may suggest that NMCPs play some functions of lamins in the plant cell.

1. Lamins are expressed in all metazoans as NMCPs are expressed in all land plants. Many lines of studies suggest that lamins evolved to facilitate the integration of cell types into highly elaborated tissue organization in animals since mutations in these proteins result in developmental aberrations (Zuela et al. 2012). Similarily the mutations of the four *At*NMCP/*LINC* genes and some combinations of triple mutations are lethal or cause whole-plant dwarfing defects (Dittmer and Richards 2008; Graumann et al. 2013; Sakamoto and Takagi 2013) suggesting that functionality of at least one of the NMCP protein is essential for proper development of the plant.
2. Lamins are highly conserved proteins in metazoans (Franke et al. 1987; Weber et al. 1989a). NMCPs also make up a protein family with a high conservation degree which suggests they play essential functions in plants.
3. Invertebrates usually express one B-type lamin. Mammals contain three lamin genes, two encoding B-type lamins: *LMNB1* (encoding lamin B1), *LMNB2* (encoding lamin B2 and B3) and one encoding A-type lamins *LMNA* (encoding lamins A, AΔ10, C and C2) (HIFD: www.interfil.org) (Ostlund and Worman 2003; Broers et al. 2004; Peter and Stick 2012; Machiels et al. 1996). Analogously to lamins, there are two types of NMCP proteins: NMCP1 and

NMCP2. Monocots contain one gene coding for each type whereas dicots contain three or four *NMCP* genes: *NMCP1* and *NMCP3* (one or two) (encoding NMCP1-type proteins) and one *NMCP2*.

4. NMCPs and lamins represent a similar tripartite structure with a central coiled-coil domain predicted to form dimers. Lamins oligomerize into dimers and protofilaments in head-to-tail fashion. The highly conserved regions at the ends of the rod domain are the prime candidates to mediate the head-to-tail association of two dimers (Kapinos et al. 2010) and the phosporylation sites located in close proximity to the conserved regions probably regulate the polymerization state during cell cycle. In NMCP proteins the ends of the rod domain are also highly conserved and also contain predicted cdk1 phosphorylation sites flanking the ends of the rod domain which could suggest a similar oligomerization mechanism.
5. Lamin binding proteins (LBPs) form a vast group of proteins that associate with lamins. Most of them are not conserved in plants and are thought to be metazoan-specific. Very few lamin-binding proteins have been identified in plants, the only clear orthologs are the SUN proteins which contain the SUN-domain conserved across the kingdoms (Graumann et al. 2010; Murphy et al. 2010; Oda and Fukuda 2011). In addition, a functional homolog of Nup153 was described in *Arabidopsis thaliana* and although it does not share significant sequence similarity with its animal counterpart, it was confirmed to play the functions of the lamin-binding nucleoporin Nup153 (Tamura and Hara-Nishimura 2011). The interactions between these proteins and NMCPs are not yet confirmed. In fact the possible binding of SUN-domain proteins to NMCP are currently under investigations by FRET and co-immunopreciptation

and the preliminary results from FRET suggest such interaction (personal communication, Prof. K. Graumann).

6. Some biochemical properties of NMCPs are similar to those of lamins and IFs. A hallmark feature of IFs is their insolubility in buffers of physiological ionic strength and pH (Herrmann and Aebi 2004). Also, they are resistant to extraction with buffers of high ionic strength and high concentrations of non-ionic detergents. They require drastic conditions to solubilize, like for example, inclusion of 8M urea or 3M guanidinium hydrochloride. These biochemical properties characterize NMCP proteins as well.
7. Although we did not investigate the possibility that NMCPs form filaments, its predicted structure and properties strongly suggest they do. Also, filaments of 6-12 nm in diameter were observed under the electron microscope in the isolated pea nuclear matrix fraction (Li and Roux 1992; Blumenthal et al. 2004). One of the constituent proteins of this fraction is a protein with the same MW (70 kDa) as PsNMCP1. A filament meshwork with attached nuclear pore complexes similar to metazoan lamina was observed on the inner side of the tobacco nuclear envelope (Fiserova et al. 2009). In collaboration with the group of Dr Goldberg we are investigating if NMCP1 is a component of this filamentous meshwork lining the INE by immunodetection of AcNMCP1 in feSEM preparations of nuclei.
8. AcNMCP1 has a subnuclear distribution similar to that of lamins. It is abundant in the lamina and in a minor degree also present in the nucleoplasm (Dechat et al. 2010b). In electron miscroscopy sections AcNMCP1 seems to be localized in close proximity to NPCs, which

is characteristic for lamins that are involved in the distribution of NPCs on the NE (Fiserova and Goldberg 2010).

9. The expression of NMCP1 is developmentally regulated as is also the expression of lamins (Peter and Stick 2012). The NMCP1 expression pattern resembles that of lamin B1 (Shimi et al. 2011).
10. NMCP proteins are involved in the maintenance of nuclear shape and size as are lamins in metazoan cells (Edens et al. 2012; Dechat et al. 2010a). In addition, lamins play numerous functions in metazoan cells like for example regulation of chromatin organization, cell cycle, transcription, replication, differentiation etc. The involvement of NMCP proteins in these functions is yet to be investigated.

NMCPs display many similarities to lamins (Ciska et al. 2013) and in the future even more analogies may emerge as the knowledge of these proteins develops. Based on our present and previous results we propose NMCPs to be candidates to fulfill some functions of lamins in plants.

Nevertheless, it is possible that due to the differences between plant and animal cells the shared functions of lamins and NMCP proteins may be limited to just few and also the plant analogues may play specific functions not fulfilled by the animal counterparts.

NMCP proteins, as lamins play functions in maintenance of nuclear size and shape. On the other hand, latest studies on LINC/NMCP and plant SUN proteins suggest they do not share some functions with their animal counterparts. The mechanism of nuclear movement in animal cell involves lamins, SUN- and KASH-proteins (Starr 2009; Brosig et al. 2010; Luxton et al. 2010). Nevertheless, in the plant cell neither SUN-proteins nor NMCPs appear to be involved. The disruption of two *sun* genes or *linc* genes in *A.*

	NMCP	**Lamins**
Presence	land plants	Metazoans
Genes	*NMCP1*, *NMCP2*, *NMCP3* (dicots)	*LMNB1, LMNB2*, *LMNA* (vertebrates) Single *LMNB* in most invertebrates
Sequence	Highly conserved across species	
Structure	Tripartite structure with central coiled-coil domain	
	Coiled coils form dimers	
	Short head domain containing phosphorylation site	
	Rod domain contains two segments separated with linker	
	Highly conserved regions at the ends of rod domain and at the positions of linkers	
	-	Ig fold in the tail
	R**YNLRR** (tail domain; NMCP1)	E**YNLR**S**R**T (tail domain; lamin A)
	Stretch of acidic amino acids (except dicot NMCP2)	Stretch of acidic amino acids (vertebrates)
	Conserved region at the C-terminus (except dicot NMCP2)	CaaX box at the C-terminus
Properties	70-200 kDa	65-70 kDa
	Acidic pI	Acidic pI (B-type lamins) Neutral pI (A-type lamins)
	Unsoluble	Generally unsoluble
		Form 10 nm filaments
Localization	Nuclear periphery at the lamina, a minor fraction in nucleoplasm	
	In close proximity to heterochromatin masses and NPCs	
Protein levels	Developmentally regulated	
Funcions	Maintenance of nuclear size and shape	
		Functions in essential cellular processes: transcription, DNA replication, cell cycle progression and chromatin organization

Table 14. Comparison of the main features of NMCP proteins and lamins.

thaliana did not affect the nuclear movement in the root hair cells or in response to light which suggest an alternative mechanism that does not

include the SUN-KASH bridge (Oda and Fukuda 2011) nor NMCP proteins (Sakamoto and Takagi 2013).

Further studies are needed to fully elucidate the functions of NMCPs including the analysis of their involvement in different nuclear activities studying mutants; identification of their protein partners (such as SUN domain proteins, Nup136, actin and other plant-specific proteins); and their in vitro polymerization.

CONCLUSIONS

1. NMCPs are plant specific proteins that form a highly conserved protein family. They are expressed in multicellular but not in single-cell plants.

2. The NMCP protein family consists of two clusters, one containing NMCP1-type and the second containing NMCP2-type proteins.

3. Monocots express one protein of each type whereas dicots contain two or three NMCP1-type proteins (designated NMCP1 and NMCP3) and a single NMCP2-type.

4. The two members in *Physcomitrella patens* evolved from a common NMCP progenitor which seems to be related to the NMCP2 cluster.

5. *Arabidopsis thaliana*, *Capsella rubella*, *Brassica rapa* and *Dacus carota* express four NMCP proteins: one NMCP1 (LINC1/AtNMCP1), one NMCP2 (LINC4/AtNMCP2) and two NMCP3-type proteins (LINC2, LINC3).

6. NMCPs have a tripartite structure with a central α-helical rod domain that is predicted to form coiled coils, similar to that in lamins although twice as long. The coiled-coil domain is interrupted by one or two linkers whose position is conserved across the NMCP family.

7. Members of this protein family contain five highly conserved motifs within the coiled-coil domains whose positions correspond to the beginning and the end of rod domain and the linkers. The tail domain contains three conserved regions, some of which are type-specific. Additionally, most NMCP proteins contain predicted phosphorylation sites at the ends of the rod domain and an NLS sequence in the tail domain, whose position and sequence are conserved across NMCP1-type proteins.

8. The molecular weights of the endogenous NMCP proteins in various species are different from the predicted ones, indicating the presence of alternative transcripts and/or post-translational modifications. The difference between predicted and detected molecular weights is not caused by incomplete denaturation nor formation of oligomers.

9. AcNMCP1 is predicted to contain 1,217 aa and shares the predicted structure with other NMCP proteins. It also contains all the conserved regions characteristic for the NMCP family.

10. The endogenous AcNMCP1 has a molecular weight of 200 kDa and an isoelectric point of 5.2 and 5.8. The difference between the predicted and the detected MW is not due to incomplete protein denaturation or oligomerization. The mass spectrometry analysis confirms the identity of the endogenous AcNMCP1.

11. AcNMCP1 is mainly distributed at the nuclear periphery and to a lower extent in the nucleoplasm. High resolution immunogold localization revealed that AcNMCP1 is preferentially localized in the lamina.

12. AcNMCP1 is highly insoluble and is a component of the nucleoskeleton. It is mainly localized in the lamina and to a lower extent in the internal nucleoskeleton.

13. The expression levels of AcNMCP1 are devopmentally regulated. It is most abundant in meristems, either proliferating or quiescent but the levels decrease in the differentiated cells of the upper parts of the root.

14. The subnuclear distribution of AcNMCP1 also changes in cells at various differentiation states in the onion root. In all cases AcNMCP1 is predominant at the nuclear periphery. In quiescent meristems,

AcNMCP1 also forms large aggregates in the nucleoplasm. On the other hand the differentiated nuclei show discontinuity in the distribution of the NMCP1 at the nuclear periphery with large areas lacking the protein.

15. Double and single mutations of *linc1* and *linc2* genes do not produce apparent ultrastructural changes in root meristematic nuclei compared to WT nuclei. These mutants still contain functional LINC3 and LINC4/AtNMCP2 proteins that probably complement the functions of the disrupted NMCPs in nuclear organization.

16. NMCP proteins share several important features with metazoan lamins including: 1) a tripartite structure containing a central coiled-coil domain with highly conserved motifs at both ends; 2) the presence of phosphorylation sites in close proximity to the rod domain that could play a role in the formation of filaments; 3) a highly conserved C-terminus of the protein 4) identical localization in the lamina and to a lesser extent in the internal NSK; 5) its expression seems to be developmentally regulated. Together, these similarities are in agreement with the hypothesis that NMCP proteins could be the analogues of lamins in plants and play some lamin functions.

ADDENDUM

Protein	ID/ Transcript Name	Length	Predicted pI	Predicted MW
Mes3	**cassava4.1_000491m**	1183 aa	5.38	137 530
Mes1	**cassava4.1_000510m**	1163 aa	5.20	134 100
Mes2	**cassava4.1_000625m**	1103 aa	5.40	127 606
Rco1	**29673.m000916**	1163 aa	5.16	133 876
Rco3	**29738.m001028**	1172 aa	5.17	135 330
Rco2	**29825.m000318**	1052 aa	5.31	121 267
Lus1	**Lus10034075**	1007 aa	5.34	116 178
Lus3	**Lus10034263**	1217 aa	5.25	139 389
Lus2	**Lus10019257**	1008 aa	5.25	116 404
Ptr3	**POPTR_0008s11380.1 (primary)**	1205 aa	5.15	138 172
	POPTR_0008s11380.2	1149 aa	5.17	132 030
Ptr2	**POPTR_0012s01110.1**	1043 aa	5.25	120 462
Ptr1	**POPTR_0017s14050.1**	1156 aa	5.26	133 230
Pvu3	**Phvulv091022727m**	1216 aa	5.22	139 567
Pvu1	**Phvulv091023539m**	1181 aa	5.06	134 845
Pvu2	**Phvulv091014376m**	1046 aa	5.52	120 798
Gma3	**Glyma02g11330.1**	1024 aa	5.55	118 422
Gma2	**Glyma05g23100.1**	1054 aa	5.49	121 636
Gma1	**Glyma18g51560.1**	1194 aa	5.14	136 018
Csa2	**Cucsa.103490.1 (primary)**	1025 aa	5.16	119 429
	Cucsa.103490.2	912 aa	5.19	105 841
Csa1	**Cucsa.238180.1 (primary)**	1201 aa	5.18	137 184
	Cucsa.238180.2	851 aa	5.14	97 677
Csa3	**Cucsa.280830.1 (primary)**	1169 aa	5.42	135 601

	Cucsa.280830.2	1053 aa	5.87	122 708
Ppe3	**ppa000415m**	1198 aa	5.27	137 913
Ppe1	**ppa000399m**	1208 aa	5.09	138 164
Ppe2	**ppa016288m**	1059 aa	5.28	123 048
Mdo2	**MDP0000322171**	1154 aa	5.53	133 235
Mdo3	**MDP0000208604**	1217 aa	5.10	139 456
Mdo1	**MDP0000312257**	1265 aa	5.13	144 653
LINC2	**AT1G13220.2 (primary)**	1128 aa	5.08	129 924
	AT1G13220.1	391 aa	5.96	45 365
LINC1	**AT1G67230.1**	1132 aa	5.24	129 093
LINC3	**AT1G68790.1**	1085 aa	5.27	127 204
LINC4	**AT5G65770.2**	1042 aa	5.28	121 222
	AT5G65770.1	1010 aa	5.13	117 086
Aly3	**476006**	1085 aa	5.19	126 955
Cru3	**Carubv10011605m**	1169 aa	5.00	134 204
Cru1	**Carubv10019693m**	1130 aa	5.26	129 270
Cru2	**Carubv10025809m**	1001 aa	5.17	115 764
Bra1	**Bra034012**	1115 aa	5.14	127 803
Bra3	**Bra019819**	1503 aa	5.87	172 610
Bra2	**Bra037827**	1012 aa	5.25	117 283
Tha3	**Thhalv10006601m**	1178 aa	5.09	135 928
Tha2	**Thhalv10003578m**	1019 aa	5.23	118 241
Tha1	**Thhalv10018034m**	1127 aa	5.29	128 984
Cpa3	**evm.model.supercontig_1.235**	1086 aa	5.15	126 921
Cpa1	**evm.model.supercontig_179.33**	674 aa	5.33	77 994
Csi2	**orange1.1g001119m (primary)**	1150 aa	5.51	132 925
	orange1.1g001600m	1047 aa	5.43	121 197
	orange1.1g002268m	944 aa	5.67	109 994
Csi3	**orange1.1g000847m (primary)**	1255 aa	5.27	145 080
	orange1.1g001278m	1109 aa	5.26	128 488

	orange1.1g003017m	857 aa	5.23	98 755
Csi1	**orange1.1g048767m**	1041 aa	5.45	120 907
Ccl2	**clementine0.9_000926m (primary)**	1116 aa	5.36	128 732
	clementine0.9_000939m	1113 aa	5.47	128 484
Ccl1	**clementine0.9_028880m**	1166 aa	5.18	133 605
Egr3	**Eucgr.G02361.1**	1213 aa	5.40	139 337
	Eucgr.G02361.4	1050 aa	5.52	121 795
Egr2	**Eucgr.I00661.1**	1073 aa	5.44	123 257
Egr1	**Eucgr.J01462.1**	1178 aa	5.24	135 213
	Eucgr.J01462.2	1054 aa	5.48	122 263
Vvi3	**GSVIVT01011972001**	1122 aa	5.51	129 172
Vvi1	**GSVIVT01031076001**	964 aa	5.50	109 194
Vvi2	**GSVIVT01007428001**	1117 aa	5.34	129 161
Mgu1	**mgv1a000432m**	1157 aa	5.28	133 628
Mgu2	**mgv1a000959m**	932 aa	5.27	109 417
Mgu3	**mgv1a000453m**	1144 aa	5.37	133 168
Aco1	**Aquca_006_00294.1**	1198 aa	5.15	139 115
	Aquca_006_00294.2	1013 aa	5.14	118 242
Aco2	**Aquca_017_00100.1**	1081 aa	5.05	124 612
	Aquca_017_00100.2	999 aa	5.22	115 891
	Aquca_017_00100.3	991 aa	5.03	114 873
Sbi2	**Sb03g035670.1 (primary)**	818 aa	5.21	93 968
	Sb03g035670.2	804 aa	5.32	92 429
Sbi1	**Sb04g030240.1 (primary)**	1156 aa	5.22	132 155
	Sb04g030240.2	1023 aa	5.49	118 277
	Sb04g030240.3	1022 aa	5.49	118 206
Zma2	**GRMZM2G320013_T01**	970 aa	5.03	112 642
Zma1	**GRMZM2G015875_T01**	1156 aa	5.13	132 820
Sit1	**Si016142m**	1151 aa	5.32	131 882
Sit2	**Si000171m**	1002 aa	5.03	115 668
Osa2	**LOC_Os01g56140.1**	987 aa	5.23	113 614

Osa1	**LOC_Os02g48010.1**	1155 aa	5.12	132 331
Bdi2	**Bradi2g50990.1**	997 aa	5.03	115 693
Bdi1	**Bradi3g53047.1**	1157 aa	5.10	132 374
Ppa1	**Pp1s76_81V6.1**	1418 aa	4.80	165 625
Ppa1	**Pp1s200_64V6.1**	1548 aa	4.71	179 107
AgNMCP1	**BAI67715.1**	1171 aa	5.26	134 598
DcNMCP1	**BAA20407**	1119 aa	5.35	128 775
AgNMCP2	**BAI67716**	925 aa	5.43	108 005
DcNMCP2	**BAI67718**	927 aa	5.13	108 898
AcNMCP1	**AB673103**	1217 aa	5.39	139 272

BIBLIOGRAPHY

Aaronson RP, Blobel G (1975) Isolation of nuclear pore complexes in association with a lamina. *Proc Natl Acad Sci U S A* 72 (3):1007-1011

Abedin M, King N (2010) Diverse evolutionary paths to cell adhesion. *Trends Cell Biol* 20 (12):734-742

Aebi U, Cohn J, Buhle L, Gerace L (1986) The nuclear lamina is a meshwork of intermediate-type filaments. *Nature* 323 (6088):560-564

Al-Haboubi T, Shumaker DK, Koser J, Wehnert M, Fahrenkrog B (2011) Distinct association of the nuclear pore protein Nup153 with A- and B-type lamins. *Nucleus* 2 (5):500-509

Alfaro JF, Gong CX, Monroe ME, Aldrich JT, Clauss TR, Purvine SO, Wang Z, Camp DG, 2nd, Shabanowitz J, Stanley P, Hart GW, Hunt DF, Yang F, Smith RD (2012) Tandem mass spectrometry identifies many mouse brain O-GlcNAcylated proteins including EGF domain-specific O-GlcNAc transferase targets. *Proc Natl Acad Sci U S A* 109 (19):7280-7285

Alsheimer M, von Glasenapp E, Schnolzer M, Heid H, Benavente R (2000) Meiotic lamin C2: the unique amino-terminal hexapeptide GNAEGR is essential for nuclear envelope association. *Proc Natl Acad Sci U S A* 97 (24):13120-13125

Anderson CT, Carroll A, Akhmetova L, Somerville C (2010) Real-time imaging of cellulose reorientation during cell wall expansion in *Arabidopsis* roots. *Plant Physiol* 152 (2):787-796

Avisar D, Abu-Abied M, Belausov E, Sadot E, Hawes C, Sparkes IA (2009) A comparative study of the involvement of 17 *Arabidopsis* myosin family members on the motility of Golgi and other organelles. *Plant Physiol* 150 (2):700-709

Bailey TL, Boden M, Buske FA, Frith M, Grant CE, Clementi L, Ren J, Li WW, Noble WS (2009) MEME SUITE: tools for motif discovery and searching. *Nucleic Acids Research* 37 (Web Server issue):W202-208

Baines AJ (2009) Evolution of spectrin function in cytoskeletal and membrane networks. *Biochem Soc Trans* 37 (Pt 4):796-803

Bank EM, Gruenbaum Y (2011a) *Caenorhabditis elegans* as a model system for studying the nuclear lamina and laminopathic diseases. *Nucleus* 2 (5):350-357

Bank EM, Gruenbaum Y (2011b) The nuclear lamina and heterochromatin: a complex relationship. *Biochem Soc Trans* 39 (6):1705-1709

Batsios P, Peter T, Baumann O, Stick R, Meyer I, Graf R (2012) A lamin in lower eukaryotes? *Nucleus* 3 (3):237-243

Beams HW, Tahmisian TN, Devine R, Anderson E (1957) Ultrastructure of the nuclear membrane of a gregarine parasitic in grasshoppers. *Exp Cell Res* 13 (1):200-204

Belmont AS, Zhai Y, Thilenius A (1993) Lamin B distribution and association with peripheral chromatin revealed by optical sectioning and electron microscopy tomography. *J Cell Biol* 123 (6 Pt 2):1671-1685

Ben-Harush K, Wiesel N, Frenkiel-Krispin D, Moeller D, Soreq E, Aebi U, Herrmann H, Gruenbaum Y, Medalia O (2009) The supramolecular organization of the *C. elegans* nuclear lamin filament. *J Mol Biol* 386 (5):1392-1402

Benavente R, Krohne G (1985) Change of karyoskeleton during spermatogenesis of *Xenopus*: expression of lamin LIV, a nuclear lamina protein specific for the male germ line. *Proc Natl Acad Sci U S A* 82 (18):6176-6180

Benavente R, Krohne G, Franke WW (1985) Cell type-specific expression of nuclear lamina proteins during development of *Xenopus laevis*. *Cell* 41 (1):177-190

Bennett T, Scheres B (2010) Root development-two meristems for the price of one? *Curr Top Dev Biol* 91:67-102

Berezney R, Coffey DS (1974) Identification of a nuclear protein matrix. *Biochem Biophys Res Commun* 60 (4):1410-1417

Berezney R, Coffey DS (1975) Nuclear protein matrix: association with newly synthesized DNA. *Science* 189 (4199):291-293

Berezney R, Coffey DS (1977) Nuclear matrix. Isolation and characterization of a framework structure from rat liver nuclei. *J Cell Biol* 73 (3):616-637

Berkelman T (2008) Quantitation of protein in samples prepared for 2-D electrophoresis. *Methods in Molecular Biology* 424:43-49

Birnbaum K, Shasha DE, Wang JY, Jung JW, Lambert GM, Galbraith DW, Benfey PN (2003) A gene expression map of the *Arabidopsis* root. *Science* 302 (5652):1956-1960

Blom N, Sicheritz-Ponten T, Gupta R, Gammeltoft S, Brunak S (2004) Prediction of post-translational glycosylation and phosphorylation of proteins from the amino acid sequence. *Proteomics* 4 (6):1633-1649

Blumenthal SS, Clark GB, Roux SJ (2004) Biochemical and immunological characterization of pea nuclear intermediate filament proteins. *Planta* 218 (6):965-975

Boschmann M, Engeli S, Moro C, Luedtke A, Adams F, Gorzelniak K, Rahn G, Mahler A, Dobberstein K, Kruger A, Schmidt S, Spuler S, Luft FC, Smith SR, Schmidt HH, Jordan J (2010) LMNA mutations, skeletal muscle lipid metabolism, and insulin resistance. *J Clin Endocrinol Metab* 95 (4):1634-1643

Bossie CA, Sanders MM (1993) A cDNA from *Drosophila melanogaster* encodes a lamin C-like intermediate filament protein. *J Cell Sci* 104 (Pt 4):1263-1272

Brachner A, Reipert S, Foisner R, Gotzmann J (2005) LEM2 is a novel MAN1-related inner nuclear membrane protein associated with A-type lamins. *J Cell Sci* 118 (Pt 24):5797-5810

Brady SM, Orlando DA, Lee JY, Wang JY, Koch J, Dinneny JR, Mace D, Ohler U, Benfey PN (2007) A high-resolution root spatiotemporal map reveals dominant expression patterns. *Science* 318 (5851):801-806

Brameier M, Krings A, MacCallum RM (2007) NucPred--predicting nuclear localization of proteins. *Bioinformatics* 23 (9):1159-1160

Broers JL, Hutchison CJ, Ramaekers FC (2004) Laminopathies. *J Pathol* 204 (4):478-488

Broers JL, Machiels BM, Kuijpers HJ, Smedts F, van den Kieboom R, Raymond Y, Ramaekers FC (1997) A- and B-type lamins are differentially expressed in normal human tissues. *Histochem Cell Biol* 107 (6):505-517

Broers JL, Machiels BM, van Eys GJ, Kuijpers HJ, Manders EM, van Driel R, Ramaekers FC (1999) Dynamics of the nuclear lamina as monitored by GFP-tagged A-type lamins. *J Cell Sci* 112 (Pt 20):3463-3475

Brosig M, Ferralli J, Gelman L, Chiquet M, Chiquet-Ehrismann R (2010) Interfering with the connection between the nucleus and the cytoskeleton affects nuclear rotation, mechanotransduction and myogenesis. *Int J Biochem Cell Biol* 42 (10):1717-1728

Brown R (1833) On the Organs and Mode of Fecundation of Orchidex and Asclepiadea. *Trans Linnean Soc London* (16):685-745

Bruston F, Delbarre E, Ostlund C, Worman HJ, Buendia B, Duband-Goulet I (2010) Loss of a DNA binding site within the tail of prelamin A contributes to altered heterochromatin anchorage by progerin. *FEBS Lett* 584 (14):2999-3004

Burke B, Stewart CL (2013) The nuclear lamins: flexibility in function. *Nat Rev Mol Cell Biol* 14 (1):13-24

Ciska M, Masuda K, Moreno Diaz de la Espina S (2013) Lamin-like analogues in plants: the characterization of NMCP1 in *Allium cepa*. *J Exp Bot* 64 (6):1553-1564

Cladaras MH, Kaplan A (1984) Maturation of alpha-mannosidase in *Dictyostelium discoideum*. Acquisition of endoglycosidase H resistance and sulfate. *J Biol Chem* 259 (22):14165-14169

Cordes VC, Reidenbach S, Rackwitz HR, Franke WW (1997) Identification of protein p270/Tpr as a constitutive component of the

nuclear pore complex-attached intranuclear filaments. *J Cell Biol* 136 (3):515-529

Crick FH (1952) Is alpha-keratin a coiled coil? *Nature* 170 (4334):882-883

Crick FHC (1953a) The Fourier transform of a coiled-coil. *Acta Crystallogr* 6:685-689

Crick FHC (1953b) The packing of alpha-helices:Simple coiled-coils. *Acta Crystallogr* 6:689-697

Crisp M, Liu Q, Roux K, Rattner JB, Shanahan C, Burke B, Stahl PD, Hodzic D (2006) Coupling of the nucleus and cytoplasm: role of the LINC complex. *J Cell Biol* 172 (1):41-53

Cruz JR, Moreno Diaz de la Espina S (2009) Subnuclear compartmentalization and function of actin and nuclear myosin I in plants. *Chromosoma* 118 (2):193-207

Csoka AB, Cao H, Sammak PJ, Constantinescu D, Schatten GP, Hegele RA (2004) Novel lamin A/C gene (LMNA) mutations in atypical progeroid syndromes. *J Med Genet* 41 (4):304-308

Cui P, Moreno Diaz de la Espina S (2003) Sm and U2B" proteins redistribute to different nuclear domains in dormant and proliferating onion cells. *Planta* 217 (1):21-31

Chen B, Cai ST, Zhai ZH (1994) [Investigation of nuclear lamina in Tetrahymena thermophila]. *Shi Yan Sheng Wu Xue Bao* 27 (2):153-163

Chuang CH, Carpenter AE, Fuchsova B, Johnson T, de Lanerolle P, Belmont AS (2006) Long-range directional movement of an interphase chromosome site. *Curr Biol* 16 (8):825-831

Dahl KN, Kalinowski A (2011) Nucleoskeleton mechanics at a glance. *J Cell Sci* 124 (Pt 5):675-678

De Sandre-Giovannoli A, Bernard R, Cau P, Navarro C, Amiel J, Boccaccio I, Lyonnet S, Stewart CL, Munnich A, Le Merrer M, Levy N (2003) Lamin a truncation in Hutchinson-Gilford progeria. *Science* 300 (5628):2055

Dechat T, Adam SA, Taimen P, Shimi T, Goldman RD (2010a) Nuclear lamins. *Cold Spring Harb Perspect Biol* 2 (11):a000547

Dechat T, Gesson K, Foisner R (2010b) Lamina-independent lamins in the nuclear interior serve important functions. *Cold Spring Harb Symp Quant Biol* 75:533-543

Dechat T, Korbei B, Vaughan OA, Vlcek S, Hutchison CJ, Foisner R (2000) Lamina-associated polypeptide 2alpha binds intranuclear A-type lamins. *J Cell Sci* 113 Pt 19:3473-3484

Delbarre E, Tramier M, Coppey-Moisan M, Gaillard C, Courvalin JC, Buendia B (2006) The truncated prelamin A in Hutchinson-Gilford progeria syndrome alters segregation of A-type and B-type lamin homopolymers. *Hum Mol Genet* 15 (7):1113-1122

Delorenzi M, Speed T (2002) An HMM model for coiled-coil domains and a comparison with PSSM-based predictions. *Bioinformatics* 18 (4):617-625

den Boer BG, Murray JA (2000) Triggering the cell cycle in plants. *Trends Cell Biol* 10 (6):245-250

Devos D, Dokudovskaya S, Williams R, Alber F, Eswar N, Chait BT, Rout MP, Sali A (2006) Simple fold composition and modular architecture of the nuclear pore complex. *Proc Natl Acad Sci U S A* 103 (7):2172-2177

Ding D, Muthuswamy S, Meier I (2012) Functional interaction between the Arabidopsis orthologs of spindle assembly checkpoint proteins MAD1 and MAD2 and the nucleoporin NUA. *Plant Mol Biol* 79 (3):203-216

Dinneny JR, Long TA, Wang JY, Jung JW, Mace D, Pointer S, Barron C, Brady SM, Schiefelbein J, Benfey PN (2008) Cell identity mediates the response of *Arabidopsis* roots to abiotic stress. *Science* 320 (5878):942-945

Dittmer TA, Misteli T (2011) The lamin protein family. *Genome Biol* 12 (5):222

Dittmer TA, Richards EJ (2008) Role of LINC proteins in plant nuclear morphology. *Plant Signal Behav* 3 (7):485-487

Dittmer TA, Stacey NJ, Sugimoto-Shirasu K, Richards EJ (2007) *LITTLE NUCLEI* genes affecting nuclear morphology in *Arabidopsis thaliana*. *Plant Cell* 19 (9):2793-2803

Dorner D, Gotzmann J, Foisner R (2007) Nucleoplasmic lamins and their interaction partners, LAP2alpha, Rb, and BAF, in transcriptional regulation. *FEBS J* 274 (6):1362-1373

Dubois KN, Alsford S, Holden JM, Buisson J, Swiderski M, Bart JM, Ratushny AV, Wan Y, Bastin P, Barry JD, Navarro M, Horn D, Aitchison JD, Rout MP, Field MC (2012) NUP-1 Is a Large Coiled-Coil Nucleoskeletal Protein in Trypanosomes with Lamin-Like Functions. *PLoS Biology* 10 (3):e1001287

Dundr M, Ospina JK, Sung MH, John S, Upender M, Ried T, Hager GL, Matera AG (2007) Actin-dependent intranuclear repositioning of an active gene locus in vivo. *J Cell Biol* 179 (6):1095-1103

Dwyer N, Blobel G (1976) A modified procedure for the isolation of a pore complex-lamina fraction from rat liver nuclei. *J Cell Biol* 70 (3):581-591

Edens LJ, White KH, Jevtic P, Li X, Levy DL (2012) Nuclear size regulation: from single cells to development and disease. *Trends Cell Biol*

Egelman EH (2003) Cell walls, cell shape, and bacterial actin homologs. *Dev Cell* 5 (1):4-5

Erber A, Riemer D, Hofemeister H, Bovenschulte M, Stick R, Panopoulou G, Lehrach H, Weber K (1999) Characterization of the

Hydra lamin and its gene: A molecular phylogeny of metazoan lamins. *J Mol Evol* 49 (2):260-271

Eriksson M, Brown WT, Gordon LB, Glynn MW, Singer J, Scott L, Erdos MR, Robbins CM, Moses TY, Berglund P, Dutra A, Pak E, Durkin S, Csoka AB, Boehnke M, Glover TW, Collins FS (2003) Recurrent de novo point mutations in lamin A cause Hutchinson-Gilford progeria syndrome. *Nature* 423 (6937):293-298

Evans DE, Irons SL, Graumann K, Runions J (2009) The plant nuclear envelope Meier I (ed) Functional Organization of The Plant Nucleus

Fang Y, Spector DL (2005) Centromere positioning and dynamics in living *Arabidopsis* plants. *Mol Biol Cell* 16 (12):5710-5718

Fawcett DW (1966) On the occurrence of a fibrous lamina on the inner aspect of the nuclear envelope in certain cells of vertebrates. *Am J Anat* 119 (1):129-145

Faye L, Gomord V, Fitchette-Laine AC, Chrispeels MJ (1993) Affinity purification of antibodies specific for Asn-linked glycans containing alpha 1-->3 fucose or beta 1-->2 xylose. *Anal Biochem* 209 (1):104-108

Felsenstein J (1988) Phylogenies from molecular sequences: inference and reliability. *Annu Rev Genet* 22:521-565

Ferraro A, Eufemi M, Cervoni L, Marinetti R, Turano C (1989) Glycosylated forms of nuclear lamins. *FEBS Lett* 257 (2):241-246

Field MC, Horn D, Alsford S, Koreny L, Rout MP (2012) Telomeres, tethers and trypanosomes. *Nucleus* 3 (6):478-486

Fiserova J, Goldberg MW (2010) Relationships at the nuclear envelope: lamins and nuclear pore complexes in animals and plants. *Biochem Soc Trans* 38 (3):829-831

Fiserova J, Kiseleva E, Goldberg MW (2009) Nuclear envelope and nuclear pore complex structure and organization in tobacco BY-2 cells. *Plant J* 59 (2):243-255

Fisher DZ, Chaudhary N, Blobel G (1986) cDNA sequencing of nuclear lamins A and C reveals primary and secondary structural homology to intermediate filament proteins. *Proc Natl Acad Sci U S A* 83 (17):6450-6454

Foeger N, Wiesel N, Lotsch D, Mucke N, Kreplak L, Aebi U, Gruenbaum Y, Herrmann H (2006) Solubility properties and specific assembly pathways of the B-type lamin from *Caenorhabditis elegans*. *J Struct Biol* 155 (2):340-350

Fontoura BM, Dales S, Blobel G, Zhong H (2001) The nucleoporin Nup98 associates with the intranuclear filamentous protein network of TPR. *Proc Natl Acad Sci U S A* 98 (6):3208-3213

Ford BJ (2009) Did physics matter to the pioneers of microscopy? . *Advances in imaging and electron physics* 158:27-87

Frajola WJ, Greider MH, Kostir WJ (1956) Electron microscopy of the nuclear membrane of *Amoeba proteus*. *J Biophys Biochem Cytol* 2 (4 Suppl):445-448

Franke J, Podgorski GJ, Kessin RH (1987) The expression of two transcripts of the phosphodiesterase gene during the development of *Dictyostelium discoideum*. *Dev Biol* 124 (2):504-511

Franke WW (1987) Nuclear lamins and cytoplasmic intermediate filament proteins: a growing multigene family. *Cell* 48 (1):3-4

Frederick SE, Mangan ME, Carey JB, Gruber PJ (1992) Intermediate filament antigens of 60 and 65 kDa in the nuclear matrix of plants: their detection and localization. *Exp Cell Res* 199 (2):213-222

Frosst P, Guan T, Subauste C, Hahn K, Gerace L (2002) Tpr is localized within the nuclear basket of the pore complex and has a role in nuclear protein export. *J Cell Biol* 156 (4):617-630

Fujimoto S, Matsunaga S, Yonemura M, Uchiyama S, Azuma T, Fukui K (2004) Identification of a novel plant MAR DNA binding protein localized on chromosomal surfaces. *Plant Mol Biol* 56 (2):225-239

Fujiwara S, Matsuda N, Sato T, Sonobe S, Maeshima M (2002) Molecular properties of a matrix attachment region-binding protein located in the nucleoli of tobacco cells. *Plant Cell Physiol* 43 (12):1558-1567

Furukawa K, Kondo T (1998) Identification of the lamina-associated-polypeptide-2-binding domain of B-type lamin. *Eur J Biochem* 251 (3):729-733

Geisler N, Schunemann J, Weber K, Haner M, Aebi U (1998) Assembly and architecture of invertebrate cytoplasmic intermediate filaments reconcile features of vertebrate cytoplasmic and nuclear lamin-type intermediate filaments. *J Mol Biol* 282 (3):601-617

Georgiev GP, Chentsov JS (1962) On the structural organization of nucleolo-chromosomal ribonucleoproteins. *Exp Cell Res* 27:570-572

Gerace L, Blobel G (1980) The nuclear envelope lamina is reversibly depolymerized during mitosis. *Cell* 19 (1):277-287

Gerace L, Blum A, Blobel G (1978) Immunocytochemical localization of the major polypeptides of the nuclear pore complex-lamina fraction. Interphase and mitotic distribution. *J Cell Biol* 79 (2 Pt 1):546-566

Gerner C, Gotzmann J, Frohwein U, Schamberger C, Ellinger A, Sauermann G (2002) Proteome analysis of nuclear matrix proteins during apoptotic chromatin condensation. *Cell Death Differ* 9 (6):671-681

Gindullis F, Meier I (1999) Matrix attachment region binding protein MFP1 is localized in discrete domains at the nuclear envelope. *Plant Cell* 11 (6):1117-1128

Gindullis F, Peffer NJ, Meier I (1999) MAF1, a novel plant protein interacting with matrix attachment region binding protein MFP1, is located at the nuclear envelope. *Plant Cell* 11 (9):1755-1768

Gindullis F, Rose A, Patel S, Meier I (2002) Four signature motifs define the first class of structurally related large coiled-coil proteins in plants. *BMC Genomics* 3:9

Gob E, Schmitt J, Benavente R, Alsheimer M (2010) Mammalian sperm head formation involves different polarization of two novel LINC complexes. *PLoS One* 5 (8):e12072

Goldberg MW, Blow JJ, Allen TD (1992) The use of field emission in-lens scanning electron microscopy to study the steps of assembly of the nuclear envelope in vitro. *J Struct Biol* 108 (3):257-268

Goldberg MW, Fiserova J, Huttenlauch I, Stick R (2008a) A new model for nuclear lamina organization. *Biochem Soc Trans* 36 (Pt 6):1339-1343

Goldberg MW, Huttenlauch I, Hutchison CJ, Stick R (2008b) Filaments made from A- and B-type lamins differ in structure and organization. *J Cell Sci* 121 (Pt 2):215-225

Goldman RD, Gruenbaum Y, Moir RD, Shumaker DK, Spann TP (2002) Nuclear lamins: building blocks of nuclear architecture. *Genes Dev* 16 (5):533-547

Goodstein DM, Shu S, Howson R, Neupane R, Hayes RD, Fazo J, Mitros T, Dirks W, Hellsten U, Putnam N, Rokhsar DS (2012) Phytozome: a comparative platform for green plant genomics. *Nucleic Acids Res* 40 (Database issue):D1178-1186

Graumann K, Bass HW, Parry G (2013) SUNrises on the International Plant Nucleus Consortium: SEB Salzburg 2012. *Nucleus* 4 (1):1-5

Graumann K, Irons SL, Runions J, Evans DE (2007) Retention and mobility of the mammalian lamin B receptor in the plant nuclear envelope. *Biol Cell* 99 (10):553-562

Graumann K, Runions J, Evans DE (2010) Characterization of SUN-domain proteins at the higher plant nuclear envelope. *Plant J* 61 (1):134-144

Gruber M, Soding J, Lupas AN (2006) Comparative analysis of coiled-coil prediction methods. *J Struct Biol* 155 (2):140-145

Gruenbaum Y, Landesman Y, Drees B, Bare JW, Saumweber H, Paddy MR, Sedat JW, Smith DE, Benton BM, Fisher PA (1988) *Drosophila* nuclear lamin precursor Dm0 is translated from either of two developmentally regulated mRNA species apparently encoded by a single gene. *J Cell Biol* 106 (3):585-596

Guelen L, Pagie L, Brasset E, Meuleman W, Faza MB, Talhout W, Eussen BH, de Klein A, Wessels L, de Laat W, van Steensel B

(2008) Domain organization of human chromosomes revealed by mapping of nuclear lamina interactions. *Nature* 453 (7197):948-951

Haithcock E, Dayani Y, Neufeld E, Zahand AJ, Feinstein N, Mattout A, Gruenbaum Y, Liu J (2005) Age-related changes of nuclear architecture in *Caenorhabditis elegans*. *Proc Natl Acad Sci U S A* 102 (46):16690-16695

Hamant O, Heisler MG, Jonsson H, Krupinski P, Uyttewaal M, Bokov P, Corson F, Sahlin P, Boudaoud A, Meyerowitz EM, Couder Y, Traas J (2008) Developmental patterning by mechanical signals in *Arabidopsis*. *Science* 322 (5908):1650-1655

Haque F, Lloyd DJ, Smallwood DT, Dent CL, Shanahan CM, Fry AM, Trembath RC, Shackleton S (2006) SUN1 interacts with nuclear lamin A and cytoplasmic nesprins to provide a physical connection between the nuclear lamina and the cytoskeleton. *Mol Cell Biol* 26 (10):3738-3751

Harborth J, Elbashir SM, Bechert K, Tuschl T, Weber K (2001) Identification of essential genes in cultured mammalian cells using small interfering RNAs. *J Cell Sci* 114 (Pt 24):4557-4565

Harborth J, Wang J, Gueth-Hallonet C, Weber K, Osborn M (1999) Self assembly of NuMA: multiarm oligomers as structural units of a nuclear lattice. *EMBO J* 18 (6):1689-1700

Hatton D, Gray JC (1999) Two MAR DNA-binding proteins of the pea nuclear matrix identify a new class of DNA-binding proteins. *Plant J* 18 (4):417-429

He DC, Nickerson JA, Penman S (1990) Core filaments of the nuclear matrix. *J Cell Biol* 110 (3):569-580

Hegele RA, Cao H, Anderson CM, Hramiak IM (2000) Heterogeneity of nuclear lamin A mutations in Dunnigan-type familial partial lipodystrophy. *J Clin Endocrinol Metab* 85 (9):3431-3435

Herrmann H, Aebi U (2004) Intermediate filaments: molecular structure, assembly mechanism, and integration into functionally distinct intracellular Scaffolds. *Annu Rev Biochem* 73:749-789

Ho CY, Lammerding J (2012) Lamins at a glance. *J Cell Sci* 125 (Pt 9):2087-2093

Hofemeister H, Kuhn C, Franke WW, Weber K, Stick R (2002) Conservation of the gene structure and membrane-targeting signals of germ cell-specific lamin LIII in amphibians and fish. *Eur J Cell Biol* 81 (2):51-60

Hofemeister H, Weber K, Stick R (2000) Association of prenylated proteins with the plasma membrane and the inner nuclear membrane is mediated by the same membrane-targeting motifs. *Mol Biol Cell* 11 (9):3233-3246

Hoffmann K, Dreger CK, Olins AL, Olins DE, Shultz LD, Lucke B, Karl H, Kaps R, Muller D, Vaya A, Aznar J, Ware RE, Sotelo Cruz N, Lindner TH, Herrmann H, Reis A, Sperling K (2002) Mutations in the gene encoding the lamin B receptor produce an altered nuclear morphology in granulocytes (Pelger-Huet anomaly). *Nat Genet* 31 (4):410-414

Hofmann WA, Johnson T, Klapczynski M, Fan JL, de Lanerolle P (2006) From transcription to transport: emerging roles for nuclear myosin I. *Biochem Cell Biol* 84 (4):418-426

Hoger TH, Krohne G, Franke WW (1988) Amino acid sequence and molecular characterization of murine lamin B as deduced from cDNA clones. *Eur J Cell Biol* 47 (2):283-290

Hoger TH, Zatloukal K, Waizenegger I, Krohne G (1990) Characterization of a second highly conserved B-type lamin present in cells previously thought to contain only a single B-type lamin. *Chromosoma* 100 (1):67-69

Holaska JM, Lee KK, Kowalski AK, Wilson KL (2003) Transcriptional repressor germ cell-less (GCL) and barrier to autointegration factor (BAF) compete for binding to emerin in vitro. *J Biol Chem* 278 (9):6969-6975

Houben F, Ramaekers FC, Snoeckx LH, Broers JL (2007) Role of nuclear lamina-cytoskeleton interactions in the maintenance of cellular strength. *Biochim Biophys Acta* 1773 (5):675-686

Irons SL, Evans DE, Brandizzi F (2003) The first 238 amino acids of the human lamin B receptor are targeted to the nuclear envelope in plants. *J Exp Bot* 54 (384):943-950

Jacob Y, Mongkolsiriwatana C, Veley KM, Kim SY, Michaels SD (2007) The nuclear pore protein AtTPR is required for RNA homeostasis, flowering time, and auxin signaling. *Plant Physiol* 144 (3):1383-1390

Jakob KM, Bovey F (1969) Early nucleic acid and protein syntheses and mitoses in the primary root tips of germinating *Vicia faba*. *Exp Cell Res* 54 (1):118-126

Jones DT, Taylor WR, Thornton JM (1992) The rapid generation of mutation data matrices from protein sequences. *Comput Appl Biosci* 8 (3):275-282

Kalderon D, Roberts BL, Richardson WD, Smith AE (1984) A short amino acid sequence able to specify nuclear location. *Cell* 39 (3 Pt 2):499-509

Kandasamy MK, Deal RB, McKinney EC, Meagher RB (2004) Plant actin-related proteins. *Trends Plant Sci* 9 (4):196-202

Kandasamy MK, McKinney EC, Meagher RB (2003) Cell cycle-dependent association of *Arabidopsis* actin-related proteins AtARP4 and AtARP7 with the nucleus. *Plant J* 33 (5):939-948

Kandasamy MK, McKinney EC, Meagher RB (2010) Differential sublocalization of actin variants within the nucleus. *Cytoskeleton (Hoboken)* 67 (11):729-743

Kapinos LE, Schumacher J, Mucke N, Machaidze G, Burkhard P, Aebi U, Strelkov SV, Herrmann H (2010) Characterization of the head-to-tail overlap complexes formed by human lamin A, B1 and B2 "half-minilamin" dimers. *J Mol Biol* 396 (3):719-731

Karabinos A, Schunemann J, Meyer M, Aebi U, Weber K (2003) The single nuclear lamin of *Caenorhabditis elegans* forms in vitro stable intermediate filaments and paracrystals with a reduced axial periodicity. *J Mol Biol* 325 (2):241-247

Kaufmann A, Heinemann F, Radmacher M, Stick R (2011) Amphibian oocyte nuclei expressing lamin A with the progeria mutation E145K exhibit an increased elastic modulus. *Nucleus* 2 (4)

Kennedy BK, Barbie DA, Classon M, Dyson N, Harlow E (2000) Nuclear organization of DNA replication in primary mammalian cells. *Genes Dev* 14 (22):2855-2868

Kessin RH (2000) Evolutionary biology. Cooperation can be dangerous. *Nature* 408 (6815):917, 919

Kim Y, Sharov AA, McDole K, Cheng M, Hao H, Fan CM, Gaiano N, Ko MS, Zheng Y (2011) Mouse B-type lamins are required for proper organogenesis but not by embryonic stem cells. *Science* 334 (6063):1706-1710

Kim YG, Raunser S, Munger C, Wagner J, Song YL, Cygler M, Walz T, Oh BH, Sacher M (2006) The architecture of the multisubunit TRAPP I complex suggests a model for vesicle tethering. *Cell* 127 (4):817-830

Kimura Y, Kuroda C, Masuda K (2010) Differential nuclear envelope assembly at the end of mitosis in suspension-cultured *Apium graveolens* cells. *Chromosoma* 119 (2):195-204

Kleffmann T, Hirsch-Hoffmann M, Gruissem W, Baginsky S (2006) plprot: a comprehensive proteome database for different plastid types. *Plant Cell Physiol* 47 (3):432-436

Kobata A (1979) Use of endo- and exoglycosidases for structural studies of glycoconjugates. *Anal Biochem* 100 (1):1-14

Kolb T, Maass K, Hergt M, Aebi U, Herrmann H (2011) Lamin A and lamin C form homodimers and coexist in higher complex forms both in the nucleoplasmic fraction and in the lamina of cultured human cells. *Nucleus* 2 (5):425-433

Krohne G, Waizenegger I, Hoger TH (1989) The conserved carboxy-terminal cysteine of nuclear lamins is essential for lamin association with the nuclear envelope. *J Cell Biol* 109 (5):2003-2011

Kruger A, Batsios P, Baumann O, Luckert E, Schwarz H, Stick R, Meyer I, Graf R (2012) Characterization of NE81, the first lamin-like nucleoskeleton protein in a unicellular organism. *Mol Biol Cell* 23 (2):360-370

Kruse T, Gerdes K (2005) Bacterial DNA segregation by the actin-like MreB protein. *Trends Cell Biol* 15 (7):343-345

Laguri C, Gilquin B, Wolff N, Romi-Lebrun R, Courchay K, Callebaut I, Worman HJ, Zinn-Justin S (2001) Structural characterization of the LEM motif common to three human inner nuclear membrane proteins. *Structure* 9 (6):503-511

Lammerding J, Fong LG, Ji JY, Reue K, Stewart CL, Young SG, Lee RT (2006) Lamins A and C but not lamin B1 regulate nuclear mechanics. *J Biol Chem* 281 (35):25768-25780

Lammerding J, Hsiao J, Schulze PC, Kozlov S, Stewart CL, Lee RT (2005) Abnormal nuclear shape and impaired mechanotransduction in emerin-deficient cells. *J Cell Biol* 170 (5):781-791

Lammerding J, Schulze PC, Takahashi T, Kozlov S, Sullivan T, Kamm RD, Stewart CL, Lee RT (2004) Lamin A/C deficiency causes defective nuclear mechanics and mechanotransduction. *J Clin Invest* 113 (3):370-378

Lang S, Loidl P (1993) Identification of proteins immunologically related to vertebrate lamins in the nuclear matrix of the myxomycete *Physarum polycephalum*. *Eur J Cell Biol* 61 (1):177-183

Larkin MA, Blackshields G, Brown NP, Chenna R, McGettigan PA, McWilliam H, Valentin F, Wallace IM, Wilm A, Lopez R, Thompson JD, Gibson TJ, Higgins DG (2007) Clustal W and Clustal X version 2.0. *Bioinformatics* 23 (21):2947-2948

Lee KK, Haraguchi T, Lee RS, Koujin T, Hiraoka Y, Wilson KL (2001) Distinct functional domains in emerin bind lamin A and DNA-bridging protein BAF. *J Cell Sci* 114 (Pt 24):4567-4573

Lee SH, Sterling H, Burlingame A, McCormick F (2008) Tpr directly binds to Mad1 and Mad2 and is important for the Mad1-Mad2-mediated mitotic spindle checkpoint. *Genes Dev* 22 (21):2926-2931

Lehner CF, Stick R, Eppenberger HM, Nigg EA (1987) Differential expression of nuclear lamin proteins during chicken development. *J Cell Biol* 105 (1):577-587

Lenz-Bohme B, Wismar J, Fuchs S, Reifegerste R, Buchner E, Betz H, Schmitt B (1997) Insertional mutation of the *Drosophila* nuclear lamin Dm0 gene results in defective nuclear envelopes, clustering of nuclear

pore complexes, and accumulation of annulate lamellae. *J Cell Biol* 137 (5):1001-1016

Levesque AA, Compton DA (2001) The chromokinesin Kid is necessary for chromosome arm orientation and oscillation, but not congression, on mitotic spindles. *J Cell Biol* 154 (6):1135-1146

Levy DL, Heald R (2010) Nuclear size is regulated by importin alpha and Ntf2 in *Xenopus*. *Cell* 143 (2):288-298

Li H, Roux SJ (1992) Casein kinase II protein kinase is bound to lamina-matrix and phosphorylates lamin-like protein in isolated pea nuclei. *Proc Natl Acad Sci U S A* 89 (18):8434-8438

Libotte T, Zaim H, Abraham S, Padmakumar VC, Schneider M, Lu W, Munck M, Hutchison C, Wehnert M, Fahrenkrog B, Sauder U, Aebi U, Noegel AA, Karakesisoglou I (2005) Lamin A/C-dependent localization of Nesprin-2, a giant scaffolder at the nuclear envelope. *Mol Biol Cell* 16 (7):3411-3424

Lin F, Worman HJ (1993) Structural organization of the human gene encoding nuclear lamin A and nuclear lamin C. *J Biol Chem* 268 (22):16321-16326

Lindsay AJ, McCaffrey MW (2009) Myosin Vb localises to nucleoli and associates with the RNA polymerase I transcription complex. *Cell Motil Cytoskeleton* 66 (12):1057-1072

Liu J, Rolef Ben-Shahar T, Riemer D, Treinin M, Spann P, Weber K, Fire A, Gruenbaum Y (2000) Essential roles for *Caenorhabditis elegans* lamin gene in nuclear organization, cell cycle progression, and spatial organization of nuclear pore complexes. *Mol Biol Cell* 11 (11):3937-3947

Lombardi ML, Jaalouk DE, Shanahan CM, Burke B, Roux KJ, Lammerding J (2011) The interaction between nesprins and sun proteins at the nuclear envelope is critical for force transmission between the nucleus and cytoskeleton. *J Biol Chem* 286 (30):26743-26753

Louvet E, Percipalle P (2009) Transcriptional control of gene expression by actin and myosin. *Int Rev Cell Mol Biol* 272:107-147

Luderus ME, den Blaauwen JL, de Smit OJ, Compton DA, van Driel R (1994) Binding of matrix attachment regions to lamin polymers involves single-stranded regions and the minor groove. *Mol Cell Biol* 14 (9):6297-6305

Lundin LG, Larhammar D, Hallbook F (2003) Numerous groups of chromosomal regional paralogies strongly indicate two genome doublings at the root of the vertebrates. *J Struct Funct Genomics* 3 (1-4):53-63

Lupas A (1996) Prediction and analysis of coiled-coil structures. *Methods Enzymol* 266:513-525

Lupas A, Van Dyke M, Stock J (1991) Predicting coiled coils from protein sequences. *Science* 252 (5009):1162-1164

Lupas AN, Gruber M (2005) The structure of alpha-helical coiled coils. *Adv Protein Chem* 70:37-78

Lussi YC, Hugi I, Laurell E, Kutay U, Fahrenkrog B (2011) The nucleoporin Nup88 is interacting with nuclear lamin A. *Mol Biol Cell* 22 (7):1080-1090

Luxton GW, Gomes ER, Folker ES, Vintinner E, Gundersen GG (2010) Linear arrays of nuclear envelope proteins harness retrograde actin flow for nuclear movement. *Science* 329 (5994):956-959

Machiels BM, Zorenc AH, Endert JM, Kuijpers HJ, van Eys GJ, Ramaekers FC, Broers JL (1996) An alternative splicing product of the lamin A/C gene lacks exon 10. *J Biol Chem* 271 (16):9249-9253

Macho B, Brancorsini S, Fimia GM, Setou M, Hirokawa N, Sassone-Corsi P (2002) CREM-dependent transcription in male germ cells controlled by a kinesin. *Science* 298 (5602):2388-2390

Mahen R, Hattori H, Lee M, Sharma P, Jeyasekharan AD, Venkitaraman AR (2013) A-type lamins maintain the positional stability of DNA damage repair foci in mammalian nuclei. *PLoS One* 8 (5):e61893

Mancini MA, Shan B, Nickerson JA, Penman S, Lee WH (1994) The retinoblastoma gene product is a cell cycle-dependent, nuclear matrix-associated protein. *Proc Natl Acad Sci U S A* 91 (1):418-422

Mans BJ, Anantharaman V, Aravind L, Koonin EV (2004) Comparative genomics, evolution and origins of the nuclear envelope and nuclear pore complex. *Cell Cycle* 3 (12):1612-1637

Mansharamani M, Wilson KL (2005) Direct binding of nuclear membrane protein MAN1 to emerin in vitro and two modes of binding to barrier-to-autointegration factor. *J Biol Chem* 280 (14):13863-13870

Masuda K, Haruyama S, Fujino K (1999) Assembly and disassembly of the peripheral architecture of the plant cell nucleus during mitosis. *Planta* 210 (1):165-167

Masuda K, Takahashi S, Nomura K, Arimoto M, Inoue M (1993) Residual structure and constituent proteins of the peripheral framework of the cell nucleus in somatic embryos from *Daucus carota* L. *Planta* 191 (4):532-540

Masuda K, Xu ZJ, Takahashi S, Ito A, Ono M, Nomura K, Inoue M (1997) Peripheral framework of carrot cell nucleus contains a novel protein predicted to exhibit a long alpha-helical domain. *Exp Cell Res* 232 (1):173-181

Mazumdar M, Misteli T (2005) Chromokinesins: multitalented players in mitosis. *Trends Cell Biol* 15 (7):349-355

McClintock D, Ratner D, Lokuge M, Owens DM, Gordon LB, Collins FS, Djabali K (2007) The mutant form of lamin A that causes Hutchinson-Gilford progeria is a biomarker of cellular aging in human skin. *PLoS One* 2 (12):e1269

McKeon FD, Kirschner MW, Caput D (1986) Homologies in both primary and secondary structure between nuclear envelope and intermediate filament proteins. *Nature* 319 (6053):463-468

McMahon LW, Zhang P, Sridharan DM, Lefferts JA, Lambert MW (2009) Knockdown of alphaII spectrin in normal human cells by siRNA leads to chromosomal instability and decreased DNA interstrand cross-link repair. *Biochem Biophys Res Commun* 381 (2):288-293

McNulty AK, Saunders MJ (1992) Purification and immunological detection of pea nuclear intermediate filaments: evidence for plant nuclear lamins. *J Cell Sci* 103 (Pt 2):407-414

Mehta IS, Amira M, Harvey AJ, Bridger JM (2010) Rapid chromosome territory relocation by nuclear motor activity in response to serum removal in primary human fibroblasts. *Genome Biol* 11 (1):R5

Meier I, Phelan T, Gruissem W, Spiker S, Schneider D (1996) MFP1, a novel plant filament-like protein with affinity for matrix attachment region DNA. *Plant Cell* 8 (11):2105-2115

Mejat A, Misteli T (2010) LINC complexes in health and disease. *Nucleus* 1 (1):40-52

Mekhail K, Moazed D (2010) The nuclear envelope in genome organization, expression and stability. *Nat Rev Mol Cell Biol* 11 (5):317-328

Melcer S, Gruenbaum Y, Krohne G (2007) Invertebrate lamins. *Exp Cell Res* 313 (10):2157-2166

Meyerzon M, Gao Z, Liu J, Wu JC, Malone CJ, Starr DA (2009) Centrosome attachment to the *C. elegans* male pronucleus is dependent on the surface area of the nuclear envelope. *Dev Biol* 327 (2):433-446

Minguez A, Franca S, Moreno Diaz de la Espina S (1994) Dinoflagellates have a eukaryotic nuclear matrix with lamin-like proteins and topoisomerase II. *J Cell Sci* 107 (Pt 10):2861-2873

Minguez A, Moreno Diaz de la Espina S (1993) Immunological characterization of lamins in the nuclear matrix of onion cells. *J Cell Sci* 106 (Pt 1):431-439

Mislow JM, Holaska JM, Kim MS, Lee KK, Segura-Totten M, Wilson KL, McNally EM (2002) Nesprin-1alpha self-associates and binds directly to emerin and lamin A in vitro. *FEBS Lett* 525 (1-3):135-140

Moir RD, Montag-Lowy M, Goldman RD (1994) Dynamic properties of nuclear lamins: lamin B is associated with sites of DNA replication. *J Cell Biol* 125 (6):1201-1212

Moir RD, Spann TP, Lopez-Soler RI, Yoon M, Goldman AE, Khuon S, Goldman RD (2000a) Review: the dynamics of the nuclear lamins during the cell cycle-- relationship between structure and function. *J Struct Biol* 129 (2-3):324-334

Moir RD, Yoon M, Khuon S, Goldman RD (2000b) Nuclear lamins A and B1: different pathways of assembly during nuclear envelope formation in living cells. *J Cell Biol* 151 (6):1155-1168

Moreno Diaz de la Espina S (1995) Nuclear matrix isolated from plant cells. *Int Rev Cytol* 162B:75-139

Moreno Diaz de la Espina S, Barthellemy I, Cerezuela MA (1991) Isolation and ultrastructural characterization of the residual nuclear matrix in a plant cell system. *Chromosoma* 100 (2):110-117

Moriguchi K, Suzuki T, Ito Y, Yamazaki Y, Niwa Y, Kurata N (2005) Functional isolation of novel nuclear proteins showing a variety of subnuclear localizations. *Plant Cell* 17 (2):389-403

Morisawa G, Han-Yama A, Moda I, Tamai A, Iwabuchi M, Meshi T (2000) AHM1, a novel type of nuclear matrix-localized, MAR binding protein with a single AT hook and a J domain-homologous region. *Plant Cell* 12 (10):1903-1916

Muralikrishna B, Thanumalayan S, Jagatheesan G, Rangaraj N, Karande AA, Parnaik VK (2004) Immunolocalization of detergent-susceptible nucleoplasmic lamin A/C foci by a novel monoclonal antibody. *J Cell Biochem* 91 (4):730-739

Murphy SP, Simmons CR, Bass HW (2010) Structure and expression of the maize (*Zea mays* L.) SUN-domain protein gene family: evidence for the existence of two divergent classes of SUN proteins in plants. *BMC Plant Biol* 10:269

Nalepa G, Harper JW (2004) Visualization of a highly organized intranuclear network of filaments in living mammalian cells. *Cell Motil Cytoskeleton* 59 (2):94-108

Narayan KS, Steele WJ, Smetana K, Busch H (1967) Ultrastructural aspects of the ribonucleo-protein network in nuclei of Walker tumor and rat liver. *Exp Cell Res* 46 (1):65-77

Navarro M, Penate X, Landeira D (2007) Nuclear architecture underlying gene expression in *Trypanosoma brucei*. *Trends Microbiol* 15 (6):263-270

Nemeth A, Langst G (2011) Genome organization in and around the nucleolus. *Trends Genet* 27 (4):149-156

Neuhoff V, Arold N, Taube D, Ehrhardt W (1988) Improved staining of proteins in polyacrylamide gels including isoelectric focusing gels with clear background at nanogram sensitivity using Coomassie Brilliant Blue G-250 and R-250. *Electrophoresis* 9 (6):255-262

Newman JR, Wolf E, Kim PS (2000) A computationally directed screen identifying interacting coiled coils from *Saccharomyces cerevisiae*. *Proc Natl Acad Sci U S A* 97 (24):13203-13208

Oda Y, Fukuda H (2011) Dynamics of *Arabidopsis* SUN proteins during mitosis and their involvement in nuclear shaping. *Plant J* 66 (4):629-641

Osborne CS, Chakalova L, Brown KE, Carter D, Horton A, Debrand E, Goyenechea B, Mitchell JA, Lopes S, Reik W, Fraser P (2004) Active genes dynamically colocalize to shared sites of ongoing transcription. *Nat Genet* 36 (10):1065-1071

Ostlund C, Worman HJ (2003) Nuclear envelope proteins and neuromuscular diseases. *Muscle Nerve* 27 (4):393-406

Ozaki T, Saijo M, Murakami K, Enomoto H, Taya Y, Sakiyama S (1994) Complex formation between lamin A and the retinoblastoma gene product: identification of the domain on lamin A required for its interaction. *Oncogene* 9 (9):2649-2653

Padmakumar VC, Libotte T, Lu W, Zaim H, Abraham S, Noegel AA, Gotzmann J, Foisner R, Karakesisoglou I (2005) The inner nuclear membrane protein Sun1 mediates the anchorage of Nesprin-2 to the nuclear envelope. *J Cell Sci* 118 (Pt 15):3419-3430

Pappas GD (1956) The fine structure of the nuclear envelope of *Amoeba proteus*. *J Biophys Biochem Cytol* 2 (4 Suppl):431-434

Parry DA (1975) Analysis of the primary sequence of alpha-tropomyosin from rabbit skeletal muscle. *J Mol Biol* 98 (3):519-535

Parry DA (1982) Coiled-coils in alpha-helix-containing proteins: analysis of the residue types within the heptad repeat and the use of these data in the prediction of coiled-coils in other proteins. *Biosci Rep* 2 (12):1017-1024

Parry DA, Conway JF, Steinert PM (1986) Structural studies on lamin. Similarities and differences between lamin and intermediate-filament proteins. *Biochem J* 238 (1):305-308

Patel S, Brkljacic J, Gindullis F, Rose A, Meier I (2005) The plant nuclear envelope protein MAF1 has an additional location at the Golgi and binds to a novel Golgi-associated coiled-coil protein. *Planta* 222 (6):1028-1040

Pederson T (2000) Half a century of "the nuclear matrix". *Mol Biol Cell* 11 (3):799-805

Pekovic V, Gibbs-Seymour I, Markiewicz E, Alzoghaibi F, Benham AM, Edwards R, Wenhert M, von Zglinicki T, Hutchison CJ (2011) Conserved cysteine residues in the mammalian lamin A tail are essential for cellular responses to ROS generation. *Aging Cell* 10 (6):1067-1079

Percipalle P (2013) Co-transcriptional nuclear actin dynamics. *Nucleus* 4 (1):43-52

Peremyslov VV, Mockler TC, Filichkin SA, Fox SE, Jaiswal P, Makarova KS, Koonin EV, Dolja VV (2011) Expression, splicing, and evolution of the myosin gene family in plants. *Plant Physiol* 155 (3):1191-1204

Perez-Munive C, Blumenthal SS, de la Espina SM (2012) Characterization of a 65 kDa NIF in the nuclear matrix of the monocot *Allium cepa* that interacts with nuclear spectrin-like proteins. *Cell Biol Int* 36 (12):1097-1105

Perez-Munive C, Moreno Diaz de la Espina S (2011) Nuclear spectrin-like proteins are structural actin-binding proteins in plants. *Biol Cell* 103 (3):145-157

Peric-Hupkes D, Meuleman W, Pagie L, Bruggeman SW, Solovei I, Brugman W, Graf S, Flicek P, Kerkhoven RM, van Lohuizen M, Reinders M, Wessels L, van Steensel B (2010) Molecular maps of the reorganization of genome-nuclear lamina interactions during differentiation. *Mol Cell* 38 (4):603-613

Peric-Hupkes D, van Steensel B (2010) Role of the nuclear lamina in genome organization and gene expression. *Cold Spring Harb Symp Quant Biol* 75:517-524

Pestic-Dragovich L, Stojiljkovic L, Philimonenko AA, Nowak G, Ke Y, Settlage RE, Shabanowitz J, Hunt DF, Hozak P, de Lanerolle P (2000) A myosin I isoform in the nucleus. *Science* 290 (5490):337-341

Peter A, Stick R (2012) Evolution of the lamin protein family: What introns can tell. *Nucleus* 3 (1):44-49

Pickersgill H, Kalverda B, de Wit E, Talhout W, Fornerod M, van Steensel B (2006) Characterization of the *Drosophila melanogaster* genome at the nuclear lamina. *Nat Genet* 38 (9):1005-1014

Pranchevicius MC, Baqui MM, Ishikawa-Ankerhold HC, Lourenco EV, Leao RM, Banzi SR, dos Santos CT, Roque-Barreira MC, Espreafico EM, Larson RE (2008) Myosin Va phosphorylated on Ser1650 is found in nuclear speckles and redistributes to nucleoli upon inhibition of transcription. *Cell Motil Cytoskeleton* 65 (6):441-456

Radulescu AE, Cleveland DW (2010) NuMA after 30 years: the matrix revisited. *Trends Cell Biol* 20 (4):214-222

Riemer D, Dodemont H, Weber K (1993) A nuclear lamin of the nematode *Caenorhabditis elegans* with unusual structural features; cDNA cloning and gene organization. *Eur J Cell Biol* 62 (2):214-223

Riemer D, Stuurman N, Berrios M, Hunter C, Fisher PA, Weber K (1995) Expression of *Drosophila* lamin C is developmentally regulated:

analogies with vertebrate A-type lamins. *J Cell Sci* 108 (Pt 10):3189-3198

Riemer D, Wang J, Zimek A, Swalla BJ, Weber K (2000) Tunicates have unusual nuclear lamins with a large deletion in the carboxyterminal tail domain. *Gene* 255 (2):317-325

Risueno MC, Moreno Diaz de la Espina S (1979) Ultrastructural and cytochemical study of the quiescent root meristematic cell nucleus. *J Submicr Cytol* 11 (1):85-98

Rober RA, Weber K, Osborn M (1989) Differential timing of nuclear lamin A/C expression in the various organs of the mouse embryo and the young animal: a developmental study. *Development* 105 (2):365-378

Rose A, Manikantan S, Schraegle SJ, Maloy MA, Stahlberg EA, Meier I (2004) Genome-wide identification of *Arabidopsis* coiled-coil proteins and establishment of the ARABI-COIL database. *Plant Physiol* 134 (3):927-939

Rose A, Schraegle SJ, Stahlberg EA, Meier I (2005) Coiled-coil protein composition of 22 proteomes-differences and common themes in subcellular infrastructure and traffic control. *BMC Evol Biol* 5:66

Rout MP, Field MC (2001) Isolation and characterization of subnuclear compartments from *Trypanosoma brucei*. Identification of a major repetitive nuclear lamina component. *J Biol Chem* 276 (41):38261-38271

Rudzinska MA (1956) Further observations on the fine structure of the macronucleus in *Tokophrya infusionum*. *J Biophys Biochem Cytol* 2 (4 Suppl):425-430

Saitou N, Nei M (1987) The neighbor-joining method: a new method for reconstructing phylogenetic trees. *Mol Biol Evol* 4 (4):406-425

Sakaki M, Koike H, Takahashi N, Sasagawa N, Tomioka S, Arahata K, Ishiura S (2001) Interaction between emerin and nuclear lamins. *J Biochem* 129 (2):321-327

Sakamoto Y, Takagi S (2013) LITTLE NUCLEI 1 and 4 Regulate Nuclear Morphology in *Arabidopsis thaliana*. *Plant Cell Physiol* 54 (4):622-633

Samaniego R, de la Torre C, Moreno Diaz de la Espina S (2008) Characterization, expression and subcellular distribution of a novel MFP1 (matrix attachment region-binding filament-like protein 1) in onion. *Protoplasma* 233 (1-2):31-38

Samaniego R, Jeong SY, de la Torre C, Meier I, Moreno Diaz de la Espina S (2006) CK2 phosphorylation weakens 90 kDa MFP1 association to the nuclear matrix in *Allium cepa*. *J Exp Bot* 57 (1):113-124

Schape J, Prausse S, Radmacher M, Stick R (2009) Influence of lamin A on the mechanical properties of amphibian oocyte nuclei measured by atomic force microscopy. *Biophys J* 96 (10):4319-4325

Scheer U, Kartenbeck J, Trendelenburg MF, Stadler J, Franke WW (1976) Experimental disintegration of the nuclear envelope. Evidence for pore-connecting fibrils. *J Cell Biol* 69 (1):1-18

Schirmer EC, Gerace L (2004) The stability of the nuclear lamina polymer changes with the composition of lamin subtypes according to their individual binding strengths. *J Biol Chem* 279 (41):42811-42817

Schmidt M, Grossmann U, Krohne G (1995) The nuclear membrane-associated honeycomb structure of the unicellular organism *Amoeba proteus*: on the search for homologies with the nuclear lamina of metazoa. *Eur J Cell Biol* 67 (3):199-208

Schoenenberger CA, Mannherz HG, Jockusch BM (2011) Actin: from structural plasticity to functional diversity. *Eur J Cell Biol* 90 (10):797-804

Schutz W, Benavente R, Alsheimer M (2005) Dynamic properties of germ line-specific lamin B3: the role of the shortened rod domain. *Eur J Cell Biol* 84 (7):649-662

Sellers JR (2000) Myosins: a diverse superfamily. *Biochim Biophys Acta* 1496 (1):3-22

Shimada N, Inouye K, Sawai S, Kawata T (2010) SunB, a novel Sad1 and UNC-84 domain-containing protein required for development of *Dictyostelium discoideum*. *Dev Growth Differ* 52 (7):577-590

Shimi T, Butin-Israeli V, Adam SA, Hamanaka RB, Goldman AE, Lucas CA, Shumaker DK, Kosak ST, Chandel NS, Goldman RD (2011) The role of nuclear lamin B1 in cell proliferation and senescence. *Genes Dev* 25 (24):2579-2593

Shimi T, Pfleghaar K, Kojima S, Pack CG, Solovei I, Goldman AE, Adam SA, Shumaker DK, Kinjo M, Cremer T, Goldman RD (2008) The A- and B-type nuclear lamin networks: microdomains involved in chromatin organization and transcription. *Genes Dev* 22 (24):3409-3421

Shoeman RL, Traub P (1990) The in vitro DNA-binding properties of purified nuclear lamin proteins and vimentin. *J Biol Chem* 265 (16):9055-9061

Shopland LS, Lynch CR, Peterson KA, Thornton K, Kepper N, Hase J, Stein S, Vincent S, Molloy KR, Kreth G, Cremer C, Bult CJ, O'Brien TP (2006) Folding and organization of a contiguous chromosome region according to the gene distribution pattern in primary genomic sequence. *J Cell Biol* 174 (1):27-38

Shumaker DK, Solimando L, Sengupta K, Shimi T, Adam SA, Grunwald A, Strelkov SV, Aebi U, Cardoso MC, Goldman RD (2008) The highly conserved nuclear lamin Ig-fold binds to PCNA: its role in DNA replication. *J Cell Biol* 181 (2):269-280

Simon DN, Wilson KL (2011) The nucleoskeleton as a genome-associated dynamic 'network of networks'. *Nat Rev Mol Cell Biol* 12 (11):695-708

Simon DN, Wilson KL (2013) Partners and post-translational modifications of nuclear lamins. *Chromosoma* 122 (1-2):13-31

Simon DN, Zastrow MS, Wilson KL (2010) Direct actin binding to A- and B-type lamin tails and actin filament bundling by the lamin A tail. *Nucleus* 1 (3):264-272

Sohaskey ML, Jiang Y, Zhao JJ, Mohr A, Roemer F, Harland RM (2010) Osteopotentia regulates osteoblast maturation, bone formation, and skeletal integrity in mice. *J Cell Biol* 189 (3):511-525

Sosa BA, Kutay U, Schwartz TU (2013) Structural insights into LINC complexes. *Curr Opin Struct Biol* 23 (2):285-291

Sosa BA, Rothballer A, Kutay U, Schwartz TU (2012) LINC complexes form by binding of three KASH peptides to domain interfaces of trimeric SUN proteins. *Cell* 149 (5):1035-1047

Spann TP, Moir RD, Goldman AE, Stick R, Goldman RD (1997) Disruption of nuclear lamin organization alters the distribution of replication factors and inhibits DNA synthesis. *J Cell Biol* 136 (6):1201-1212

Sparkes I (2011) Recent advances in understanding plant myosin function: life in the fast lane. *Mol Plant* 4 (5):805-812

Speckman RA, Garg A, Du F, Bennett L, Veile R, Arioglu E, Taylor SI, Lovett M, Bowcock AM (2000) Mutational and haplotype analyses of families with familial partial lipodystrophy (Dunnigan variety) reveal recurrent missense mutations in the globular C-terminal domain of lamin A/C. *Am J Hum Genet* 66 (4):1192-1198

Spencer VA, Costes S, Inman JL, Xu R, Chen J, Hendzel MJ, Bissell MJ (2011) Depletion of nuclear actin is a key mediator of quiescence in epithelial cells. *J Cell Sci* 124 (Pt 1):123-132

Sridharan DM, McMahon LW, Lambert MW (2006) AlphaII-Spectrin interacts with five groups of functionally important proteins in the nucleus. *Cell Biol Int* 30 (11):866-878

Starr DA (2009) A nuclear-envelope bridge positions nuclei and moves chromosomes. *J Cell Sci* 122 (Pt 5):577-586

Stenoien DL, Simeoni S, Sharp ZD, Mancini MA (2000) Subnuclear dynamics and transcription factor function. *J Cell Biochem* Suppl 35:99-106

Stewart C, Burke B (1987) Teratocarcinoma stem cells and early mouse embryos contain only a single major lamin polypeptide closely resembling lamin B. *Cell* 51 (3):383-392

Stick R (1988) cDNA cloning of the developmentally regulated lamin LIII of *Xenopus laevis*. *EMBO J* 7 (10):3189-3197

Stick R (1992) The gene structure of *Xenopus* nuclear lamin A: a model for the evolution of A-type from B-type lamins by exon shuffling. *Chromosoma* 101 (9):566-574

Stick R, Hausen P (1985) Changes in the nuclear lamina composition during early development of *Xenopus laevis*. *Cell* 41 (1):191-200

Strambio-De-Castillia C, Niepel M, Rout MP (2010) The nuclear pore complex: bridging nuclear transport and gene regulation. *Nat Rev Mol Cell Biol* 11 (7):490-501

Strelkov SV, Herrmann H, Aebi U (2003) Molecular architecture of intermediate filaments. *Bioessays* 25 (3):243-251

Strelkov SV, Schumacher J, Burkhard P, Aebi U, Herrmann H (2004) Crystal structure of the human lamin A coil 2B dimer: implications for the head-to-tail association of nuclear lamins. *J Mol Biol* 343 (4):1067-1080

Stuurman N, Heins S, Aebi U (1998) Nuclear lamins: their structure, assembly, and interactions. *J Struct Biol* 122 (1-2):42-66

Sweeney HL, Houdusse A (2010) Myosin VI rewrites the rules for myosin motors. *Cell* 141 (4):573-582

Szeverenyi I, Cassidy AJ, Chung CW, Lee BT, Common JE, Ogg SC, Chen H, Sim SY, Goh WL, Ng KW, Simpson JA, Chee LL, Eng GH, Li B, Lunny DP, Chuon D, Venkatesh A, Khoo KH, McLean WH, Lim YP, Lane EB (2008) The Human Intermediate Filament Database: comprehensive information on a gene family involved in many human diseases. *Hum Mutat* 29 (3):351-360

Takamori Y, Tamura Y, Kataoka Y, Cui Y, Seo S, Kanazawa T, Kurokawa K, Yamada H (2007) Differential expression of nuclear lamin, the major component of nuclear lamina, during neurogenesis in two germinal regions of adult rat brain. *Eur J Neurosci* 25 (6):1653-1662

Tamura K, Fukao Y, Iwamoto M, Haraguchi T, Hara-Nishimura I (2010) Identification and characterization of nuclear pore complex components in *Arabidopsis thaliana*. *Plant Cell* 22 (12):4084-4097

Tamura K, Hara-Nishimura I (2011) Involvement of the nuclear pore complex in morphology of the plant nucleus. *Nucleus* 2 (3):168-172

Tamura K, Peterson D, Peterson N, Stecher G, Nei M, Kumar S (2011) MEGA5: molecular evolutionary genetics analysis using maximum likelihood, evolutionary distance, and maximum parsimony methods. *Mol Biol Evol* 28 (10):2731-2739

Taniura H, Glass C, Gerace L (1995) A chromatin binding site in the tail domain of nuclear lamins that interacts with core histones. *J Cell Biol* 131 (1):33-44

Trigg J, Gutwin K, Keating AE, Berger B (2011) Multicoil2: predicting coiled coils and their oligomerization states from sequence in the twilight zone. *PLoS One* 6 (8):e23519

Tsai MY, Wang S, Heidinger JM, Shumaker DK, Adam SA, Goldman RD, Zheng Y (2006) A mitotic lamin B matrix induced by RanGTP required for spindle assembly. *Science* 311 (5769):1887-1893

van Zanten M, Carles A, Li Y, Soppe WJ (2012) Control and consequences of chromatin compaction during seed maturation in *Arabidopsis thaliana*. *Plant Signal Behav* 7 (3):338-341

van Zanten M, Koini MA, Geyer R, Liu Y, Brambilla V, Bartels D, Koornneef M, Fransz P, Soppe WJ (2011) Seed maturation in *Arabidopsis thaliana* is characterized by nuclear size reduction and increased chromatin condensation. *Proc Natl Acad Sci U S A* 108 (50):20219-20224

Vaughan A, Alvarez-Reyes M, Bridger JM, Broers JL, Ramaekers FC, Wehnert M, Morris GE, Whitfield WGF, Hutchison CJ (2001) Both emerin and lamin C depend on lamin A for localization at the nuclear envelope. *J Cell Sci* 114 (Pt 14):2577-2590

Vergnes L, Peterfy M, Bergo MO, Young SG, Reue K (2004) Lamin B1 is required for mouse development and nuclear integrity. *Proc Natl Acad Sci U S A* 101 (28):10428-10433

Vigouroux C, Magre J, Vantyghem MC, Bourut C, Lascols O, Shackleton S, Lloyd DJ, Guerci B, Padova G, Valensi P, Grimaldi A, Piquemal R, Touraine P, Trembath RC, Capeau J (2000) Lamin A/C gene: sex-determined expression of mutations in Dunnigan-type familial partial lipodystrophy and absence of coding mutations in congenital and acquired generalized lipoatrophy. *Diabetes* 49 (11):1958-1962

Visa N, Percipalle P (2010) Nuclear functions of actin. *Cold Spring Harb Perspect Biol* 2 (4):a000620

Vlcek S, Foisner R (2007) A-type lamin networks in light of laminopathic diseases. *Biochim Biophys Acta* 1773 (5):661-674

von Moeller F, Barendziak T, Apte K, Goldberg MW, Stick R (2010) Molecular characterization of *Xenopus* lamin LIV reveals differences in the lamin composition of sperms in amphibians and mammals. *Nucleus* 1 (1):85-95

Vorburger K, Lehner CF, Kitten GT, Eppenberger HM, Nigg EA (1989) A second higher vertebrate B-type lamin. cDNA sequence determination and in vitro processing of chicken lamin B2. *J Mol Biol* 208 (3):405-415

Vreugde S, Ferrai C, Miluzio A, Hauben E, Marchisio PC, Crippa MP, Bussi M, Biffo S (2006) Nuclear myosin VI enhances RNA polymerase II-dependent transcription. *Mol Cell* 23 (5):749-755

Wagner S, Chiosea S, Nickerson JA (2003) The spatial targeting and nuclear matrix binding domains of SRm160. *Proc Natl Acad Sci U S A* 100 (6):3269-3274

Wang N, Tytell JD, Ingber DE (2009) Mechanotransduction at a distance: mechanically coupling the extracellular matrix with the nucleus. *Nat Rev Mol Cell Biol* 10 (1):75-82

Wang TY, Han ZM, Chai YR, Zhang JH (2010a) A mini review of MAR-binding proteins. *Mol Biol Rep* 37 (7):3553-3560

Wang W, Shi Z, Jiao S, Chen C, Wang H, Liu G, Wang Q, Zhao Y, Greene MI, Zhou Z (2012) Structural insights into SUN-KASH complexes across the nuclear envelope. *Cell Res* 22 (10):1440-1452

Wang Z, Udeshi ND, Slawson C, Compton PD, Sakabe K, Cheung WD, Shabanowitz J, Hunt DF, Hart GW (2010b) Extensive crosstalk between O-GlcNAcylation and phosphorylation regulates cytokinesis. *Sci Signal* 3 (104):ra2

Ward GE, Kirschner MW (1990) Identification of cell cycle-regulated phosphorylation sites on nuclear lamin C. *Cell* 61 (4):561-577

Waterhouse AM, Procter JB, Martin DM, Clamp M, Barton GJ (2009) Jalview Version 2--a multiple sequence alignment editor and analysis workbench. *Bioinformatics* 25 (9):1189-1191

Weber K, Plessmann U, Dodemont H, Kossmagk-Stephan K (1988) Amino acid sequences and homopolymer-forming ability of the intermediate filament proteins from an invertebrate epithelium. *EMBO J* 7 (10):2995-3001

Weber K, Plessmann U, Traub P (1989a) Maturation of nuclear lamin A involves a specific carboxy-terminal trimming, which removes the polyisoprenylation site from the precursor; implications for the structure of the nuclear lamina. *FEBS Lett* 257 (2):411-414

Weber K, Plessmann U, Ulrich W (1989b) Cytoplasmic intermediate filament proteins of invertebrates are closer to nuclear lamins than are vertebrate intermediate filament proteins; sequence characterization of two muscle proteins of a nematode. *EMBO J* 8 (11):3221-3227

Wilson KL, Berk JM (2010) The nuclear envelope at a glance. *J Cell Sci* 123 (Pt 12):1973-1978

Wilson KL, Foisner R (2010) Lamin-binding Proteins. *Cold Spring Harb Perspect Biol* 2 (4):a000554

Wilson N, Simpson R, Cooper-Liddell C (2009) Introductory glycosylation analysis using SDS-PAGE and peptide mass fingerprinting. *Methods Mol Biol* 534:205-212

Wolf E, Kim PS, Berger B (1997) MultiCoil: a program for predicting two- and three-stranded coiled coils. *Protein Sci* 6 (6):1179-1189

Wolin SL, Krohne G, Kirschner MW (1987) A new lamin in *Xenopus* somatic tissues displays strong homology to human lamin A. *EMBO J* 6 (12):3809-3818

Xu XM, Meulia T, Meier I (2007) Anchorage of plant RanGAP to the nuclear envelope involves novel nuclear-pore-associated proteins. *Curr Biol* 17 (13):1157-1163

Yang SH, Chang SY, Yin L, Tu Y, Hu Y, Yoshinaga Y, de Jong PJ, Fong LG, Young SG (2011) An absence of both lamin B1 and lamin B2 in keratinocytes has no effect on cell proliferation or the development of skin and hair. *Hum Mol Genet* 20 (18):3537-3544

Ye Q, Worman HJ (1994) Primary structure analysis and lamin B and DNA binding of human LBR, an integral protein of the nuclear envelope inner membrane. *J Biol Chem* 269 (15):11306-11311

Ye Q, Worman HJ (1995) Protein-protein interactions between human nuclear lamins expressed in yeast. *Exp Cell Res* 219 (1):292-298

Young KG, Kothary R (2005) Spectrin repeat proteins in the nucleus. *Bioessays* 27 (2):144-152

Yu W, Moreno Diaz de la Espina S (1999) The plant nucleoskeleton: ultrastructural organization and identification of NuMA homologues in the nuclear matrix and mitotic spindle of plant cells. *Exp Cell Res* 246 (2):516-526

Zastrow MS, Flaherty DB, Benian GM, Wilson KL (2006) Nuclear titin interacts with A- and B-type lamins in vitro and in vivo. *J Cell Sci* 119 (Pt 2):239-249

Zbarsky IB, Debov SS (1948) On the proteins of the cell nucleus. *Dokl Akad Nauk SSSR* 63

Zhong R, Ye ZH (2007) Regulation of cell wall biosynthesis. *Curr Opin Plant Biol* 10 (6):564-572

Zhou X, Graumann K, Evans DE, Meier I (2012) Novel plant SUN-KASH bridges are involved in RanGAP anchoring and nuclear shape determination. *J Cell Biol* 196 (2):203-211

Zimek A, Weber K (2005) Terrestrial vertebrates have two keratin gene clusters; striking differences in teleost fish. *Eur J Cell Biol* 84 (6):623-635

Zimek A, Weber K (2008) In contrast to the nematode and fruit fly all 9 intron positions of the sea anemone lamin gene are conserved in human lamin genes. *Eur J Cell Biol* 87 (5):305-309

Zuela N, Bar DZ, Gruenbaum Y (2012) Lamins in development, tissue maintenance and stress. *EMBO Rep* 13 (12):1070-1078

Zuleger N, Robson MI, Schirmer EC (2011) The nuclear envelope as a chromatin organizer. *Nucleus* 2 (5):339-349

Zwerger M, Ho CY, Lammerding J (2011) Nuclear mechanics in disease. *Annu Rev Biomed Eng* 13:397-428

PUBLICATIONS